AN ATMOSPHERIC DISPERSION MODEL

FOR THE

SUDBURY, ONTARIO, AREA

By

© FRANK J. HUHN, M.Sc.

A Thesis

Submitting To The School Of Graduate Studies

In Partial Fulfillment Of The Requirements

For The Degree

Doctor Of Philosophy

McMaster University

March 1981

AN ATMOSPHERIC DISPERSION MODEL

FOR THE

SUDBURY, ONTARIO, AREA

DOCTOR OF PHILOSOPHY (1981) (Geology)

McMASTER UNIVERSITY
Hamilton, Ontario

TITLE: An Atmospheric Dispersion Model For The Sudbury, Ontario, Area

AUTHOR: Frank J. Huhn, B.Sc. (Rutgers University)
M.Sc. (University of Toronto)

SUPERVISOR: Professor J. R. Kramer

NO. OF PAGES: 404

ABSTRACT

The objectives of the study are to predict the relationship of atmospheric emissions from smelters to atmospheric and precipitation chemistry, and to lake water and sediment chemistry.

A mathematical model was developed and tested to simulate atmospheric, precipitation, lake water and sediment chemistry of selected lakes in an approximate 0.3×10^6 square kilometre area around the city of Sudbury, Ontario.

The model consists of two basic parts; an atmospheric portion and a lake chemistry portion. The atmospheric model is a Gaussian crosswind distribution modification to a box model with a uniform vertical concentration gradient limited by a mixing height (for the far field). In the near field, plume rise and vertical dispersion terms are utilized. First order chemical reaction kinetics are utilized to model the production of hydrogen ion and sulphate ion by the oxidation of sulphur dioxide. Oxidation processes in both the gas phase and the liquid phase are incorporated.

Losses en route are accounted for by the incorporation of deposition mechanisms. Losses result from the operation of these mechanisms over a period determined by plume travel time from the source to the receptor. Separate wet and dry deposition mechanisms acting on the different physical phases of pollutant species in the atmosphere are considered. These include pollutants in the gas phase, the liquid phase (dissolved in cloud droplets) and particulates or aerosols.

The mass flux of pollutant onto a unit surface (loading rate) at the receptor is accounted for by the incorporation of deposition mechanisms. While the physical processes involved are the same as those producing enroute losses, loadings result from the operation of these mechanisms at the receptor over the time period of model operation.

The continued oxidation of sulphur dioxide in samplers after deposition is also modeled.

The model can be operated in the Gaussian crosswind mode or the box mode. Advection, dispersion and boundary conditions are described by using hourly and daily meteorological data from a series of meteorological stations in the study area. These data are preprocessed by a subprogram. Provision for

six alternative schemes for combining the data from the meteorological stations are included.

Important improvements over previous models include

- computations for near and far field conditions in a single model

- direct linkage of crosswind dispersion to daily and hourly meteorological parameters

- utilization of minimum and maximum input driving parameters and theoretical parameter measurement accuracy to realistically model the range of outputs

- direct linkage of the atmospheric model to a lake water and sediment model.

The second portion of the model is the lake model. Precipitation chemistry as calculated by the atmospheric model is related to lake water and sediment chemistry utilizing a mass balance approach and assuming a continuously stirred reactor(CSTR) model to describe lake circulation. In the model surface water, the epilimnion; and the hypolimnion are considered as a single unit.

All inputs to the lake model are determined by predicted atmospheric and precipitation chemistry, modified by hydrology, soil chemistry and sedimentation in the drainage basin. Lake model outputs are stream flow and sedimentation.

A field program was carried out to collect sediment and lake chemistry data with which to test the lake model. These observations of lake water and sediment chemistry, geological observations and measurements supplement atmospheric chemistry, precipitation chemistry, meteorological and topographic data and available literature concerning the Sudbury study area.

The study area chosen surrounds the smelters at Sudbury and Falconbridge. Eight pollutant species were selected for modeling--sulphur dioxide, sulphate ion, hydrogen ion, copper, nickel, lead, zinc and iron particulates. The INCO and Falconbridge copper/nickel ore smelters in the Sudbury, Ontario area are among the largest single sources of sulphur dioxide in the world, emitting approximately 1 percent of the anthropogenic total. Significant quantities of particulates containing iron, copper, nickel, lead and other trace elements are also emitted. Sulphur dioxide, copper, iron and nickel are important smelter emissions. Zinc and iron are also indicators of natural geological

processes affecting atmospheric chemistry, while lead and zinc also provide indicators of urban processes other than smelter operation.

The Sudbury source is relatively isolated from other sources of comparable magnitude, and topographic and meteorological conditions are relatively uniform across the study area. This presents advantages for model verification.

The study area contains large numbers of accessible lakes in a variety of geological formations, including small unbuffered lakes in small bedrock basins in the Lorraine Quartzite formation. Several of these lakes were examined in comparison to large basin lakes with higher buffering capacities in order to effectively gauge the effects of atmospheric inputs from Sudbury on lakewater and sediment chemistry.

Results indicate that the model effectively predicts precipitation chemistry within approximately 150 kilometres of Sudbury. Predictions of precipitation chemistry range from approximately 22±36 percent of measured values for hydrogen ion to approximately 242±179 for copper. The average ratio of predicted to measured precipitation chemistry values is approximately 90±80 percent. Beyond 150

kilometres the effects of other pollutant sources begin to dominate. Utilization of Sudbury centered sources only in the model is invalid at these distances.

Predictions of precipitation chemistry are calculated from model predictions of atmospheric concentrations. Therefore the accuracy of the atmospheric concentration predictions defines an upper limit to the accuracy of the precipitation chemisty predictions. Therefore atmospheric concentration predictions will be at least as accurate as precipitation chemisty predictions. Results indicated that excellent prediction of atmospheric concentrations are achieved with the model within 80 kilometres of the smelters. Predictions of atmospheric concentrations range from approximately 69±26 percent of measured values for sulphur dioxide, to approximately 105±37 percent of measured values for nickel. The average ratio of predicted to measured atmospheric concentrations is approximately 81±21 percent.

Predictions of lake water chemistry are calculated from predictions of precipitation chemistry, hence the accuracy of precipitation chemistry predictions defines an upper limit to the accuracy of lake chemistry predictions. Results indicate that good predictions of lake chemistry are achieved with the model. Predictions of lake water chemistry

range from approximately 10±6 percent of measured values for hydrogen ion, to approximately 270±265 percent of measured values for zinc. The average ratio of predicted to measured lake chemistry values is approximately 140±124 percent. Ratios of predicted to measured lake water chemistry exhibit a clear bimodal pattern for pH, copper, nickel, zinc and iron. pH predictions for large drainage basin lakes are high, and pH predictions for small drainage basin lakes are low. Geological controls of lake chemistry, especially of pH and the control pH exerts on trace metal chemistry, may account for this pattern. These results indicate that adequate lake chemistry modeling requires a more complex model then a simple CSTR mass balance.

Predictions of sediment chemistry are calculated from model predictions of lake water chemistry. Therefore the accuracy of sediment chemistry predictions are limited by the accuracy of lake water chemistry predictions. Results indicate that good predictions are achieved with the model. Predictions of sediment chemistry range from approximately 102±78 percent of measured values for nickel, to 263±228 percent of measured values for lead. The average ratio of predicted to measured sediment chemistry is approximately 166±122 percent.

ACKNOWLEDGEMENTS

I extend the warmest thanks to my supervisor, Dr. J. R. Kramer, for his great patience, interest, and guidance during the planning, research, and writing of this thesis, and to the members of my committee, Dr. B. J. Burley, Dr. J. H. Crocket, Dr. H. D. Grundy, and Dr. W. J. Snodgrass, and to the staff of the Geology Department for guidance and helpful suggestions.

Thanks to Mark Burley for assistance in the field, Mrs. Jill Gleed for the analysis of samples, and special thanks to Victor Di Angelo for assistance both in the field and in the laboratory.

My thanks to the staff of the McMaster Data Processing and Computing Center for guidance and assistance, and to Joe Bowman and the staff of the Minnesota Copper Nickel Project for their intensive interest and assistance in improving the model and computer coding.

Thanks also to Fred Reuter, Al Coons, Doreen Williams, and to Acres Consulting Services Limited for assistance with graphics, typing, and reproductions of this thesis.

This research was supported by grants to Dr. J. R. Kramer from Inland Waters Subvention Program of Environment Canada, and the National Research Council of Canada.

I am most grateful to my wife Anne for assisting in the proofreading of the manuscript, and for her patience and constant encouragement, without which the writing of this thesis would have been infinitely more difficult.

TABLE OF CONTENTS

LIST OF TABLES

List of Tables - 2

List of Tables - 3

LIST OF FIGURES

1 - INTRODUCTION

The purpose of my research is to develop and test a reliable predictive model capable of describing the relationships of atmospheric emissions from smelters in the Sudbury area to atmospheric and rainfall chemistry, and to lake water and sediment chemistry of selected lakes in an approximately 0.3×10^6 square kilometre area around the city of Sudbury, Ontario.

Evidence from extensive measurements indicates that a relationship exists between emissions from the smelters at Sudbury and the chemistry of precipitation and soil up to at least 16 kilometres. This evidence consists of patterns of vegetation damage by sulphur dioxide, and patterns of nickel and copper concentrations in soil, vegetation and precipitation, centered on Sudbury.

In the vicinity of Sudbury vegetation damage by sulphur dioxide is a well-documented phenomenon (Thomas and Hendricks, 1956). Approximately 1,557 square kilometres were subject to ground level air concentrations of 0.005 ppm of sulphur dioxide ten or more times in the period 1964 to 1968, and an area of 5,468 square kilometres

was subject to at least one such episode in the same time period (Dreisinger, 1970). This can be compared to average growing season sulphur dioxide concentrations at between approximately 0.002 ppm and 0.010 ppm associated with trace amounts of damage to jack pine, trembling aspen and white birch (Linzon et al, 1979). Sulphate levels are elevated significantly above background levels in the soil up to 16 kilometres from the smelters (Gorham and Gordon, 1960). Copper, nickel and trace metals associated with them in the complex nickel-copper sulphide of the Sudbury area are also significantly higher in the soil, plants and snowfall within 16 kilometres of the smelters (McGovern and Balsillie, 1973).

The influence of the smelting of copper-nickel sulphide is clearly visible near the smelters, inside city limits and up to 3 to 5 kilometres along the major highways into Sudbury. Areas of obvious damage include areas denuded of trees, with bare, etched rock surfaces. At greater distances the effects of the smelters are not as obvious. Tree and shrub growth is reduced and leaves and needles are often yellowed or killed. More subtle effects, such as the presence of trace metal residues, can be detected in lakes and lake sediments (Semkin, 1975; Beamish, 1974; Huhn, 1974; Conroy, 1971). Of lakes

examined by the author, the most strongly affected are poorly buffered lakes, such as the majority of the lakes in the Lorraine quartzite of the LaCloche mountains, which are located to the north and east of the North Channel of the Georgian Bay, at an approximate distance of 40 to 90 kilometres southwest of the city of Sudbury. In some of these lakes the pH of the water is less than 5.0, so that most of the fish populations are nonviable, (Beamish and Harvey, 1972; Beamish, 1974). When variations in local lake basin geology and stream flow patterns are considered, copper and nickel concentration in the lake sediments and hydrogen ion concentration in the lake water tend to decrease with increasing distances from the smelters in and near Sudbury (Semkin, 1975; Conroy, 1971).

Examination of lake sediments for trace metals, notably copper and nickel, suggests that concentrations of these metals have increased up to ten-fold in some lakes, in the time period 1885 to 1974. Examination of plant microfossils in these lake sediments indicates significant changes in vegetation patterns in the Sudbury area since the inception of smelting there in the 1880's, (Huhn, 1974). These include loss of lichen populations; loss of white pine and changes in other conifer, maple, birch and poplar species populations.

Analyses of airborne dust near the ground and rain-water indicate that a significant proportion of the iron, copper, nickel, sulphate and hydrogen ion concentrations found in the soil and vegetation within 16 kilometres of Sudbury is of atmospheric origin (Costescu and Hutchinson, 1972). Concentrations of copper, nickel, sulphate and hydrogen ion in rainfall collected over five years, at distances up to 350 kilometres from Sudbury indicates a clear pattern of decreasing concentration with increasing distances in all direction from the centres of smelting in and near Sudbury (Kramer, 1973, 1974, 1975). Within 50 kilometres of Sudbury high volume air sampling of airborne copper, nickel and sulphate particulates indicates a similar pattern of decreasing concentrations with distance (Ontario Ministry of the Environment, 1974, 1975, 1976).

These patterns indicate sources of airborne copper, nickel, sulphate and hydrogen ion at or near the city of Sudbury.

The smelting of copper-nickel sulphide ores at Sudbury and at Falconbridge 15 kilometres to the north-east produces more than enough sulphur dioxide, copper and nickel to account for the observed concentrations in

the air, precipitation, soil and in lake water and sediments. This can be demonstrated by the comparison of Sudbury emission rates and atmospheric loading rates within the surrounding area (Muller and Kramer, 1970). A single smelter at Copper Cliff in Sudbury is the largest industrial point source of sulphur dioxide in Canada, releasing into the atmosphere in 1969, $2,300 \times 10^6$ kilograms of sulphur dioxide (Beamish and Harvey, 1972). This is equivalent to approximately 6 to 10 percent of the total sulphur dioxide emissions of the United States in 1968 (Mass. Inst. Tech., 1970).

Yearly total emission are summarized in Table 1, (Kramer and Muller, 1977; Acres 1980; Environment Canada, 1977). Emissions are compared to depositions in Table 2, (Muller and Kramer, 1977). These estimates can be compared to $1,452 \times 10^6$ kilograms of sulphur dioxide emitted into the atmosphere annually from the entire industrial area of Chicago, Milwaukee and Northwest Indiana, (Air Quality Control Regions 67, 68, 69, 71, 73, 81, 82, 239 and 240) (E.P.A., 1976).

It is apparent from these studies that a model capable of quantitatively relating emissions to precipitation chemistry is desirable. In its barest

Table 1

Estimates of Annual SO_2 Emissions in the Sudbury Area, from Production Data, 10^6 kilograms Annually

Source	Stack Height(s) m	Year 1970	1971	1972	1973	1974 (est.)
Copper Cliff						
Smelter	(2 x 152,107)/381*	1,530	1,362	1,227	1,079	1,720
Iron ore plant	194	220	289	256	104	122
Coniston						
Smelter	120,114	242	216	35	nil	nil
Falconbridge						
Smelter	91,137	271	301	259	269	281
Pyrrhotite plant	122	70	60	16	nil	nil

*381 m stack operational in 1972

(from Muller and Kramer, 1977)

Table 2

Material Balance for Emitted vs Deposited Materials in the Sudbury Region, 106 kilograms Annually

Time Period	Pollutant Species SO_2	SO_4	Fe	Ni	Cu
1970-1972					
Emission	2,100*	----------not known----------			
Deposition	-	32.00	1.22	0.16	0.18
1972-1974					
Emissions by 381 m INCO stack at Copper Cliff	1,450*	5.66	1.99	0.42	0.57
Deposition	4.00**	13.60	2.38	0.29	0.24

* Total SO_2 emission in Sudbury area

**Deposition as sulphate, assuming that 75 percent of the total SO_4 emission in the Sudbury region originates from the 381 m INCO stack at Copper Cliff.

(from Muller and Kramer, 1977)

essentials such a system must consider three basic processes as material is transported from source to receptor

- the rise and mixing of emitted material into the ambient atmosphere
- processes of transformation in the atmosphere
- process removing emitted material and material derived from emissions from the atmosphere.

For a more practical model framework these basic processes can be further subdivided into

- plume rise
- advection and dilution
- dispersion
- chemical decay
- losses
- scavenging or loading.

Emissions from a smokestack rise into the atmosphere as a distinct plume under the influence of ejection velocity and bouyancy forces. The height to which the plume rises depends chiefly on the vertical temperature structure of the atmosphere above the stack. As it rises it is transported away from the point of emission by the wind. As it moves downwind it is mixed with the ambient air by vertical and horizontal wind turbulence. In the atmosphere the emissions react with

each other and with the constituents of the ambient air to form new products. Forces act upon both the original emissions and their new products to remove them from the atmosphere. Two important examples of these processes are gravitational settling and washout by rainfall. There are losses enroute to the receptor which can be estimated but are not directly measurable. A proportion of the material removed from the atmosphere reaches rainfall receptors and therefore is measurable. These are termed scavenging, or loading processes.

These processes form the basis of the predictive model developed in this research. The model was developed by abstracting the best information on each aspect from previous work. This forms the framework of the model. This framework was developed and refined as required to incorporate aspects of atmospheric, chemical and physical studies in the literature, and the results of a testing program.

The model can be tested in two steps. The first step is to compare the atmospheric and rainfall concentrations calculated by the model with high volume air sampler data (Ontario Ministry of the Environment, 1974) and precipitation chemistry data (Kramer, 1973) for a small

time period and a limited number of receptor sites. This comparison is the basis for "tuning" or "calibrating" the model to a maximum practical accuracy. The model is designed to predict the maximum and minimum concentrations compatible with the range and measurement accuracies of input parameters. A sensitivity analysis identifies the most important system parameters. In the second step the model is used to predict precipitation chemistry over three years for a 0.3×10^6 square kilometre area around Sudbury. From this step a comparison is made of measured and calculated lake water and sediment chemistry. Precipitation chemistry as calculated by the atmospheric model is related to lake water and sediment chemistry utilizing a mass balance approach and assuming a continuously stirred reactor (CSTR) model. The basic lake model parameters are calculated from the topographic and geological characteristics of lake drainage basins in the Sudbury area. The model is used to predict lake water and sediment chemistry in 36 lakes in and near the LaCloche mountains, 80 kilometres WSW of Sudbury.

2 - PREVIOUS WORK

2.1 - Atmospheric Modeling

It is useful to examine previous work in the area of atmospheric modeling under five headings

- model types and approaches
- atmospheric physics, as it relates to plume rise
- dispersion and advection of stack emissions
- atmospheric chemistry, primarily the oxidation of sulphur dioxide
- depositional mechanisms.

2.1.1 - Model Types

Four source oriented model types are briefly examined in a logical developmental sequence. This sequence is a series of simplifications, from diffusion models through three, two and one dimensional Gaussian distributions, as applied to Gaussian puff kernel models and steady state Gaussian plume models, to the box model, which does not incorporate a Gaussian term.

Models can be broadly classified into two major groups

- source oriented
- receptor oriented.

The first group consists of models that apply an appropriate mathematical algorithm to a source or sources. Emissions are followed from sources to receptors. The second group consists of models that apply mathematical algorithms to receptor parameters. Source oriented models are most useful when a source or sources are known and quantifiable. Receptor oriented models are most useful when the receptor is better quantified. As Sudbury has only a few major point sources, well defined in terms of location, emission constituents, emission rates, and other relevant parameters, only source oriented models are considered in this research.

Source oriented models can be classified into four major groups

- a diffusion model
- a Gaussian puff kernel model
- a steady state Gaussian plume model
- a box model.

2.1.1.1 - Diffusion Models

The basic idea of diffusion model, developed by Adolphe Fick, 1855, is that the dominant transport mechanism causing

change in concentration of a substance at a point in space results from the existence of a concentration gradient at that point. The diffusive behavior of a medium can be characterized by its diffusivity, K_d. Diffusivity is defined mathematically in Equation 1.

$$\partial X/\partial t = K_d \nabla^2 X \qquad (1)$$

Where

∇ is the mathematical operator specifying the gradient in all three dimensions

X is the concentration

dX/dt is the rate of concentration change.

This diffusivity equation describes diffusion in three dimensions from a point with zero velocity in relation to the coordinate system.

If a steady state is assumed, or dX/dt=0 (uniform wind speed, diffusivity independent of time and spatial dimensions) Equation 1 can be expanded into Equation 2.

$$U(dX/dx) = K_x(d^2X/dx^2) + K_y(d^2X/dy^2) + K_z(d^2X/dz^2) \quad (2)$$

This expansion is valid for a coordinate system at rest or moving at a uniform wind speed along the X axis, the point of diffusion moving at a velocity U in the x dimension with respect to the coordinate system, (Stern et al, 1973). An approximate solution to Equation 2 is

$$X_{(x,y,z)} = [Q/4\pi r(K_y K_z)^{\frac{1}{2}}] \exp \{[-U/4x][(y^2/K_y)+(z^2/K_z)]\} \quad (3)$$

Where

$$r = (x^2+y^2+z^2)^{\frac{1}{2}}$$

U is the mean wind speed

Q is the source emission rate

$X_{(x,y,z)}$ is the concentration at a point defined by x, y and z.

2.1.1.2. - Gaussian Puff Kernel Models

Diffusion from a point of concentration into a static isotropic medium theoretically results in a concentration gradient that describes a normal, or Gaussian, distribution in three dimensions.

Puff kernel models basically are equations for a Gaussian distribution in three dimensions, with modifications to describe the movement of the distribution, or "puff", downwind.

An example of a Gaussian puff kernel model, applicable to an instantaneous point source, is summarized in Equation 4, (Shieh et al, 1970).

$$X_{(x,y,z,t)} = \frac{Q(t)}{(2\pi)^{3/2} s_x(t) s_y(t) s_z(t)} \exp\{-\tfrac{1}{2}[(\frac{x-ut-x'}{s_x(t)})^2 + (\frac{y-vt-y'}{s_y(t)})^2 + (\frac{z-wt-z'}{s_z(t)})^2]\} \quad (4)$$

Where

$s_x(t), s_y(t)$ and $s_z(t)$ are instantaneous standard deviations of concentrations in the x,y and z dimensions

u,v and w are velocities in the x,y and z directions

x',y' and z' are the rectangular coordinates of the point of release.

In this model the point of diffusion is moving with respect to the coordinate system. The other parameters are as previously defined.

Instantaneous point source models can be modified for application to continuous sources by integration over time. One such time integrated Gaussian puff kernel model is described by Equations 5 and 6, (Roberts et al, 1971).

$$G_{(x,y,z,t-t')} = \exp-\left\{\frac{[x-u(t-t')]^2}{2(s_x^2)^2} + \frac{y^2}{2(s_y^2)^2} + \frac{z^2}{2(s_z^2)^2}\right\} \left[(2\pi)^{3/2} s_x s_y s_z\right]^{-1} \quad (5)$$

$$X_{(x,y,z,t)} = \int_0^t dt' Q(t') G_{(x,y,z,t-t')} \exp\left(-0.693\frac{t-t'}{T_{\frac{1}{2}}}\right) \quad (6)$$

Where

$T_{\frac{1}{2}}$ is a decay term to account for loss processes, chemical reactions and radioactive decay

G is the intermediate term for the Gaussian distribution

The other parameters are as previously defined.

This model is applicable to such problems as radioactivity due to an atomic explosion. $T_{\frac{1}{2}}$ is then the time required

for the original radioactivity of the atmospheric explosion residues to be reduced by one half.

2.1.1.3 - Steady-state Gaussian Plume Models

For many continuous source applications it is possible to assume that advection, the transportation of emissions by the wind, is much greater than the dispersion rate along the wind direction. This allows the simplification of the three dimensional Gaussian distribution. This is described mathematically by Equation 7 (Pasquill, 1961; Gifford, 1961).

$$X_{(x,y,z)} = \frac{Q}{2\pi s_y s_z U} \exp\left[-\tfrac{1}{2}(y/s_y)^2 - \tfrac{1}{2}(z/s_z)^2\right] \qquad (7)$$

Where

Q is the emission rate of the source

U is the wind velocity in the x direction

Other parameters are as previously defined.

Equation 8 (Slade, 1967), describes a variation applicable to a finite area source.

$$X_{(x,y,z)} = \frac{Q}{(2\pi)^{\frac{1}{2}}(s_{y_0}^2 + s_y^2)^{\frac{1}{2}} Hu} \exp\left[- \frac{y^2/4}{2(s_{y_0}^2 + s_y^2)} - \frac{0.693t}{T_{\frac{1}{2}}} \right] \quad (8)$$

Where

y is the equivalent diameter of the emisson source area.

It is assumed that vertical diffusion is limited by atmospheric conditions. This limit, H, is the mixing height. Like Equation 6 this model incorporates an exponential decay term.

Another steady-state Gaussian plume model, including an emission height term, h, for smoke stacks or similar elevated point sources, is described by Equation 9, (Turner, 1964).

$$X/Q = \frac{\exp\left(- \frac{0.693t}{T_{\frac{1}{2}}} \right) \exp -\frac{1}{2}\left[\frac{y^2}{(s_y + 402)^2} - \frac{(z-h)^2}{s_z^2} \right]}{\pi u (s_y + 402) s_z} \quad (9)$$

As in Equations

4, 5, 6 and 7, s_x, s_y and s_z are standard deviations of concentrations in the x, y and z directions. The other

parameters are also as previously defined. In Equations 8 and 9 the horizontal standard deviations are subdivided into a fixed and a variable component. This form is convenient to use if it is assumed that the emissions diffuse under the influence of local conditions before downwind transport becomes effective. A hypothetical example is the case of a factory stack that is downwind of a large building. Dispersion in the immediate vicinity of the stack is strongly affected by the building. s_{y_0} (Equation 8), is the horizontal standard deviation (equal to 402 in Equation 9), or dispersion coefficient, at the emission point, and s_y is the dispersion coefficient applicable to the remaining plume transport distance.

Equation 10 is a form of the Gaussian plume model that assumes that as emissions diffuse downward from the centerline of the plume, they are totally reflected from the earth's surface. It is assumed that there is no reaction or deposition at the surface. This is treated mathematically as a reflected source at a distance below the surface equal to the distance of the source above the surface (Turner, 1969; Dana et al, 1973).

$$X_{(x,y,z;H)} = \frac{Q}{2\pi s_y s_z u} \exp\left[-\tfrac{1}{2}(y/s_y)^2\right] \left\{\exp\left[-\tfrac{1}{2}\left(\frac{z-H'}{s_z}\right)^2\right] + \right. \qquad (10)$$

$$\exp\left[-\tfrac{1}{2}\left(\frac{z+H'}{s_z}\right)^2\right]\}$$ (10 cont)

Where

H' is the effective plume centreline height, and the other parameters are as previously defined. The system of a Gaussian plume with total ground plane reflection is illustrated in Figure 1. It is valid to assume that total reflection can also occur at the mixing height. This is treated mathematically by multiple z terms in the two dimensional Gaussian distribution equation. Each z term is the contribution of the source, its reflection from the ground or the mixing height, and their reflections in turn. The contributions of these multiple reflection terms produce a vertical concentration gradient that approaches uniformity downwind of the source. The three cases of

- a Gaussian distribution with absorption at the ground plane
- Gaussian distribution with total reflection at the ground plane
- total reflection at both the ground plane and the mixing height,

are illustrated in Figure 2.

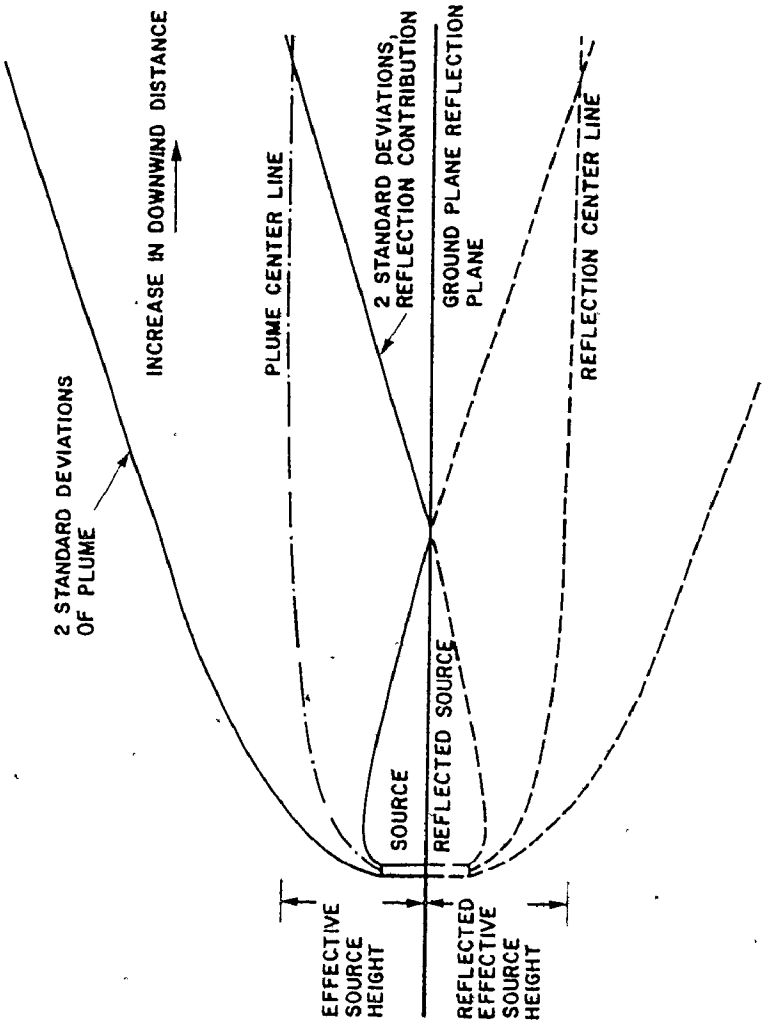

FIGURE 1
PLUME WITH REFLECTED COMPONENT

FIGURE 2
PLUME CONCENTRATION DISTRIBUTIONS

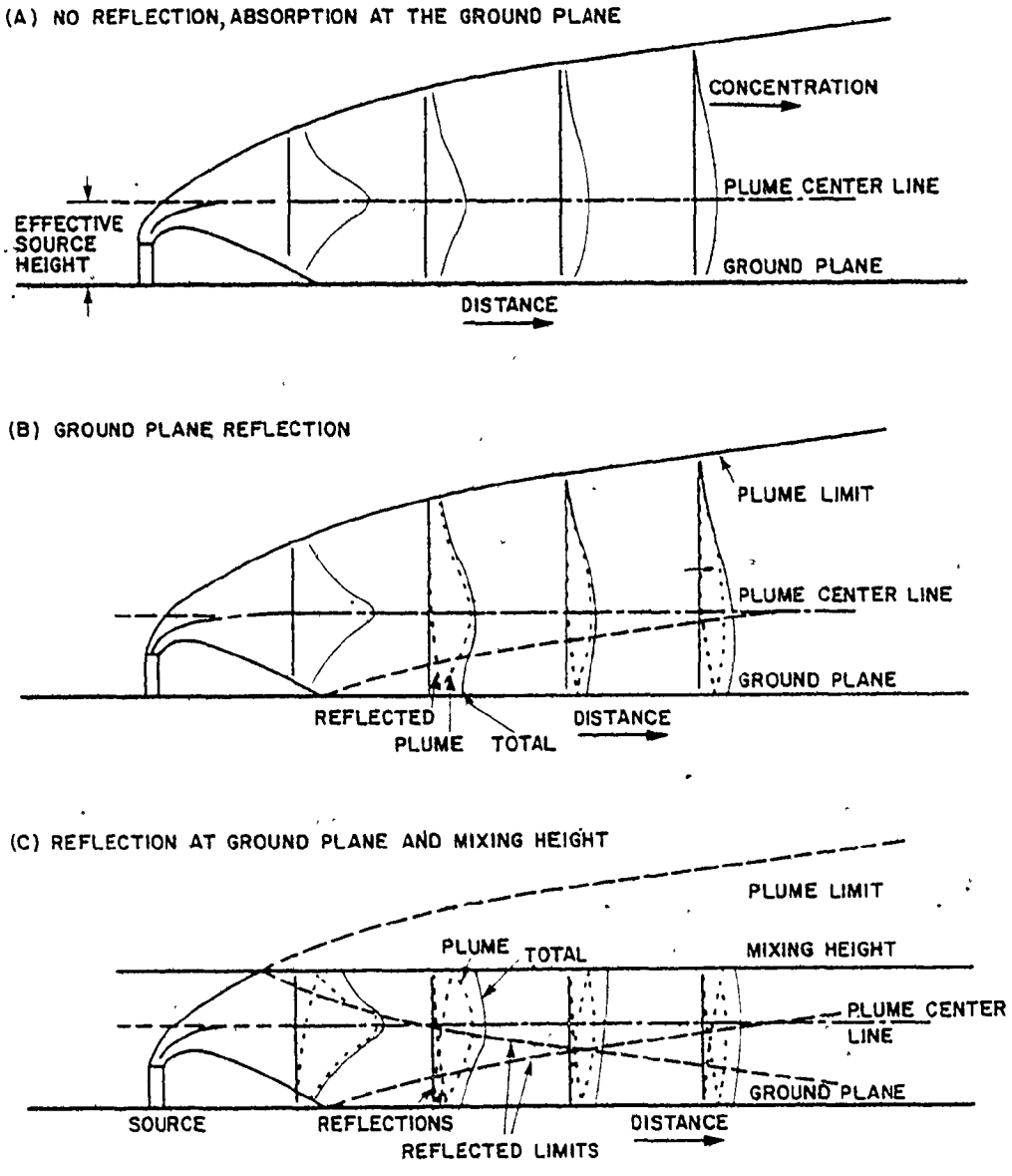

If a uniform vertical concentration can be assumed, the Steady-state Gaussian plume equation can be further simplified; only the cross wind horizontal concentration distribution is assumed to be Gaussian. This is expressed mathematically in Equation 11 (Carpenter et al, 1976).

$$X/Q = \frac{1}{(2\pi)^{\frac{1}{2}} s_y(t)} \exp\ (-\tfrac{1}{2}y^2/s_y(t)^2) \qquad (11)$$

Where

the parameters are as previously defined

2.1.1.4 - Box Models

For a system containing multiple finite sources and long transport distances further simplification may be in some cases justifiable. The Gaussian distribution is eliminated altogether. At a given downwind distance the concentration is assumed to be uniform across a rectangular area defined vertically by a dispersion angle. Outside these limits the concentration is assumed to be zero. One such "box" model, applicable to all directions around a source, is described mathematically by Equation 12 (Slade, 1967).

$$X = \frac{}{H(\frac{2\pi r}{16} + y_1)\,u} \exp\ (-\frac{0.693t}{T_{\frac{1}{2}}}) \qquad (12)$$

Where

W is the fractional frequency of the wind direction into each of 16 direction sectors

y_1 is the equivalent diameter of the source area. The other parameters are as previously defined.

One sector of the circle can be treated as a system if the wind direction is assumed to be constant. This is equivalent to making W=1 for one sector and W=0 for all other directions in Equation 12. The box angle is not necessarily one sixteenth of the circle, or 22.5 degrees. The box angle, or dispersion angle is related to atmospheric conditions, primarily wind speed and the vertical temperature structure of the atmosphere. A modification of Equation 12, incorporating a dispersion angle related to atmospheric conditions, is described by Equation 13 (Acres, 1975).

$$X_{(x)} = \frac{QDL}{u(A_i x + y_1)H_i} \qquad (13)$$

Where

A_i is the dispersion angle associated with an atmospheric condition i

H_i is the mixing height associated with the same condition

D is a decay term to account for chemical reactions in the atmosphere

L is a loss term equal to the proportion of the emissions or emission product remaining after losses from the atmosphere.

Other parameters are as previously defined.

2.1.1.5 - Summary

Four source oriented model types have been briefly examined in a logical sequence. This sequence is a series of simplifications, from diffusion models through three, two and one dimensional Gaussian distributions, as applied to Gaussian puff kernel models and steady state Gaussian plume models, to the box model, which does not incorporate a Gaussian term.

The diffusion model has the theoretical potential for predictions at the gridpoints of a three dimensional array, but it is dependent on theoretical characterization or representative measurements of many parameters over each gridpoint in question. Gaussian models are easier to apply as they require fewer

parameters to produce useful predictions.

For a system like the Sudbury region, with one or a small number of large sources, and a large spatial scale, the one dimensional Gaussian distribution model is the most applicable. The horizontal distance scale of the system is large compared to the vertical limitations of atmospheric mixing. The surface distances involved are hundreds of kilometres, and mixing heights are in the range of 0.5 to 1.5 kilometres (Turner, 1969). Therefore the assumption of uniform vertical concentration is justified. Further simplification to the box model is justified if there are many sources, as the abrupt limits of the different boxes obscure each other. The concentrations over an area change in a series of steps that approximate a smooth distribution. If the concentrations of one source are summed over a period of time, the normal distibution of weather parameters around an average should produce a (Gaussian) concentration distribution across the average wind axis. Over time the one dimensional Gaussian distribution model approaches the box model.

2.1.2 - Atmospheric Physics

Atmospheric physics, as applied to plume rise, will be examined under three headings.

- Atmospheric stability
- wind velocity profile
- plume rise expressions.

2.1.2.1 - Stability and Lapse Rates

Atmospheric stability is a measure of the tendency of the air column to produce vertical motion, driven by the vertical temperature gradient. The rate of decrease of temperature with increase in height is the temperature lapse rate. If this temperature gradient is such that a parcel of air rising in the atmosphere expands and cools without exchanging heat with its environment, then that temperature gradient is termed the adiabatic lapse rate. Cooling of rising air parcels and the warming of descending air parcels is exactly equal to the ambient temperature gradient. No bouyancy forces are produced to act upon the air parcel , it is in neutral equilibrium at any height.

If the temperature decreases with height at a greater rate the lapse rate is termed superadiabatic. An air parcel rising in the atmosphere would cool at the adiabatic rate, and would become relatively warmer than the ambient temperature. It would experience an acceleration due to bouyancy forces. Vertical upward and downward motions are reinforced. This is the unstable condition. If the

temperature decrease with increasing height is less than the adiabatic lapse rate, air parcels in vertical motion will experience deccelerating buoyancy forces. Vertical motions are suppressed. This is the stable condition. If the temperature increases with increasing height this is termed an inversion. An inverted or negative lapse rate produces conditions of extreme atmospheric stability.

Atmospheric stability can be expressed as the potential temperature gradient. This is the sum of the adiabatic temperature gradient, expressed as a positive term, and the actual temperature gradient. This relation is given in Equation 14.

$$dT_p/dz = dT/dz + L \qquad (14)$$

Where

dT/dz is the real temperature gradient, in $^{o}C/100$ m

L is the adiabatic temperature gradient, or dry adiabatic lapse rate, as a positive term.

It is usually given as $1^{o}C/100$ m (Stern, 1976). From this definition it is evident that the potential temperature gradient is zero for neutral conditions, positive for stable

conditions, and negative for unstable conditions.

The lapse rate may vary considerably at different heights. An inversion or stable condition at the ground surface may change to neutral or unstable conditions above an altitude. The stable layer near the ground effectively isolates the surface from the unstable layer. The opposite condition, an unstable layer near the ground, with a stable layer or an inversion above it isolates near surface processes from the remainder of the atmosphere. The base of the inversion or stable layer is considered to be the mixing height, H, as used in Equations 8, 12 and 13. In the absence of a well defined inversion or stable layer the mixing height is the approximate maximum height to which an air parcel at the surface can rise before reaching equilibrium with the surrounding air mass. This height is a function of the heating of the air mass by the sun and of the temperature, moisture content and wind turbulence of the air mass.

Four air mass types, named by their source areas, are important to the Sudbury area. These are

- Continental Arctic
- Maritime Arctic
- Maritime Polar
- Maritime Tropical.

Mixing heights associated with these air masses vary from 0.5 kilometres in winter for Continental Arctic to 1.5 kilometres in summer for Maritime Tropical. This is expanded upon in Table 3 (Turner, 1969).

TABLE 3

Mixing Depths Associated with Air Mass Types (Acres, 1975, 1980)

Air Mass Type	Mixing Depths Winter (m)	Spring (m)	Summer (m)	Fall (m)
Continental Artic	525	rare	-	rare
Maritime Arctic	675	780	900	780
Maritime Polar	900	1,050	1,200	1,050
Maritime Tropical	-	rare	1,500	rare

The mixing height, as a function of the season and the air mass, or as a function of the vertical temperature profile of the atmosphere, determines the height to which the emission plume rises. Different stabilities are also associated with the four air mass types. The six stability classes are reproduced in Table 4.

TABLE 4

Stability Classes
(Pasquill, 1961)

wind speed at 10 m (m/s)	Day incoming solar radiation strong, moderate, slight			Night thinly overcast, or ≥4/8 cloud cover	Night ≤3/8 cloud cover
<2	A	A-B	B		
2-3	A-B	B	C	E	F
3-5	B	B-C	C	D	E
5-6	C	C-D	D	D	D
>6	C	D	D	D	D

This classification is an attempt to quantify stability from surface weather observations. Strong incoming solar radiation corresponds to a solar altitude greater than 60 degrees with clear skies; slight insolation corresponds to a solar altitude of from 15 degrees to 35 degrees with clear skies. Class A stability is the most unstable class and Class F stability is the most stable class considered by Pasquill. This definition of stability classes leads to estimations of average stability classes for each air mass type. These estimates are given in Table 5.

TABLE 5

Pasquill's Stability Classes Associated With Air Mass Types (Acres, 1975, 1980)

Air Mass Type	Stability
Continental Arctic	D
Maritime Arctic	C
Maritime Polar	A-B
Maritime Tropical	A

2.1.2.2 - Wind Velocity Profiles

As the plume rises into the atmosphere it is swept away from the point of emission by the wind. For large spatial scale models, such as the box models, the average wind velocity from the surface to the mixing height is found to produce acceptable calculations (Acres, 1975, 1980 and Slade, 1967). Due to the surface friction of the ground, the velocity of the wind tends to decrease as the surface is approached.

The simplest way to estimate the average wind velocity is to assume a linear relation with the mixing height, as demonstrated in Equation 15 (Acres, 1975).

$$u_a = u_s + 0.0018H \qquad (15)$$

Where

u_a is the average wind velocity throughout the mixing layer, in m/s

u_s is the average surface wind speed

H is the mixing depth between 525 and 1,500 m.

For very small mixing depths, such as are sometimes caused by inversion conditions, this equation does not adequately account for the retarding effects of surface friction.

For Gaussian models, plume rise is a more critical parameter and must therefore be calculated with greater accuracy than can be afforded with an average wind velocity for the entire mixed layer. Theoretical and empirical rules relating height to wind velocities are in common use, (Stern, 1976). The logarithmic velocity profile is based on the assumption of constant shear stress with elevation and neutral atmospheric stability. A modified form, the log-linear velocity profile, an empirical formulation, is used in many plume diffusion studies, (Stern, 1976).

A common form of the logarithmic velocity profile is given in Equation 16 below.

$$u_z=(u_*/k)\ln(z/z_0) \tag{16}$$

Where

k is the von Karman constant

z_0 is the roughness length

u_* is the friction velocity

z is the height

u_z is the wind velocity at height z.

The von Karman constant is experimentally determined to have the value 0.4 (Rohsenow and Choi, 1961). Friction velocity is related to surface shear stress, τ_0, by Equation 17.

$$u_*=(\tau_0/p)^{\frac{1}{2}} \tag{17}$$

Where

p is the density of the air

The logarithmic velocity profile is empirical in that the controlling parameter friction velocity is usually found

experimentally from the measured wind velocity profile data. The roughness length depends on the surface roughness, which is also usually obtained by extrapolation from the velocity profile data. Typical values of roughness length and friction velocity divided by measured velocities at specific heights are given in Table 6.

TABLE 6

Parameters for Logarithmic Wind Velocity Profile Equation (Stern, 1976)

Surface	z_o, cm	u_*/u	u, m/s	z, m	Ref.
Mud flats-ice	.001	.03-.08	5	2	Sutton, 1953
Even snow cover	.05	-			Orlenko, 1970
Prairie snow cover	.10	.053		2	Priestly, 1959
Desert	.03	.045		2	Priestly, 1959
Semidesert	0.3				Orlenko, 1970
Bare ground	1.0				Orlenko, 1970
Plowed ground	2.0				Orlenko, 1970
Flat open country	3.0	.071		10	Davenport, 1965
Woodland forest	30	0.12		10	Davenport, 1965
Town	100				Orlenko, 1970
City	200				Orlenko, 1970
Urban area	300	0.22		10	Davenport, 1965

Roughness length can be roughly estimated in terms of the dimensions and distributions of roughness elements (Lettau, 1969). This is expressed mathematically by Equation 18.

$$z_o = 0.5 h^* s/S \qquad (18)$$

Where

h^* is the average element height

s is the average silhouette area on the vertical plane normal to the wind direction for the elements

S is the specific area.

Specific area is the average plan view area per element. Roughness lengths obtained by this calculation range from 0.025 centimetres for sand grains to 12.5 and 125 centimetres for suburban and urban housing densities.

The simplest modification of the logarithmic wind velocity profile equation for calculations with non-neutral atmospheric conditions is the addition of a term that is linear with height. This is expressed as in Equation 19.

$$u=\frac{u_*}{k}[\ln(z/z_0) + a(z/L)] \qquad (19)$$

Where

a is a constant determined by extrapolation from measurements

L is the Monin-Obukhov stability length, defined in Equation 20 (Obukhoff, 1941).

$$L=-u_*^3 T\rho c_p/kgq_h \qquad (20)$$

Where

q_h is the heat transfer from the surface to the air

c_p is the specific heat of air at constant pressure

ρ is the density of the air

g is the acceleration of gravity.

The difficulty in accurately measuring heat transfer makes the Monin-Obukhov stability length hard to evaluate, reducing the value of the log-linear velocity profile equation.

A more practical wind velocity profile equation is the power law velocity profile. It is an empirical formulation, simply formulated, and does not require the evaluation of theoretical terms. The usual form of the power law velocity profile is given in Equation 21.

$$u=u_1(z/z_1)^m \qquad (21)$$

Where

u_1 and z_1 are reference velocity and height, selected from the available data or to suit a particular application. The key parameter is the exponent m, which is dependent on surface characteristics and atmospheric stability. Pipe flow experiments indicate a median figure of 1/7 for neutral stability and flat surfaces of low roughness (Rohsenow and Choi, 1961). The exponent generally increases with increasing stability and with increasing surface roughness (Stern, 1976). Investigation by a number of workers indicates a range of values for various conditions. Some of these results are presented in Table 7.

TABLE 7

Exponent m for Power Law Wind Velocity Profile Equation (Stern, 1976)

Surface	Stability	m	Ref.
Smooth open country	Unstable	0.11	Sutton, 1947
	Neutral	0.14	Sutton, 1947
	Moderately stable	0.20	Sutton, 1947
	Large stability	0.33	Sutton, 1947
Nonurban terrain of varying roughness	Daytime-unstable and neutral	0.1-0.3	DeMarris, 1959
	Night-stable, inc. inversion	0.2-0.8	DeMarris, 1959
Urban Liverpool	Unstable	0.20	Jones, 1971
	Neutral	0.21	Jones, 1971
Flat open country	Neutral	0.16	Davenport, 1965
Woodland forest	Neutral	0.28	Davenport, 1965
Urban area	Neutral	0.40	Davenport, 1965

2.1.2.3 - Plume Rise Expressions

Plume rise is the elevation of the plume centreline above the point of emission as a function of the distance downwind (Stern, 1976). In an atmospheric layer characterized by a single stability and wind direction, plume rise can be approximated by relatively simple equations. Equations in common use are based in part on theoretical considerations and in part on observations of plume rise.

The important driving forces causing the plume to rise are momentum forces and buoyancy forces. Momentum forces refer to the kinetic energy of the effluent due to the velocity with which it is emitted from the stack. In most cases momentum forces are important only close to the point of emission. Buoyancy forces acting on the plume are due to the lesser density of the emissions. The density of the emission is usually due to the higher temperature of the emissions relative to the surrounding air. While momentum forces are rapidly dissipated by fluid friction with the ambient atmosphere, buoyancy forces continue to cause the plume to rise until the emissions have cooled sufficiently to reduce the plume's average density to that of the ambient air. In general the time required for this equilibrium to occur is a function of the heat emission rate, wind velocity, ambient

air temperatures, and atmospheric stability.

Most plume rise equations are simple one term power laws with exponents for the parameters based on observations. Equation 22 is the general form.

$$dh(x) = KQ_h{}^a x^b u^c \qquad (22)$$

Where

$dh(x)$ is the plume rise at distance downwind x

Q_h is the heat emission rate

u is the wind velocity

a,b and c are exponents evaluated from theoretical or experimental considerations

K is a constant.

The units of the constant depend on the units chosen for Q_h, x, u and dh; and on the exponents a, b and c. The heat emission rate Q_h is evaluated in various ways depending on available stack effluent data. It is a pure heat emission only if there is no effluent mass flow. If a mass flow

exists Q_h is the equivalent heat emission required to produce the same buoyancy relative to the ambient air. It can therefore be expressed as;

$$Q_h = Q_m c_p (T_s - T) \qquad (23)$$

Where

Q_m is the effluent mass emission rate

c_p is the specific heat of the effluent at constant pressure

T_s is the absolute temperature of the effluent at the stack outlet

T is the absolute temperature of the ambient atmosphere.

The effluent mass emission rate can be expressed in terms of the effluent density and stack parameters, as in Equation 24.

$$Q_m = p_s A_s V_s \qquad (24)$$

Where

p_s is the mass density of the effluent at the stack outlet

A_s is the stack outlet area

V_s is the effluent emission velocity at the stack outlet.

Studies by Briggs (1969), Bringfelt (1969) and Fay et al (1970), indicate from field data and on theoretical grounds that values for a, b and c in Equation 22 are; a=1/3, b=2/3 and c=1. For these exponent values, and assuming the parameters to be in compatible units, the constant K is dimensionless. There is agreement on the value for c, but various investigators find different values for a and b. Values for a range from 0.25 to 0.40 and values for b range from 0.26 to 0.67 (Stern, 1976).

Briggs (1969, 1972) related Q_h to a bouyancy flux parameter, F_b, given in Equation 25.

$$F_b=gQ_h/\pi c_p p_s T \qquad (25)$$

Where

g is the acceleration due to gravity, and the other terms are defined as for Equations 22, 23 and 24. For all stability classes and x larger than a critical distance x^*, Briggs (1968, 1972) uses an equation of the following form.

$$dh_x=C_1 F_b^{1/3} x^{2/3} u^{-1} \qquad (26)$$

Briggs (1969) recommends a value of 1.6 for the dimensionless constant C_1. Beyond x^* ambient atmospheric turbulence dominates the plume rise. The critical distance x^* is a function of atmospheric turbulence and the buoyancy flux parameter (Equation 25). For mks units Equations 27 and 28 give approximations of the critical distance.

$$x^* = 2.16 F_b^{2/5} h_s^{3/5} \qquad h_s < 305 \text{ metres} \qquad (27)$$

$$x^* = 67 F_b^{2/5} \qquad h_s > 305 \text{ metres} \qquad (28)$$

Where

h_s is the stack height, h_s and x^* are in metres and F_b must be in units of $m^4 s^{-3}$. A good approximation of dh_x for distances up to 10 times stack height is given by Equation 29 (Briggs, 1969).

$$dh_x = 1.6 F_b^{1/3} x^{2/3} \qquad (29)$$

Bringfelt (1968) collected extensive field data from the literature and made measurements at fossil fuel fired electrical generation stations and industrial plants in Sweden. He summarized these data in three equations for plume rise at three downwind distances. These are given in Equations

30, 31 and 32.

$$dh = 103 Q_h^{0.39} u^{-1} \qquad x = 250 \text{ metres} \qquad (30)$$

$$dh = 167 Q_h^{0.36} u^{-1} \qquad x = 500 \text{ metres} \qquad (31)$$

$$dh = 224 Q_h^{0.34} u^{-1} \qquad x = 1{,}000 \text{ metres} \qquad (32)$$

Where

dh is in metres

u is the wind velocity in metres/second

the heat emission Q_h is in terms of power plant electrical generating capacity, in megawatts.

Carpenter et al (1971) and Montgomery et at (1972) studied various plume dispersion models for the coal burning power plants of the Tennessee Valley Authority (TVA). Carpenter et al (1971) expressed plume rise in the form of Equation 33, which is the same as Equation 26 (Briggs, 1969) with modified buoyancy flux and temperature gradient terms.

$$dh_x = C_1 F_{ba}^{1/3} x^{2/3} u^{-1} \quad (33)$$

Where

F_{ba} and C_1 are defined by Equations 34 and 35.

$$F_{ba} = g V_s r_s^2 (T_s - T)/T_s \quad (34)$$

Where

r_s is the radius of the stack outlet and the other terms are as defined for Equations 23, 24 and 26.

$$C_1 = 1.58 - 0.414(dT_p/dz) \quad (35)$$

Where

dT_p/dz is the potential temperature gradient.

Three stability categories are emphasized for the range covered by Equation 35. These are tabulated in Table 8.

TABLE 8

Stability Categories for the Tennessee Authority Plume Rise Equation

Stability Class	dT_p/dz, C°/100 m	C_1
1	1.3	1.04
2	0.3	1.46
3	-0.06	1.60

Montgomery et al (1972) later developed separate plume rise equations for three stability ranges. These are given in Equations 36, 37 and 38.

Neutral stability; Potential temperature gradient from -0.17 to 0.16

$$dh_x = 2.50x^{0.56}F_{ba}{}^{1/3}u^{-1} \quad \text{for x less than 3,000 metres} \quad (36)$$

Moderate stability; Potential temperature gradient from 0.16 to 0.70

$$dh_x = 3.75x^{0.49}F_{ba}{}^{1/3}u^{-1} \quad \text{for x less than 2,800 metres} \quad (37)$$

Very stable; Potential temperature gradient from 0.70 to 1.87

$dh_x 13.8x^{0.26}F_{ba}{}^{1/3}u^{-1}$ for x less than 1,960 metres (38)

Where

dh_x and x are in metres

u is in metres/second

potential temperature gradient is in $^{o}C/100$ metres

F_{ba} (Equation 34) is in m^4/s^3.

For plume rise expressions with dh_x related to an x term raised to a power larger than zero, there is no theoretical limit to plume rise in a non-stable atmosphere. A final rise must be based on practical considerations derived from experimental data. This is usually at a selected downwind distance beyond which further plume rise is negligible.

Holland (1953) was one of the first workers to develop a relationship between final plume rise, wind velocity, heat emission rate and stack parameters. This relationship is expressed in Equation 39.

$$dh=(1.5V_s d_s + 0.00004Q_h)u^{-1} \quad (39)$$

Where

d_s is the stack outlet diameter in metres. Other units are as previously defined.

Q_h is in units of cal/s.

The equation (Equation 39) separates the momentum and buoyancy contribution to plume rise into two separate terms.

In contrast to Equation 22, Equation 40 gives the general form of the plume rise equation with additional terms for source elevation and momentum.

$$dh=C_3 + C_4(V_s/u)^e d_s + C_5 Q_h^f/u \quad (40)$$

Where

C_3 is the source elevation

C_4 and e are a constant and exponent giving the momentum contribution to plume rise

C_5 and f are a constant and exponent giving the buoyancy contribution to plume rise.

As for the parameters of the buoyancy terms previously discussed (Equation 25 and 34) the constant and exponent of the momentum term are derived from the measurement of real plumes.

Moses and Carson (1968) derived three equations for three stability groups, as given in Equations 41, 42 and 43.

Unstable; Potential temperature gradient less than -0.22

$$dh=3.47(V_s/u)d_s + 10.53Q_h^{\frac{1}{2}}/u \quad (41)$$

Neutral; Potential temperature gradient between -0.22 to 0.85

$$dh=0.35(V_s/u)d_s + 5.41Q_h^{\frac{1}{2}}/u \quad (42)$$

Stable; Potential temperature gradient greater than 0.85

$$dh=-1.04(V_s/u)d_s + 4.58Q_h^{\frac{1}{2}}/u \quad (43)$$

Units for potential temperature gradient are $^{o}C/100$ m;

V_s, m/s; u, m/s; d_s, m; and Q_h, kcal/s.

Briggs' (1969, 1972) equations for final plume rise include calm as well as the usual windy condition. These relations are given in Equations 44, 45, 46, 47 and 48. For neutral and unstable conditions

$$dh=1.6F_b^{1/3}(3x^*)^{2/3}/u \qquad (44)$$

Equation 44 is obtained by setting x in Equation 29 equal to $3x^*$. x^* is given by Equations 27 and 28.

According to Briggs (1969) Equation 45 is a good approximation for fossil fuel power plants with heat emission rates of 20 megawatts or more.

$$dh=1.6F_b^{1/3}(10h_s)^{2/3}/u \qquad (45)$$

Where

h_s is the emission source height in metres. Equation 45 is obtained by setting x in Equation 29 equal to $10h_s$. For stable conditions

$$dh=C_2(F_b/us)^{1/3} \qquad (46)$$

Where

s is a stability parameter given in terms of the temperature and the potential temperature gradient as expressed in Equation 47.

$$s=g(dT_p/dz)/T \qquad (47)$$

Briggs (1969) recommended a value of 2.9 for C_2. Later research indicated a range of values of C_2 from 2.4 to 2.6. A conservative value for C_2 is 2.4 (Briggs, 1972).

For calm conditions the final plume rise is given by Equation 48 (Briggs, 1969).

$$dh=5.0F_b^{1/4}s^{-3/8} \qquad (48)$$

If the plume has sufficient buoyancy it may rise beyond an inversion layer. This occurs if the final plume rise calculated for the stability conditions of an atmospheric layer of a given depth is greater than that depth.

A plume rising through a neutral layer may be stopped at the base of a stable or inversion layer. Resistance to penetration of an inversion is given in

Equation 49.

$$b_i = g(dT_i/T) \tag{49}$$

Where dT_i is the temperature increase through the inversion layer. If the inversion is less than a critical thickness z_i, the plume will penetrate the inversion and continue to rise above it. The critical thickness is given in Equations 50 and 51 (Stern, 1976).

For windy conditions,

$$z_i = 2.0(F_b/ub_i)^{\frac{1}{2}} \tag{50}$$

For calm conditions,

$$z_i = 4.0F_b^{0.4}b_i^{-0.6} \tag{51}$$

Where

z_i is the critical inversion thickness and the other parameters are as defined for Equations 25 and 49.

Plume height as a function of distance downwind of an emission source can be described as a function of heat

emission rate, stack parameters, wind and atmospheric stability parameters. While in theory plume rise continues in a nonstable layer without limit, a practical final rise is reached when the rate is no longer detectable in measurements of real plumes. In reality the paramenters effecting plume rise in the atmosphere may change with altitude, modifying the rate of plume rise and further limiting the final rise height. Under inversion or strongly stable atmospheric conditions the plume may cease to rise or even descend. However, if the stable or inversion layer is not too thick the plume may penetrate it and continue to rise.

2.1.2.4 - Dispersion

Dispersion is a measure of the rate at which the emissions mix with the ambient air through which the plume is transported. The primary agent of dispersion in the atmosphere is eddy diffusion. This is the rate with which momentum is transferred through the atmosphere by fluid friction in and between eddies (Rohsenow and Choi, 1961). These eddies are caused primarily by two agencies
- friction between the wind and the surface of the earth
- thermal instabilities

Friction reduces the wind to zero at or near the ground. Friction against this layer of still air reduces the

velocity of the air in the layer above, and friction against this slow moving layer reduces the velocity of the air in the layer above it. This is the basis of the wind velocity profile expressions given in Equation 15 through 21. If conservation of fluid momentum is maintained, the fluid momentum that is lost from the wind velocity near the surface is transferred to random wind variation, analogous to the production of heat by friction.

Atmospheric stability is a measure of thermal instabilities, as described in Section 2.1, Atmospheric Stability. It is evident that dispersion must be related to the wind velocity profile and to atmospheric stability. Many workers have derived expressions for this theoretical relationship. However, the majority of the practical relationships have been worked out by the substitution of field data in Gaussian distribution equations.

Sutton (1947, 1953) relates diffusion coefficients C_y and C_z to s_y and s_z, the horizontal and vertical standard deviation terms in the Gaussian plume equation, as given in Equation 52 and 53.

$$s_y = 2^{-\frac{1}{2}} C_y x^{(2-n_y)/2} \tag{52}$$

$$s_z = 2^{-\frac{1}{2}} C_z x^{(2-n_z)/2} \tag{53}$$

Where

x is the downwind distance

n is related to the exponent m of the power law wind velocity profile given in Equation 21.

This relationship is given in Equation 54.

$$m = n/(2-n) \tag{54}$$

C_y and C_z depend on components of turbulence in the y and z directions. In practice they are determined by fitting Gaussian diffusion equations to the concentration profile data.

Sutton (1953) eventually determined n_y and n_z in the same manner, by fitting the diffusion equation to the measured concentration data. The relationship of n to the power law velocity profile exponent (Equation 54) was retained only if no adequate concentration data could be obtained.

Montgomery et al (1973) developed simplified equations for neutral conditions of atmospheric stability, given by Equation 55 and 56.

$$s_y=0.42x^{0.75} \quad (55)$$

$$s_z=0.39x^{0.75} \quad (56)$$

For stable atmospheric conditions, Equations 57 and 58 are appropriate (Montgomery et al, 1973).

$$s_y=1.32x^{0.55} \quad (57)$$

$$s_z=6.71x^{0.21} \quad (58)$$

Where

horizontal and vertical standard deviations and downwind distance , s_y, s_z and x respectively, are all in metres.

Hinds (1970), working in a complex area of canyons and ridges typically 300 to 500 metres high found that the data fitted Equation 59 for horizontal standard deviation with a scatter of a factor of 2.0 above and below the mean.

$$s_y = 0.65x^{0.75} \qquad (59)$$

This equation includes data for all conditions; stable, neutral and unstable.

Singer and Smith (1966) found Equations 60 to 67 to produce good fits, with a scatter of plus or minus a factor of 3.0, for downwind distances of 50 to 150 kilometres over a 24 hour averaging period. Table 9 lists the appropriate equations for a range of atmospheric stabilities.

TABLE 9

Standard Deviations for a Range of Stabilities

Stability	Wind, m/s at 9 m	Wind, m/s at 108 m	s_y, m	s_z, m	
B	2.5	3.8	$.40x^{.91}$	$.41x^{.91}$	(60,61)
B-C	3.4	7.0	$.36x^{.86}$	$.33x^{.86}$	(62,63)
C	4.7	10.4	$.32x^{.78}$	$.22x^{.78}$	(64,64)
D	1.9	6.4	$.31x^{.71}$	$.06x^{.71}$	(66,67)

Many workers designate a horizontal angle of diffusion, or a standard deviation of the wind direction. This is defined as the angle, measured from the wind direction, that includes 95 percent of the plume material

(Acres, 1975) to define the crosswind limits of a box model. Angles range from 30 degrees for unstable to 2.5 degrees for stable atmospheric conditions. This is detailed in Table 10.

TABLE 10

Standard Deviation of the Wind Direction for Stability Classes

Stability Class	Standard Deviation, degrees	Reference
A	25	Slade, 1968
B	20	Slade, 1968
C	15	Slade, 1968
D	10	Slade, 1968
E	5	Slade, 1968
F	2.5	Slade, 1968
Unstable	18-13	McElroy, 1969
Neutral	15-20	McElroy, 1969
Stable	8-13	McElroy, 1969
A	27	Acres, 1975
A-B	20	Acres, 1975
C	12	Acres, 1975
D	9	Acres, 1975

The combined effects of atmospheric stability, wind, momentum and buoyancy forces, and dispersion produce several different plume configurations. The six most common plume configurations are

- looping
- coning
- fanning
- lofting

- fumigation
- trapping.

Looping occurs in unstable atmospheric conditions where large scale thermal turbulence forms the plume into irregular loops, waves and patches. Over a time scale that is long relative to the time scale of the thermal turbulence, dispersion is rapid. Standard deviation terms for the Gaussian plume model are large. On a short time scale concentrations at any given point tend to fluctuate widely. Coning occurs for neutral to stable atmospheric conditions, where mechanical turbulence induced by the wind is more important then thermal turbulence induced by the wind is more important than thermal turbulence. The plume appears to be more or less conical in form, and changes much more slowly than does the looping plume. Dispersion is less than for the looping plume, but the standard deviation terms vary less over a given time interval. Fanning occurs for conditions of stability or extreme stability such as are cause by an inversion. The plume rises to its maximum rise height with very little vertical dispersion. Under these conditions there is no thermal instability to cause vertical mixing. The horizontal dispersion, caused by wind eddies, is also. small. These three plume, types, looping, coning, and fanning occur when the plume rises in an atmospheric

layer characterized by a single stability. The form of lofting, fumigating and trapped plumes is dictated by the presence of a stable and an unstable atmospheric layer. Lofting occurs when an inversion or a relatively stable layer occurs near the surface, and the plume has sufficient buoyancy to penetrate the stable layer and rise in the more unstable layer above. The plume has a coning or sometimes looping configuration but with downward motions and dispersion limited or halted by the stable or inversion layer. Fumigation is the opposite case. An inversion or relatively stable layer above the surface limits the plume rise and upward dispersion. The emissions are confined in contact with the surface. Trapping occurs when the stable layer or inversion is high enough for a coning plume to form beneath it, but with upward motions and dispersion limited or halted by the stable layer.

Each type of plume can be modeled by a Gaussian two dimensional concentration pattern with appropriate standard deviation terms and limitations. For a looping plume both vertical and horizontal standard deviation terms must be large. For a coning plume both standard deviation terms can be much smaller. For a fanning plume the vertical standard deviation of the concentration can be almost zero. For a lofting plume the standard deviation terms

change at the top of the inversion layer. They are small below, in the inversion, and larger above it in the unstable layer. For trapping the opposite applies. The standard deviation terms are large in the unstable layer near the surface and become relatively small at the base of the inversion layer. For fumigation the vertical standard deviation term can be eliminated, and the assumption made that the concentration will be constant with height up to the base of the inversion. This is a logical successor to the trapping case as the vertical standard deviation increases.

The Gaussian model variation appropriate to a situation depends on the frequency with which the different atmospheric stabilities occur , and the spatial and temporal scale of interest.

2.1.3 - Chemistry

It is apparent from a study of forms of emissions compared to forms of deposition that a portion of the sulphur dioxide emitted from the stacks at Sudbury is oxidized to sulphates before it is deposited (Kramer, 1975). A summary of the emissions and depositions measured at Sudbury is given in Tables 1 , 2, and Appendix B.

The pathways by which this oxidation occurs are exceedingly complex (Greenfield, 1957; Van der Westhuizen, 1969; Beilke, 1978; Eggleton and Cox. 1978; Altshuller, 1979; Möller, 1980). Many sulphur containing species have been found in the atmosphere and in precipitation, many may be important intermediaries in the oxidation of sulphur dioxide to sulphate (Altshuller et al, 1971; Sidle, 1967). Research has indicated that a large number of the constituents of clean or polluted air may be catalysts in sulphur oxidation processes (Hallsworth and Adams, 1973; Harrison et al, 1971; Bufalini, 1971; Hegg and Hobbs, 1978, Calvert et al, 1978).

In general the basic reaction pathways can be categorized as oxidation in the gas phase or in the liquid phase. Oxidation in the gas phase can be examined under the headings of direct and indirect oxidation. Oxidation in the liquid phase can be examined under the headings of catalyzed and uncatalyzed oxidation reactions.

In the gas phase, the production of the product sulphuric acid and its subsequent reactions involves the oxidation of sulphur dioxide to sulphur trioxide, hydration of the trioxide, condensation of the resulting sulphuric acid, and reactions with particulates and droplets of

atmospheric water. This is illustrated by Equation 68.

$$SO_{2(g)} + \tfrac{1}{2}O_{2(g)} = SO_{3(g)} \qquad (68)$$

The equilibrium constant for this reaction strongly favors the formation of the trioxide at the temperatures at which, typically, sulphur dioxide is emitted from the stack and enters the plume (300 to 500 degrees Kelvin). Kinetic factors prevent the immediate oxidation of all the sulphur dioxide to the trioxide. As the gases cool the equilibrium constant increases. This is less favorable for reaction to completion. A summary of the relationship of the equilibrium constant to temperature is given in Table 11.

TABLE 11

Equilibrium Constants for the Oxidation of Sulphur Dioxide in the Gas Phase (Levy et al, 1976)

Temperature (^{o}K)	Equilibrium Constant
300	2.069×10^{12}
400	1.088×10^{8}
500	2.608×10^{5}
600	4.892×10^{3}

Thermodynamically, the hydration of SO_3 to sulphuric acid also becomes more favorable as the temperature drops. At the temperatures existing in plumes essentially all the SO_3 is converted to H_2SO_4. The reaction is illustrated by Equation 69.

$$SO_{3(g)} + H_2O_{(g)} = H_2SO_{4(g)} \quad (69)$$

Direct oxidation is driven by the energy of sunlight; the basic equation is Equation 68. Indirect oxidation is driven by chemical energy from high energy reactive species in the atmosphere, such as ozone or nitrate radicals. Two examples, out of a large number of possible indirect oxidation reactions, are illustrated by Equations 70 and 71.

$$SO_{2(g)} + O_{3(g)} = SO_{3(g)} + O_{2(g)} \quad (70)$$

$$SO_{2(g)} + NO_3 = SO_{3(g)} + NO_2 \quad (71)$$

One of the basic questions in assessing the importance of gas phase oxidation is the rate at which the reaction proceeds in clean air at plume temperatures. Gerhard and Johnstone (1955) reported an oxidation rate of 0.1 percent

per hour in natural sunlight and rates averaging 0.68 percent per hour in ultraviolet light irradiated (2,950 to 3,650 Å) systems containing NO_2. Oxidation of SO_2 by ozone is also a slow process, approximately 0.25 percent per hour (Levy et al, 1976). These rates can be compared to direct oxidation rates of 0.001 to 0.05 percent per hour, estimated by Levy, et al (1976) and 0.021 percent per hour estimated by Castleman (1975). These can be compared to overall oxidation rates of from 0.5 percent per hour (Chan et al, 1980) to 2 to 3 percent per hour (Katz, 1950) at Sudbury.

The process involved in the oxidation of SO_2 in the aqueous phase includes absorption of SO_2, oxygen and other gases, hydration and subsequent dissociation of the dissolved species, and the oxidation of sulfite or bisulfite ions. These processes are strongly dependent on thermodynamic factors and the presence and concentrations of reactants and catalysts. In general, however, oxidation in the aqueous phase is favoured in the conditions prevailing in plumes.

A consideration of primary importance to the problem of aqueous phase oxidation of sulphur dioxide is the dissociation behaviour of SO_2 and its associated oxidation products and intermediaries in water.

Spectroscopic studies indicate that while SO_2, HSO_3^-, and $SO_3^=$ are the most abundant species, pyrosulphate ion, $HS_2O_5^-$, and hydrates $SO_2 \cdot nH_2O$, exist in measurable quantities (Falk and Giguere, 1958). This is an indication that the SO_2-H_2O system is in reality far more complex than was previously assumed. For application to plume studies the dissociation processes can be represented in terms of three equations interrelating the most abundant species, (Levy et al, 1976; Möller, 1980). These are illustrated by Equations 72, 73 and 74.

$$SO_{2(g)} \overset{k_o}{=} SO_{2(aq)} \tag{72}$$

$$SO_{2(aq)} + H_2O \overset{k_1}{=} HSO_3^- + H^+ \tag{73}$$

$$HSO_3^- \overset{k_2}{=} SO_3^= + H^+ \tag{74}$$

The values of these equilibrium constants as functions of temperature are given in Table 12.

TABLE 12

Equilibrium Constants for the Dissociation of Sulphur Species in the Aqueous Phase (Yue et al, 1975)

Temperature (degrees C)	k_0 (mol/atm)	k_1 (mol)	k_2 (mol)
25	1.24	0.0174	6.3×10^{-8}
15	1.83	0.0219	7.9×10^{-8}
10	2.25	0.0247	8.9×10^{-8}
0	3.46	0.0319	11.4×10^{-8}
-3	3.97	0.0346	12.4×10^{-8}

The oxidation reaction itself may be oxidation of sulphite to sulphate or bisulphite to bisulphate, as illustrated by Equations 75 and 76.

$$HSO_3^- + \tfrac{1}{2}O_2 = HSO_4^- \quad (75)$$

$$SO_3^= + \tfrac{1}{2}O_2 = SO_4^= \quad (76)$$

There is a general agreement in the literature that in the aqueous phase the oxidation of SO_2 by oxygen must be catalyzed to proceed at an appreciable rate (Levy et al, 1976). Almost without exception the suggested catalyst has been either ammonia or a metal salt or oxide, most likely Fe^{+++} or Mn^{++}.

Fuller and Crist (1941) found that at 25 degrees C in a pure oxygen atmosphere that the uncatalyzed oxidation reaction exhibited a first order rate constant of 0.013 ± .0015 s^{-1}. The addition of Cu^{++} to act as a catalyst increased the rate constant proportional to the copper concentration. The modified rate constant is described in Equation 77.

$$\frac{-d(SO_3^{=})}{dt} = \left[k_1 + k_3(Cu^{++})\right](SO_3^{=}) \qquad (77)$$

Where

k_1 is the uncatalyzed rate constant

k_3 is equal to $2.5 \pm 0.33 \times 10^6$ $mol^{-1}sec^{-1}$.

The effect of pH on the oxidation rate was also investigated. The oxidation rate increases with increasing pH, as is illustrated in Equation 78.

$$\frac{-d(SO_3^{=})}{dt} = \left[k_1 + k_4(H^{+})^{\frac{1}{2}}\right](SO_3^{=}) \qquad (78)$$

Where

k_4 is equal to 6.6 ± 0.47 $mol^{-\frac{1}{2}}$ s^{-1}.

More recent research indicated that this value should be equal to 59 $mol^{-\frac{1}{2}}$ s^{-1} (Sillen, 1964).

Junge and Ryan (1958) found that the uncatalyzed reaction produced a negligible amount of sulfate. In the presence of $FeCl_2$ catalyst the formation of sulfate was found to reach a limiting value after a time period, typically 1 to 3 hours. For a given concentration of catalyst the final sulfate concentration depended linearly on the initial SO_2 concentration. The pH of the solution dropped during the course of the reaction, and sulphate production nearly ceased by the time the pH dropped to 2.2.

Other catalysts examined (Junge and Ryan, 1958), in decreasing order of effectiveness in promoting oxidation were $MnCl_2$, $CuCl_2$, $FeCl_2$, $CoCl_2$, NH_4OH and NaCl. Ammonia is not a catalyst in the oxidation reaction, but neutralizes the sulfate formed, thereby shifting the system toward the oxidized product. An investigation of the oxidation process in fog droplets indicates that an atmosphere containing initially 20 $\mu g/m^3$ of SO_2 and 3 $\mu g/m^3$ of NH_3, with a liquid water content of 0.1 gm/m^3 forms an estimated 2.9 $\mu g/m^3$ of sulphate. This ammonia concentration is suggested to be proper for "clean country air". 500 $\mu g/m^3$

of SO_2 and 10 $\mu g/m^3$ of NH_3 in the same fog produces an estimated 26.2 $\mu g/m^3$ of sulphate (Levy et al, 1976).

Van den Heuval and Mason (1963) experimented with water droplets suspended on a fibre grid, exposed to controlled amounts of SO_2 and NH_3. Ammonium sulfate, produced in the droplet, is proportional to the surface area of the droplet and to time. In an atmosphere containing 100 $\mu g/m^3$ SO_2 and 10 $\mu g/m^3$ NH_3 a conversion rate of 2.5 percent per minute was obtained.

Scott and Hobbs (1967) approached the problem theoretically, by assuming that the system of gaseous and dissolved SO_2, NH_3 and CO_2 and product ions is in equilibrium. It is then possible to derive the theoretical oxidation rate. Oxidation rates calculated are of the order of 2.5 percent per hour.

Foster (1969) examined the role of metal catalysts in power plant plumes. The source of these metals are fly ash from the combustion of coal in the power plant itself, natural and anthropogenic dust in the atmosphere. Foster estimated oxidation rates of 0.09 percent per minute for manganese and 0.15 to 1.5 percent per minute for iron catalysts. Cheng et al, (1971), found that metal catalyzed oxidation proceeded at about 20 percent per

hour for a 0.1 ppm level of SO_2. In order of decreasing catalytic efficiency are $MnSO_4$, $MnCl_2$, $CuSO_4$ and NaCl.

None of these studies claim to effectively model the real atmosphere in plumes, but only to be indicators of the true condition. For practical purposes it is necessary to make measurements in real plumes in the field. Unfortunately in the field it is nearly impossible to control conditions, and difficult to make the required measurements. Therefore the various studies attempted are not always directly comparable.

In general it was found that oxidation rates depended on atmospheric moisture content and plume age. Oxidation rates decreased with decreasing humidity and with increasing plume age. Also typical is the wide range of oxidation rates measured or estimated within single studies; Gartrell et al (1963) reported oxidation rates from essentially zero to 1 to 3 percent per hour for low relative humidities to 30 percent per hour at high relative humidity; Coutant et al (1972) report first order rate constants for the loss of SO_2 that vary from 2×10^{-3} to 13×10^{-3} min^{-1}; Roberts et al (1975) report pseudo-first order rate constants for the oxidation of SO_2 in the Los Angeles basin of from 1.2 to 13.8 percent per hour; and Lusis et al

(1975) report oxidation rates of from 0.2 to 7 percent in the plume of the Sudbury smelters. More recently reported oxidation rates for the INCO smelter at Copper Cliff are as low as 0.5 percent per hour (Chan et al, 1980). These rates are approximately 20 percent of oxidation rates, between 2 and 3 percent per hour, from early ground measurements at Sudbury (Katz, 1950). From the wide range of oxidation rates measured it is clear that factors other than time in the plume are important determining parameters. This variability may have been the result of changing meteorological conditions, the difficulties of analysis, or other factors unknown (Levy et al, 1976).

Table 13 is a short summary of some measured oxidation rates in plumes.

TABLE 13

Summary of Oxidation Rates in Plumes, SO_2 to $SO_4^=$.

Oxidation rates	Half lifes	Rel. Hum.	Ref.
*2-3% /hr	-	-	Katz, 1950
12% /min	-	-	Shirai et al, 1962
0-4% /hr	-	45-70%	Gartrell et al, 1963
8-55% /hr	-	73%	Gartrell et al, 1963
-	1.0-2.8 hr	36-53%	Dennis et al, 1969
-	0.3-1.0 hr	-	Weber, 1970
-	1.2-2.4 hr	40-80%	Stephens & McCaldin, 1971
0	-	<35%	Stephens & McCaldin, 1971
-	1.0-6.0 hr	40-90%	Coutant et al, 1972
0-1% /min	-	-	Manowitz et al, 1972
0.37-0.76% /hr	-	26-50%	University of Utah, 1975
2.2×10^{-4} /s	-	-	Dana et al, 1973
7.7×10^{-4} /s	-	-	Dana et al, 1973
-	10	-	Newman et al, 1975
*1% /hr	-	-	Lusis et al, 1975
1.5-1.8% /hr	-	-	Whitby et al, 1976
*0.5% /hr	-	-	Chan et al, 1980

*These studies refer to the Sudbury area.

In general, more recent studies indicate lower oxidation rates. This may indicate that progressively better, or more reliable experiments are being carried out (Levy et al, 1976).

2.1.4 - Loss and Scavenging Mechanisms

If a parcel of air containing stack emissions is considered to move with the wind, the parcel will experience a loss of emission products. The processes causing these losses can be divided into two by an operational consideration. All processes that remove emissions and emission products from the atmosphere enroute, which do not reach the receptor, are termed enroute loss mechanisms. All processes that lead to measurable loadings at the receptor are termed loading mechanisms. The actual processes involved are for all practical purposes identical. The differences are where and when the mechanism acts.

Losses enroute occur during the time the air parcel is moving downwind from the stack or point of emission to the receptor. If this air parcel is considered to be independent of the emission source and other air parcels, it will contain a fixed amount of emissions, assuming no in-plume decay or transformation processes. If it is further assumed that the loss mechanisms act uniformly over the

extent of the parcel, and over time, then the remaining concentration in the parcel after any time period can be described by a simple exponential expression, as given in Equation 79.

$$C_{(t)} = C_0 e^{-kt} \tag{79}$$

Where

C_0 is the original concentration

$C_{(t)}$ is the concentration remaining after losses at a fixed rate over time t

K is the loss rate per unit time.

Equation 79 is the solution to a differential equation of the form given in Equation 80, where the rate of change of concentration is directly proportional to the concentration.

$$\frac{dC}{dt} = -kC \tag{80}$$

Loading mechanisms are defined for the purposes of this research as deposition processes at the point where the air

parcel contributes to the receptor. During the time scale chosen for modeling or measurements, it is assumed that the plume maintains a constant relationship to the receptor. This implies that the air parcel over the receptor is continuously renewed, and the air concentration is not reduced by loading to the receptor. This is illustrated by the basic loading equation, Equation 81.

$$L_{(t)} = kCt \qquad (81)$$

Where

$L_{(t)}$ is the amount deposited, or the total loading, in time period t

Here t is the time scale of operation of the model, typically 24 hours, or the time between measurements

C is the concentration in the air above the receptor

k is the loading rate, equal to the loss rate as defined in Equation 79 and 80.

For convenience both loss and loading mechanisms will be termed depositional processes in the following discussion.

The many processes by which pollutants are removed from the air can be divided into wet and dry processes. Wet processes involve the interaction of emissions and emission products with rainfall, cloud droplets and other forms of liquid water in the atmosphere, dry processes are all those processes that do not involve interactions with liquid water. Practically, these categories can be subdivided according to the physical phase of the material acted upon; gas, liquid, or solid phase.

All wet deposition processes can be taken together and termed "precipitation scavenging". Wet processes include washout and rainout. Washout is the removal of particles or droplets by the impact of falling raindrops, or the absorption of gases into falling drops. Rainout involves the condensation of liquid water on particles or smaller drops as nuclei. These newly formed or enlarged drops grow large enough to fall from the plume as rain or present larger targets for rain falling through the plume. In practical terms it is usually impossible to determine by which process a pollutant entered rainfall measured on the ground. Scavenging coefficients in the literature are the result of both processes.

Washout is a bulk process. That is, washout is

dependent on the pathway through the plume taken by a raindrop. The number of particles impacted by a falling drop depends on the concentration of particles, the relative sizes and velocities of the impacting raindrops and the impacted particles, and the pathlength through the plume. Pathlength is a function of depth of plume through which the rain must fall, the wind velocity, which causes the rain to fall at an angle along the direction of the wind, and wind turbulence, which increases the pathlength, increases the relative velocities of drops and particles and increases the probability of contact.

As a drop falls through the air the air is divided to flow around it. The paths taken by the air as it flows past the drop are termed streamlines. Particles in the path of a falling drop are disturbed by the moving air in front of the drop, and tend to move around the drop with the streamlines. This is the effect of fluid friction between the air and the particles.. Opposing this force is inertia, which tends to keep the particle in place. The effective result of this interaction of forces is a reduction of the apparent cross-sectional area of the falling drop, as seen from the point of view of the particle. The effective collision diameter is smaller than the sum of the drop and particle diameters. The correction for

effectiveness of impaction is given in Equation 82 (Marchello, 1976).

$$E = N^2_{st}/(N_{st} + 0.06)^2 \qquad N_{st} > 0.08$$

$$E = 0.0 \qquad N_{st} < 0.08 \qquad (82)$$

Very small particles follow the streamlines, exhibiting essentially no inertial effect.

E is the correction factor for impaction effectiveness

N_{st}, Stokes number, is described in Equation 83.

$$N_{st} = 2\, u\rho_p d_p^2/9\mu_a R \qquad (83)$$

Where

ρ_p is the particle density

u is the relative velocity between the drop and the particle

d_p is the particle diameter

R is the droplet radius

μ_a is the viscosity of air equal to 0.00018 gm/cm s at

20 degrees C and 1 atm.

A complete theoretical expression for particle washout by raindrops requires integration of the basic impaction expression over the range of particle size and frequencies, raindrop sizes and frequencies and across concentration changes through the plume along the path of the raindrops. As pathlength and drop and particle velocities are size dependent, the integration becomes complex (Dana et al, 1973). For most practical studies a simple relationship derived from measurements is used. Table 14 is a brief summary of some of the scavenging coefficients in use for particulates.

TABLE 14

Scavenging Coefficients for Particulates

Scavenging Coefficient (s^{-1})	Reference
3×10^{-5}	Chamberlain, 1955
$16 \times 10^{-5} I^{0.8}$, I is rain rate in mm/hr; particle size 5μ	Englemann, 1965
8×10^{-5}	Makhon'ko, 1976
0.01×10^{-5}; particles size .1μ	Slinn and Hales, 1970
0.1×10^{-5}; particles size .5μ	Slinn and Hales, 1970
3×10^{-5}; particles size 1μ	Slinn and Hales, 1970
0.4×10^{-5}	Esmen, 1972
$3 \times 10^{-5} I$, I is rain rate in mm/hr	Acres, 1977

Kramer (1976) related measured washout of particulates to precipitation velocity, using a relationship based on data from Engelmann (1965) for a fixed particle size of 5 μm, for rainfall rates between .03 and 3 mm/hr, as given in Equation 84.

$$\lambda = 10^{(-0.24 + 0.8 \log J)} \quad (84)$$

Where

λ is the washout coefficient in hr^{-1} and J is the rainfall rate in mm/hr.

Makhon'ko (1967) developed an exponential expression for wet deposition, relating rain time, washout and rain-out coefficients to air and rainwater concentrations. The relationship is given in Equation 85.

$$C_t = aq_0 + bq_0e^{-s_0t} + dq_0e^{-st} \quad (85)$$

Where

C_t is the contaminant concentration in rainwater at time t after the start of the rain

q_0 is the contaminant concentration in the subcloud layer at time t = 0.0

s_o is the rainout coefficient

s is the washout coefficient

a,b and d are independent factors dependent on meteorological conditions.

Assuming q_0 to be constant with elevation, Makhon'ko (1967) concluded from field data that s_o ranged from 10^{-3} to 10^{-4} s^{-1} and s ranged from 10^{-4} to 10^{-5} s^{-1}.

Gas washout is the absorption of gases by falling raindrops during the time that a raindrop is falling through a concentration of gas. The amount absorbed by a drop depends on the drop surface area, the relative concentration of the gas in the atmosphere and dissolved in the drop, the nature of the gas, other chemicals and reaction products in the drop, and the velocity of fall of the drop.

Gas washout is treated in great detail by Danà et al (1973). Transfer of SO_2 into a raindrop is calculated

in terms of an overall mass transfer coefficient for each drop size. This mass transfer is the overall effective rate of gas transfer through three drop regions in turn; the air boundary layer; the air/water interface and the water boundary layer. The gas diffuses through the boundary layer in air at a rate determined by the gas' diffusivity in air at the prevailing temperature and pressure conditions and by the gas concentration gradient across the air boundary layer. The steady state ratio of gas concentration in air at the surface of a raindrop to that dissolved in it is determined by the Henry's law constant. This constant is a function of the dissolving gas, the temperature, atmospheric pressure, and the chemistry of the water in the raindrop. The dissolved gas diffuses into the drop, through the water boundary layer, at a rate determined by the gas' diffusivity in water, driven by the concentration gradient across the water boundary layer in the drop. It is also a function of temperature and water droplet chemistry. Equation 86 gives the overall mass transfer coefficient in terms of the air, water and interface mass transfer rates (Dana et al, 1973).

$$1/K_y = H/k_x + 1/k_y \qquad (86)$$

Where

K_y is the overall mass transfer coefficient of gas into the drop

H is the Henry's law constant

k_x and k_y are the mass transfer coefficients for the gas in water and in air, respectively.

In Dana et al (1973), the Henrys' law constant is replaced by an expression that is continuously modified, as gas diffuses into, or out of, the drop, to account for the oxidation of sulfur dioxide in the drop.

The mass transfer coefficients for sulphur dioxide in air and in water are related to gas diffusivities by the gas concentrations and the boundary layer thickness, as given in Equations 87 and 88.

$$k_x = C_x D_{ex}/S_x \tag{87}$$

$$k_y = C_y D_{ey}/S_y \tag{88}$$

Where

C_x and C_y are the concentrations of sulphur dioxide in

water and in air respectively

D_{ex} and D_{ey} are the diffusivities of sulphur dioxide in water and air

S_x and S_y are the effective boundary layer thickness on the water and air sides of the air/water interface.

As for impaction on suspended particles, realistic theoretical solutions, relating bulk air concentrations to bulk rainfall concentrations, require integration over all droplet sizes and frequencies, and across concentration changes along the raindrop trajectories. As the absorption rate for each drop is dependent on the drop and ambient air concentrations of sulphur dioxide, simple integration along the range of conditions existing along the raindrop trajectory is not sufficient to produce a solution.

Iterative calculation techniques are required. This is the approach taken for much of the power plant effluent modeling at Batelle-Northwest Laboratories (Dana et al, 1973; Hales, Thorp and Wolf, 1970).

Most practical studies do not attempt to relate the gas washout coefficient to the actual physical processes

taking place. Instead, an overall washout coefficient or simple expression relating rainfall rates to washout coefficients is derived from measurements. A few of these coefficients and relationships are summarized briefly in Table 15.

TABLE 15

Washout Coefficients for Gases,
J = rainfall rate in mm/hr

Washout Coefficient (s^{-1})	Reference
1×10^{-4}	Chamberlain, 1955
6×10^{-5}	Makhon'ko, 1967
$1.7 \times 10^{-4} J^{0.6}$	Beille, 1970
2×10^{-5}	Hales, Thorp and Wolf, 1970
0.4×10^{-5}	Hales, Thorp and Wolf, 1970
$6 \times 10^{-5} J$	Acres, 1977

Another process for removing gases from the atmosphere is adsorption of surfaces. In extremely dusty atmospheres adsorption of gases onto solid particulate surfaces may be

a significant process. The adsorbed gases then are scavenged or fall out at rates applicable to the particulates.

Transport of gases to the surface can be described by Fick's diffusion law. The rate of change in concentration is dependent on the concentration gradient, as is given in Equation 89.

$$\frac{dC_a}{dt} = D_{ab} \frac{d^2C_a}{dz^2} \qquad (89)$$

Where

dC_a/dt is the rate of change of concentration

d^2C_a/dz^2 is the second derivative of the concentration profile along the distance z

C_a is the concentration

D_{ab} is the diffusivity of constituent a in medium b.

This is the single dimensional modification of the general Fick's law expression, given in Equation 1. The one dimensional case is applicable to the problem of gas diffusion

through a plume or an atmospheric layer to the surface of the earth.

At the surface the gas is absorbed at varying rates, dependent to a large extent on the character of the surface. Over water surfaces gases are absorbed by the same basic processes by which they are absorbed into raindrops (Liss, 1976). Absorption rates are dependent on the surface roughness, which modifies the amount of absorbing surface per unit of ground surface, and increases micro-scale turbulence.

Due to the difficulty of effectively describing real absorbing surfaces mathematically, most gas deposition studies use an empirical deposition velocity parameter, based on measurements. Measured air concentrations are divided into the measured mass deposition rate per unit area, producing a number with units of velocity. It is difficult to summarize deposition velocities because of the many factors affecting the estimates. Experimental method, reference height, type of surface, moisture condition of surface and atmospheric conditions all affect estimates (Denison, McMahon and Kramer, 1979). Nevertheless, the estimates tabulated in Table 16 exhibit a fair degree of consistency

(The standard deviation for the six deposition velocity estimates for SO_2 is 0.795).

TABLE 16

Deposition Velocities for Gases

Deposition Velocity (cm/s)	Gas	Surface	Reference
1.2	I	flat plate	Chamberlain, 1955
2.5	I	grass	Chamberlain, 1955
2.0	I	grass,water	Slade, 1968.
0.5	I	soil, snow	Slade, 1968
1.2	SO_2	grass	Garland & Clough,1973
0.8	SO_2	grass	Garland & Clough,1973
2.2	SO_2	grass	Whelpdale & Shaw,1974
2.3	SO_2	water	Whelpdale & Shaw,1974
0.3	SO_2	snow	Whelpdale & Shaw,1974
1.0	SO_2	-	Acres, 1977

Dry depositional processes affecting particulates are as follows

- gravitational settling
- Brownian motion
- inertial and diffusional deposition
- particle collisions
- static electrical and magnetic coagulation processes.

Gravitational settling, or sedimentation, is the fall of particles by their own weight. It is dependent on the size, configuration, and mass of particles. Inertial deposition occurs in the turbulent area between tree leaves, grass, weeds and near waves on water surfaces. The air streamlines follow sharply curved trajectories which change randomly and rapidly, so that inertial forces prevent the particles being carried along by the air from following the streamlines. They tend to follow straight lines tangent to the curves of the streamlines, hitting vegetation and other obstacles which effectively remove them from the air. Impaction on wet surfaces or waves is a very efficient depositional mechanism, as reentrainment is prevented. Particles also collide with each other (sometimes to form aggregations, with increased settling velocities), but this process is not important at commonly observed particle concentration levels (Ledbetter, 1972). Most often when particles do collide, the collision is elastic and the velocity vectors that describe the trajectories taken by

the colliding particles tend to shift away from the direction of the air streamlines. Elastic collisions between particles tend to produce a particle diffusion effect across the direction of particle transport.

Many natural processes occuring in the atmosphere, such as friction and the freezing of water droplets, produce a separation of electrical charges. Through the action of these processes atmospheric particles, aerosols and raindrops may acquire electric charges. Stack effluents may contain particles that have become electrically charged by electrostatic precipitators.

Coalesence of particles or particles and droplets of opposite charge produces particles or drops of higher mass modifying their depositional characteristics.

Small crystalline particles of materials such as iron oxides or clays have areas of positive and negative surface charges. In a particle collision the existence of these surface charges on the colliding particles increases the probability that the particles will stick together, rather than bounce off one another. Some metal oxides, such as iron oxides, may be magnetized. Collisions between magnetized particles are more likely to lead to

coagulation of fine particles into coarser ones than are collisions between unmagnetized particles.

Brownian motion is the diffusion of very fine particles through a medium due to collisions with the molecules of the medium. It is analagous to molecular diffusion. In both processes the driving force is the random motion of the molecules of the medium. For very small particles, the probability is high that a significant number of the molecules colliding with the particle will have velocity vectors that do not completely cancel each other. There will be a net force on the particle. As the individual molecular velocity vectors are random, the net force vector will also be random. Allowing for the effects of inertia and friction forces, the particle will be moved in a manner similar to the motion of a single molecule in the medium. This is Browian motion.

For particles with diameters less then 0.1 μm, diffusion by Brownian motion predominates over settling. The Brownian motion relation, expressed in the same form as gas diffusion, as given in Equation 89. In the case of Brownian motion diffusion the diffusion constant is a function of the inertia of the particle and the viscosity of the air, as expressed in Equation 90 (Bird et al, 1960).

$$D = kTK_m/3\pi\mu_a d_p \qquad (90)$$

Where

k is Boltzmann's constant

K_m is the Cunningham correction (Rohsenow and Choi, 1966)

μ_a is the viscosity of air, equal to 0.00018 gm/cm-s at 20 degrees C and at 1 atm

d_p is the effective particle diameter in cm.

Cunningham's correction is a function of the finite size of the particle, while a molecule can be treated as a mathematical point. Cunningham's correction is expressed in Equation 91.

$$K_m = 1 + \frac{\lambda}{d_p}\left[1.644 + 0.552\exp\left(-0.656\frac{d_p}{\lambda}\right)\right] \qquad (91)$$

Where

λ is the mean free path, the average distance that a molecule travels between collisions. At standard conditions of

25 degrees C and 1 atm the mean free path is equal to 0.066 μm.

Air velocity and Brownian motion bring aerosol particulates close enough together for van der Waal's forces to cause coagulation or agglomeration, leading to size and volume distribution changes with time. The process may be accelerated or decelerated by the presence of electric surface charges or magnetic dipole fields associated with the particulates.

Larger particles are less affected by molecular collisions (Brownian motion) and proportionately more affected by gravity (settling). Particles larger than 0.1 μm settle out of the air predominantly by gravitational sedimentation; the balance of gravitational acceleration and aerodynamic drag leads to the formulation of the generalized Stoke's law expression for fall velocity as given in Equation 92.

$$V_t = \left[4gd(p_p-p_a)/3p_aC\right]^{\frac{1}{2}} \qquad (92)$$

Where

V_t is the terminal fall velocity

p_a is the density of the air, equal to 0.0013 gm/cm^3 at standard conditions

g is the gravitational constant

C is the drag coefficient.

The drag coefficient is a function of air viscosity, density, particle size and shape. It is related to the Reynolds number, N_{re}. The mathematical definition of the Reynolds number is given is Equation 93.

$$N_{re} = d_p p_a V_t / \mu_a \qquad (93)$$

Where

μ_a is the viscosity of air

p_a is the density of the air

V_t is the fall velocity of the particle

d_p is the effective particle diameter.

For spherical particles C can be represented by

three relationships, each applicable to a different range of Reynolds numbers. These relationships are given in Equations 94, 95 and 96.

$$C = 24N_{re}^{-1} \qquad \text{for } N_{re} \text{ less than 2} \qquad (94)$$

$$C = 18.5N_{re}^{-0.6} \qquad \text{for } N_{re} \text{ between 2 and 500} \qquad (95)$$

$$C = 0.44 \qquad \text{for } N_{re} \text{ greater than 500} \qquad (96)$$

The fall velocity is dependent on the drag coefficient, which is defined in terms of the fall velocity. Complex interaction of forces control the fall of a drop or particle through the air. Measured fall velocities, expressed as functions of particle sizes, do not always match theoretical fall velocities. Gunn and Kinzer (1949) developed an empirical expression for the terminal fall velocity of raindrops in stagnant air, given in Equation 97.

$$V_t = 8710.858R - 18029.72R^2 - 32184.48R^3 \qquad (97)$$

Where

R is the droplet radius in cm

V_t is the fall velocity in cm/s.

The relationship was obtained by fitting a polynomial to rainfall data. The curve applies to droplets with radii greater then 40 μm; below this size fall velocities follow Stokes law (Stern et al, 1973).

As is the case with other depositional process parameters discussed the relationship of theoretical to measured particle deposition velocities is not thoroughly understood. For this reason many practical deposition velocities for particles have been obtained by experiment or measurements in the field.

Table 17 is a short summary of some of the deposition velocities measured for particles.

TABLE 17

Deposition Velocities for Particulates

Deposition Velocity, V_d cm/s	Particle Diameter μm	Roughness Length, z_0 cm	Wind Velocity, V m/s	Surface	Reference
1.1	16	-	-	grass	Chamberlain, 1955
.03	.1	-	-	grass	Chamberlain, 1967
.03	1	-	-	grass	Chamberlain, 1967
.1	2	-	-	grass	Chamberlain, 1967
.8	5	-	-	grass	Chamberlain, 1967
.4	-	.6	2	grass	Chamberlain, 1976
.7	-	.6	4	grass	Chamberlain, 1976
1.4	-	.6	8	grass	Chamberlain, 1976
.24	-	.001	6	filter paper	Clough, 1973
.11	-	.002	2.2	water	Sehmel & Sutter, 1974
.44	-	.02	7.2	water	Sehmel & Sutter, 1974
1.17	-	.1	13.8	water	Sehmel & Sutter, 1974
.1	.5	-	-	membrane filter	Esman & Corn, 1971
.2	1	-	-	membrane filter	Esman & Corn, 1971
.8	5	-	-	membrane filter	Esman & Corn, 1971
.1	-	-	-	-	Acres, 1977
.1-.6	-	-	-	-	Pierson, Cawse, Salmon & Cambry, 1973

An extensive examination of the literature reveals ranges of values for washout coefficients and deposition velocities of sulphur dioxide and sulphates of from two to seven orders of magnitude. Table 18 is a summary of the ranges and median values of depositional parameters in the literature (Denison et al, 1979).

TABLE 18

Summary of Depositional Parameter Values

Species & Process	Deposition Velocity cm s^{-1}		Washout Coefficient 10^{-5} s^{-1}	
	Gas	Particulate	Gas	Particulate
Geometric Frequency Median	0.50	0.50	5.27I	5.48I
Arithmetic Frequency Median	0.94	0.60	8.98I	9.40I
Range of Literature Values				
Laboratory	0.04 to 3.90	0.002 to 20000	$17I^{0.6}$ to $9.0I^{-0.54}$	----
Field	0.30 to 3.70	0.10 to 100	0.40I to 6.0I	0.40I to 300I

Where

I is rainfall rate in mm hr^{-1}.

2.2 - Lake Modeling

Rainfall receptors are one means of estimating the rate of deposition of air pollution constituents. They are limited by practical considerations to a small number of receptors and a short time span. Sampling the water of natural lakes provides an indication of loading rates over an area, the drainage basin of the lake, and over time (roughly the detention time) of the pollution constituent under examination.

Basic parameters to consider are input terms for water and pollutant constituents, loss terms, transformation terms, and transportation terms. Transportation terms include all those factors that influence the movement and mixing of materials in the lake.

For the purposes of this study it is assumed that all materials entering a lake are uniformly distributed in a time that is negligible in comparison to the sampling time scale. Transformation terms include all those factors

that change the state of the pollutant constituents after they enter the lake basin. Transformation in the drainage basin must be included in these terms. Included in these terms are coagulation of fine particulates, surface reactions such as the adsorption of ions onto the surface of clay particulates, the solution of particulates, reaction of atmospheric constituents with lake water chemistry, and the incorporation of atmospheric inputs into the biological cycles of the lake. All of these processes are important to the relationships between observed precipitation and lake water chemistries. For the purposes of this study all detailed transformations have been ignored. The only chemistry noted is geology related buffering effects on lake water chemistry.

Most lake models are concerned with nonconservative constituents, such as oxygen, nutrients such as nitrogen and phosphorus and living organic material. Such models generally are based on the extremely complex interactions of the biological cycles in lakes, estuaries, streams and seas (O'Connor, 1966; DiToro et al, 1972; Snodgrass and O'Melia, 1974; Thomann et al, 1975). Models for conservative constituents, materials that do not take part in complex chemical and biological reactions, are usually more complex in terms of transport and diffusion factors.

One example of such a model is that of O'Connor and Mueller (1970) for the movements of chloride ion in the Great Lakes and Great Lakes Basin. If terms describing transport and transform within the lake can be ignored, the model may be reducible to a simple mass balance equation. For each constituent measured in the lake water, including water, all pathways entering and leaving the system are identified and quantified. Inputs and outputs are set equal to each other, plus a difference term, which must be equal to retention in the lake. In order for input and output terms to be equated in this manner, all gradients betweem points of inputs, outputs and concentration measurements must be assumed to be negligible. This is the basic assumption of the CSTR (continuously stirred reactor) model. That is, any inputs or outputs affect the whole volume of the reactor equally and instantaneously.

Equation 98 gives the basic form of the mass balance. The rate of change of mass in the system is equal to the inflow less the output of the mass.

$$\frac{d(VC)}{dt} = (QC)_{in} - Q_{out}C \qquad (98)$$

which can be expanded mathematically to

$$\frac{VdC}{dt} + \frac{CdV}{dt} = (QC)_{in} - Q_{out}C$$

Where

V is the volume of the system or the lake

C is the concentration of the constituent in the lake water, and hence, also in the water leaving the system

Q_{out} is the total water flux out

$(QC)_{in}$ is the total mass of a constituent in.

If the total water volume of the system is considered to remain constant over the sampling period or the modeling time scale, the system is in a steady state in regard to water. If V is constant over time the derivative of V over time is equal to zero. Equation 98 can therefore be reduced to Equation 99 as given below.

$$\frac{VdC}{dt} = (QC)_{in} - Q_{out}C \qquad (99)$$

Where

the input and output terms represent sums of all input and

output terms, as given in Equations 100 and 101.

$$(QC)_{in} = \sum_{i=1}^{i=n} c_i q_i \qquad (100)$$

$$Q_{out} = \sum_{j=1}^{j=m} q_j \qquad (101)$$

Where q_i and q_j are individual input and output fluxes

c_i is the concentration in input flux q_i.

The solution to this first order differential Equation is given in Equation 102.

$$C = \left[1-\exp(-tQ_{out}/V)\right](QC)_{in}/VQ_{out} \qquad (102)$$

Where

t is the time.

This is the form of the simplest type of lake model, and is the most useful for the purposes of this study. Input terms include inputs by stream flow, surface run off, subsurface seepage and streams, and direct atmospheric inputs

to the surface of the lake. If the entire drainage basin collecting atmospheric inputs to the lake is considered all inputs can be considered as atmospheric inputs to the lake surface, atmospheric inputs to the surface of waters upstream of the lake, and atmospheric inputs to the land surface. Inputs to the lake from deposition onto upstream water surfaces must be related to lake inputs by relationships to account for constituent losses by sedimentation before reaching the lake. Inputs to the land surface of the basin must be related to inputs to the lake by relationships to account for constituent losses by uptake by the soil.

Loss terms include outputs by stream flow, subsurface seepage and streams, evaporative losses and sedimentation. Losses by water flux out of the lake includes stream flow, subsurface seepage and streams. Evaporative losses affect water only, tending to increase the concentration of pollution constituents in the lake water. Sedimentation losses are the net depositions of pollution constituents in lake water to the sediments at the bottom of the lake.

Input terms are a function of the surface area of the lake and the lake basin, while of the loss terms, the evaporative term is a function of surface area. Stream flow

losses are a function of constituent concentration in the water and stream outflow rate. For steady state conditions for water (no net gain or loss of water volume in the lake) stream outflow is equal to total water input, which is in turn dependent on the lake and lake basin surface areas. Sedimentation losses are directly proportional to constituent concentrations in the lake water, analogous to dry deposition by gravitational settling from the air.

3 - METHODS

An atmospheric dispersion model was developed to quantitatively describe the relationship between emissions at Sudbury and atmospheric chemistry, precipitation chemistry, and loading rates in the study area.

Measured atmospheric and precipitation chemistry and loading rate data are utilized to calibrate the model. The calibrated model was then utilized to make predictions of atmospheric chemistry, precipitation chemistry, and loading rates. Predictions were compared with measured data to evaluate the accuracy of the model.

A lake water and sediment chemistry model was developed to quantitatively describe the relationship between precipitation chemistry and lake chemistry. This model is linked directly to the atmospheric model.

The lake model is calibrated utilizing data from the literature. It was then utilized to make predictions of lake water and sediment chemistry.

Lake water and sediment analyses for lakes in the study area were made in order to evaluate the predictive accuracy of the lake model.

3.1 - Atmospheric Model

The basic type of model chosen as the basis of a predictive model for loadings in the Sudbury area was the Acres (1975) box model, modified by a Gaussian crosswind concentration distribution term. The Gaussian concentration term is related to the daily measured wind variabilities. To account for near-field loadings an expression for plume rise is incorporated. Chemical transform terms are included to account for the oxidation of sulphur dioxide to sulphate, with the subsequent production of hydrogen ion. Loss and scavenging terms for five metal particulates and four sulphur containing constituents are included. A term for continued production of hydrogen ion in the water of the rainfall receptor is included.

The model and model details are discussed under eight basic headings

- plume rise
- dispersion

- advection and dilution
- model type alternatives
- chemistry in the plume
- losses from the plume
- loading or deposition to rainfall receptors
- postdepositional chemistry

Figure 3 is a schematic flow diagram of the model, giving the various processes that affect the material from the source to the receptor. For calculation purposes, the Basic FORTRAN code structure of the Acres box model (Acres, 1975, 1977, 1980) was utilized (Appendix C). Subroutine and extensive code modifications were made to represent the mechanisms required for this study.

These can be summarized briefly as

Description	Source	Location
Atmospheric model	Box model, modified as required, Acres (1975)	Equation 13
Plume rise	Briggs (1969, 1970, 1972) Smith and Singer (1966) Turner (1969) Roth et al (1975) Modifications as required	Equation 24, 25, 26, 27 45, 63 Table 2 Section 4.1.1
Dispersion	Smith and Singer (1966) Roth et al (1975) Modifications as required	Table 9 Section 4.1.1

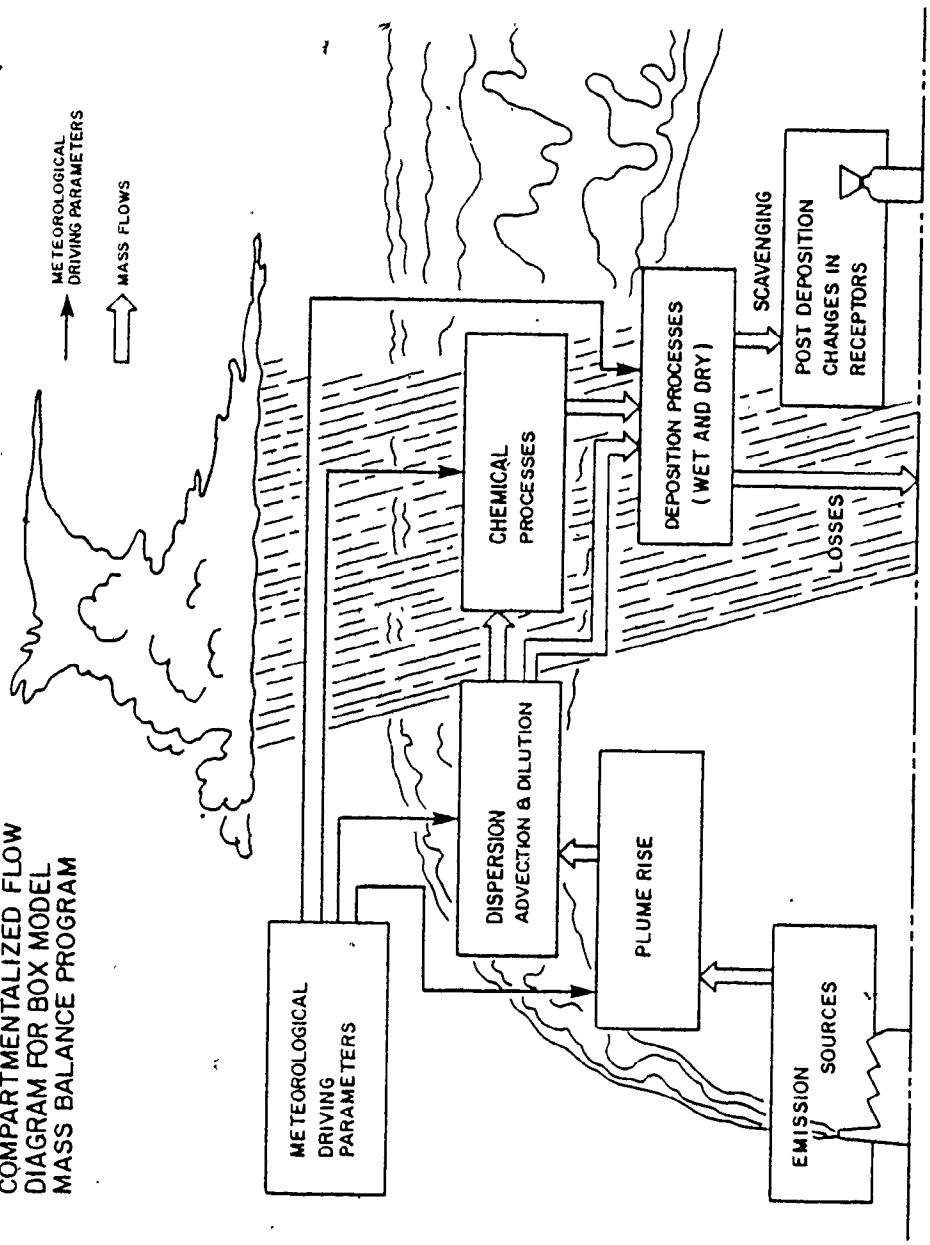

FIGURE 3
COMPARTMENTALIZED FLOW
DIAGRAM FOR BOX MODEL
MASS BALANCE PROGRAM

Description	Source	Location
Advection and dilution	Power law, box model, modification as required Acres (1975) Roth et al (1975)	Equation 13, 27, Table 7 Section 4.1.1
Gaussian crosswind concentration distribution	Modifications as required from Pasquill (1961) Gifford (1961)	Equation 7, 109
Chemistry - oxidation of SO_2	Modifications as required Dana et al (1973) Levy et al (1975) Lusis et al (1975)	Equation 68, 69 70, 72, 73, 74, 75, 76 Figure 5 Table 13
Mass transport to droplets, droplet evaporation	Modifications as required Dana et al (1973) Tverskoi (1962) Briggs (1969, 1970, 1972)	Equation 25, 45, 86, 87, 88
Deposition - dry	First order exponential Literature values, including Acres (1975) Chamberlain (1967) Stern (1976)	Equation 16, 17, 18, 79, 80, 82, 83 Table 16, 17, 18
Deposition - wet	Modifications as required from Engelmann (1965) Dana et al (1973) Marchello (1976) Mason and Berry (1968) Tverskoi (1962) Kinzer and Gunn (1949) Roth et al (1975)	Equation 79, 80, 82, 83, 84, 86, 87, 88, 97 Table 14, 15, 18 Section 4.1.1
Post - depositional chemistry	Modificaions as required from Levy et al (1975) Kramer (1973, 1975) Stumm and Morgan (1970)	Equation 152, 153 Appendix B

3.1.1 - Plume Rise

I have utilized Briggs' (1969, 1970, 1972) plume rise equations in the model. Briggs' equations produce the best description of real plumes from tall stacks (Dana et al, 1973). For vertical dispersion I have utilized Smith and Singer's (1966) expressions for slightly unstable atmospheric conditions. In the model, plume rise is limited by a seasonally determined mixing height. Based on Turners (1969) mixing heights for air mass types and seasons, I have derived an expression giving mixing heights on a monthly time scale.

As a true mixing height cannot be precisely defined, I have made provision for all model calculations to be repeated as required utilizing both minimum and maximum estimates of mixing height.

Minimum and maximum mixing heights are derived from the calculated mean mixing height by applying estimates of measurement accuracies as given in Roth et al, (1975). These equations and modifications can be summarized as follows.

Description	Source	Location
Plume rise	Briggs (1969, 1970 1972)	Equation 24, 25, 26, 45
Vertical dispersion	Smith and Singer (1966)	Equation 63
Mixing height	Modifications as required, based on Turner (1969)	Table 2
Range of mixing heights	Modifications as required, based on Roth et al (1975)	Section 4.1.1 Driving parameter treatment

The equation describing loft, or final plume rise in the model is Briggs' (1970) revised final rise formula (given in its basic form by Equation 45) for downwind distances greater than a critical distance dependent on heat output rates and stack height (given by Equations 26 and 27). For lesser distances downwind it is assumed that final height is not reached, and Equation 25 applies.

The plume rise formulas used are for rise under neutral and unstable conditions. The forms of the plume rise equations are those used by Dana et al, (1973). The expression used for less than critical downwind distances is Equation 25, and the expression used for greater than critical downwind distances is Equation 45. The critical distance calculation is in a modified form derived from

Equations 26 and 27, as given in Equation 103.

$$x^* = 3.5C_bF_b^{5/8} \quad (103)$$

Where

x^* is the critical downwind distance

F_b is the bouyancy flux parameter

C_b is Briggs' constant

F_b, given in Equation 104, is in units of m^4/s^3

$$F_b = 3.7 \times 10^{-5}Q_h \quad (104)$$

This is a form of Equation 24 for the bouyancy parameter.

Where

Q_h is the heat emission rate of the stack in calories per second

C_b is a function of the potential temperature gradient (Equation 34) and the heat emission rate.

The values used in this study are those given by Dana et al, (1973)

C_b = 14 m for F_b less than 55 m^4/s^3 and

C_b = 34 m for F_b greater than 55 m^4/s^3.

The maximum height of pollutant constituent mixing is termed the mixing height. The mixing height utilized in the model is the maximum daily mixing height during each 24-hr period. Diurnal cycles of inversion (low-level inversion caused by the cooling of the surface at night and inversion breakup by insolation induced near-surface turbulence) are not considered in the model.

Conditions of stability and extreme stability or inversions are not considered in the model. Mixing heights are calculated as a function of frequency of occurence or air mass type and season, as given in Table 2. For this study, I developed a relationship of mixing height to month of the year as a smooth function, given by a least squares fit of sinusoidally transformed data from Turner (1969):

$$H_{maq} = 0.616 + 0.497\sin[(m_{nr}-4)-.524] \quad (105)$$

Where

H_{maq} is the mixing height in kilometres

m_{nr} is the month of the year

This expression produces 12 average values for the mixing height, with a range from a minimum of 0.700 kilometres in January to a maximum of 1.200 kilometres in July.

For the purpose of this model, the mixing height is considered to present an effective barrier to further plume rise. The top of the "box" of the box model (Equations 12 and 13) is given by the mixing height if the final plume rise exceeds the mixing height; by the final plume rise (Equation 45) if the downwind distance is greater than the critical distance and the final rise is less than the mixing height; and by the plume rise with downwind distance expression (Equation 25) if the downwind distance is less than the critical distance.

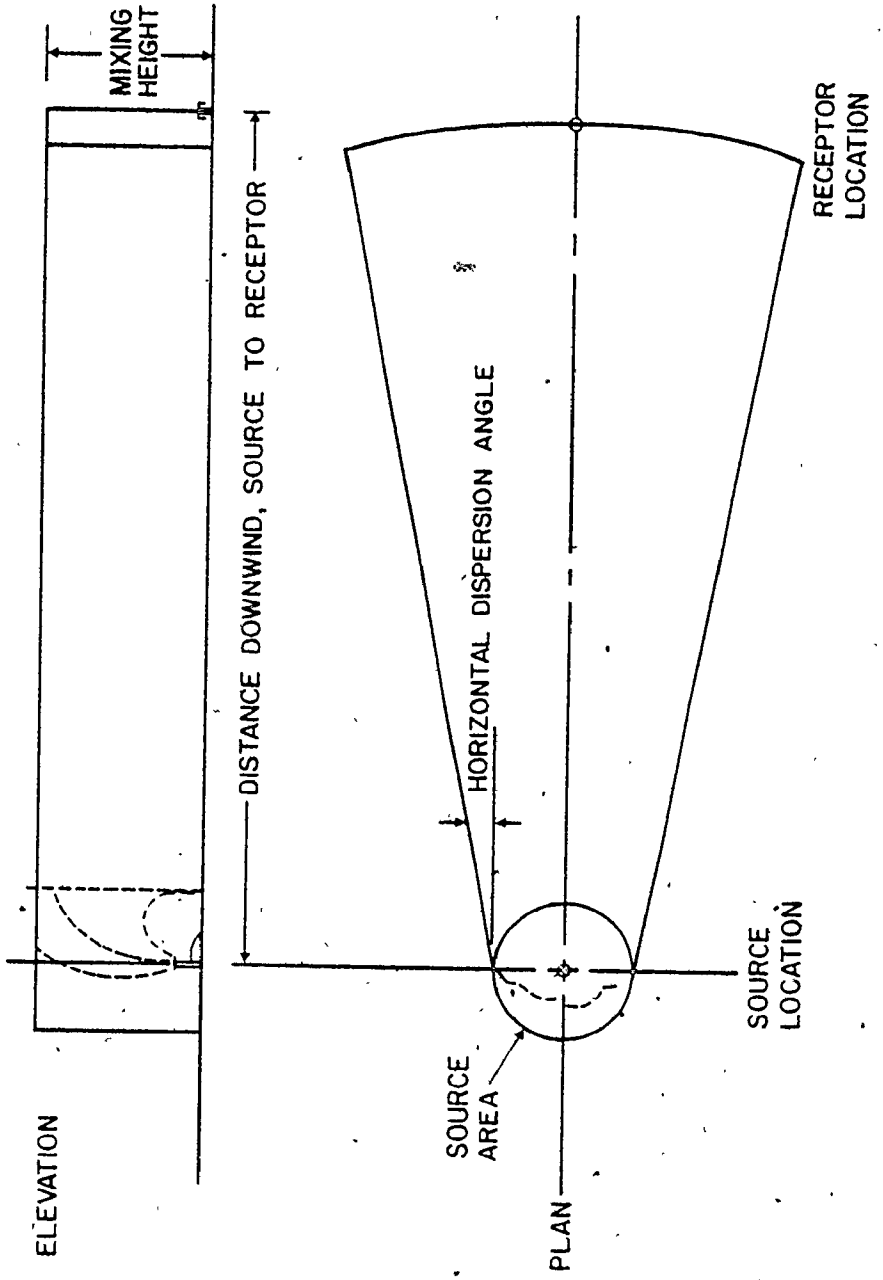

FIGURE 4
BOX MODEL DIMENSIONS

These expressions describe the plume vertical centreline with downwind distance and the vertical limitations of the plume according to the box concept. This is illustrated in Figure 4. In the basic box concept a uniform vertical concentration of the pollutant is assumed. In the modified box concept vertical dispersion from the centreline of the plume is assumed. Smith and Singer's (1966) expression for vertical dispersion under slightly unstable atmospheric conditions is used to describe the vertical extent of the plume due to vertical dispersion (Equation 63).

As the pollutant disperses upward and downward, and away from the plume centreline, it encounters both the mixing height and the ground plane. For the purposes of this model these are both considered to be perfect reflectors, as illustrated in Figures 1 and 2. Beyond this distance the effect of the sum of the reflected Gaussian terms is to produce a vertical concentration profile that rapidly approaches a uniform concentration between the ground and the mixing height. The distance downwind required for this effect is typically 5 to 10 times the mixing height, dependent on the wind speed

and plume rise. This distance is approximately half the distance from the smelter at Copper Cliff to the nearest rainfall receptor (6.6 kilometres) considered in this study. Hence, for the purposes of this study, plume rise, vertical dispersion and non-uniformity of the vertical pollution distribution at short distances downwind are of minor importance.

At shorter distances, the vertical extent of the plume is defined as follows. The top of the plume is defined as the stack height plus plume rise plus vertical dispersion, limited by the mixing height. The bottom of the plume is defined as the stack height plus plume rise minus vertical dispersion, limited by the ground plane. Between these vertical limits a uniform pollutant concentration is assumed.

3.1.2 - Dispersion

To adequately model horizontal dispersion, I have modified Smith and Singer's (1966) expression for horizontal dispersion (Table 9) by incorporating a factor describing the standard deviations of hourly wind heading over each 24-hr diurnal period. Standard deviation of the wind

heading is derived by standard statistical methods. (This is discussed in greater detail in Section 4.1.1, Driving Parameter Treatment.)

As the true dispersion angle cannot be precisely defined, I have made provision for all model calculations to be repeated as required utilizing minimum and maximum estimated dispersion angles. Minimum and maximum values are derived from the calculated mean dispersion angle by applying standard measurement accuracies (Roth et al, 1975).

These derivations can be summarized as follows.

Description	Source	Location
Horizontal dispersion	Modifications as required, based on Smith and Singer (1966)	Table 9 Section 4.1.1
Range of dispersion angles	Modifications as required, based on Roth et al (1975)	Section 4.1.1

In the box concept model the horizontal dispersion angle, which describes the width of the box (Figure 4), is related closely to daily weather statistics defined by wind speed

and direction variations during each 24-hr period. The relation used is given in Equation 106.

$$D_x = 0.3\ S_{dw} X^{0.86} \qquad (106)$$

Where

D_x is the box horizontal dispersion angle

X is the distance downwind

S_{dw} is the standard deviation of the hourly wind headings over the 24-hr day.

This equation is a form of Sutton's (1947, 1953) relation for horizontal diffusion coefficients given in Equation 52. The exponent is related to the power law wind velocity profile, as given in Equation 54. The values chosen for the constant are derived from Smith and Singer (1966), Equation 60 to 67 (Table 9).

In the box concept model the pollutant concentration is assumed to be constant across the width of the box, between the limits described by the horizontal dispersion

angle (Equation 13). Outside these limits the pollutant concentration is assumed to be zero. In the modified box model concept a Gaussian crosswind distribution of pollutant concentrations is assumed (Equation 11). The standard deviation term in the Gaussian distribution is equal to the horizontal dispersion angle of the box model concept. After integration over 360 degrees across the wind direction, this produces a total concentration of pollutant of approximately 92 percent of the total concentration given by the box concept.

3.1.3 - Advection and Dilution

In the box model, dilution of the pollutant is a function of average wind velocity and box dimensions (Acres, 1975).

To calculate wind velocity at the calculated centre-line of the plume, I have utilized the power law wind velocity profile utilizing exponents appropriated to the topography of the Sudbury area (DeMarris, 1959; Davenport, 1965).

As the wind velocity cannot be precisely defined, I have made provision for all model calculations to be

repeated as required utilizing minimum and maximum estimated wind velocities. I have derived minimum and maximum values from mean wind velocity by applying the calculated standard deviation of hourly wind velocities over each 24-hr diurnal period, and by the application of standard measurement accuracies (Roth et al, 1975).

These derivations can be summarized as follows.

Description	Source	Location
Dilution factor, box concept	Acres (1975) Slade (1967)	Equation 13
Average wind velocity	Power law	Equation 21 Table 7
Range of wind velocities	Modifications as required, based on statistical analysis of meteorological data and Roth et al (1975)	Section 4.1.1

The box height and width defined by vertical and horizontal dispersion have been discussed in the previous sections. The other important parameter is the advection term. This is a function equivalent to the length of the box. This term is a function of the average wind velocity during a 24-hr period.

The average wind velocity increases substantially with altitude. Therefore, the wind velocity, calculated by the power law velocity profile (Equation 21) at an altitude equal to half the plume height, was used to calculate the advection term. The form used is given in Equation 107.

$$U = U_s (H_k/0.018)^{\frac{1}{4}} \qquad (107)$$

Where

U_s is the surface wind velocity measured from a 10 metre meteorological tower

H_k is the plume height in kilometres

U is the wind velocity at half the plume height.

This midpoint is assumed to be roughly equivalent to the plume centreline altitude. The exponent value of 0.25 is a good median value for neutral conditions and the ground surface characteristics in the Sudbury area (DeMarris, 1959; Davenport, 1965).

The three relevant terms in the box concept; box height, width, and length, determine the dilution of the pollutant as it moves downwind from the source. This is given in Equation 108, the dilution factor:

$$D_{lf} = \frac{1}{(D_x + Y_c)UD_y} \qquad (108)$$

Where

D_{lf} is the dilution factor

D_x is the horizontal dispersion angle (Equation 106)

U is the wind velocity at plume centreline height (Equation 107)

D_y is the vertical extent of the plume, equivalent to the box height

Y_c is the source area diameter.

This diameter is twice the approximate downwind distance required for the attainment of a uniform vertical pollutant concentration between the ground and the mixing height.

Multiplication of D_{lf} by the pollutant emission rate, and an appropriate constant for units of measurement used, gives the box model pollutant concentration.

This dilution is a consequence of the conservation of mass and the defined shape of the box. As the pollutant is swept downwind through the box, its concentration is inversely proportional to the cross-sectional area of the box and the wind velocity.

3.1.4 - Gaussian Crosswind Concentration Distribution

I have made provision for alternative modes of calculation. Calculations can be made utilizing the box model concept or utilizing a Gaussian crosswind pollutant distribution (Equation 7) (Pasquill, 1961; Gifford, 1961).

A Gaussian crosswind pollutant distribution is assumed with a uniform vertical concentration distribution; the pollutant concentration calculated by the box concept (Equation 108) is multiplied by a Gaussian concentration distribution factor, as given in Equation 109.

$$F_{gc} = 0.398\exp -\tfrac{1}{2}\frac{A_x^2 X^2}{(D_x + Y_c)^2} \qquad (109)$$

Where

D_x and Y_c are as defined for Equation 99, the dilution factor. Together these terms define the standard deviation term of the Gaussian distribution.

A_x is the angle, in radians, between the wind heading and the vector from the source to the receptor.

X is the source to receptor distance.

Hence, these two terms together describe the distance of the receptor away from the average plume centreline.

As an option to be used when testing the sensitivity of the model to changes in deposition and oxidation parameters, calculations may be made without utilizing the Gaussian crosswind distribution.

3.1.5 - Chemistry

I have assumed that there are five main pollutant species of concern emitted by the Sudbury smelters. These

are copper, nickel, sulphur dioxide, sulphate, and hydrogen ion. I have assumed that copper and nickel from the smelters are in relatively inert forms. The chemical reactions of trace metals in the atmosphere is not considered in this study.

From the Sudbury stacks the only species emitted in significant amounts is sulphur dioxide. This is oxidized in the atmosphere to yield a mixture containing sulphate ion, hydrogen ion, and unoxidized sulphur dioxide.

To effectively model the production of sulphate and hydrogen ion from sulphur dioxide emissions, I have assumed a first order oxidation reaction (Dana et al, 1973). This is modified by utilizing gas phase and wet phase oxidation rates. These rates decrease exponentially with plume age to a fixed minimum oxidation rate, as derived from Sudbury plume data (Lusis et al, 1975).

I have incorporated terms for the effects of hydrogen and sulphate ion atmospheric background levels, the effects of sulphuric acid emissions, and the activity of atmospheric background ammonia concentrations as a

sink for hydrogen ions (Levy et al, 1975). No attempt was made to model atmospheric nitrogen chemistry.

The majority of the oxidation of sulphur dioxide takes place in the liquid phase, therefore I have incorporated an overall mass transfer term for the solution of sulphur dioxide in suspended cloud droplets (Dana et al, 1973). The required droplet parameters are derived from the cloud physics literature (Tverskoi, 1962).

I have assumed that the rate of production of dry sulphate particulates would be proportional to the rate of evaporation of cloud droplets, which was derived as a function of the difference in temperature of the plume over the ambient atmospheric temperature. As this is also the driving buoyancy force of plume rise, the evaporation rate was made directly proportional to the derivative of the plume rise (Briggs, 1969, 1970, 1972).

These derivations and modifications can be summarized as follows.

Description	Source	Location
Oxidation process	Dana et al (1973) Levy et al (1975)	Equation 68, 69, 70, 72, 73, 74, 75, 76
Oxidation rates	Modifications as required Lusis et al (1975)	Figure 5 Table 13
Mass transport rates, cloud droplet statistics	Modifications as required Dana et al (1973) Tverskoi (1962)	Equation 86, 87, 88
Evaporation rates	Modifications as required Briggs (1969, 1970, 1972)	Equation 25, 45

The model considers chemical changes in the sulphur species system only. It is assumed that the metal particulates present in the plume are not chemically modified in the atmosphere. Emissions of oxides of nitrogen from the Sudbury area smelters are negligible, therefore, nitrogen chemistry is not considered in the model. The process considered is the oxidation of sulphur dioxide to sulphate in the atmosphere, with the consequent production of hydrogen ion (Equations 68, 69, 70, 72, 73, 74, 75, 76). The reaction is assumed to be a first order reaction (Dana et al, 1973), as given in Equation 110.

$$C_1 = 1.5C_0\{1 - \exp[-T(R_1 + R_3)]\} \quad (110)$$

Where

C_0 is the original concentration of sulphur dioxide in $\mu g/cm^3$

C_1 is the concentration of sulphate ion in the same units

T is the time, or plume age, in hours

R_1 and R_3 are the oxidation rates, in hr^{-1}, for two major oxidation pathways. The numeric constant corrects for the mass difference between sulphur dioxide and sulphate ion.

R_1 is descriptive of the oxidation rate for sulphur dioxide in solution in droplets. Values for R_1 are given in Equations 111 and 112.

$$R_1 = 10^{(-1.45-0.45T)} \quad \text{for T less than 2 hours} \quad (111)$$

$$R_1 = 0.5 \times 10^{-4} \quad \text{for T greater than 2 hours} \quad (112)$$

Equation 111 is a least squares best fit curve to exponentially transformed oxidation rate data from Lusis et al, (1975). Beyond 2 hours the average oxidation rate can be described by a low, constant value, as given by Equation 112. Equation 111, and the data points from which the relationship is derived, are plotted in Figure 5.

R_3 is the oxidation rate for homogeneous gas phase photooxidation equal to approximately 25 percent of the liquid phase oxidation rate (Penzhorn et al, 1974).

If equation 110 gives the amount of sulphate produced by oxidation, the remaining unoxidized sulphur dioxide is given in Equation 113.

$$C_{1R} = C_0 \exp -T(R_1 + R_3) \qquad (113)$$

Where

C_{1R} is the concentration of sulphur dioxide remaining after oxidation. Other parameters are as defined for Equation 110.

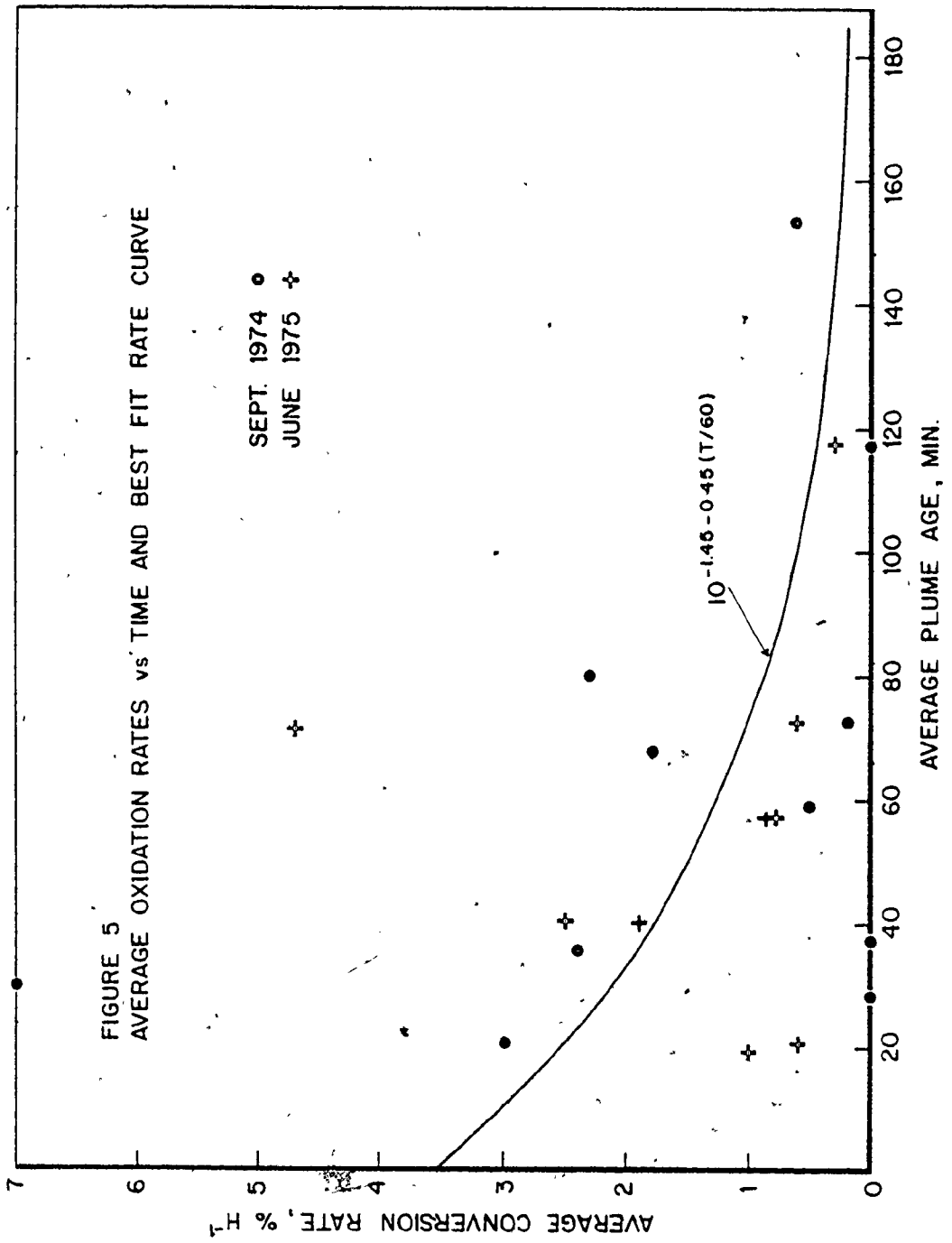
FIGURE 5
AVERAGE OXIDATION RATES vs TIME AND BEST FIT RATE CURVE
SEPT. 1974 •
JUNE 1975 +
$10^{-1.45-0.45(T/60)}$
AVERAGE CONVERSION RATE, % H^{-1}
AVERAGE PLUME AGE, MIN.
0
1
2
3
4
5
6
7
20
40
60
80
100
120
140
160
180

A product of the oxidation of sulphur dioxide, in the presence of water, is hydrogen ion. Hydrogen ion concentrations are given in Equation 114.

$$C_H = (C_1 + C_E)10^{-3}/48 + C_{ha} - C_{NH_4}10^{-3}/18 \qquad (114)$$

Where

C_H is the hydrogen ion concentration in droplets, in equivalents per liter

C_1 is the sulphate ion generated by oxidation, in $\mu g/cm^3$

C_E is the sulphuric acid emission of the smelters, in the same units

C_{ha} is the ambient atmospheric hydrogen ion concentration in equivalents per liter

C_{NH_4} is the atmospheric ambient concentration of ammonium ion NH_4^+, in $\mu g/cm^3$.

The numerical terms convert to equivalents.

The chief source of the hydrogen ion is the oxidation of sulphur dioxide, but the hydrogen ion concentration is increased by the hydrogen ion background level and the direct emission of sulphuric acid by the smelters. Ammonia, NH_3, hydrolyzes in the cloud droplets to form NH_4OH, which reacts with sulphate and hydrogen ions to form ammonium sulphate and water. Hence, ammonia acts as a sink for hydrogen ion.

As most of the oxidation takes place in the liquid phase, the availability of liquid water, and the rate at which the reacting species are dissolved in cloud droplets will influence the overall effective oxidation rate. Dana et al (1973) treats the overall mass transfer rate of sulphur dioxide into a droplet in detail (Equations 86, 87, 88). The availability of liquid water is a function of total water content, temperature, and atmospheric pressure. In the absence of this data for plumes from the Sudbury smelter stacks, standard figures from the literature are utilized. An average cloud droplet radius was assumed to be 5 μm, and the average liquid water content for a typical cloud was assumed to be approximately 1.0 gm/m^3 (Tverskoi, 1962). Then the average droplet population can be calculated to be approximately 550 droplets per cm^3.

Combining the overall mass transfer coefficient with values for droplet size and droplet density, the overall solution rate, E_{sr}, into the available liquid water can be derived (Dana et al, 1973),

$$E_{sr} = T_{ky} R_{dl}^2 N_{dl} \times 2.533 \times 10^8 \quad (115)$$

Where

E_{sr} is the solution rate in hr^{-1}

T_{ky} is the mass transfer coefficient

R_{dl} is the average droplet radius in centimetres

N_{dl} is the droplet density, or the equivalent number of average droplets per unit air volume

T_{ky} is equivalent to K_y (Equation 86), and has a value for cloud droplets of 0.0351 moles/cm^2/s

Values for k_x and k_y in Equation 86 were calculated with practical formulations of Equations 87 and 88, given in Equations 116 and 117 (Dana et al, 1973).

$$k_x = 0.2778D_{ex}/R \tag{116}$$

$$k_y = (1 + .3R_e^{\frac{1}{2}}S_c^{1/3})D_{ey}P/(82.057RT) \tag{117}$$

Where

k_x, k_y, D_{ex} and D_{ey} are as defined for Equations 87 and 88

R is the droplet radius in centimetres

P is the ambient air pressure in atmospheres

T is the temperature in degrees Kelvin

R_e is the Reynolds number

S_c is the Schmidt number for a falling drop.

Dana et al (1973) define R_e and S_c as;

$$R_e = -2RV_r/X_{nu} \tag{118}$$

$$S_c = S_{nu}/D_{ey} \tag{119}$$

Where

X_{nu} is the viscosity of the air

V_r is the terminal fall velocity of droplets, in cm/s (Equation 97).

In the calculation of T_{ky} standard values were assumed (Dana et al, 1973): H in Equation 86 equal to 1/18 gram moles/cm^3; D_{ey} equal to 9 x 10^{-6} cm^2/s; D^{ey} equal to 0.136 cm^2/s; P equal to 1.00; T equal to 330 K^o; X_{nu} equal to 0.0133 cm^2/s; and V_r equal to zero. Cloud droplets were assumed to have a negligible fall velocity.

The relative concentrations of dissolved (C_l) and gas phase (C_g) sulphur dioxide can then be described by

$$C_l = C_0[1-\exp(-TE_{sr})] \qquad (120)$$

$$C_g = C_0\exp(-TE_{sr}) \qquad (121)$$

Where

C_0 is the original sulphur dioxide concentration in the gas phase

C_l is the liquid phase concentration

C_g is the subsequent gas phase concentration

T is the time or plume age

E_{sr} is the total solution rate.

For two reasons the total solution rate E_{sr} is not the limiting factor in determining the effective overall oxidation rate.

- E_{sr} is much greater than R_1 and R_3

- The liquid water portion of the total water in the cloud is in a state of dynamic equilibrium with the water vapor in the cloud.

Although the relative proportion of liquid water to water vapor in the cloud may remain constant, determined by temperature and atmospheric pressure, individual droplets are always forming and growing while others are evaporating. While a static droplet, with a fixed volume, has a finite maximum capacity for sulphur dioxide or sulphate in solution, new droplets with negligible amounts of sulphur species contents are always available. Evaporating droplets leave their sulphate content behind as sulphate particulates.

For equilibrium, rates of evaporation must equal rates of condensation; this is assumed to be the case after the plume has risen to its maximum altitude. At this altitude the plume is in thermal equilibrium with the ambient atmosphere, so that bouyancy forces cease.

It is assumed that the approximate rate of evaporation of cloud droplets is proportional to the difference in temperature of the plume over the ambient atmospheric temperature. This temperature difference is the same factor that produces the bouyancy forces that cause the plume to rise. The evaporation rate is set equal to the rate of plume rise, or the derivative of Equations 25 and 45 for plume rise, as given in Equations 122 and 123:

$$E_{vp} = 1.6F^{1/3}/X^{1/3}, \text{ for X less than } X^* \quad (122)$$

$$E_{vp} = 1.6F^{1/3}(10H)^{2/3}/X, \text{ for X greater than } X^* \quad (123)$$

Where

E_{vp} is the evaporation rate in hr^{-1}, and the other parameters are as defined for Equations 25, 45, 94, and 97.

The relative concentrations of dissolved and particulate sulphate can then be described by Equations 124 and 125.

$$C_l = C_0 \exp(-TE_{vp}) \quad (124)$$

$$C_p = C_e + C_0[1-\exp(-TE_{vp})] \quad (125)$$

Where

C_l is the concentration of sulphate, in $\mu g/cm^3$ of air, in dissolved form

C_p is the concentration of particulate sulphate, in $\mu g/cm^3$

C_e is the concentration of particulate sulphate emitted by the smelter

C_0 is the original dissolved sulphate concentration

T is the time in hours

E_{vp} is the net evaporation rate in hr^{-1}, as calculated by Equations 122 and 123.

3.1.6 - Losses

I have assumed dry losses to be proportional to dry deposition velocities, atmospheric concentrations, and the vertical extent of the plume. The gaseous sulphur dioxide deposition velocity utilized is a median value from the literature (Tables 16 and 18) (Acres, 1975; McMahon, et al, 1978). Direct deposition of cloud droplets was assumed to be determined by Stokes law for sedimentation of particles, and on deposition velocities from Clough (1973), Chamberlain (1967), and Sehmel and Sutton (1974).

Deposition velocities for particulates were estimated from size and mass data, and applying the methods of the above noted authors (Clough, 1973; Chamberlain, 1967;

Sehmel and Sutton, 1974; Kramer, 1976; Stern, 1976). I have modified the dry deposition velocities with a wind velocity factor, to more effectively model increased deposition at higher wind speeds (based on Chamberlain, 1967).

I have utilized Engelmanns (1965) scavenging expression for the removal of sulphur dioxide from the atmosphere by falling raindrops. For the purposes of this research the scavenging expression is split into two coefficients, one for the absorption of gas phase sulphur dioxide into falling raindrops, and one for modeling the scavenging of sulphur dioxide dissolved in cloud droplets, by the collision of falling raindrops and cloud droplets. The gas phase mass absorption rate is calculated as in Dana et al, (1973), utilizing cloud droplet and raindrop size, mass and population density statistics from the meteorological literature (Tverskoi, 1962). Raindrop terminal fall velocities are calculated by the method of Gunn and Kinzer (1949).

Wet phase scavenging is a function of the population densities of cloud droplets and raindrops, and the fall velocities of raindrops. Effective cloud droplet

diameters are calculated by applying methodology from Marchello (1976).

Particulate washout rates are modeled by a method similar to the washout of cloud droplets by the impaction of falling raindrops. Particle effective diameters are derived from measurements at Sudbury (Kramer, 1976), and in the literature (Gatz, 1974, 1976; Cawse, 1974; Slinn and Hales, 1970). I have estimated particle densities (Mason and Berry, 1968) assuming that the particles consist of the most stable oxides and sulphides of the trace metals.

As rainfall intensity and duration cannot be precisely defined, I have made provisions for all model calculations to be repeated as required (Section 4.1.1, Driving Parameter Treatment) utilizing minimum and maximum rainfall durations and intensities. Maximum rainfall durations include trace rainfall indications. A trace rainfall indication is less than 0.1 mm recorded for a 6 hour measurement period. Minimum rainfall durations exclude trace rainfall indications. The range between

minimum and maximum rainfall intensities and durations is further expanded by applying standard measurement accuracies (Roth et al, 1975).

These can be summarized as follows.

Description	Source	Location
Dry and wet losses	First order exponential	Equation 79, 80
Dry deposition velocities	Derived from literature, including Acres (1975) Tverskoi (1962) Clough (1973) Chamberlain (1967) Sehmel and Sutton (1974), Stern (1976)	Tables 16, 17, 18
Wind speed effect	Modifications as required Chamberlain (1967)	Equation 82, 83
Rainfall scavenging losses	First order exponential	Equation 79, 80
Coefficient	Modifications as required Engelmann (1965) Mason and Berry (1968)	Equation 84 Tables 14, 15, 18
Gas phase coefficient	Modifications as required Dana et al (1973) Tverskoi (1962) Gunn and Kinzer (1949)	Equation 86, 87 88, 97

Description	Source	Location
Dissolved phase coefficient	Modifications as required Marchello (1976)	Equation 82, 83
Range of rainfall durations and intensities	Modifications as required; from meteorological data, Roth et al (1975)	Section 4.1.1

Losses are separated into dry and wet losses in the model. Dry depositional mechanisms considered are

- direct gas impingement, or the diffusion of sulphur dioxide to the surface and absorption

- deposition of dissolved sulphur dioxide and sulphates by the fall of droplets from the plume

- the sedimentation of sulphate and metal particulates.

Wet depositional processes considered parallel the dry depositional processes. These are

- the washout of gaseous sulphur dioxide by solution in falling raindrops

- the washout of sulphur dioxide and sulphate containing plume droplets by collision with falling raindrops

- the washout of sulphate and metal particulates by collision with falling raindrops.

For the purposes of this study, it is assumed that dry depositional processes are significant only during periods of no precipitation, and wet depositional processes are significant only during periods of precipitation. The total losses experienced by the plume are directly proportional to the concentration of the pollutant in the plume (Equation 80), so that a simple exponential expression derived from Equation 79 and given in Equation 126, describes these losses.

$$C_{(t)} = C_0 \exp(-k_w t_w - k_d t_d) \qquad (126)$$

Where

C_0 is the pollutant concentration before the calculation of losses by wet and dry depositional mechanisms

$C_{(t)}$ is the concentration after losses are calculated, at a plume age or travel time t

t_w is the length of time that a parcel of air travelling in the plume from the source to the receptor experiences precipitation. The plume age is the sum of t_w and t_d

t_d is the length of time the parcel experiences dry conditions enroute

k_w and k_d are the wet and dry depositional process rate constants.

The time parameters t, t_w and t_d are calculated from the travel distance or the distance from the source to the receptor, the component of the average wind velocity along the heading from the source to the receptor, and the hours of precipitation per day. The relationships are given in Equations 127, 128 and 129.

$$t = X/u_x \qquad (127)$$

$$t_w = tT_p/24 \qquad (128)$$

$$t_d = t + t_w \qquad (129)$$

Where

X is the source to receptor distance in kilometres

u_x is the wind component in the X direction, in kilometres per hour

T_p is the hours of precipitation during the 24 hours of the day. The time parameters are as previously defined (Equation 126).

The rate at which sulphur dioxide is lost from the plume by dry deposition is the result of two mechanisms

- diffusion of sulphur dioxide through the air, to leave the "box" at the mixing height

- by deposition at the ground plane.

Diffusion in the crosswind direction is already accounted for in the Gaussian crosswind concentration profile term.

At the surface of the earth, it is assumed that sulphur dioxide is absorbed by leaf surfaces, water surfaces, snow and other natural surfaces.

For this study, it is assumed that diffusion through the air is not the limiting mechanism for the direct loss of gaseous sulphur dioxide. If a uniform vertical sulphur dioxide concentration profile is assumed, deposition is a function of the deposition velocity (Table 16), concentration, and an average "fall distance" parameter, as given in Equation 130.

$$F_{ldg} = \exp(-t_d k_{dg}/D_y) \qquad (130)$$

Where

F_{ldg} is the dry loss factor for gaseous sulphur dioxide

t_d is the dry deposition time (Equation 129)

D_y is the vertical extent of the plume

k_{dg} is the deposition velocity for sulphur dioxide.

The value chosen for k_{dg} is 1 cm/s, or .036 km/hr, (Acres 1975, 1977; Denison, et al, 1979).

By definition, the box model and the modified box model have no gaseous sulphur dioxide losses through the mixing height.

The effective dry deposition of sulphur species dissolved in cloud droplets is calculated by assuming an average droplet size of 5 μm (Tverskoi, 1962), and extrapolating a Stokes law-type of deposition velocity from figures in Clough (1973), Chamberlain, (1967), and Sehmel and Sutton (1974). These figures give deposition velocities as a function of particle sizes from 0.01 to 100 μm in diameter, for a variety of surfaces. For zero wind velocity, an effective deposition velocity of 0.081 cm/s was assumed.

Increasing wind velocities produce greater deposition velocities (Equations 82 and 83). Deposition velocity is an exponential function of the wind velocity (Chamberlain, 1967) as given in Equation 131.

$$F_{wd} = 10^{(0.065U)} \qquad (131)$$

Where

F_{wd} is the factor giving the increase in depositional velocity for an average wind velocity in the plume, U.

The effective dry deposition of sulphate and metal particulates is treated in the same manner as the cloud droplets. Table 19 below gives sizes and deposition velocities for sulphate and five metal particulates.

TABLE 19

Particulate size ranges observed at Sudbury and estimated depositional velocity ranges

Particulate Species	Equivalent Diameter min (mean) max (μm)	Depositional Velocities min (mean) max (cm/s)
Sulphate	1.0(1.10)1.2	.0023(.0083).0230
Copper	1.0(2.65)3.0	.0023(.0800).0950
Nickel	1.8(1.75)5.9	.0050(.0080).2000
Lead	(est. 0.38)	.0012(.0033).0130
Zinc	(est. 2.96)	.0050(.0074).0850
Iron	3.2(4.38)5.3	.0230(.0283).1300

Very limited particulate size and frequency spectrum data are available in the Sudbury area. The

diameter values in Table 19 (except for the estimates for zinc and lead) are from measurements made on two occasions and at three locations in Sudbury and the nearby town of Lively, Ontario. Samples were taken with a four stage impactor with a back-up filter (Kramer, 1975). Within the observed size ranges, mean effective particulate diameters which best fitted precipitation chemistry measurements were chosen.

Lead particulate diameters are estimated from published measurements for Riverside, California (Lundgren, 1970), Fairfax, Ohio (Lee and Patterson, 1969), and for Los Angeles, California (Robinson and Ludwig, 1967).

The diameter estimate used in Table 19 for zinc is based on the relative concentrations of suspended zinc, iron, and lead particulates in the atmosphere at 35 independent locations (Stern, 1976; USEPA, 1976). The basis of this estimate is the proposition that if two metal particulates have the same source, if their emission rates are known, and if both are chemically inert in the atmosphere, then their suspended populations will be proportional to the effectiveness of depositional processes

on these particulates. Diameter is assumed to be one major parameter determining deposition, and ratios of suspended atmospheric concentrations are related to ratios of particulate effective diameters. Iron and lead were chosen for comparison with suspended zinc concentrations because it is assumed that iron and zinc, and lead and zinc particulates in the atmosphere have some sources in common. Estimation for 35 sites formed a sufficient data base for an estimate of effective median zinc particulate diameter to be made.

Deposition velocities in this research were estimated from figures in Clough (1973), Chamberlain (1967), and Sehmel and Sutton (1974) which give deposition velocity versus particulate diameters for flat surfaces, grass, and water surfaces. The estimated deposition velocities are modified by a wind factor (Equation 131).

The dry loss factor for particulates and cloud droplets is calculated for the purposes of this study by an exponential expression derived from Equation 79, given in Equation 132.

$$F_{dd} = \exp(-0.036 t_d k_{dd} F_{wd} / D_y) \quad (132)$$

Where

F_{dd} is the dry loss factor for a particulate. There are seven different dry loss factors, one for each particulate species listed in Table 19 and one for cloud droplets

F_{wd} is the wind effect factor (Equation 131)

k_{dd} is the median deposition velocity from Table 19

As k_{dd} is in cm/s, t_d is in hours, and D_y is in kilometres, the conversion factor 0.036 is required.

The scavenging rate for sulphur dioxide gas includes two components

- absorption into falling raindrops

- the collision of falling raindrops with cloud droplets containing dissolved sulphur dioxide.

The scavenging rate relating the concentration of sulphur dioxide in the air (both gas phase and dissolved in suspended cloud droplets) to the concentration of sulphur dioxide in precipitation is derived from Kramer's (1975) use of Engelmann's (1965) scavenging expression (Equation 84) as given in Equation 133.

$$W_o = \exp(2.3026(-0.24 + 0.80\log_{10}J)) \qquad (133)$$

Where

W_o is the scavenging coefficient of sulphur dioxide in hr^{-1}

J is the rainfall intensity, or rainfall rate, in mm/hr

This expression is mathematically identical to Equation 84.

For the purposes of this study, the scavenging coefficient W_o is split up into a washout coefficient for gas phase sulphur dioxide and a washout coefficient for liquid phase sulphur dioxide, as given in Equations 134 and 135.

$$W_1 = (1-f_{cx})W_o \quad (134)$$

$$W_2 = f_{cx}W_o \quad (135)$$

Where

W_1 is the gas phase washout coefficient for sulphur dioxide

W_2 is the liquid phase washout coefficient

W_o is the overall sulphur dioxide washout coefficient

f_{cx} is the proportionality constant giving the relative importance of the two washout mechanisms.

The value of f_{cx} is calculated from theoretical considerations, as given in Equation 136.

$$f_{cx} = T_{kl}/(T_{kl} + T_{kg}) \quad (136)$$

Where

T_{kl} is the rate of accumulation of sulphur dioxide in a falling raindrop by the capture of suspended cloud droplets

T_{kg} is the rate of accumulation of sulphur dioxide by absorption from the gas phase.

Both T_{kl} and T_{kg} are in units of moles/cm^2/s.

The gas phase rate is calculated by a derivation of Equation 115, modified to calculate the accumulation rate for a single falling raindrop (rather than the accumulation rate for the suspended cloud droplets in a unit volume of air. The accumulation rate for a falling raindrop 300 μm in diameter is given in Equation 137.

$$T_{kg} = T_{kydp} R^2 \times 1094.4 \qquad (137)$$

Where

R is the raindrop radius. The value chosen for R is 150 μm, approximately the frequency median radius of a normal frequency distribution of raindrops (Tverskoi, 1962).

T_{kydp} is the overall mass transfer rate of sulphur dioxide gas into the drop, which is equivalent to k_y as calculated by Equation 86, and has a calculated value of 0.006 moles/cm^2/s.

T_{kg} is the sulphur dioxide accumulation rate for the drop.

T_{kydp} was calculated with formulae equivalent to Equations 116, 117, 118, and 119 (Dana et al, 1973). Values for the parameters are the same except for the raindrop radius of 150 μm instead of a cloud droplet radius of 5 μm, and a fall velocity V_r of 64.3 cm/s, calculated by Gunn and Kinzer's (1949) relationship (Equation 97).

While the raindrop is falling, and absorbing sulphur dioxide from the atmosphere through which it is travelling, it is also intersecting the suspended cloud droplets in a cylindrical volume of space with a diameter equal to the effective diameter of the raindrop plus droplet. This relationship for calculating T_{kl} is given in Equation 138.

$$T_{kl} = 0.4112R^3E^3N_{dl}(r + RE)^2 \qquad (138)$$

Where

R is the raindrop diameter

r is the suspended cloud droplet diameter

N_{dl} is the average number of cloud droplets per cm^3

E is a factor giving the effective diameter of the raindrop in collision with a cloud droplet (Marchello, 1976) as calculated by Equations 82 and 83.

Parameter values used to calculate E are as defined for Equation 83, with a particle density p_p of 1.000, a particle diameter d_p of 5 μm, and a relative velocity μ of 64.3 cm/s.

Then, analogous to Equation 130 for dry gas deposition, and Equation 132, for dry deposition of cloud droplets and particulates, washout factors for gas and liquid phase sulphur dioxide can be derived. These are given in Equations 139 and 140.

$$F_{wg} = \exp(-t_w W_1) \tag{139}$$

$$F_{wl} = \exp(-t_w W_2) \tag{140}$$

Where

F_{wg} and F_{wl} are gas phase and liquid phase washout factors

t_w is the rainfall event time (Equation 128)

W_1 and W_2 are the washout coefficients for the gas and the liquid phases (Equations 134 and 135).

Washout rates for particulates are related to the mass median diameters (Table 19) of the particulates (Gatz, 1976, 1974; Cawse, 1974; Slinn and Hales, 1970; Kramer, 1976). Particulate washout rates incorporated into the model are estimated by multiplying the sulphur dioxide washout rate, W_o (Equation 133) by the effective cross-sectional area ratio of the particulate compared to the effective median cloud droplet cross-sectional area. The ratios are calculated as given in Equation 141.

$$R_{tp} = (r_p/r_{dl})^2 (E_p/E_{dl}) \qquad (141)$$

Where

R_{tp} is the ratio of effective cross-sectional areas of a particulate to a cloud droplet, in collision with a raindrop

r_p and r_{dl} are the diameters of the particulate and of the cloud droplet, respectively

E_p and E_{dl} are the effective diameter factors for the particulate and the cloud droplet, respectively (Marchello, 1976)

E_{dl} is the same as E in Equation 138, for the collision of a typical raindrop and cloud droplet, and E_p is calculated by Equations 82 and 83, with appropriate diameters and densities for the five metal and the sulphate particulates.

Analogous to Equations 130, 132, 139, and 140, equations for dry and wet loss factors, washout factors for sulphate and metal particulates can be derived as given in Equation 142.

$$F_{wp} = \exp(-t_w W_o R_{tp}) \qquad (142)$$

Where

F_{wp} is the washout factor for the particulate. Six different washout factors are calculated; for sulphate, copper,

nickel, zinc, lead, and iron particulates

t_w is the rainfall event time as previously calculated (Equation 128)

W_o is the washout rate as defined in Equation 133

R_{tp} is the effective cross sectional area ratio, as defined by Equation 141.

Petrographic microscopy, transmission electron microscopy, and X-ray diffraction studies of the Sudbury particulate samples (Table 19) indicate only that they are generally amorphous (Kramer, 1976). The densities of the particulates are not known. Therefore, it was assumed that the particulates consisted of the most stable high temperature oxides and sulfides of the metals. Densities were estimated from Mason and Berry (1968), and are shown in Table 20.

TABLE 20

Estimated particulate densities

Particulate species	Density (gm/cm^3)
SO_4	1.10
Cu	4.00
Ni	4.68
Zn	4.09
Pb	6.21
Fe	4.50

3.1.7 - Scavenging

Losses and scavenging are two aspects of the same depositional mechanisms: losses act on a parcel of pollutant containing air during the time it requires to move downwind from the source to the receptor, and therefore can be described by an exponential relationship (Equations 79 and 80); scavenging acts upon a continuously renewed volume of air over the receptor, on a time scale chosen for convenient operation of the model, and can therefore be described by a linear relationship (Equation 81). For this study the model is operated on a 24-hr, or daily time scale. Therefore, in analogy to Equations 128 and 129, wet and dry scavenging times can be calculated by Equations 143 and 144.

$$t_{wd} = T_p \quad (143)$$

$$t_{dd} = 24 - t_{wd} \quad (144)$$

Where

t_{wd} the time during a 24 hour day that wet depositional mechanisms are active, is equal to the hours of precipitation

t_{dd} the time during which dry deposition mechanisms are active, is equal to the balance of the 24 hours in the day

Loadings to the receptor of each species are calculated separately. Loadings of sulphur dioxide due to scavenging of gaseous sulphur dioxide are calculated using equation 145.

$$L_{gs2} = 3600 C_{gs2} k_{dg} t_{dd} \quad (145)$$

Where

L_{gs2} is the loading rate in $\mu g/cm^2/day$

C_{gs2} is the atmospheric concentration of sulphur dioxide in gaseous form over the receptor, in $\mu g/cm^3$

t_{dd} is the dry deposition time in hours

k_{dg} is the deposition velocity for sulphur dioxide used for loss calculation (Equation 130) in cm/s, or 3,600 cm/hr.

Loadings of dissolved sulphur dioxide are calculated as the sum of wet and dry loadings of sulphur dioxide dissolved in cloud droplets, plus washout of gaseous sulphur dioxide, as given in Equation 146.

$$L_{ls2} = C_{ls2}(3600t_{dd}k_{dd} + 10^5 t_{wd}W_2 D_{ya}) + C_{gs2}(10^5 t_{wd}W_1 D_{ya}) \quad (146)$$

Where

L_{ls2} is the loading rate, in $\mu g/cm^2$/day of sulphur dioxide that reaches the receptor in dissolved form

C_{ls2} is the atmospheric concentration of sulphur dioxide, in $\mu g/cm^3$, that is in the dissolved form in cloud droplets

C_{gs2} is the atmospheric concentration of sulphur dioxide that is in the gaseous form, in $\mu g/cm^3$

D_{ya} is the vertical extent of the plume, in kilometres

t_{dd} and t_{wd} are the dry and wet deposition times as defined in Equations 143 and 144

W_1 and W_2 are the washout coefficients for gaseous and dissolved sulphur dioxide, described in Equations 134 and 135.

k_{dd} is the deposition velocity for sulphur dioxide dissolved in cloud droplets. The deposition velocity k_{dd} is 0.081 cm/s.

Sulphur dioxide reaches the receptor in the gaseous or the dissolved form, sulphate reaches the receptors in the dissolved form or as particulates. Sulphate that reaches the receptor in dissolved form is the sum of the washout of

droplets containing dissolved sulphate, the washout of sulphate particles, and the dry loadings of sulphate containing cloud droplets. This is given in Equation 147.

$$L_{ls4} = C_{ls4}(3{,}600 t_{dd} k_{dd} + 10^5 t_{wd} W_2 D_{ya}) + C_{ps4}(10^5 t_{wd} W_3 D_{ya}) \quad (147)$$

Where

L_{ls4} is the loading rate, in $\mu g/cm^2/day$, of sulphate that reaches in dissolved form

C_{ls4} is the atmospheric concentration of sulphate dissolved in cloud droplets, in $\mu g/cm^3$

C_{ps4} is the atmospheric concentration of sulphate in particulate form, in $\mu g/cm^3$

t_{dd}, k_{dd}, t_{wd}, W_2, D_{ya} are as defined in Equation 146.

W_3 is the washout coefficient for sulphate particulates, calculated using Equation 148.

$$W_3 = R_{tps4} W_o \qquad (148)$$

Where

W_3 is the calculated washout coefficient for sulphate particulates, in hr^{-1}

W_o is the overall washout coefficient, described by Equation 139

R_{tps4} is the ratio of effective cross-sectional areas of a sulphate particulate to a cloud droplet, calculated by Equations 141, 82, and 83 with the appropriate parameter values for sulphate (Tables 19 and 20).

The first term in both Equations 146 and 147 have the same overall scavenging factors, as this term describes the scavenging mechanisms acting upon cloud droplets, regardless of the chemical composition of the droplet solution. Hence, this first term also describes the wash-out of hydrogen ions, produced by the oxidation of sulphur dioxide to sulphate, as given in Equation 149.

$$L_H = C_H(3600 t_{dd} k_{dd} + 10^5 t_{wd} W_2 D_{ya}) \qquad (149)$$

Where

L_H is the loading rate of hydrogen ion, in $\mu g/cm^2/day$

C_H is the atmospheric concentration of hydrogen ions dissolved in cloud droplets.

The remaining five parameters in Equation 149 are as previously defined for Equations 146, 147, and 148.

Particulate sulphate reaches the receptor by dry fall, as calculated by Equation 150.

$$L_{ps4} = C_{ps4}(3600 t_{dd} k_{dp}) \quad (150)$$

Where

L_{ps4} is the loading rate for particulate sulphate reaching the receptor by dry deposition mechanisms, in $\mu g/cm^2$/day

C_{ps4} is the atmospheric concentration of particulate sulphate

t_{dd} is the dry fall time as previously defined (Equation 144)

k_{dp} is the deposition velocity of sulphate particulates, in cm/s (Table 19).

The droplet scavenging term (Equation 149) is the basis of the scavenging expressions giving the loading rates of the five metal particulates, as given in Equation 151.

$$L_m = C_m(3600 t_{dd} k_{dm} + 10^5 t_{wd} W_o R_{tpm} D_{ya}) \quad (151)$$

Where

L_m is the metal particulate loading rate, in $\mu g/cm^2/day$.

C_m is the atmospheric concentration of the metal particulate, in $\mu g/cm^3$

t_{dd}, t_{wd}, W_o, and D_{ya} are as previously defined.

k_{dm} is the deposition velocity, in cm/s, of the metal particulate (Table 19)

R_{tpm} is the ratio of effective cross-sectional areas of the metal particulate to a cloud droplet (Equations 141, 82, and 83), with the appropriate parameter values for each metal (Tables 19 and 20).

3.1.8 - Postdepositional Chemistry

Rainfall samples may remain in the sampler for long periods before collection and analysis. Discrepancies between atmospheric concentrations and measured pH and precipitation sulphate concentration indicate that oxidation of sulphur dioxide to sulphate continues in the sampler

after deposition. I have developed an algorithm to model the postdepositional changes in precipitation chemistry.

Oxidation is assumed to be described by a first order oxidation reaction, at a rate estimated from measured concentration (Kramer, 1973, 1975). Included in the algorithm are factors to model the reduction in hydrogen ion concentration due to absorption by clay and trace metal particulates (Stumm and Morgan, 1970; Kramer, 1973, 1975).

The above can be summarized as follows.

Description	Source	Location
Postdepositional chemistry-oxidation	First order reaction, Modifications as required Levy et al, (1975)	Equation 152
Oxidation rate	Estimated from measured data Kramer (1973, 1975)	Appendix B
Hydrogen ion absorption by particulates	Estimated from Kramer (1973, 1975) Stumm and Morgan (1970)	Equation 153 Appendix B
Hydrogen ion absorption by trace metal particulates	Stumm and Morgan (1970)	Equation 153

After the scavenged pollutants and rainfall are deposited in the rainfall receptor, they remain there for the duration of the sampling period. During this time, chemical activity may continue if the solution in the receptor is not in chemical equilibrium. The major chemical change in the receptor is a decrease in pH as the sulphur dioxide in the receptor continues to oxidize to form sulphate with the production of hydrogen ion. This continued increase in the hydrogen ion concentration in the sampler is calculated using Equation 152.

$$C_{Hr} = C_H + kC_{s2}(1-\exp(-t_s r_s)) - C_{ep} \qquad (152)$$

Where

C_{Hr} is the hydrogen ion concentration in the receptor at the end of the sampling period, in $\mu g/cm^3$

C_H is the precipitation average hydrogen ion concentration, in $\mu g/cm^3$

C_{s2} is the average sulphur dioxide content of the precipitation, in $\mu g/cm^3$ (equal to the total input of sulphur dioxide, contributions by both wet and dry depositional

mechanisms, in μg, divided by the total precipitation volume, in cm^3)

t_s is the sample period, in days

r_s is the oxidation rate.

The constant k, equal to 3.125×10^{-5}, is required to correct for the molecular weights of sulphur dioxide, sulphate and hydrogen ions. The term C_{ep} is the hydrogen ion absorption capacity of the particulates in the receptor solution, in equivalents/μg, as calculated using Equation 153.

$$C_{ep} = 1.62 \times 10^{-15} C_{pt} + 0.5 \times 10^{-15} \left(\sum_{1}^{5} C_{pmi}\right) \qquad (153)$$

Where

C_{ep} is the hydrogen ion absorption capacity of the particulates in the receptor, in equivalents per μg of particulate. It is assumed that the particulates in the sampler consist largely of clay particles from the soil. An ion absorption capacity of 0.162 meq/gm was estimated (Stumm and Morgan, 1970)

C_{pt} the particulate concentration, was estimated to be 8.3 $\mu g/cm^3$. This is an average figure for measurements over a five year study period (Kramer, 1973, 1975). It is assumed that metal particulates scavenged from the plume also exhibit surface absorbing capacities, therefore, a term for the hydrogen ion absorption capacity of metal particulates is included.

C_{pmi} is the concentration, in $\mu g/cm^3$, of metal particulates in the receptor.

Contributions from the five metals (copper, nickel, lead zinc, and iron) are summed, and an average ion absorption capacity of 0.05 meq/gm is estimated (Stumm and Morgan, 1970).

The oxidation rate of sulphur dioxide in the receptors is estimated by comparing measured and calculated pH and sulphate concentration measurement data. An oxidation rate, r_s, of 0.4068×10^{-5} day^{-1} is estimated.

3.2 - Lake Model

In order to model lake water concentrations and sediment concentrations, I have utilized a simple mass balance CSTR (continuously stirred reactor) lake model. The water balance includes atmospheric input from precipitation into the lake basin, as calculated by the atmospheric model (Section 3.1) and two output terms: streamflow, and evaporation from the lake basin. The water input to the lake by precipitation is assumed equal to water outputs by streamflow and evaporation. Hence, the flux of water through the lake can be determined. Evaporation rates are from the literature (Phillips and McCulloch, 1972).

The pollutant balance consists of an atmospheric input from wet and dry deposition rates into the lake basin, as calculated by the atmospheric loading model (Section 3.1), modified by drainage basin processes, and two loss terms: streamflow, and sedimentation. I have included background concentrations (due to sources other than atmospheric loadings from the Sudbury smelters) in the lake water (Bowen, 1966) (Table 21) and sediments (Huhn, 1974) (Table 22). I have made total atmospheric input to the lake a function of the relative proportions

of lake surface, land surface, and upstream water surface areas in the lake basin. Included are terms to model the absorption of pollutants in the soil of the lake basin and for sedimentation in the water bodies upstream of the lake (Huhn, 1974). Hence, lake inputs are equal to atmospheric inputs to the drainage basin minus absorption by soil in the basin and sedimentation in lakes upstream. Lake outputs are by streamflow and sedimentation. Input and loss terms are equated to determine the flux of pollutants through the lake, then pollutant concentration in the lake water can be determined utilizing the water flux through the lake.

Sediment concentrations are modeled by applying sedimentation rates based on measurements in Sudbury area lakes (Huhn, 1974) to calculated lake water concentrations.

FORTRAN code for the lake model subroutine of the computer program is given in Appendix D.

The above can be summarized briefly as follows.

Description	Source	Location
Lake model	Mass balance, CSTR	Equations 98, 99 100, 101, 102
Evaporation rate	Phillips and McCulloch (1972)	Equation 154
Atmospheric inputs basin factor	Estimated from surface areas, soil absorption, and sedimentation rates (Huhn, 1974)	Equation 159 Table 22
Water chemistry background concentrations	Bowen (1966)	Table 21
Sediment chemistry background concentrations	(Huhn, 1974)	Table 23

Calculated loading rates for rainfall receptors form the basis for estimating the pollutant concentrations in lake water and in lake sediments.

Only a very simple lake model is considered in this paper (Equations 98 through 102). The lake model consists of two mass balances: for water, and for pollutants. Separate mass balances are calculated for each pollutant. All inputs are considered to be from the atmosphere, and the three output terms considered are

- evaporation, affecting the water volume and tending to concentrate pollutants in the lake water

- stream outflow, carrying away pollutants and water at a concentration equal to the concentration in the lake as a whole

- sedimentation, affecting pollutant particulates in the water, tending to reduce pollutant concentrations.

Transformation terms are not considered: the pollutants are considered to be conservative, and chemical or physical changes are assumed to be negligible. Transport terms are not considered: the lake is treated as a continuously stirred reactor (CSTR), as defined previously.

For the water mass balance, a state of dynamic equilibrium is assumed, i.e. over the time scale of the model, there is no net change in lake volume. This implies that total water inputs are equal to total water outputs, as calculated using Equation 154.

$$Q_{wout} = Q_{win}(1-E_{vp}) \qquad (154)$$

Where

Q_{wout} is the streamflow output flux of water from the lake, in cm^3/day

Q_{win} is the precipitation influx of water, a function of the rainfall rate and the lake basin surface area, as calculated using Equation 155.

$$Q_{win} = 2.4 \times 10^{10} P_{rc} A_{lb} \quad (155)$$

Where

Q_{win} is the average precipitation water influx to the lake, in cm^3/day

P_{rc} is the average precipitation rate in mm/hr, calculated from the total precipitation over the sample period,

A_{lb} is the lake basin area, in km^2.

The term E_{vp} in Equation 154 is the evaporation rate. This term corrects for the percentage of the precipitation falling onto the lake basin that is returned

to the atmosphere by evaporation and transpiration from vegetation. The value used in this model is an average value for the Sudbury area, equal to 30 percent (Phillips and McCulloch, 1974).

Pollutant concentrations in the lake are not necessarily in dynamic equilibrium: for the parameters utilized in this study input rates are greater than output rates, so that accumulation occurs. As inputs are independent of lake water concentrations, but both streamflow and sedimentation outputs are dependent on pollutant concentrations in the lake water, the rate of increase in concentration can be described by an exponential expression, as illustrated by Equation 102.

In a practical form utilized in this study, Equation 93 is expanded to the expression given in Equation 156.

$$C = \{1-\exp[-t(Q_{wout} + Q_{sed})/V]Q_{pin}\}/(Q_{wout} + Q_{sed}) + C_{wo} \quad (156)$$

Where

C is the lake water concentration, in $\mu g/cm^3$

Q_{wout} is the streamflow output flux of water from the lake, in cm^3/day, as calculated by Equation 154

Q_{sed} is the output flux of pollutant by sedimentation, analogous to deposition from the atmosphere

Q_{pin} is the pollutant input flux from the atmosphere, in $\mu g/cm^3$

C_{wo} is the assumed background lake water pollutant concentration, from Bowen (1966), an average value for fresh waters outside the Sudbury area.

Concentrations used in this study are given in Table 21.

TABLE 21

Pollutant Background Levels in Lake Water (Bowen, 1966)

Species	SO_4 (mg/cm^3)	Cu (mg/m^3)	Ni (mg/m^3)	Pb (mg/m^3)	Zn (mg/m^3)	Fe (mg/m^3)
Concentration	3.70	0.50	0.25	0.25	2.00	9.00

Background concentrations of trace metals and sulphate are assumed to be due to material input processes other than atmospheric deposition from the Sudbury area smelter

sources during the modeling period. These include biogenic inputs and inputs due to erosion and solution of glacial till and bedrock in the lake basin.

The time parameter t, in days, is considered to be equal to the hydraulic detention time. The detention time is the time required to replace all the water in the lake, and if it is assumed that the pollutants do not reenter the lake water from the sediments, the water turnover time must be the limiting time for accumulation of pollutants in the lake water. The detention time is a function of the lake volume and the water input rate, as calculated using Equation 157.

$$\bar{t}_w = V/Q_{wout} \qquad (157)$$

Where

$\bar{t}_w$ is the water turnover, or detention time in days

V is the volume of the lake in cm^3

Q_{wout} is the water output rate, in cm^3/day, as calculated by Equation 154.

The volume is equal to the mean lake depth multiplied by the measured lake surface area. The mean depth is an estimate derived from measurements of the lake depth made at the point of sampling and along lines across the lake defined by the sampling locations and points of access along the shoreline.

The pollutant input rate, Q_{pin}, is a function of the average precipitation pollutant concentration, the average precipitation, and a "lake basin factor", as given in Equation 158.

$$Q_{pin} = Q_{win}{}^{B}{}_{fact}{}^{C}{}_{pp} \qquad (158)$$

Where

Q_{pin} is the pollutant input rate, in µg/day

Q_{win} is the water input rate, in cm^3/day

C_{pp} is the average pollutant concentration, in µg/cm^3, calculated from the total precipitation and pollutant loadings over the sample period.

The lake basin factor, B_{fact}, corrects for the absorption of pollutants in the soil and the sedimentation of pollutants in lakes and streams upstream of the lake under examination.

The lake basin factor is calculated from the relative areas of land and water cover in the drainage basin, given in Equation 159.

$$B_{fact} = (A_{ls} + F_{sed}A_{ul} + F_s (A_{lb}-A_{ul}-A_{ls}))/A_{lb} \quad (159)$$

Where

B_{fact} is the lake basin factor

A_{ls} is the lake surface area

A_{ul} is the upstream water surface total area

A_{lb} is the total lake basin surface area.

Therefore the first term in Equation 159 accounts for the proportion of the total deposition in the lake basin onto the lake surface, the second term accounts for the

proportion of total deposition onto upstream water surfaces, such as headwater lakes and ponds, and the third term accounts for the proportion of total deposition onto the dry land surfaces in the lake basin.

F_s is a factor to correct for the absorption of pollutants in the soil and vegetation of the drainage basin. This effect is not quantified for lake basins in the Sudbury area, therefore F_s is set equal to 1.00.

For small unbuffered lakes on the LaCloche mountain ridge this is not unreasonable, as these lakes have very small drainage basins, little drainage basin soil, and the bedrock is extremely weathering-resistant Lorraine quartzite. For the larger drainage basin lakes, this is unlikely to be an appropriate value. If F_s is set equal to 1.00 this implies that none of the pollutants entering the lake from the atmosphere are absorbed by the soil in the drainage basin.

F_{sed} is a factor to correct for the loss of pollutants by sedimentation in waters upstream of the lake.

It is assumed that sedimentation processes are the same in the lake under examination and in upstream bodies of water, therefore, F_{sed} can be estimated using Equation 160.

$$F_{sed} = 1 - Q_{sed}/Q_{pin} \quad (160)$$

Where

F_{sed} is the sedimentation factor

Q_{pin} is the pollutant input rate as calculated without B_{fact}

Q_{sed} is the output flux of pollutant by sedimentation

Q_{sed}, in cm^3/day, is calculated from the lake surface area and the rate of deposition of the pollutant, as given in Equation 161.

$$Q_{sed} = 1.369 \times 10^9 R_{sed} A_{ls} d \quad (161)$$

Where

Q_{sed} is the flux of pollutant leaving the lake due to sedimentation processes, equivalent to a flux of water containing a concentration C (Equation 156) of pollutant.

R_{sed} is the sedimentation rate of the pollutant, in yr^{-1},

A_{ls} is the lake surface area, in km^2

d is the depth of the lake, in m.

The sedimentation rates, R_{sed}, for copper, nickel, lead, zinc, and iron particulates are estimated from measured bulk sedimentation rates, equal to approximately 0.266 cm/yr, and trace metal concentrations in cores taken from the bottom sediments of Sudbury area lakes (Huhn, 1974).

The surface sediment trace metal concentrations are calculated by a relationship analogous to wet deposition loading rates from the air; total loadings of the trace metal for a unit time divided by the bulk sediment deposition in the same time, as given in Equation 162.

$$C_{sed} = .50CR_{sed}d/V_{db} + C_{so} \qquad (162)$$

Where

C_{sed} is the calculated trace metal concentration in the surface layer of sediment, in $\mu g/cm^3$

C is the calculated present (1976) trace metal concentration in the lake water, in $\mu g/cm^3$

d is the depth of the lake

V_{db} is the bulk sedimentation rate, in cm/yr

C_{so} is the background sediment trace metal concentration, in $\mu g/cm^3$.

The sedimentation rates or coefficients used in this thesis for the trace metals are given in Table 22.

TABLE 22

Average estimated trace metal sedimentation coefficients, yr^{-1}, for Sudbury area lakes

Species	Cu	Ni	Pb	Zn	Fe
Sedimentation Coefficients	0.042	0.049	0.025	0.023	0.047

These figures are calculated by assuming an average exponential increase in trace metal concentrations in the sediments, from background levels before the onset of smelting (1883 - 1885) in the Sudbury area, to the present (1976). These figures represent a best-fit exponential curve fitted to trace metal concentration data from cores taken from Sudbury area lakes (Huhn, 1974). If the bulk rate of sedimentation is known, then the average rate of concentration increase for the trace metals can be calculated (Huhn, 1974).

From relatively high trace metal concentrations at the sediment surface, concentrations decrease with depth into the sediment. At a depth which varies from core to core, typically from 10 to 30 centimetres, concentration decreases are no longer detectable. This is assumed to be the estimated background concentration.

C_{so} is the background sediment trace metal concentration, given in Table 23.

TABLE 23

Estimated average sediment trace metal background concentrations for Sudbury area lakes

Species	Cu	Ni	Pb	Zn	Fe
Background Concentration	15 $\mu g/cm^3$	25 $\mu g/cm^3$	10 $\mu g/cm^3$	50 $\mu g/cm^3$	2.5 percent

4 - RESULTS AND DISCUSSION

In this section the results of model simulations are compared to actual conditions, as indicated by measurements made in the field. Results and comparisons are made and discussed under two headings

- atmospheric model
- the lake model.

4.1 - Atmospheric Model

In order to carry out model calculations for a larger number of receptor sites and sampling periods, I have developed a computer program wherein all the required calculations and derivations are expressed in Fortran computer language (Appendix C).

The following sections discuss the application of this program to modeling concentrations and loadings in the study area under five headings

- driving parameter treatment
- driving parameters
- atmospheric model sensitivity analysis

- ambient atmospheric concentrations
- precipitation chemistry.

Driving parameter treatment includes descriptions of receptor and meteorological station locations and characteristics, the different schemes utilized for pre-processing the meteorological input parameters, and the utilization of meteorological statistics and standard measurement accuracies to derive minimum and maximum input driving parameters.

The driving parameter section includes descriptions in greater detail of the emission sources driving the model, meteorological statistics, and a description and discussion of measured precipitation chemistry utilized to calibrate the model.

The atmospheric model sensitivity analysis section discusses the relative importance of the different driving parameters in controlling calculated concentrations and loading rates.

In the ambient atmospheric concentrations and precipitation chemistry sections, the results of model calculations are illustrated and compared to measured data obtained in the field program and from the literature.

9.1.1 - Driving Parameter Treatment

In order to test the usefulness of the atmospheric model, calculated precipitation concentrations of sulphate, hydrogen ion, copper, nickel, lead, zinc and iron were compared to measured precipitation concentrations (Kramer, 1975). Measured values are available for approximately 50 receptor locations over a time span of approximately 5 years. Twenty-seven of these receptor sites were selected for calculation points in this study (Table 24, Figure 6). Selection was on the basis of continued record length; receptor sites with the most number of measurements having preference (Table 24). A further condition of choice was the distance from Sudbury; the most distant receptor sites were eliminated.

Measured precipitation chemistry values are on a time scale of roughly a one month sample period. The model is operated on a one day time scale, and each day's contribution is summed over the appropriate sample period.

The basic driving parameters depend on the wind heading, source and receptor locations. The locations of the sources and receptors are input to the model in terms of latitude and longitude.

FIGURE 6
SUDBURY AREA, SOURCES, METEOROLOGICAL STATIONS AND RECEPTOR LOCATIONS

Simple spherical geometry formulations are utilized in the model to translate the relative positions of the source and receptors into terms of distances in kilometres and heading angles from source to receptor in degrees counterclockwise, with due east corresponding to 0° (Table 24).

The angle between this heading vector and the wind heading is the parameter A_x in the Gaussian distribution (Equation 109). If the parameter A_x is greater than two standard deviations for a source/receptor pair, the contribution of the source to the receptor is set to zero, and the next receptor is considered. At this point in the program a test eliminates contributions that require more than 24 hours to reach the receptor. This test reduces calculated SO_4 concentrations by less than 3 percent, but reduces calculation time.

Driving weather parameters are input from five meteorological stations in and surrounding the study area (Table 25, Figure 6). The daily weather statistics for each station can be combined in the computer program in 6 different fashions.

- any one of the weather stations can be used as the sole source of driving weather parameters

- calculations can be made for each weather station, and the calculated outputs averaged
- driving weather parameters equal to the average of parameters for all the weather stations
- driving weather parameters equal to a weighted average, weighted by the inverse of the distances from the weather stations to the receptor
- a weighted average, weighted by the inverse of the distances squared
- the weather station closest to the receptor provides the driving weather parameters.

Of the six combining schemes available to the program, the scheme combining the weather parameters by calculating an average weighted by the inverse of the distances from the meteorological stations to the receptor produced the best correlations of measured to calculated sulphate, copper and nickel loading rates and concentrations (Appendix B). This is considered the standard scheme, and was utilized in the evaluation of the calculated values in this study.

Table 26 compares the effects of utilizing the alternative combining schemes of the calculated concentrations and loading rates of sulphate, copper, nickel,

iron, and the average of the seven pollutants, sulphate, hydrogen ion, copper, nickel, zinc, lead and iron. Ratios of average values for all receptor sites over all sampling periods for the alternative schemes are compared to average values for the standard combining scheme.

The scheme utilizing meteorological data from a single meteorological station only was examined for all five meteorological stations (Table 25) with results that varied from approximately +200 percent to -100 percent. Four of these meteorological stations roughly outline the limits of the study area (Figure 6). Only the results for the most centrally located and most representative meteorological station, Sudbury Airport (Table 25, Figure 6), are presented in Table 26.

Results calculated separately for each of the meteorological stations and averaged produced values varying from the standard scheme by approximately +50 percent to -50 percent. This scheme has the serious practical problem of requiring five times the calculation time of the other schemes. This scheme is very sensitive to anomalous weather parameter values measured at a single meteorological station.

TABLE 24

LOCATION OF PRECIPITATION RECEPTORS
WITH GEOGRAPHIC RELATIONSHIP TO
COPPER CLIFF AND AVAILABILITY OF DATA

Station No.	Name	Location Latitude °N	Longitude °W	Geographic Relation Distance km	Angle CCW from E=0.0	Data Availability Number of Sample Periods
2	Skead	46.667	80.750	24.95	28.25	28
3	Killarney	45.967	81.517	62.90	-118.89	28
4	Gore Bay	45.900	82.467	135.20	-150.63	35
5	Jamot	46.100	80.567	55.88	-46.24	29
6	Windy Lake	46.633	81.467	55.88	151.27	30
8	Mount Lake	46.667	82.733	130.77	169.38	28
9	Gogama	47.700	81.733	143.06	110.42	28
10	Temagami	47.067	79.783	115.93	34.32	32
11	Espanola	46.250	81.767	61.11	-156.36	33
12	Sudbury South	46.417	80.983	11.46	-31.28	29
13	Sault Ste. Marie	46.533	84.333	245.72	179.00	26
14	Chapleau	47.833	83.400	233.60	139.24	28
15	Wawa	48.017	84.717	329.92	147.38	24
16	Timmins	48.500	81.333	223.66	95.69	29
17	Kapuskasing	49.417	82.433	342.84	107.20	26
18	Sparrow Lake	45.800	78.050	227.12	-54.83	27
23	Lake St. Peter	45.300	75.033	267.18	-28.93	25
24	Lake Traverse	46.450	81.433	236.57	-14.04	25
25	Shawanaga	45.500	80.242	123.83	-57.18	12

Table 24 contd

Station No.	Name	Location Latitude °N	Longitude °W	Geographic Relation Distance km	Angle CCW from E=0.0	Data Availability Number of Sample Periods
26	Mattawa	46.317	78.700	167.66	-6.76	26
27	Hearst	49.70	83.667	407.90	118.20	22
28	Hornepayne	49.233	83.667	413.45	131.18	24
29	Powassan	46.083	79.350	143.52	-15.30	21
21	Marten River	46.733	79.817	96.24	19.96	15
32	Verner	46.433	80.117	71.09	-4.81	19
33	River Valley	46.583	80.167	66.19	10.37	12
34	Sudbury North	46.500	81.000	6.63	29.51	20

TABLE 25

Location of Five Meteorological Stations Utilized to Define Weather Parameters in the Sudbury Study Area

Station	Latitude ^{o}N	Longitude ^{o}W
Sault St. Marie	46.533	84.333
Sudbury Airport	46.616	80.800
Timmins	48.500	81.333
North Bay	46.333	79.433
Gore Bay	45.900	82.467

TABLE 26

A Comparison of Alternative Schemes for Handling Driving Meteorological Parameters from the Five Weather Stations Utililized. (Percent Change in Calculated Concentrations, Compared to the Standard Scheme*)

Scheme	Emission Pollutant Species				
	Sulphate	Copper	Nickel	Iron	Average
Sudbury met. Data Only	-58.9	-2.8	-6.7	-3.7	-34.2
Average of Five Met. Stations	+9.5	-2.8	+5.2	+3.1	+4.2
Closest Station	+92.5	+33.2	+149.6	+116.4	+81.8
Average Weighted by the Inverse Square of the Distance to the Receptor	+30.5	+17.7	+18.2	+6.2	+9.0

*The Standard Scheme, utilized for all other model calculations, is average weighted by inverse distances from meteorological stations to receptor.

In practical terms this indicates the importance of sensitivity to errors and to statistical variation in input weather parameters.

Both these schemes were examined and discarded as serious alternatives for combining the weather parameters. Those considered were

- the use of an unweighted average
- an average weighted by the inverse square of the distance from the receptor to the meteorological station and
- the determination of driving weather parameters by the meteorological station nearest to the receptor. This has the practical advantage of requiring less computer calculation time.

The scheme utilizing Sudbury Airport meteorological data only is included in the table (Table 26) for purposes of comparison. The average for the scheme utilizing Sudbury Airport meteorological data only yields calculated values ranging from approximately 2 percent to 60 percent below those calculated utilizing the standard scheme. These figures indicate that a single meteorological station may not effectively characterize the driving weather parameters over the entire study area (approximately 0.3×10^6 km^2).

An unweighted average of the five meteorological stations yielded figures that varied from those yielded by the standard scheme by less than 10 percent. This is the same order of magnitude as the measurement accuracy of the driving weather parameters (Roth et al, 1975) and is therefore not significant. At sites close to individual meteorological stations variations much larger (up to 250 percent) than the average were produced by this scheme. This supports the intuitive assumption that the closest stations would provide the most accurate estimate of weather parameters at a receptor. For these reasons the average weighted by inverse distance was developed to combine area average weather parameters with closest station weather parameters. This is the standard procedure.

The other two schemes examined are weighted averages with different weighting functions. The average difference in concentration and loading values obtained by utilizing a weighting factor equal to the inverse square of the distances between the meteorological stations and the receptor varied from results of the standard scheme by from less than 2 percent to approximately 30 percent. The largest variations noted were exhibited by the major emission species under examination which were sulphate, copper, and nickel. This indicates that this combining scheme over-

estimates the contribution to the driving weather parameters of the nearest meteorological station, and underestimates the relative importance of the other meteorological stations indicating weather conditions along the trajectory of the plume.

For the scheme in which the weather parameters are determined by the nearest meteorological station only, calculated values differed from those obtained by the standard scheme by between 30 percent and 150 percent. This scheme had the practical advantage of reducing computing time (by approximately 6 percent), but this advantage did not outweigh its disadvantages (smallest correlation with measured values of all the schemes examined).

In summary, the standard scheme (averages weighted by inverse distance) produces the best correlations with measured values; slightly smaller correlations are obtained with an unweighted average; the use of an inverse square of the distance weighted average decreases the degree of correlation significantly; and the utilization of a nearest station scheme decreases the degree of correlation still further (Table 26).

For all the combining schemes, hourly wind headings and velocities, as obtained from the Atmospheric Environment Service (1972, 1973, 1974), are input to a subroutine that converts the figures to hourly x-vector (east/west) and y-vector (north/south) wind velocity components for each meteorological station. The combining schemes are applied to the x- and y-vector components separately, to produce a set of x and y wind velocity component vectors for each receptor location.

For each location the wind statistics are calculated separately for the x and the y components of the hourly wind velocities. The combined wind velocity vectors are then converted to polar form (wind velocity and heading).

The standard deviation of the wind velocity, as utilized in the program to calculate maximum and minimum wind velocities, is calculated as the square root of the sum of the squares of the standard deviations of the x and y components of the wind velocity over 24 hours. The standard deviation of the wind heading, the driving parameter determining the box model dispersion angle, is calculated as the arctangent (inverse tangent) of the ratio of the y component over the x component of the standard deviation of the wind heading over 24 hours.

Three of the most critical weather parameters are the wind velocity, wind heading, and mixing height. Provision is made in the model to execute all calculations with minimum and maximum values of these parameters and hence obtain results representing minimum and maximum conditions. Minimum and maximum values are equal to the input driving weather parameter value minus or plus the measurement accuracy, respectively (Roth et al, 1975).

The wind velocity measurement accuracy utilized in this study is ±0.20 metres per second, and the angular measurement accuracy utilized is ±5 degrees (Roth et al, 1975). Wind velocities as input are further modified in the program so that sets of calculations are made with the wind velocity set equal to the wind velocity plus and minus the standard deviation of the wind velocity.

The mixing height is also split into a minimum and a maximum value, calculated by adding and subtracting a measurement accuracy of ±5 percent (approximately 25 to 75 metres) (Roth et al, 1975).

Rainfall duration is input as minimum and maximum values. Maximum rainfall durations include quarters (day divided into four six-hour quarters) for which trace (less

than 0.0025 millimetres in a six hour quarter) or larger amounts of precipitation fell. Minimum rainfall durations included only quarters during which precipitation exceeded trace amounts. In the calculation of total rainfall volumes and rainfall intensities (rainfall rate) trace precipitation indications were interpreted as equal to 0.00125 millimetres of precipitation.

Parameters that drive the calculation of concentrations and loading rates in the same direction are treated together as sets in calculation. Wind velocity and mixing height are paired, as an increase in either will decrease the calculated concentrations in precipitation.

Rainfall duration and rainfall intensity are paired, as increased rainfall and increased rainfall intensity both increase the scavenging of pollutants from the atmosphere.

Minimum and maximum input values, combined with measurement accuracies, produce 16 different sets of input parameters. The 16 input data sets are generated as a cross matrix of two sets of four input parameter conditions (maximums or minimums) each. The first set of four is composed of

- maximum wind velocity, minimum rain intensity and duration
- maximum wind velocity, maximum rain intensity and duration
- minimum wind velocity, minimum rain intensity and duration and
- minimum wind velocity, maximum rain intensity and duration.

The second set of four is composed of

- the previously calculated wind velocity plus a measurement accuracy of 0.2 metres per second, the mixing height plus 25 metres, and the dispersion angle plus 5 degrees
- wind velocity plus 0.2 metres per second, mixing height plus 25 metres, and dispersion angle minus 5 degrees
- wind velocity minus 0.2 metres per second, mixing height minus 25 metres, and dispersion angle plus 5 degrees and
- wind velocity minus 0.2 metres per second, mixing height minus 25 metres, and dispersion angle minus 5 degrees.

From these input values the program calculates 16 independent sets of values (concentrations and loading rates for each pollutant species) for each sampling period and receptor location. The program selects the maximum and the minimum value for each pollutant species in each of the 16 sets for each sampling period/receptor location combination. These maximum and minimum values are outputs of the program.

4.1.2 - Driving Parameters

Driving parameters for the model can be classified as atmospheric model driving parameters and lake model driving parameters. Atmospheric model driving parameters fall into four categories

- basic model parameters
- source parameters
- receptor parameters and
- weather parameters.

Basic model parameters include oxidation rates for the oxidation of sulphur dioxide to sulphate, both in the atmosphere and in the receptor, and particulate densities. These terms and the relevant chemical and physical constants are incorporated into the calculations in the program, as given by Chapter 3 - Methods.

Other basic parameters include particulate and gas deposition velocities; particulate, droplet and raindrop sizes; and atmospheric background concentrations of the relevant sulphur species, hydrogen ion, ammonia ion and total background particulates. These basic model parameters are read into the program. Values for these parameters are given in the previous section on methods (Tables 19 and 20).

Source parameters read in include all data required to locate each source and completely characterize its emissions. The parameters read are

- source latitude, degrees north
- source longitude, degrees west
- height of stack base above datum, metres
- rate of heat emission, cal/s
- rate of SO_2 emission, gm/day
- rate of SO_4 particulate emission, gm/day
- rate of H ion emission, gm/day
- rate of H_2SO_4 emission, gm/day
- rate of Cu particulate emission, gm/day
- rate of Ni particulate emission, gm/day
- rate of Pb particulate emission, gm/day
- rate of Zn particulate emission, gm/day
- rate of Fe particulate emission, gm/day
- stack height, kilometres
- effective source diameter, kilometres.

Values for these source parameters are estimated from measurements of smelter emissions, estimated from rainfall receptor chemistry and read from published topographic maps (Kramer, 1975, E.M.R., 1960, 1975a, 1975b, 1975c).

Sulphur dioxide emission rates for Copper Cliff in Table 27 are average values for ten emission measurements made in 1973 in the 381-metre INCO stack (Table 1). Emission rates for Falconbridge for pollutants other than sulphur dioxide are estimates from the proportions of sulphur dioxide emissions contributed by Copper Cliff and Falconbridge (Kramer, 1975). The proportions assumed for copper and nickel emissions from the two sources are equal to the proportions measured for sulphur dioxide.

Sulphur dioxide contributions from Espanola are estimates based on the measured ratios of sulphate concentrations measured in rainfall receptors in and near Espanola to concentrations measured in receptors near Copper Cliff and Falconbridge.

Zinc is not a smelter effluent in the Sudbury area. Zinc is examined primarily as a measure of urbanization and industrialization not directly associated with the smelters. It is geochemically a relatively abundant element, compared to the other trace metals (copper, nickel). It is a common component of electrical machinery (brass), paint, rubber tires, plastics, automobile die castings, squeeze tubes, and many other artifacts of industrial civilization. It is one of the most commonly used metals,

and quantities are emitted into the atmosphere by building construction, automobile traffic, and incineration of trash and garbage. Levels of zinc emissions can therefore be related to population, population growth, and urbanization. A rough estimate for urban emissions of zinc from the city of Sudbury was obtained by multiplying the current annual zinc consumption of Ontario by the ratio of the population of Sudbury to the population of Ontario, and correcting for background zinc levels by subtracting the average soil zinc content (INCO, 1971, Howard-white, 1963, U.S. Bureau of Mines, 1972, Bowen, 1966). This calculation is conservative, as it assumes that all zinc consumed is emitted to the atmosphere. As zinc is also a relatively abundant element in the soil it is also a measure of natural background processes, such as the reentrainment of surface dust.

Lead emissions are linked directly to urbanization, as street and highway traffic of gasoline powered vehicles is an important source of atmospheric lead in cities. Therefore lead was also examined as another measure of urbanization and industrialization.

A rough estimate of atmospheric lead emissions by vehicular traffic in Sudbury was calculated by assuming traffic flow rates from 200 to 1,000 vehicles per hour, at

average speeds of 40 and 80 kilometres per hour on streets and highways respectively, an average fuel consumption of 0.16 litres per kilometre, and an average gasoline lead content of 0.46 gm/litre, with an emission to the atmosphere of 75 percent of the gasoline lead content (Chamberlain, 1974). These figures indicate a lead emission rate of roughly 12 to 13.5 µg per metre of road length per second. For the same estimated range of traffic densities other workers have obtained figures of 8 to 10 µg per metre per second (Boray, 1970) and 20+ µg per metre per second (Atkins, 1969). Multiplying the lead emission rate per unit length of road by the estimated street and highway total length in the city of Sudbury produces a rough estimate of the city's total atmospheric lead emissions (Table 27). More recent literature indicates that the Sudbury smelters also emit significant quantities of lead. Lead emission rates are approximately 25 percent of the emission rates of nickel and copper (Conroy et al, 1978).

The model was tested by comparison of calculated and measured concentrations and loading rates. This was accomplished in a two-phase operation. Initially, program parameters were set by utilizing theoretical relationships or the latest available literature data.

In the choice of the most representative values for deposition mechanism coefficients, this procedure was used to produce ranges of parameter values. Therefore, a representative data set of measured precipitation chemistry concentration values was utilized (Table 28) to ascertain optimum values in these ranges. Parameter values within theoretically determined ranges were chosen to produce the best correlations of calculations and measured rainwater chemistry for this small sample data set. Once all parameters were set, the second phase consisted of comparing the measured and calculated rainfall chemistry for the entire available data set (three years of data from 27 rainfall receptors).

The test case for the model is driven by three sources, as illustrated by Table 27. These sources are also located by Figure 6, a map of the Sudbury study area showing sources, meteorological stations and receptor locations.

TABLE 27

EMISSION PARAMETERS FOR THE THREE DRIVING SOURCES FOR THE MODIFIED BOX MODEL

Source	Copper Cliff	Falconbridge	Espanola
lat	81.067	80.833	81.766
long	46.467	46.567	46.275
base, m	342.9	381.0	257.2
heat, cal/s	1.7×10^8	3.7×10^7	100.0
SO_2, gm/day	3.97×10^9	7.63×10^8	4.2×10^3
SO_4, gm/day	1.55×10^5	2.33×10^4	1.0
height, km	0.381	0.091	0.03
area, km	2.50	0.75	0.50
Cu, gm/day	1.56×10^6	3.50×10^5	0.0
Ni, gm/day	1.14×10^6	2.85×10^5	0.0
Pb, gm/day	64.4	1.33	0.0
Zn, gm/day	33.3	2.00	0.0
Fe, gm/day	5.46×10^6	2.73×10^6	0.0

TABLE 28

Measured Concentrations Utilized to Set Initial Model Parameters

Station Number & Name	Distance km	Measured Concentrations SO_4 10^{-6} gm/cm^3	pH	Cu 10^{-9} gm/cm^3	Ni	Pb	Zn	Fe
12 Sudbury S.	11.5	0.5	4.05	32.0	32.5	8.0	34.0	122.0
02 Skead	25	5.5	4.00	34.0	34.0	23.0	38.0	111.0
06 Windy Lk.	56	0.5	4.20	9.0	4.5	18.0	31.0	39.0
11 Espanola	61	7.0	4.29	5.0	4.5	11.0	36.0	110.0
04 Gore Bay	135	3.5	6.06	7.0	0.0	0.0	87.0	5.0
09 Gogama	143	0.5	4.21	17.0	10.5	18.0	75.0	147.0
16 Timmins	224	0.5	5.88	4.0	9.0	31.0	75.0	149.0
18 Sparrow Lk.	227	5.5	4.09	15.0	0.0	35.0	172.0	116.0
14 Chapleau	234	4.0	4.84	7.0	4.0	38.0	96.0	188.0
13 Sault St. Marie	246	0.5	4.46	8.0	3.0	28.0	70.0	82.0

Sampling period for these measured concentrations is 8/1/72-9/1/72

The receptor parameters relevant to the model are the latitude and longitude of the receptor. Receptor locations are listed in Table 24 (Kramer, 1975).

Driving weather parameters are measured at five meteorological stations, one near Sudbury, and the remaining four roughly defining the extent of the study area. Meteorological station locations are given in Figure 6 and in Table 25. Driving weather parameters read in on a per station daily basis are

- Atmospheric Environment Service Identification number
- date: year, month, and day
- rainfall, millimetres
- minimum and maximum, rainfall rate or intensity, millimetres per hour
- minimum and maximum, rainfall duration, hours
- indicators for thunderstorm, snow, or fog
- average wind speed, kilometres per hour
- average wind heading, degrees counterclockwise from east equals 0.0
- standard deviation of the wind heading over 24 hours, degrees
- standard deviation of the wind velocity over 24 hours, kilometres per hour

Average input driving parameter and related statistics are summarized briefly in Table 29.

TABLE 29

Average Driving Parameters
for 27 Precipitation Sites

Parameter	mean	std	min	max	std/range
number of sample periods	25.22	5.76	12	35	0.25
rain volume, L	4.94	0.73	3.27	6.44	0.23
distance[a], km	163.0	117.2	6.63	413.4	0.29
angle to wind[a] heading, deg	114.1°	96.9°	0.3°	177.2°	0.55
plume age at[a] receptor, hr	13.25	9.60	0.54	33.74	0.29
precipitation[a] event time, hr/day	0.85	0.71	0.13	2.20	0.34
rainfall rate, mm/hr	0.580	0.021	0.549	0.641	0.23
wind speed, km/hr	12.35	0.32	11.99	13.57	0.20
std-wind heading, deg	45.0°	0.3°	44.7°	45.9°	0.27
std wind speed	10.06	0.21	9.56	10.85	0.16
wind heading, deg	E2.8°N	2.7°	E1.9°S	E10.7°N	0.22

[a]std/range for these parameters is above the average std/range ratio

4.1.3 - Atmospheric Model Sensitivity Analysis

A sensitivity analysis was made on the primary meteorological, chemical, and depositional mechanism parameters controlling pollutant concentrations calculated by the model. The eight parameters examined for sensitivity were

- daily average angle of wind heading
- daily average standard deviation of the wind heading
- daily average wind speed
- daily average rainfall rate
- the sulphur dioxide to sulphate oxidation rates in the atmosphere and in the receptors
- particulate scavenging rates
- sulphur dioxide gas scavenging rates.

Sensitivity is a measure of the variation in the outputs of the model caused by a variation in the inputs.

For the purposes of this study sensitivity is quantified by the ratio of differences of outputs to input parameters, as calculated using Equation 163

$$S_p = \left[\frac{C_{+n} - C_{-n}}{P_o(1+n) - P_o(1-n)}\right] / [C_o/P_o] \qquad (163)$$

Where

S_p is the relative sensitivity

C_o is the calculated output concentration for the median value of the input parameter under examination

P_o is the median value of the input parameter

C_{+n} is the calculated output concentration when P_o is increased by a factor 1+n

C_{-n} is the calculated concentration when P_o is decreased by the factor 1-n

n is the magnitude of the variation.

If the magnitude of the variation n is small compared to 1.00, Equation 163 can be approximated by Equation 164.

$$S_p = (C_{+n} - C_{-n})/2nC_o \qquad (164)$$

In Equations 163 and 164 S_p is the relative sensitivity of the parameter.

In this analysis n is always equal to 0.1 or 10 percent and the simplified expression (Equation 164) was used to calculate relative sensitivities.

The results of this sensitivity analysis are summarized in Table 30.

TABLE 30

Air Model Sensitivity Analysis

Parameter	Average Relative Sensitivity, S_p
Daily average angle of wind heading to source to receptor vector	-0.151
Daily average wind speed	0.113
Daily average standard deviation of the wind heading	0.120
Daily average rainfall rate	0.400
Particulate dry deposition mechanism rates	-0.148
Sulphur dioxide gas deposition rates	0.130
Sulphur dioxide oxidation rate in the air	0.006
Sulphur dioxide oxidation rate in the precipitation receptors	-0.040

These figures are calculated by taking the mean relative sensitivity values obtained from analyses for all seven pollutant species (sulphate ion, hydrogen ion (pH), copper, nickel, lead, zinc, and iron).

The most sensitive parameter is the average rainfall rate; a 10 percent increase in rainfall rate produced a 5 percent increase in average pollutant concentrations in the receptors. A 10 percent decrease in the rainfall rate produced an approximately 3 percent decrease in receptor average pollutant concentrations. These figures indicate that wet deposition mechanisms are the major factor in the calculation of precipitation chemistry, and that loading at the receptor outweighs losses enroute (on a one day time scale). Second in sensitivity is the angle that the daily average wind makes to the line from the source to the receptor. As this angle increases, the atmospheric concentration of the pollutant describes a Gaussian distribution centered on the average wind heading. Increasing the angle of deviation by 10 percent reduces the pollutant concentration by an average 1.5 percent.

Increasing particulate dry deposition rates by 10 percent produces approximately a 1.5 percent reduction in receptor concentrations. This indicates that on the average particulate dry deposition mechanisms are efficient enough to remove the majority of the particulates before the receptor is reached. For sulphur dioxide gas deposition mechanisms a 10 percent increase in sulphur

dioxide gas deposition rates increases receptor sulphate concentrations by approximately 1.3 percent. Gas deposition mechanisms are relatively inefficient, as indicated by the large proportion of the sulphur dioxide in the plume that reaches the receptor. Hence, the relative plume travel time to receptor deposition time has a controlling effect on the overall relative sensitivity of the sulphur dioxide gas deposition rate. The daily average standard deviation of the wind heading is the controlling parameter in determining the dispersion angle of the box model or the standard deviation term in the Gaussian crosswind concentration gradient. For the set of weather conditions, source and receptor locations considered in this study, the relative sensitivity of this term is such that a 10 percent increase in the wind heading standard deviation produces approximately a 1.2 percent increase in calculated concentrations. The larger box dispersion angle produces a lower calculated concentration inside the limits of the box, but the box covers a larger number of receptors. For the Sudbury study area the increase in the number of receptors affected outweighs the decrease in concentration in the box, hence the positive relative sensitivity. This argument also applies to the Gaussian crosswind concentration distribution. An increase in the average wind speed of 10 percent produces

an average increase of approximately 1.1 percent in calculated concentrations. For the pattern of sources and receptors in the Sudbury study area the diluting effect of increased wind speed is outweighed by the increased distance travelled by the plume in the 24-hour calculation period. For travel times greater than 24 hours this is, in part, an artifact of the model, as the plume continues to travel downwind, but no correction is made in the calculations. A 10 percent increase in the atmospheric oxidation rate for the chemical decay of sulphur dioxide to sulphate produces a calculated concentration increase of approximately 0.1 percent. This indicates that sulphate is scavenged more efficiently than sulphur dioxide. The sulphur dioxide oxidation rate in the receptors exhibits a small negative relative sensitivity; a 10 percent increase in oxidation rate produces an approximate 0.4 percent decrease in calculated sulphate concentrations. This figure indicates the level of uncertainty in the calculations of relative sensitivity. The calculated sulphate concentration is the sum of the sulphur dioxide and sulphate in the receptor (for comparison with measured sulphur dioxide plus sulphate, measured as sulphate). Hence, a change in this parameter should not produce a change in calculated sulphate concentrations. The sensitivity of this parameter should be zero. This leads to the conclusion that an uncertainty of at least ±0.04 is incorporated in the average relative sensitivities (Table 30).

In summary, the daily average rainfall rate is the most sensitive model parameter analyzed, approximately 2.6 times as sensitive as the next most sensitive model parameter, particulate dry deposition rates. At the relatively long distances of travel utilized in testing the model (Figure 6, Tables 24 and 29) sulphur dioxide oxidation rates are the least sensitive model parameters analyzed, with relative sensitivities below significant levels. This indicates that most of the oxidation of SO_2 to SO_4 takes place relatively close to the source.

4.1.4 - Ambient Atmospheric Concentrations

As previously noted, it is assumed that sulphur dioxide, copper, nickel, and iron all have common sources, the smelter stacks. In addition, it is assumed that reentrained surface dust is a significant source of atmospheric iron and zinc. The urban Sudbury area is assumed to be a significant source of atmospheric lead and zinc.

These assumptions were tested by constructing a cross correlation matrix (Table 31) between the measured ambient air concentrations of sulphur dioxide, copper, nickel, lead, zinc, and iron (Ont. Min. Envr., 1973, 1974, 1975, and 1976). Eight significant positively correlated pairs were expected: sulphur dioxide and copper, sulphur dioxide and nickel, sulphur dioxide and iron, copper and nickel, copper and iron, nickel and iron, iron and zinc, and lead and zinc. All cross correlations were tested for significance at the 95 percent confidence level. Only nickel and sulphur dioxide exhibit a correlation significant at the 95 percent confidence level. A marginally significant pair in a cross correlation matrix is indicated if the absolute value of the correlation coefficient of the pair is equal to or greater than the average absolute value of coefficient of correlation for all the pairs in the cross correlation matrix.

TABLE 31

Cross Correlations Between Pollutant Species, for Measured Ambient Air Concentrations

Pollutant Species	SO_2[c]	Copper	Nickel	Lead	Zinc
Copper	-0.2411				
Nickel	0.9127[a]	-0.3198			
Lead[c]	-0.2390	-0.5065[b]	-0.2246		
Zinc	-0.3245	0.0436	-0.6195[b]	0.6760[b]	
Iron	0.1834	0.2295	0.2205	-0.6938[b]	-0.1779

[a]Significant at the 95 percent confidence level

[b]Correlations considered marginally significant if equal to or larger than the average cross correlation

[c]9 sites, except lead with 6 sites, and SO_2, with 13 sites

By this definition, five significant pairs were indicated, two with positive and three with negative correlations. The positive pairs were sulphur dioxide and nickel, and lead and zinc, indicating some common sources for the components in these pairs. The strongest correlation indicated is between sulphur dioxide and nickel. Copper and lead, nickel and zinc, and lead and iron pairs exhibited significant negative correlations, indicating different sources for the components in these pairs.

To summarize briefly, the results of the cross correlation matrix for measured atmospheric concentrations indicate that sulphur dioxide and nickel have sources in common, and lead and zinc have sources in common. The pairs copper and lead, nickel and zinc, and lead and iron do not appear to have sources in common. However, the lack of correlations significant to the 95 percent confidence level between sulphur dioxide and copper, and between copper and nickel, when it is known that these pollutants have sources in common, indicates that the measured atmospheric concentration data is inadequate for testing the model.

The location of the ambient atmospheric concentration sites are indicated on a map of the area within approximately 75 kilometres of Sudbury (Figure 7).

FIGURE 7

LOCATIONS OF SULPHUR DIOXIDE
MONITORING STATIONS IN THE SUDBURY AREA
(ONTARIO MINISTRY OF THE ENVIRONMENT)

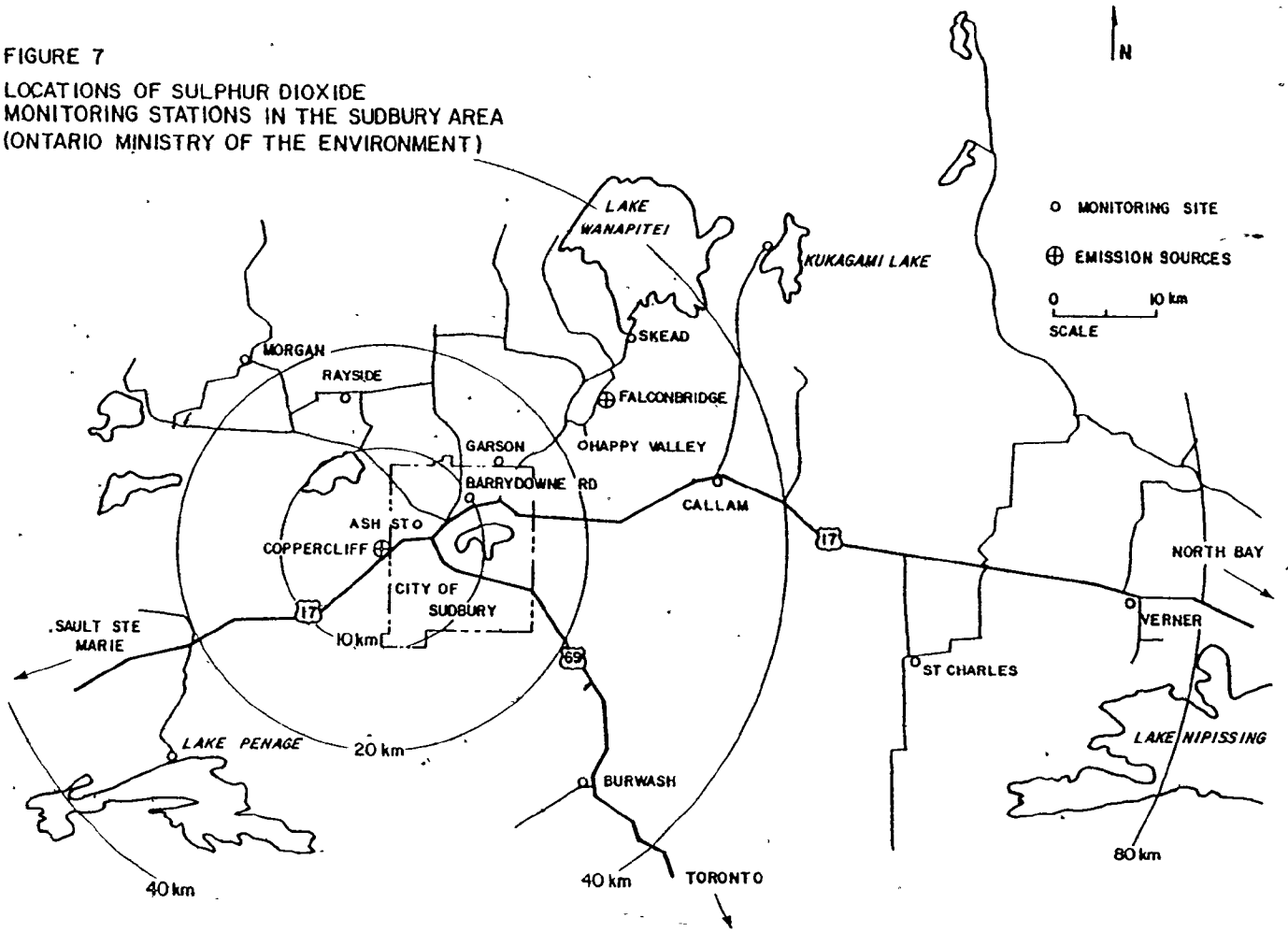

Table 32 is a comparative listing of the measured and calculated sulphur dioxide concentrations in zones at a range of distances from Copper Cliff and Table 33 is a comparison of measured and calculated ambient air concentrations of copper, nickel, lead, zinc, and iron in the same zones.

Calculated values are averages and standard deviations for from 12 to 29 calculation periods (Table 24, Appendix B). Measured trace metal values are averages and standard deviations for from 10 to 50 daily concentration measurements (Ont. Min. Envr., 1973, 1974, 1975, 1976).

As illustrated by Table 32, both measured and calculated sulphur dioxide concentrations decrease with increasing distance from the source. Both measured and calculated concentrations exhibit a large degree of scatter, which is increased close to the source. The coefficient of correlation of distance to the natural log of the measured sulphur dioxide and the nickel concentrations are significant at the 95 percent confidence level (Table 34). Logs of concentrations are used to calculate correlation coefficients because concentrations decrease exponentially with increasing distance.

TABLE 32

Comparison of Measured and Calculated Ambient Air Concentrations of Sulphur Dioxide, 10^{-9}gm/gm at STP, for 3 Years of Data at 19 Sites in the Sudbury Area

Distance from Copper Cliff (km)	Concentrations: means ± std. dev., and number of observations			
	Measured	Observations	Calculated	Observations
0-10	9.9±8.2	36	9.5±21.5	20
10-20	5.1±3.8	12	4.4±19.3	29
20-40	3.0±1.7	48	1.4± 6.0	28
40-80	3.0±1.1	24	1.4± 0.5	121

TABLE 33

Comparison of Measured and Calculated Trace Metal Ambient Air Concentrations, 10^{-9} gm/m^3, for 3 Years of Data at 15 Sites in the Sudbury Area

Distance from Copper Cliff (km)	Number of Observations Measured / Calculated	Concentrations: means ± std. dev. Copper Measured	Copper Calculated	Nickel Measured	Nickel Calculated	Iron Measured	Iron Calculated	Lead* Measured	Lead* Calculated	Zinc Measured	Zinc Calculated
0-10	36 / 20	539± 653	524±1170	198± 73	221±487	3017±1102	1783±1520	850±384	600±200	117±148	128±184
10-20	12 / 29	404± 623	320±1180	186± 46	131±480	1469± 954	1442±1290	---	700±100	110±320	81±137
20-40	48 / 28	293± 581	210± 859	65± 23	101±400	1380± 769	1085±2130	707±689	650±280	90±111	54± 38
40-80	24 / 121	42± 505	32± 160	19± 9	16± 75	1270± 499	932± 159	633± 58	410±310	81±198	49± 28

*Calculated for average meteorological conditions over 3-year study period with corrected lead emission rates

TABLE 34

Correlation Coefficients of Calculated to Measured Ambient Air Concentrations and Correlation Coefficients of Measured Ambient Air Concentrations to Distance from Source

Pollutant Species	Correlation Coefficients: Calc Conc/ Meas Conc	Log Meas Conc/ Distance
SO_2	0.7394[a]	-0.5174[a]
Copper	-0.1875	0.1783
Nickel	0.6095[a]	-0.5934[a]
Lead	-0.2663	-0.2927
Zinc	0.2951[b]	-0.1493
Iron	0.2526[b]	-0.2542

[a] significant at the 95 percent confidence level

[b] considered marginally significant if larger than the correlation with distance or the average correlation with distance for all six pollutant species

In Table 34 the correlation coefficients between measured and calculated concentrations are compared. Predicted values of sulphur dioxide and nickel exhibit correlations with measured data significant at the 95 percent confidence level. If the absolute value of the measured/calculated correlation coefficient is equal to or larger than the distance/log of measured correlation coefficient absolute value, or the average distance/ measured absolute value, then the measured calculated correlation is considered to be marginally significant. Table 34 indicates that the correlation of calculated values to measured values is better than the correlation of measured values to distance. Sulphur dioxide, copper, nickel, zinc, and iron exhibit marginally significant correlations between measured and calculated values. Calculated ambient atmospheric sulphur dioxide concentrations in the distance interval of from approximately 0 to 80 kilometres from Copper Cliff average approximately 70 percent of measured concentrations, ranging from approximately 95 percent of measured values within 10 kilometres of the smelters, to approximately 50 percent of measured values at distances of 40 to 80 kilometres.

Nickel and copper concentrations average approximately 80 to 85 percent of measured values. Copper

calculated concentrations range from 5 percent overcalculation at less than 10 kilometres to an approximately 75 percent undercalculation at distances of 40 to 80 kilometres. Nickel calculated concentrations are approximately 80 to 85 percent of measured values at distances between 0 and 80 kilometres.

Iron may be conservative, that is, measured atmospheric concentrations of iron do not decrease significantly with distance from the smelters. This may indicate that mechanisms supplying iron to the atmosphere are in equilibrium with loss processes rather than conservatism. Beyond approximately 10 kilometres, iron concentrations are not controlled by smelter emission rates. Over the distance interval of from 10 to 80 kilometres from Copper Cliff calculated iron concentrations are approximately 80 percent of measured values, ranging from 60 percent undercalculation at distances of 0 to 10 kilometres, to 35 percent undercalculation at distances of 40 to 80 kilometres. This indicates that the modified box model developed in this paper is capable of adequately modeling atmospheric concentrations of these pollutant species. For nickel, excellent predictions of atmospheric concentrations can be made.

Paired data were not available for all sites in zones in Tables 32 and 33. In order to construct Tables 31 and 34, missing data were estimated by linear regression techniques, and correlation coefficients were calculated from the series of given and estimated values.

4.1.5 - Precipitation Chemistry

Measured and calculated precipitation chemistry results are presented in tabular and graphic form.

Results in graphic form consist of comparative contour plots of measured and calculated concentrations and loading rates (Figures 8 through 20) and graphs expressing measured and calculated concentrations in precipitation to distance from the smelters (Figures 22 through 27).

Isopleth maps for comparison of measured and calculated precipitation concentrations and pollutant loading rates give the clearest visual indication of the adequacy of the modified box model (Figures 8 through 20). Calculated values, indicated by solid lines, are arithmetic means of minimum and maximum calculated values. In examining the loading and concentration isopleth maps it must be noted that the calculated isopleths do not

FIGURE 8
MEASURED AND CALCULATED PH

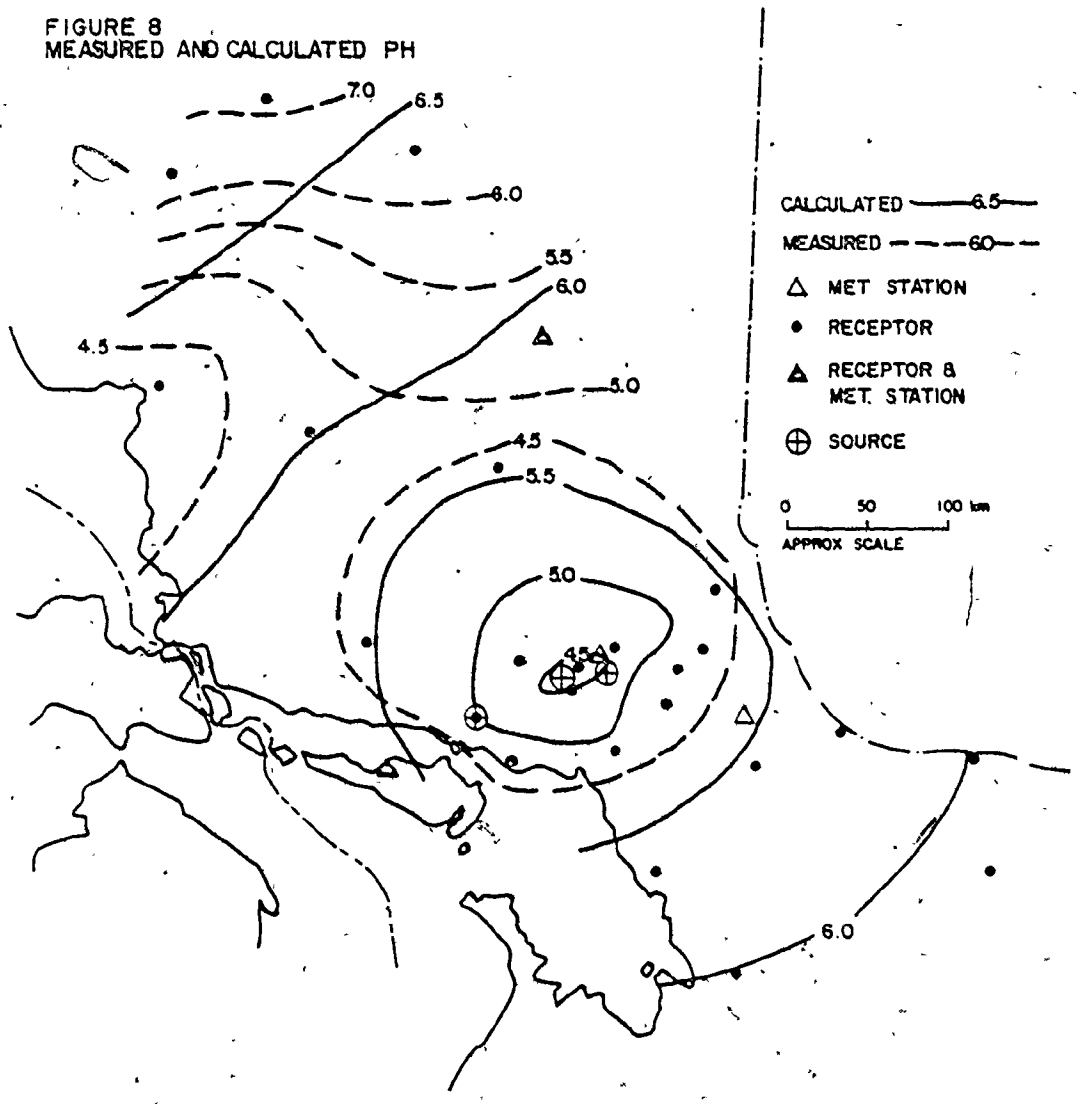

FIGURE 9
MEASURED AND CALCULATED $SO_4^=$ CONCENTRATIONS, 10×10^{-6} gm/cm^3

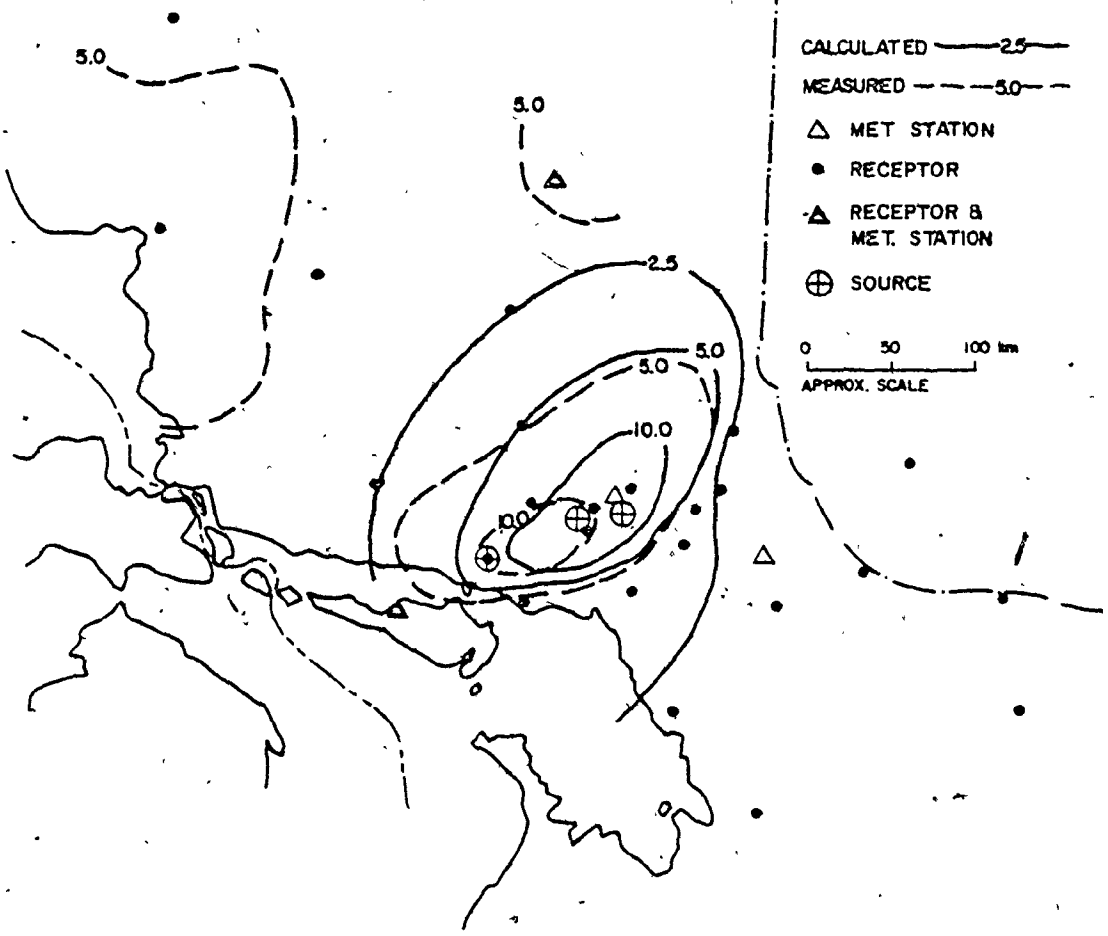

FIGURE 10
MEASURED AND
CALCULATED $SO_4^=$ LOADINGS, 10^{-9} x gm / cm^2 - DAY

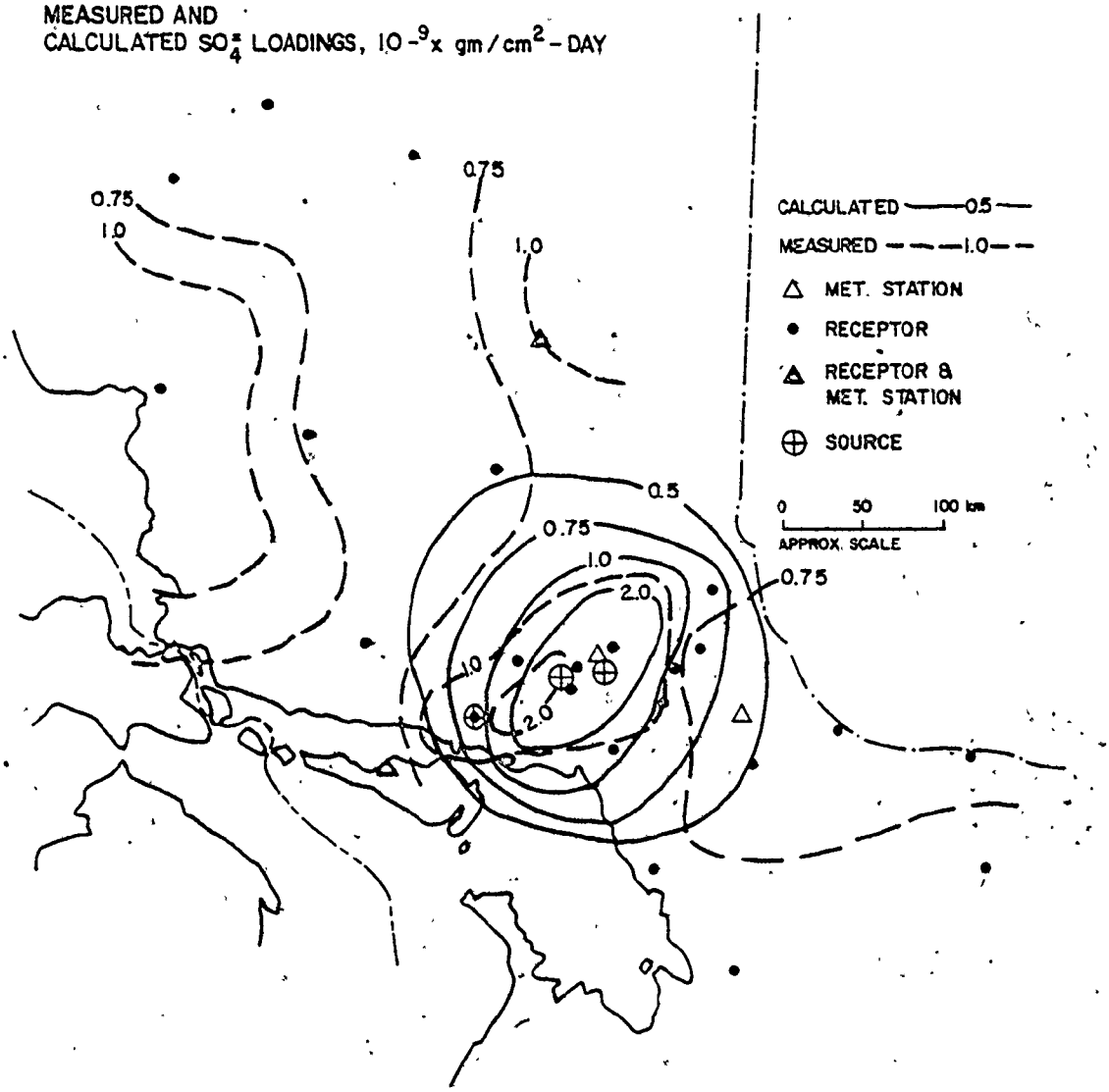

FIGURE 11
MEASURED AND
CALCULATED Cu CONCENTRATION, 10^{-9}x gm/cm^3

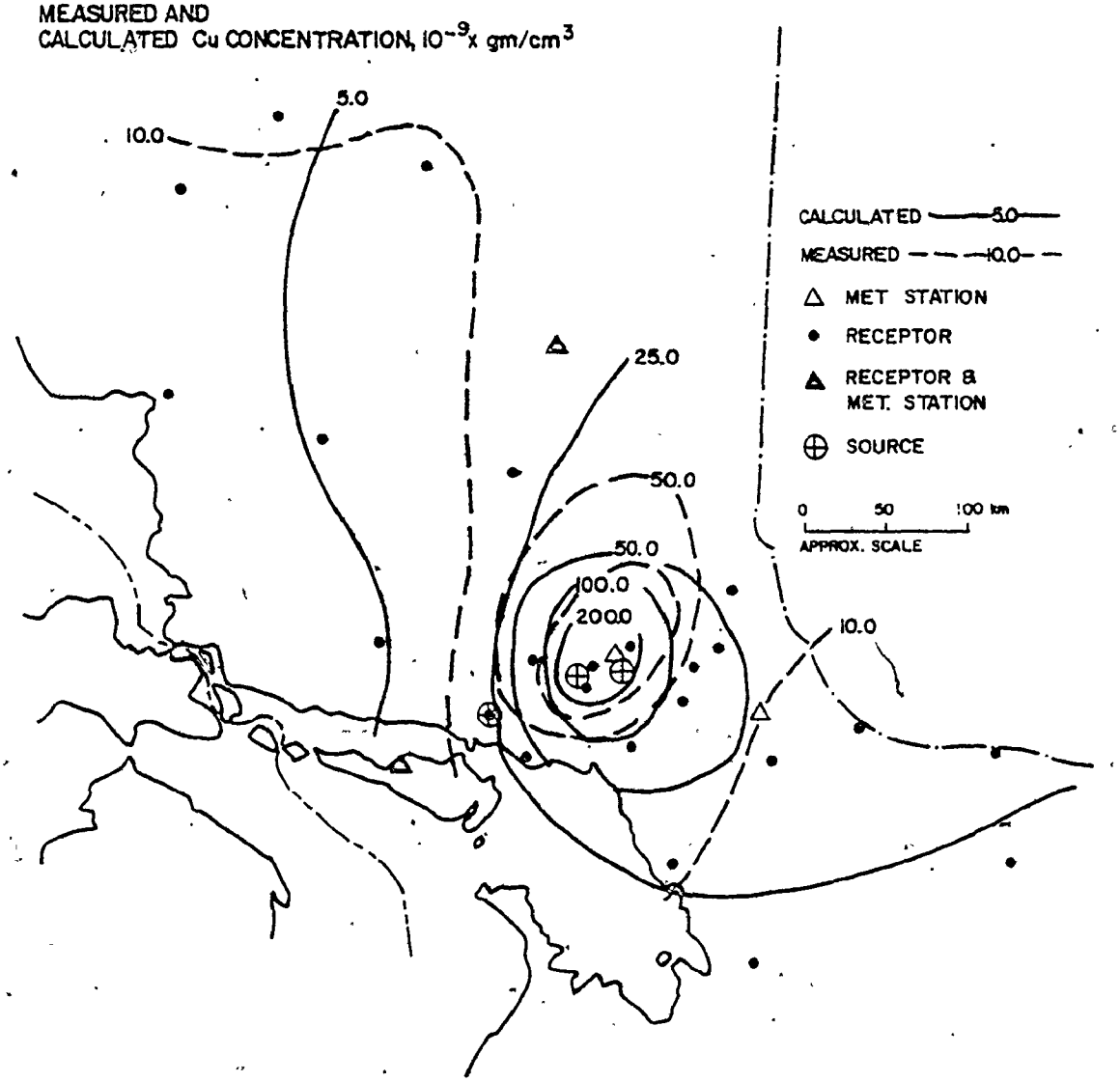

FIGURE 12
MEASURED AND CALCULATED Cu LOADINGS, 10^{-9} x gm/cm^2 - DAY

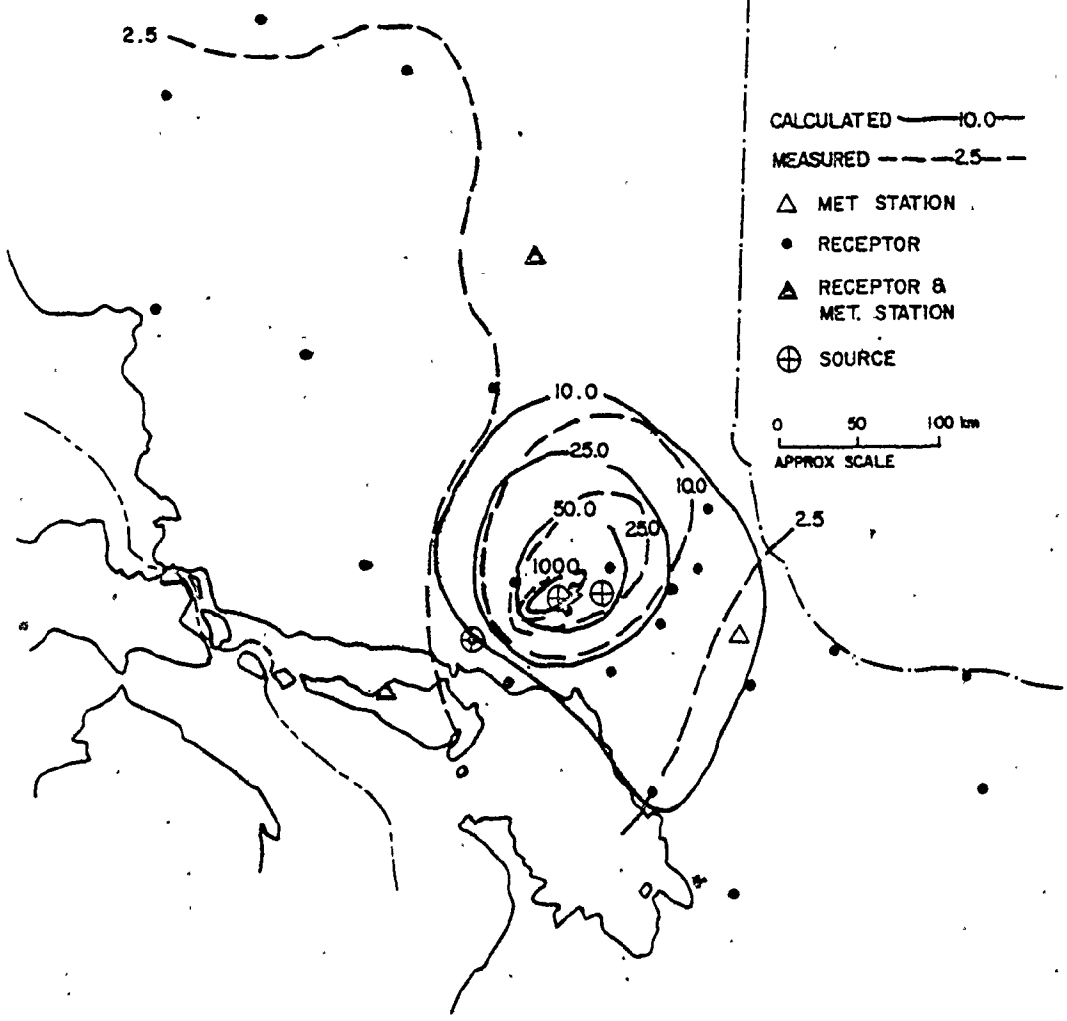

FIGURE 13
MEASURED AND CALCULATED Ni CONCENTRATIONS 10^{-9} x gm/cm^3

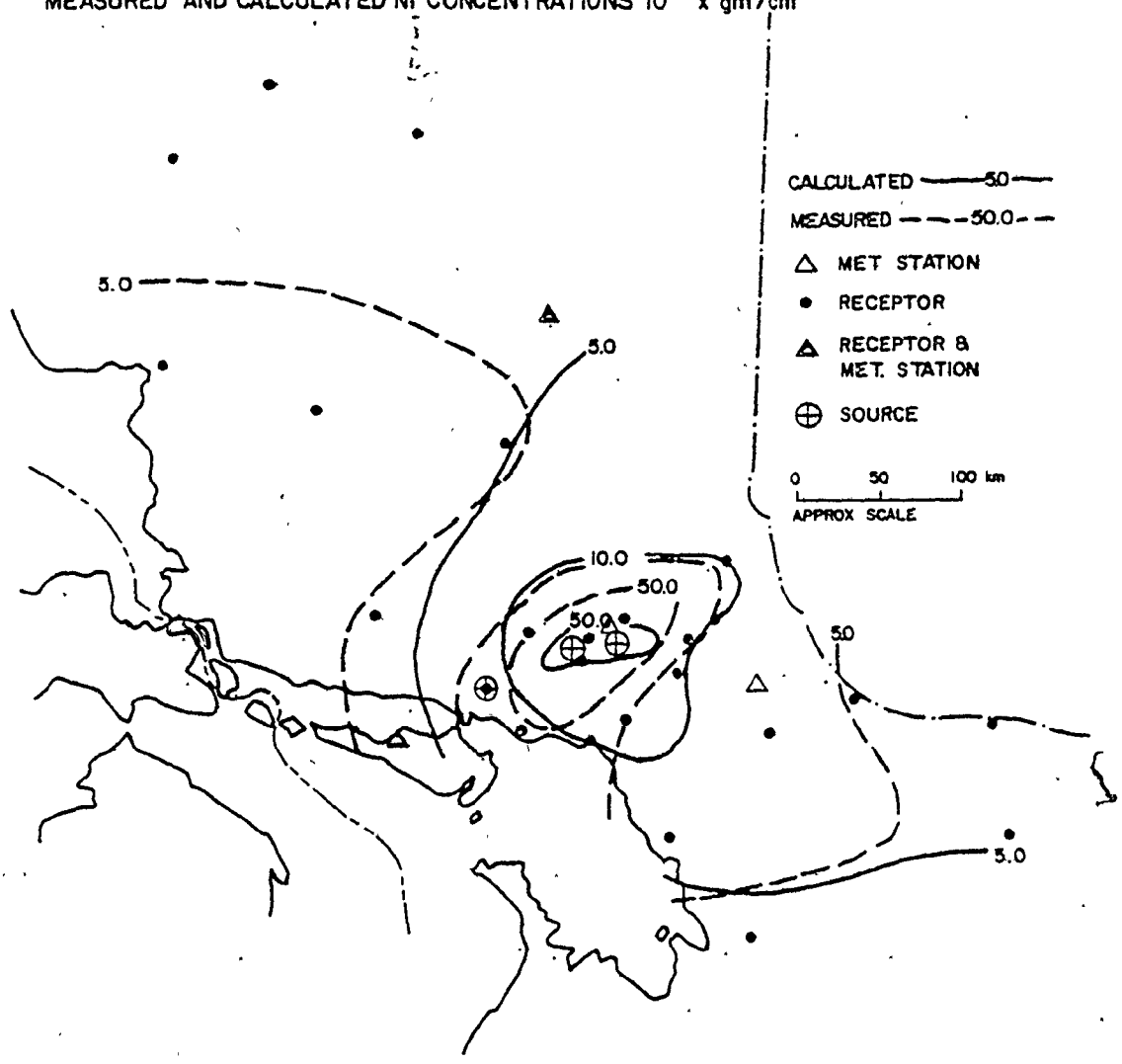

FIGURE 14
MEASURED AND CALCULATED Ni LOADINGS, 10^{-9} x gm/cm^2 - DAY

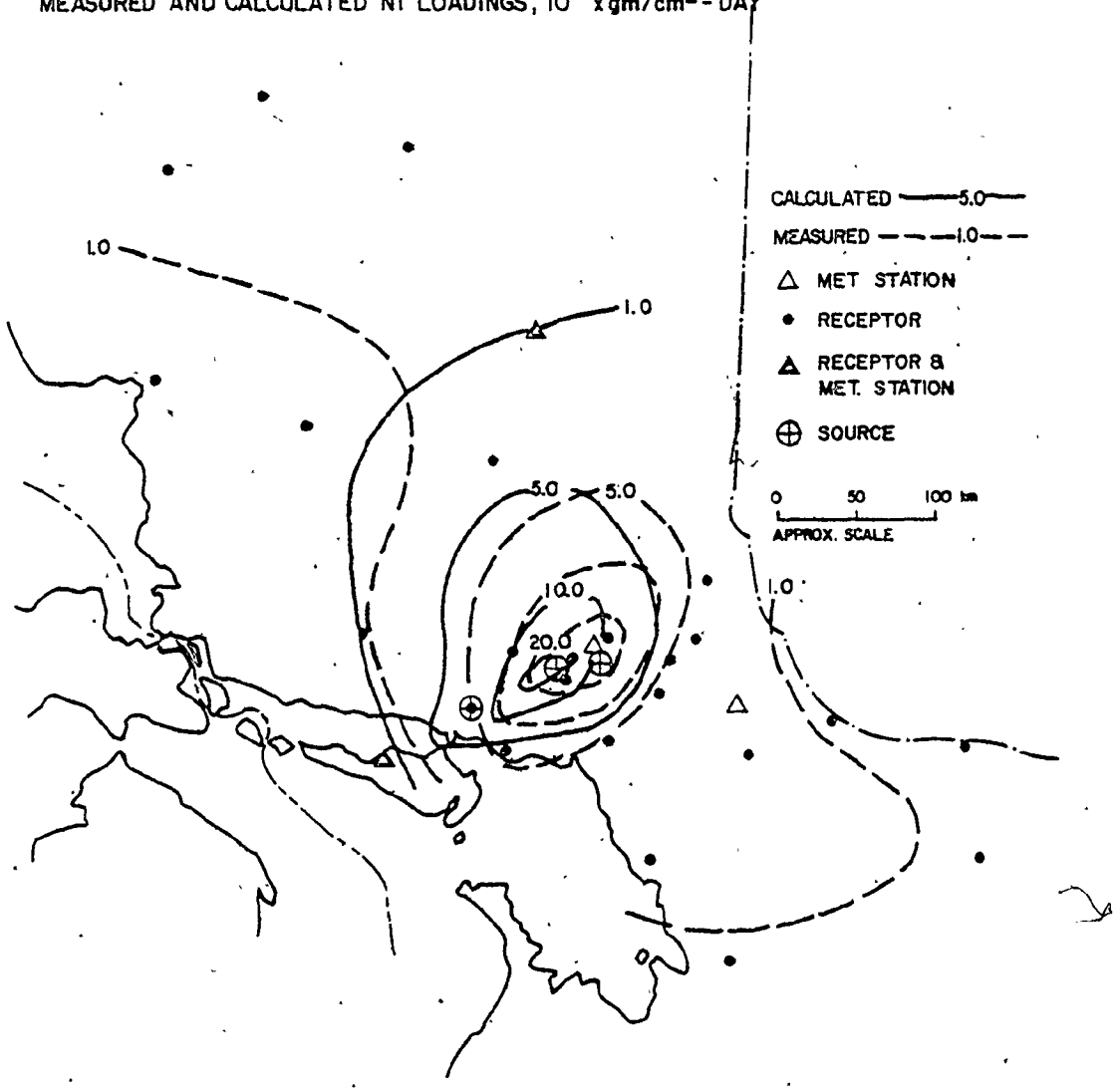

FIGURE 15
MEASURED AND CALCULATED Pb CONCENTRATIONS, 10^{-9} x gm/cm^3

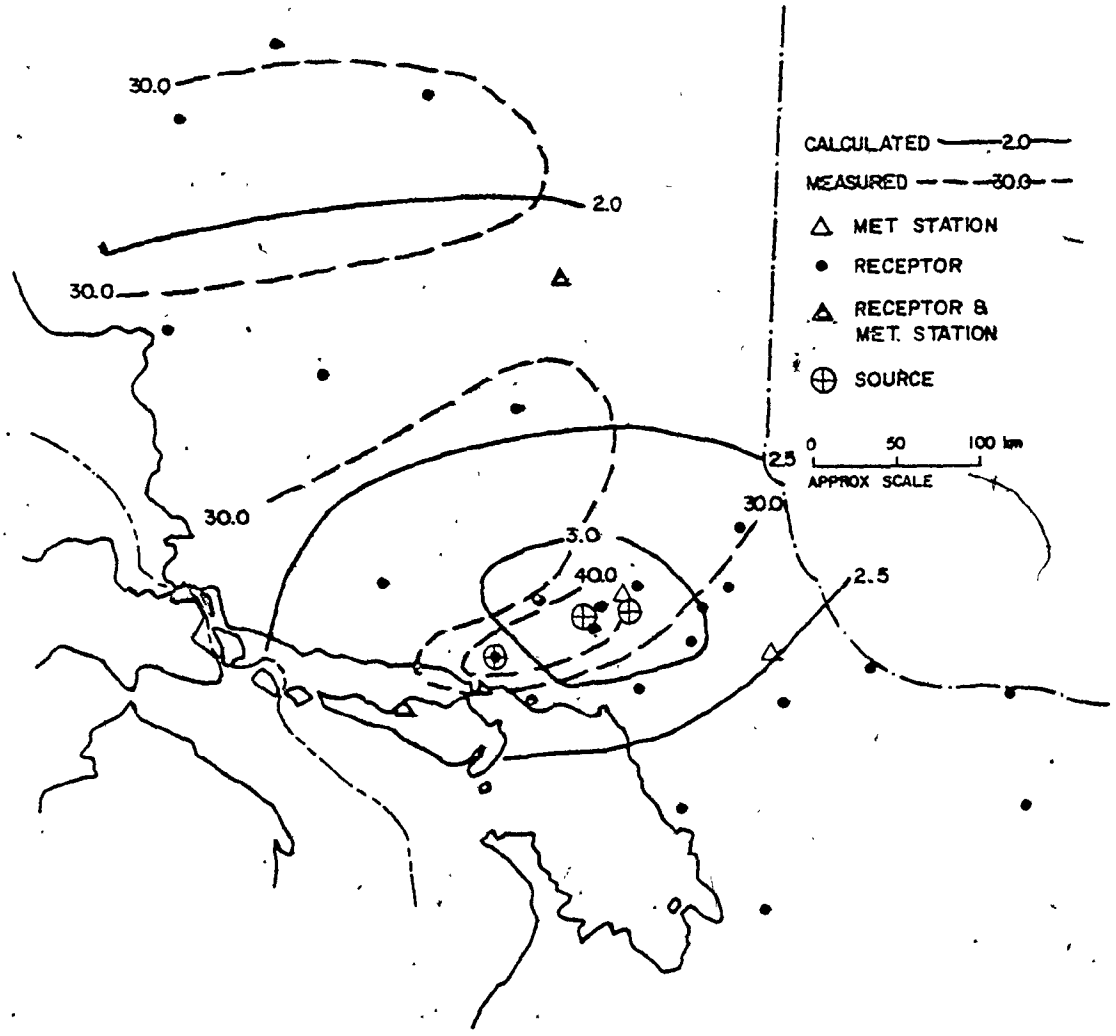

FIGURE 16
MEASURED AND CALCULATED Pb LOADINGS, 10^{-9} x gm/cm^2-DAY

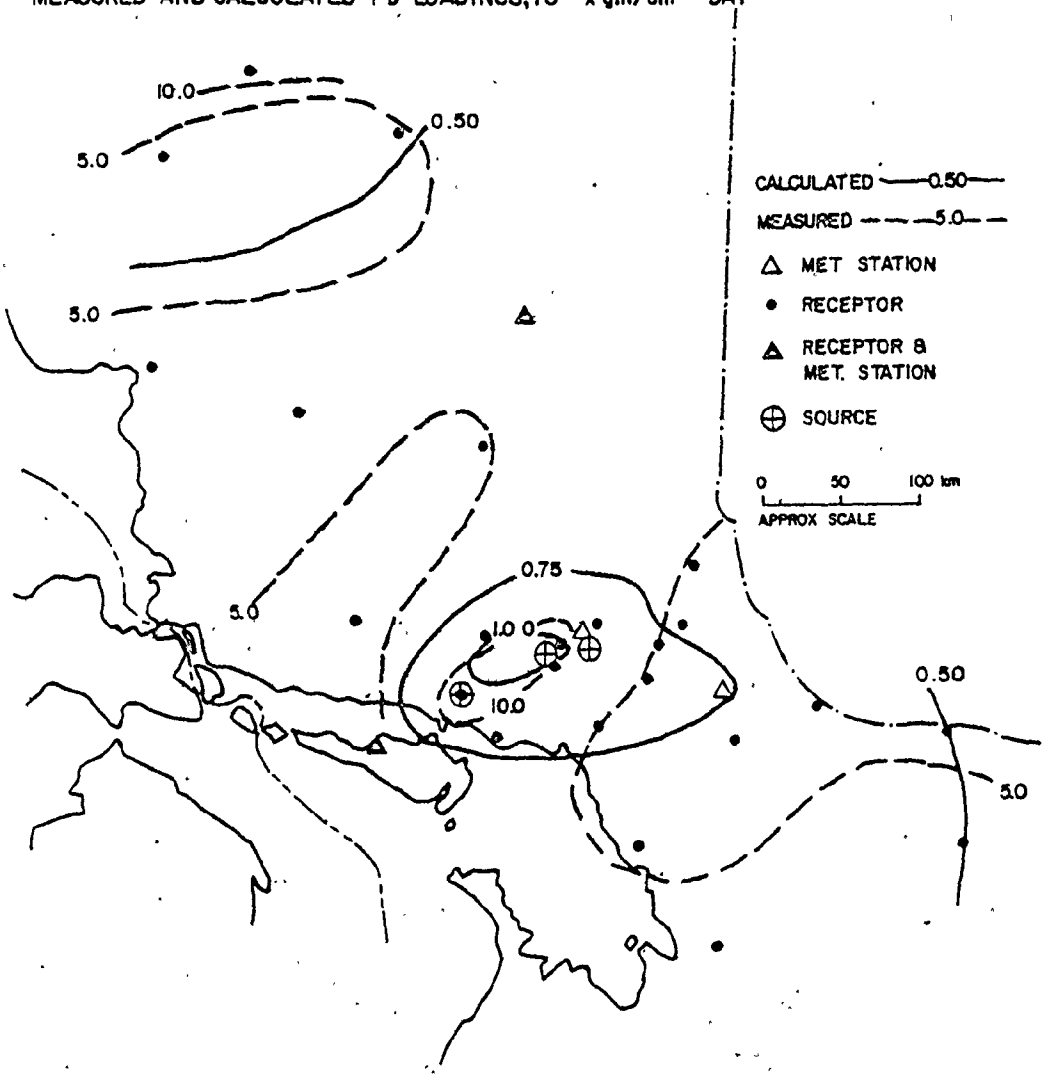

FIGURE 17
MEASURED AND CALCULATED Zn CONCENTRATIONS, 10^{-9}x gm/cm^3

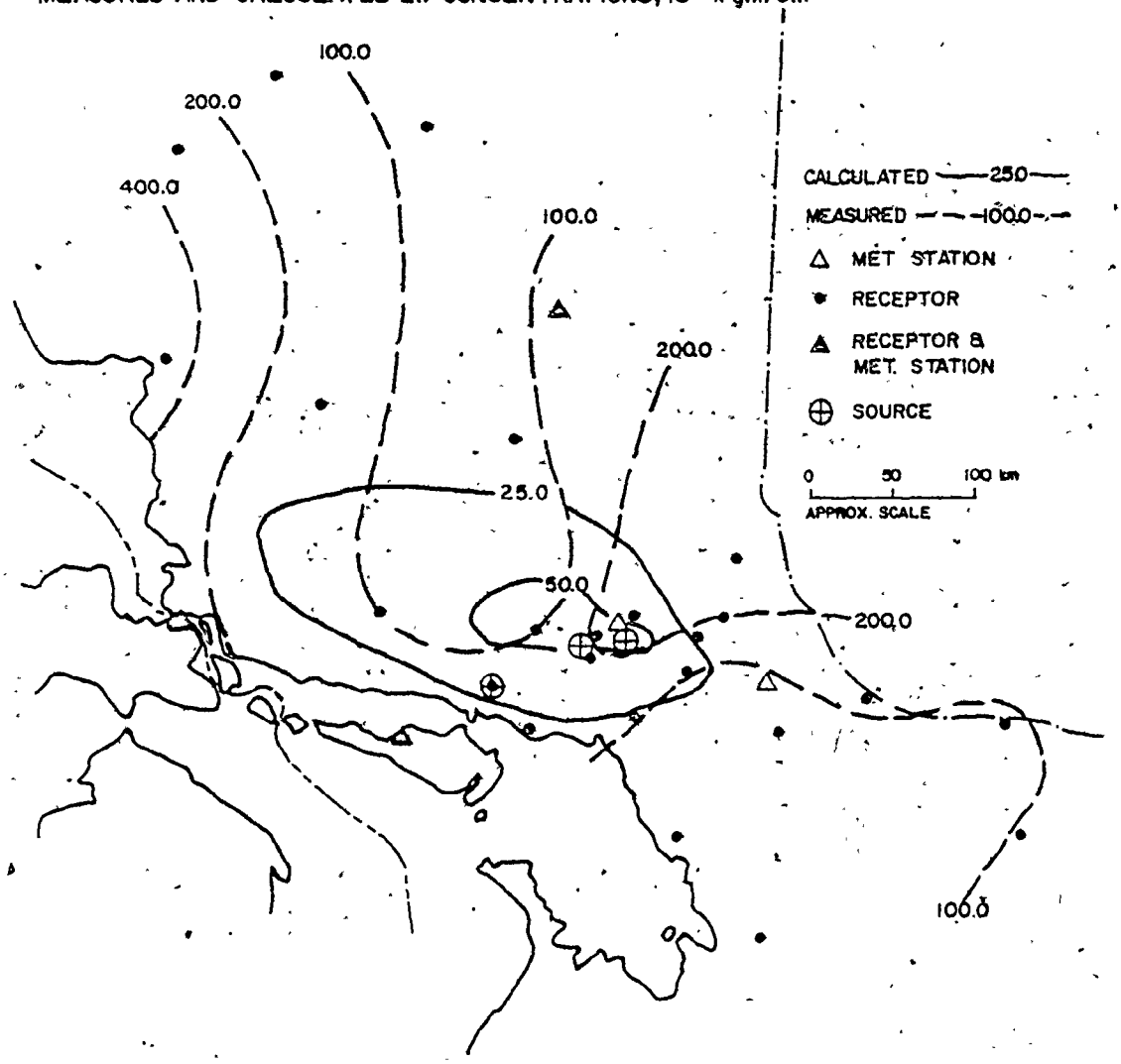

FIGURE 18
MEASURED AND CALCULATED Zn LOADINGS, 10^{-9} x gm/cm^2 - DAY

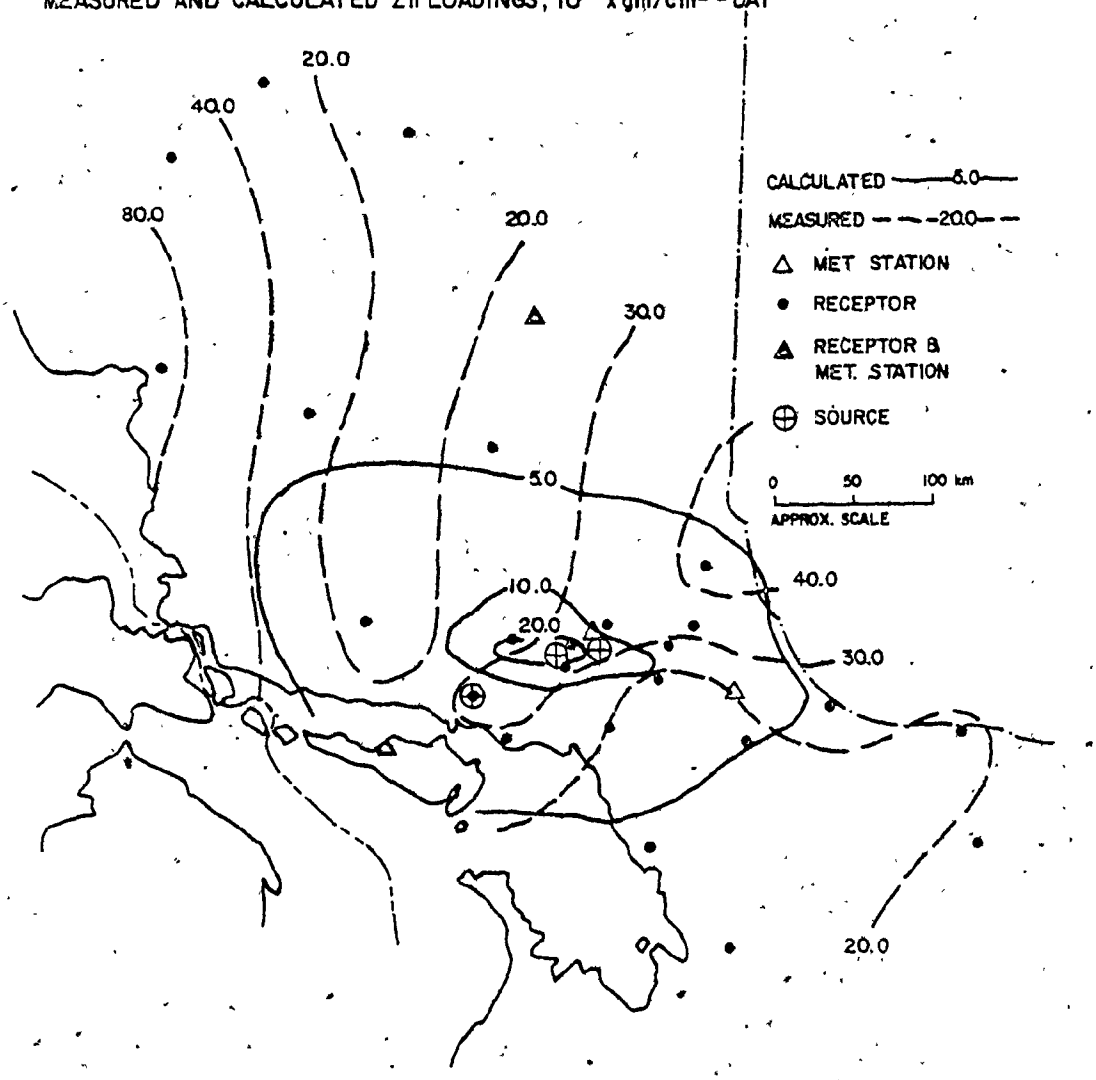

FIGURE 19
MEASURED AND CALCULATED Fe CONCENTRATIONS, 10^{-9}x gm/cm^3

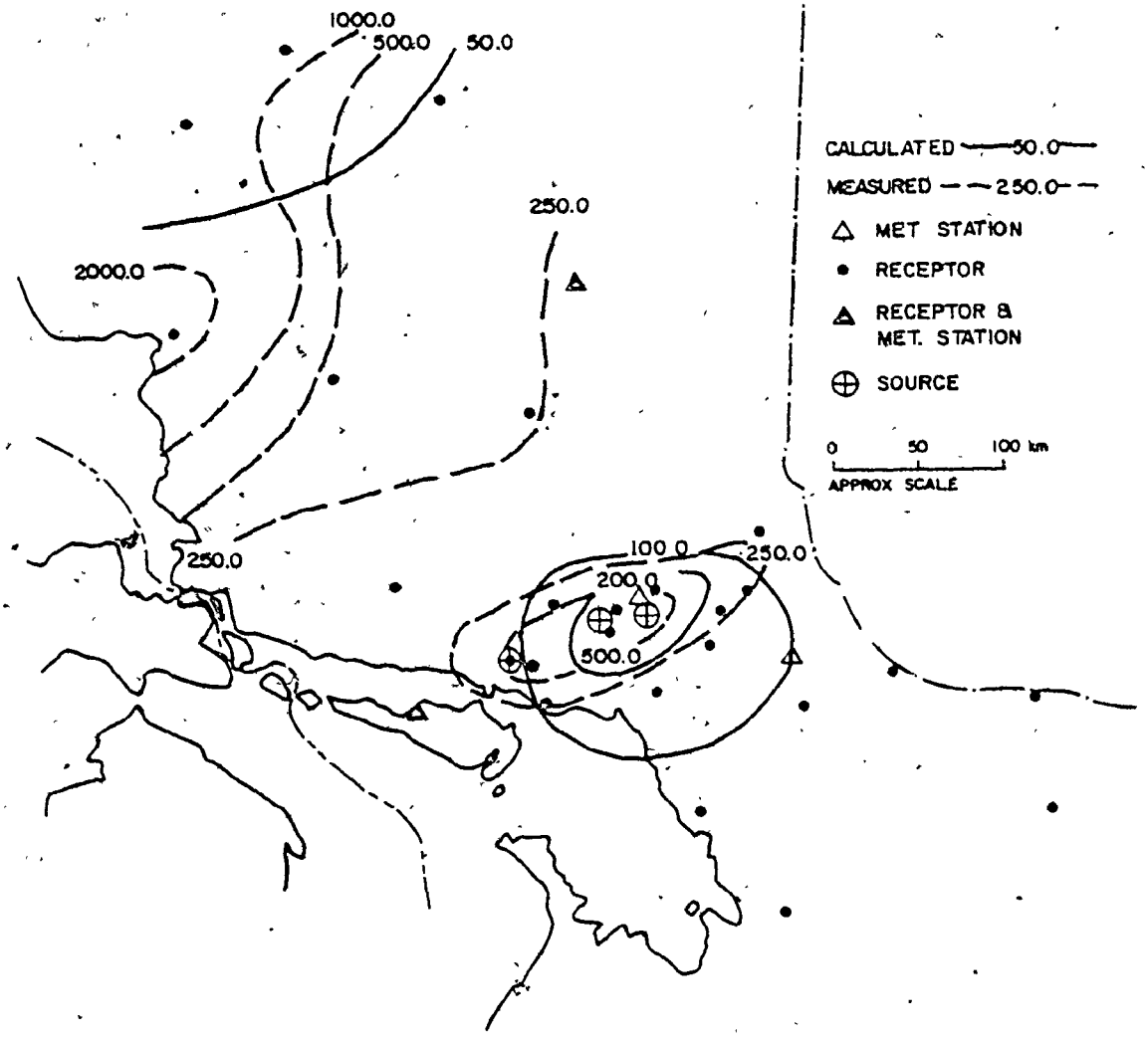

FIGURE 20
MEASURED AND CALCULATED Fe LOADINGS 10^{-9} x gm/cm^2 - DAY

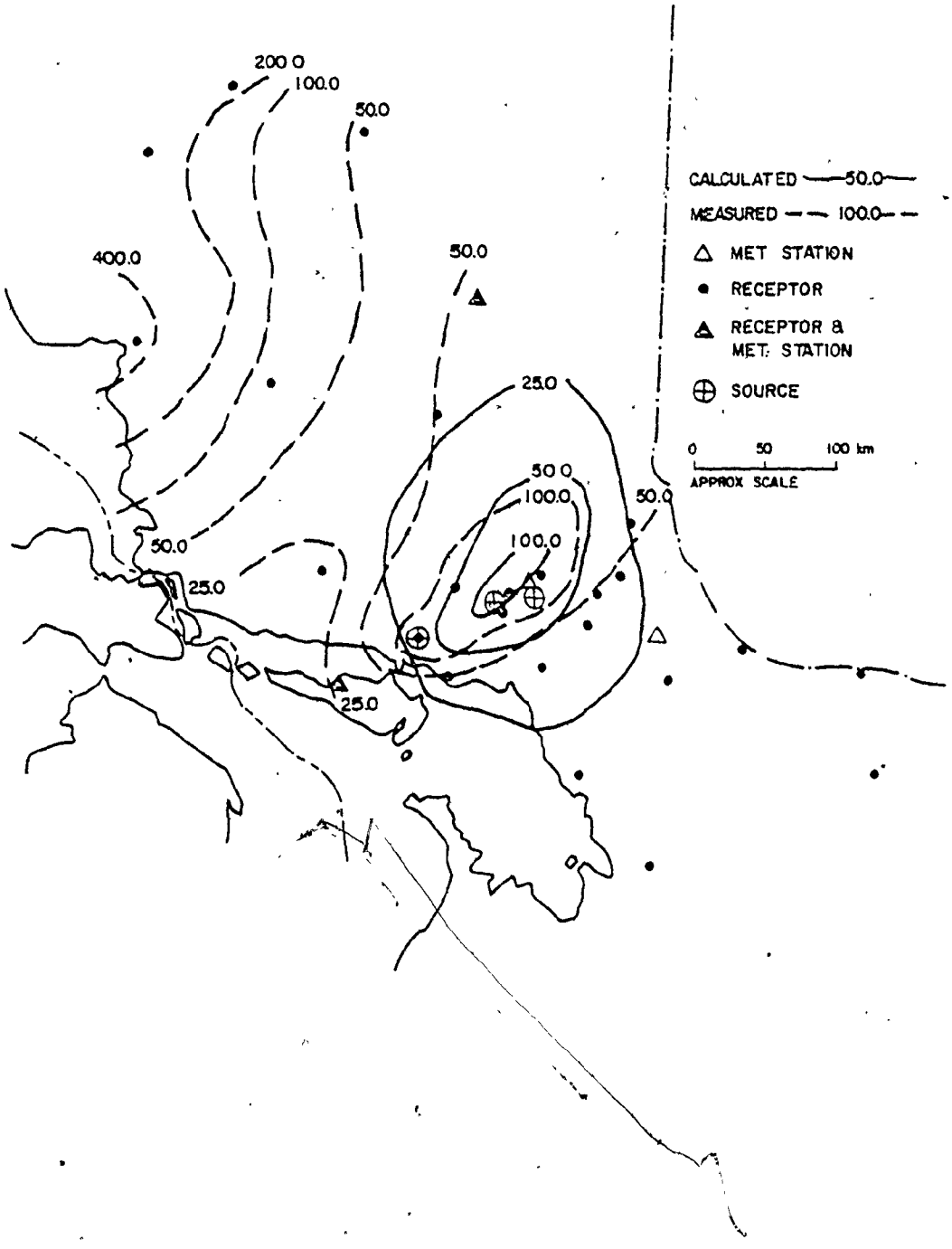

include background pollutant contributions, but only the contributions resulting from sources in the Sudbury smelter area. Background levels (contributions to measured value isopleths due to sources outside the Sudbury smelter area) will be discussed as each pollutant species is examined. Measured values, indicated by dashed lines, are geometric mean measured values from Kramer (1975) (Appendix B). Except for the case of pH, (Figure 8) patterns for both precipitation concentrations and loading rates are given. Each pollutant species is examined in turn, therefore concentration and loading rate maps are alternated.

It is apparent that the general pattern of pH distribution is accurately predicted by the model (Figure 8). Both measured and calculated concentration patterns indicate that the smelters at Sudbury are major sources of hydrogen ion in precipitation within approximately 150 to 200 kilometres of Sudbury. The major difference in measured and calculated hydrogen ion concentration patterns is due to a source (a mine and smelter for iron sulphide ores) near Wawa. This source was not utilized in driving the model, and does not contribute to the calculated hydrogen ion concentration contours. In driving the model, sources were limited to those within 50 kilometres of the city of Sudbury.

Concentration magnitude at given points differ by roughly half to one order of magnitude, except in the area of Wawa, where a difference of two orders of magnitude is approached. The ratio of calculated to measured hydrogen ion concentrations in precipitation is approximately unity at the source, and approaches one order of magnitude at approximately 100 to 150 kilometres from the source. This pattern is produced by the comparison of the exponential decrease in calculated hydrogen ion concentration with the pattern of measured hydrogen ion concentration which decreases at a greater rate with distance beyond 100 kilometres from the source.

Measured pH values lower than approximately 4.5 are rare, even close to the smelters, but this approximate pH value is common out to 100 to 150 kilometres from the smelters. In the next 150 to 200 kilometres, hydrogen ion concentrations decrease in a nearly exponential fashion, approaching the background concentration in precipitation. Measured pH does not rise with distance to the southeast as quickly as it does to the northwest. This indicates the existence of sources of hydrogen ion to the southeast in Ontario and the nearby United States. The probable sources of these hydrogen ion loadings is emissions of sulphur dioxide (and nitrogen oxides) from urban,

industrial and fossil-fuel-fired electrical generating stations outside the Sudbury study area (USEPA, 1976; Environment Canada, 1978). Approximately 45 percent of the total hydrogen ion loading from sulphate, within 80 kilometres of Sudbury, may be due to emission sources outside the Sudbury smelter area (Acres, 1975, 1977, 1980; USEPA, 1976; Environment Canada, 1978). Approximately 25 percent of the total hydrogen ion loading at Sudbury may be due to oxides of nitrogen (Acres, 1975, 1977, 1980; USEPA, 1976; Environment Canada, 1978).

This pattern of measured pH or hydrogen ion concentration may indicate that pH levels in precipitation are limited by a buffering system to a low level near 4.5, or that limitations on sulphur dioxide solubility or reaction rates limit the minimum obtainable pH.

Both sulphate loading rates (Figure 10) and concentration contour patterns (Figure 9) indicate the major contributions of sulphate made to precipitation by the smelters at Sudbury. The patterns follow closely the pH contour patterns (Figure 8), an indication that the oxidation of sulphur dioxide to sulphate is the major source of hydrogen ion in precipitation in the Sudbury area. Acidification due to nitrogen oxides may be a

significant factor near Sudbury, contributing approximately 25 percent of the total hydrogen ion (Acres, 1975, 1977, 1980; USEPA, 1976; Environment Canada, 1978).

The Wawa area is indicated as a major sulphate source by the sulphate concentration contours (a mine and smelter reducing iron sulphide ores). Within approximately 100 to 150 kilometres of Sudbury measured and calculated sulphate concentration contours correspond well, with the exception that the measured pattern is shifted 50 kilometres west of the calculated pattern, and the measured pattern decreases very little in the study area beyond 150 to 200 kilometres from the smelters at Sudbury. In the sulphate loading rate contour map (Figure 10) the pattern is more extreme, and sulphate loading rates rise at precipitation sampling sites in southern Ontario, south and east of North Bay. This pattern could best be explained by the existence of point sources of sulphur dioxide not accounted for in driving the model, at Wawa (iron sulphide ore smelter), Noranda, Quebec (copper smelting), and Timmins, Ontario (Texas Gulf) and to the existence of distant sources of sulphur dioxide in southern Ontario and to the southwest (urban areas, industrial sources, and fossil-fuel-fired electrical generating stations). Southern Ontario and the American

industrial midwest have many sources of sulphur dioxide that may contribute to precipitation sulphate concentrations and sulphate loading rates in the Sudbury study area (Acres, 1975, 1977, 1980).

Within approximately 100 to 200 kilometres from the smelters at Sudbury, calculated and measured patterns of copper and nickel concentrations in precipitation and patterns of loading rates compare closely (Figures 11 through 14). Nickel concentration patterns show better agreement than copper concentration patterns. Measured copper concentrations at given points exceed calculated values by ratios between 1:1 and 4:1 (Figure 12). The additional factor of rainfall in the calculation of copper loading rates has improved the overall match between the measured and calculated patterns. The measured copper concentration and copper loading rate patterns are shifted slightly to the northeast relative to the calculated patterns. This may indicate the contribution of copper smelting at Noranda, Quebec. The pattern of measured copper isopleths (Figures 11 and 12) indicate other sources of copper contributing to loadings in the Sudbury area. These include Texas Gulf Inc., Pamour/Porcupine in the Timmins area, Noranda GECO Division and Willroy in Manitouwadge.

Calculated and measured patterns of nickel concentrations match reasonably well over the majority of the study area, indicating the suitability of the model for modeling nickel concentrations (Figure 13). Inside approximately 75 kilometres of the smelters measured nickel concentrations exceed calculated concentrations by approximately 2:1. A comparison of measured and calculated nickel loading rates exhibits the same pattern (Figure 14). The pattern of measured nickel isopleths (Figures 13 and 14) indicate other sources of nickel contributing to loadings in the Sudbury study area. These include Teck, in the Cobalt district, and the Willroy mine, Manitouwadge. Copper and nickel sulphide ores are often found together, as at Sudbury, therefore sources of nickel emissions in northern Ontario may include copper mining and smelting districts.

Patterns of measured and calculated lead concentrations in precipitation both indicate the importance of the Sudbury urban area as a source of lead in the atmosphere (Figure 15). Patterns of measured lead concentrations indicate that most other urban and suburban centres, highways, etc, are also important sources of lead in the atmosphere and in precipitation. Measured lead concentrations in precipitation exceeded calculated concentrations

by factors between approximately 10:1 near Sudbury to 15:1 at distances beyond approximately 75 to 150 kilometres from Sudbury. Measured and calculated lead loading rate patterns match better (Figure 16) than concentration patterns. Measured and calculated lead loading rates differ consistently by a factor of 10, except for higher measured lead loading rates in the far northern portion of the study area, along the Lake Superior shore between Sault St. Marie and Wawa, and in the southeastern Ontario area, south of North Bay. From the pattern of measured lead isopleths it is clear that Sudbury is a much larger source of atmospheric lead than originally assumed. New research indicates that lead emission rates at Sudbury are approximately 25 percent of nickel and copper emission rates (Conroy et al, 1978). If the same ratio can be applied to the modeling period (1972 to 1974 emission rates), lead emission rates to drive the model should be corrected to approximately 0.11 to 0.15 x 10^6 kg/yr. When this correction is made, predicted and measured lead values are in much better agreement. Calculated lead values range from approximately a 75 percent undercalculation to a 150 percent overcalculation in the study area.

In addition, the measured lead isopleth pattern indicates that distributed sources, such as highway traffic outside the Sudbury urban area (Highways 17, 69, and 11), and other urban areas (Sault Ste. Marie and North Bay), as well as mining areas (including Sturgeon Lake, Manitouwadge, and Timmins) for copper, nickel, lead, and zinc, may be important sources of atmospheric lead concentrations.

Patterns of measured and calculated iron concentrations in precipitation and iron loading rates (Figures 19 and 20) are analogous to the patterns exhibited by copper (Figures 11 and 12) and by nickel (Figures 13 and 14). Measured and calculated iron concentrations and loading rates both indicate the importance of the Sudbury smelters as sources of atmospheric iron. The pattern of measured iron concentration and loading rate is shifted west and north relative to calculated iron concentrations and loading rates.

The pattern of measured iron concentrations and loadings indicates the major importance of Wawa as a source of atmospheric iron. Wawa is indicated to be between 2 and 4 times as important as the Sudbury area as a source of atmospheric iron (Figures 19 and 20), while it is roughly of equal importance to Sudbury as a source of

atmospheric sulphate (Figures 9 and 10). Relative importance is estimated subjectively, by comparing measured concentrations and loading rates at approximately equal distances from each indicated source, as well as by extrapolation from production figures (approximately 3 times higher iron production at Wawa). Atmospheric iron contributions from Wawa and other sources in the north and west of the study area (including Adams mine, Kirkland Lake, Sherman mine, Temagami, and National Steel, Capreol. This last is close to the Sudbury smelter area and is approximately the same size as the INCO iron recovery operation at Copper Cliff) are the reason for the relative northwest shift of the measured iron patterns in comparison to calculated iron patterns.

Measured zinc patterns for both precipitation concentrations (Figure 17) and loading rates (Figure 18) indicate a broad distribution of zinc in the atmosphere of the study area. Southern Ontario, Sudbury, the shores of Georgian Bay and Lake Superior exhibit relatively higher atmospheric zinc levels, as indicated by precipitation zinc concentrations and loading rates. The major source of the zinc emissions at Sudbury is probably from traces of zinc in the Sudbury area copper/nickel sulphide ores. Although zinc is not a product of the Sudbury smelters,

zinc is mined with copper and nickel at many Ontario mines (including mines in the Sturgeon Lake, Manitouwadge, and Timmins areas).

The measured zinc isopleth pattern indicates a major zinc source at or to the west of Wawa. Zinc is not a product of the Wawa smelter, but may be a component of the Wawa ore. It is more probable that the source of the zinc is the Noranda and Willroy mines at Manitouwadge, outside the Sudbury study area 140 kilometres northwest of Wawa. This pattern of atmospheric zinc distribution may indicate that a large proportion of the zinc may have as its source reentrained surface soil, dust, and tailings. Relatively higher atmospheric zinc levels to the southeast may be in part dust raised by traffic, construction activity, and in part from paint, filler for rubber tires and other industrial and urban sources of zinc.

The relative magnitude of average measured concentrations and calculated maximum and minimum concentrations in precipitation are illustrated in graphic form in relation to distance from the smelters (Figures 21 through 27). Distance from source to receptors was chosen for the x-axis (Figures 21 through 27) because this allows a more convenient basis for comparison with the isopleth maps (Figures 8,

through 20). The distance scale is nearly equivalent to the plume time of travel scale (for the modeling time period and the Sudbury study area) because the annual average wind velocity and direction exhibits a small variability (approximately 2.5 percent)(Table 29).

Average measured concentrations in precipitation are indicated by dots, each dot representing from 12 to 35 sampling periods at a receptor site (Table 24, Appendix B). Triangles indicate single sample periods utilized to set initial model parameters (Table 28, Section 4.1.1). Maximum and minimum calculated concentrations are indicated by two to three straight (on a log concentration scale) lines. Each line is a least squares regression fit to log concentrations calculated for from 12 to 27 receptor sites and from 12 to 35 sampling periods (Table 24, Appendix B). The minimum calculated concentration lines are a best fit for 27 sites at distances of from less than 10 kilometres to more than 400 kilometres distance from the source. The maximum calculated concentration line is broken into two best fit lines, one a best fit line for 15 receptor sites between 10 and 150 kilometres from the source, and the other a best fit line for 12 remaining sites at distances between approximately 150 and 400 kilometres from the source. Close to the source dry deposition mechanisms tend to

dominate atmospheric removal processes, and at greater distances wet deposition mechanisms dominate. For the meteorological conditions in the Sudbury area used as driving parameters in this study (Table 29), a distance of 150 kilometres approximates the dominance crossover point for maximum calculated concentration conditions. For meteorological driving parameters producing minimum calculated concentrations the dominance crossover point is between 5 and 25 kilometres. Minimum deposition rates dominated by wet or dry processes are calculated to be insignificantly different, and a single best fit line is adequate to approximate the minimum calculated concentration for all receptors at distances between 10 and 400 kilometres from the source.

It is clear from the graphical representations (Figures 21 through 27) that sulphate, copper, nickel, and iron concentrations are modeled adequately by the modified box model as utilized in this study, for receptors less than 200 kilometres from the source. Measured copper concentrations fall within the calculated limitations out to distances of approximately 400 kilometres. Beyond approximately 175 kilometres the influence of the smelters on the measured concentrations is obscured by background concentrations (contributions from other sources) and

FIGURE 21
CALCULATED AND MEASURED $SO_4^=$ CONCENTRATIONS PLOTTED AGAINST DISTANCE

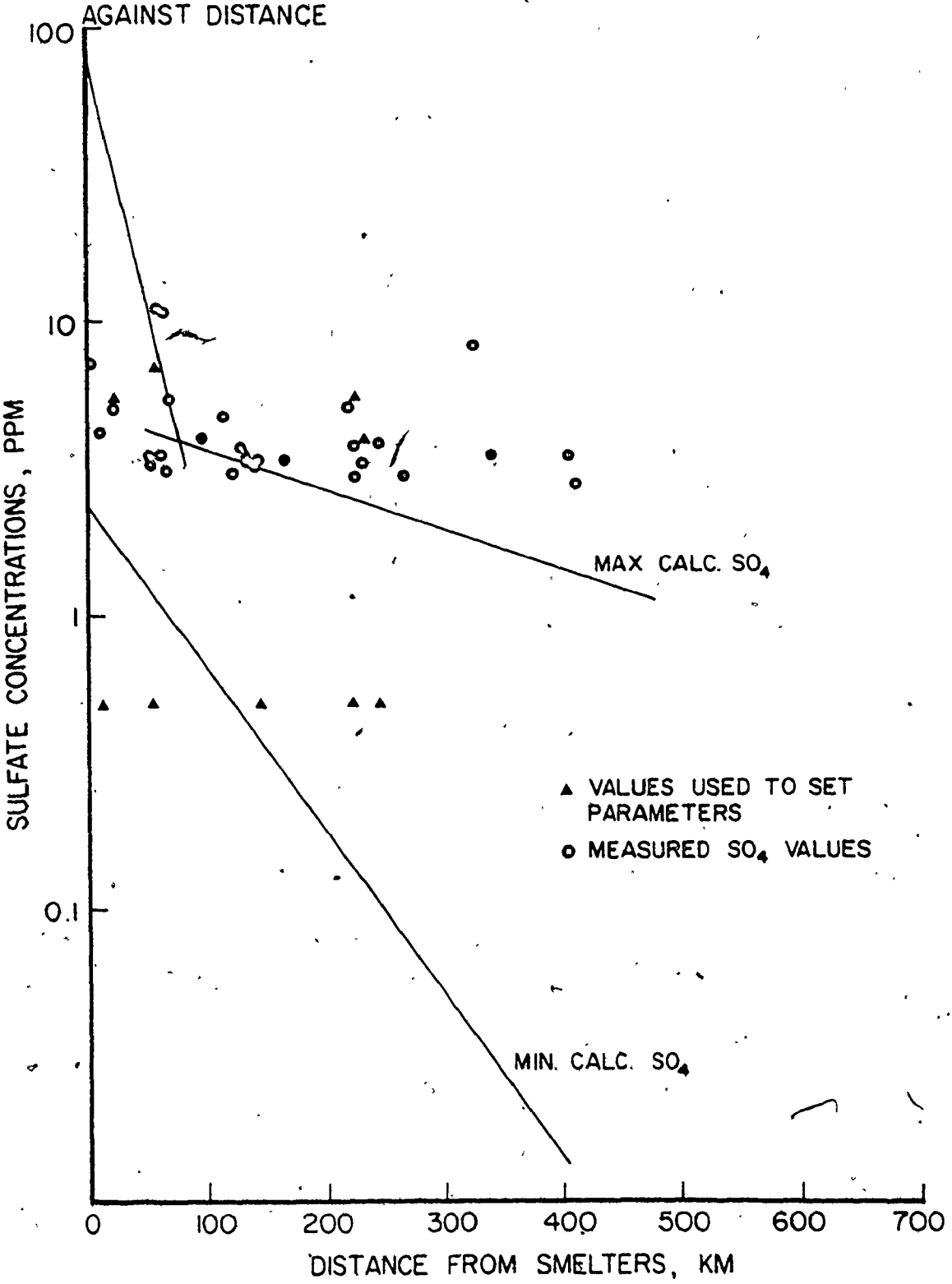

FIGURE 22
CALCULATED AND MEASURED pH, PLOTTED AGAINST DISTANCE.

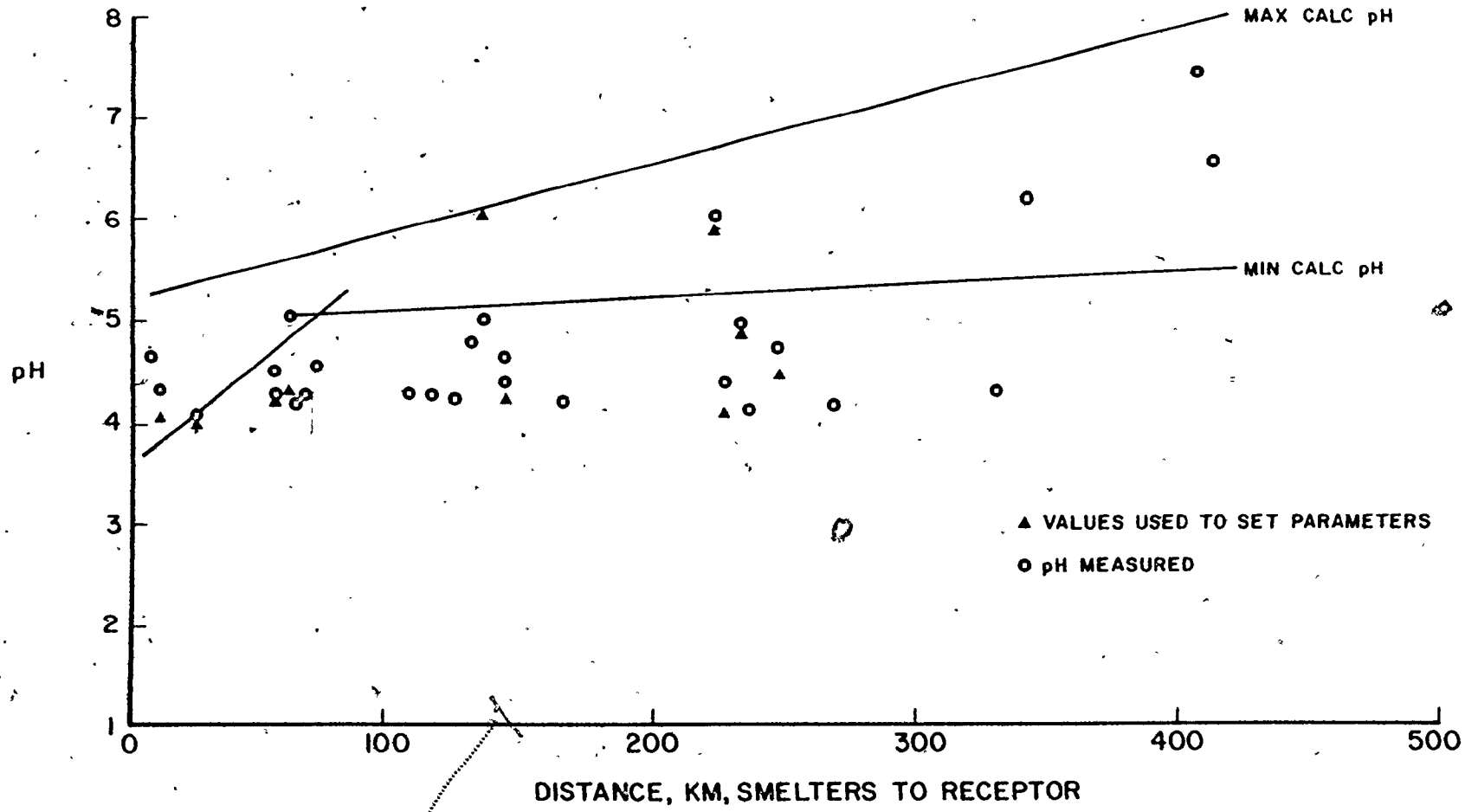

FIGURE 23
CALCULATED AND MEASURED Cu CONCENTRATIONS PLOTTED AGAINST DISTANCE

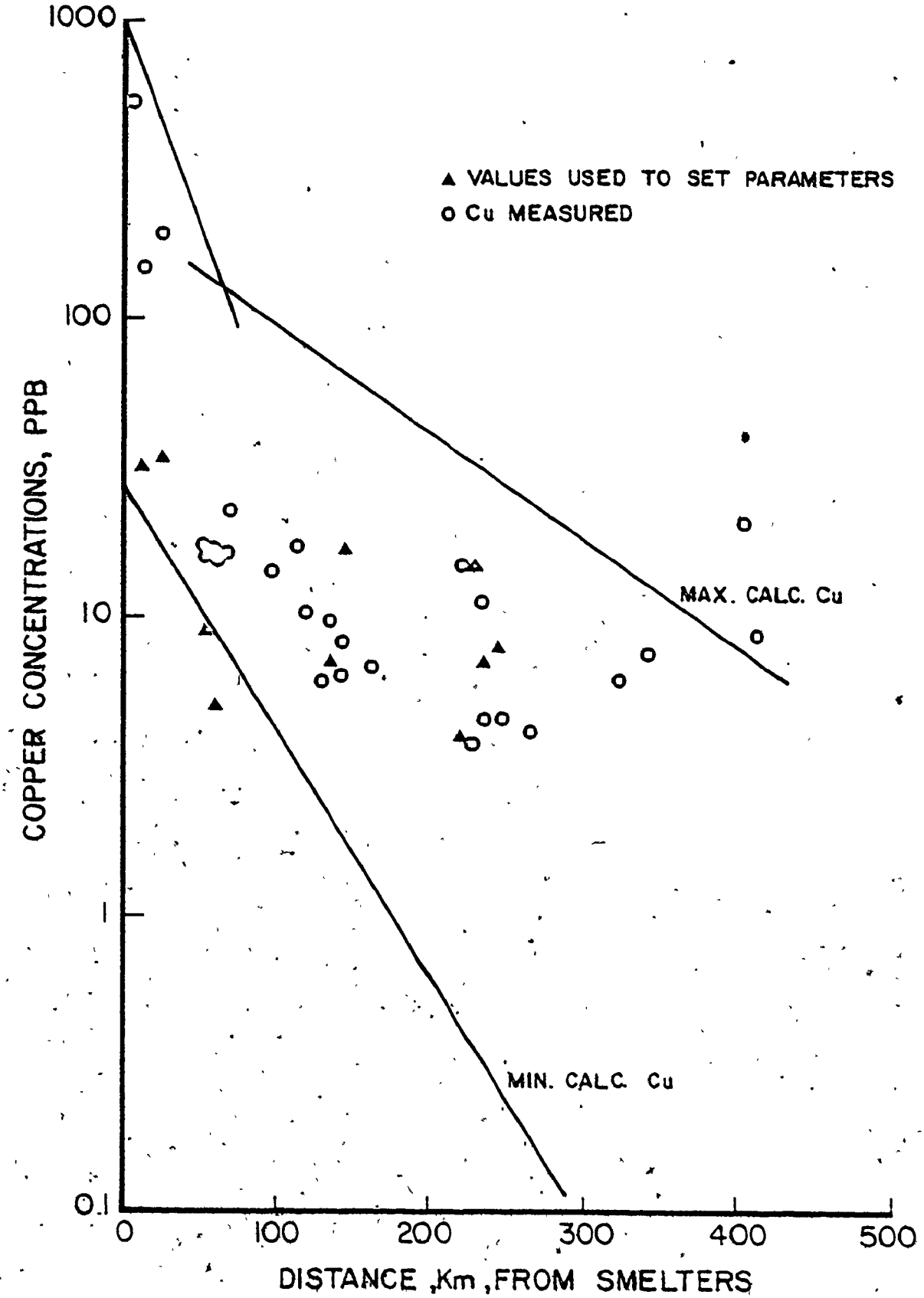

FIGURE 24
CALCULATED AND MEASURED Ni CONCENTRATIONS, PLOTTED AGAINST DISTANCE

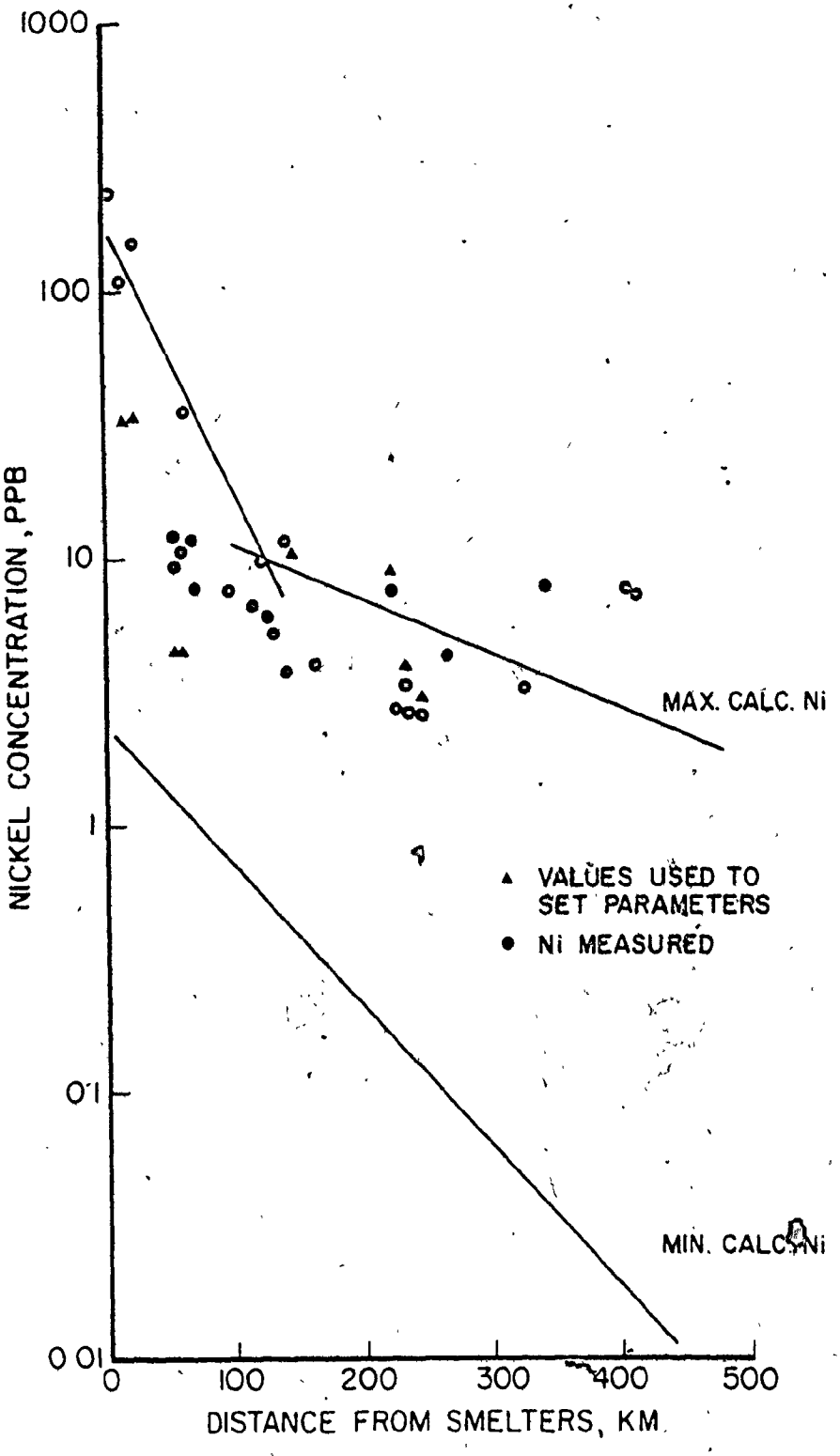

FIGURE 25
CALCULATED AND MEASURED Pb CONCENTRATIONS, PLOTTED AGAINST DISTANCE

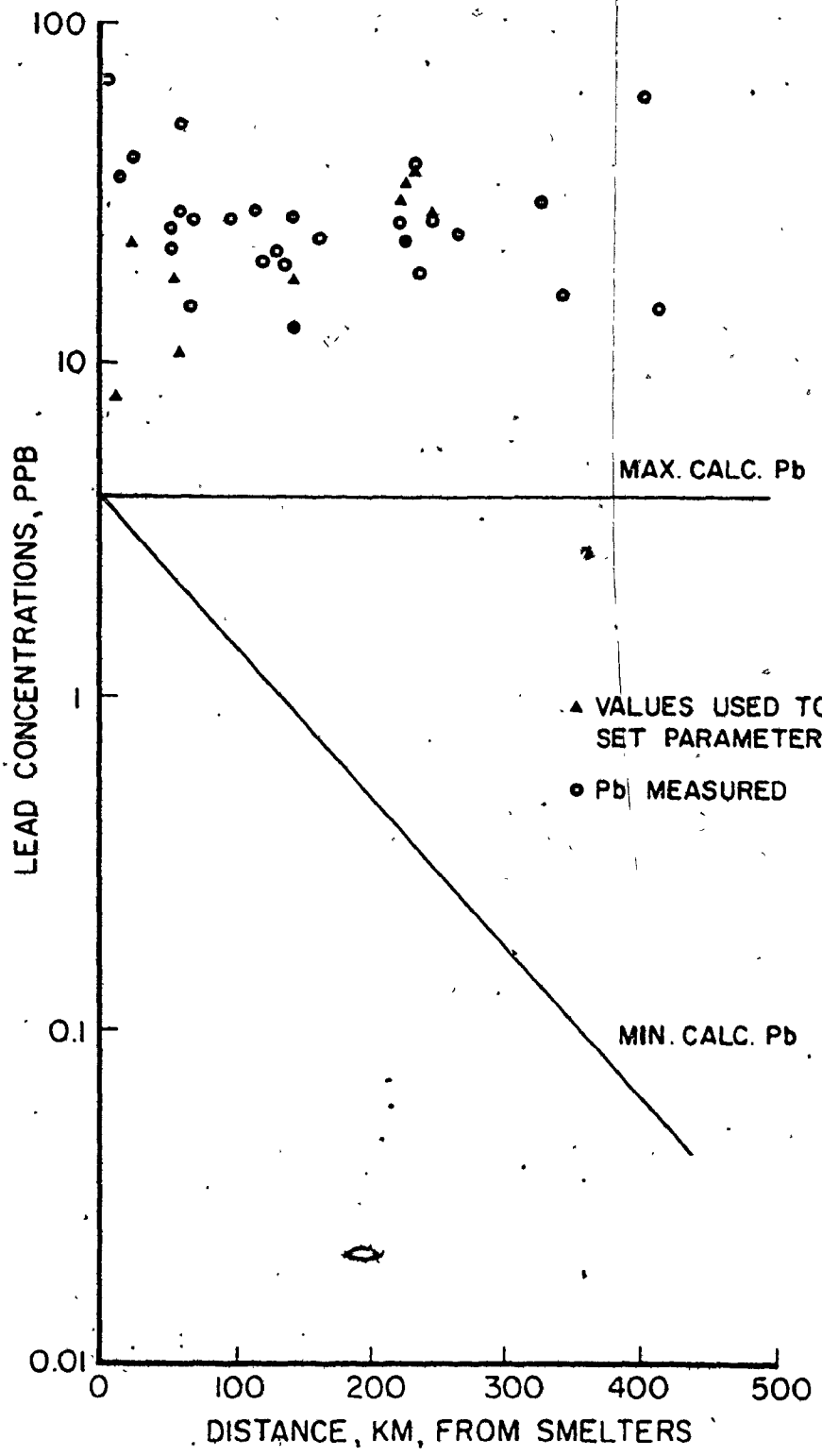

FIGURE 26
CALCULATED AND MEASURED Zn CONCENTRATION, PLOTTED AGAINST DISTANCE

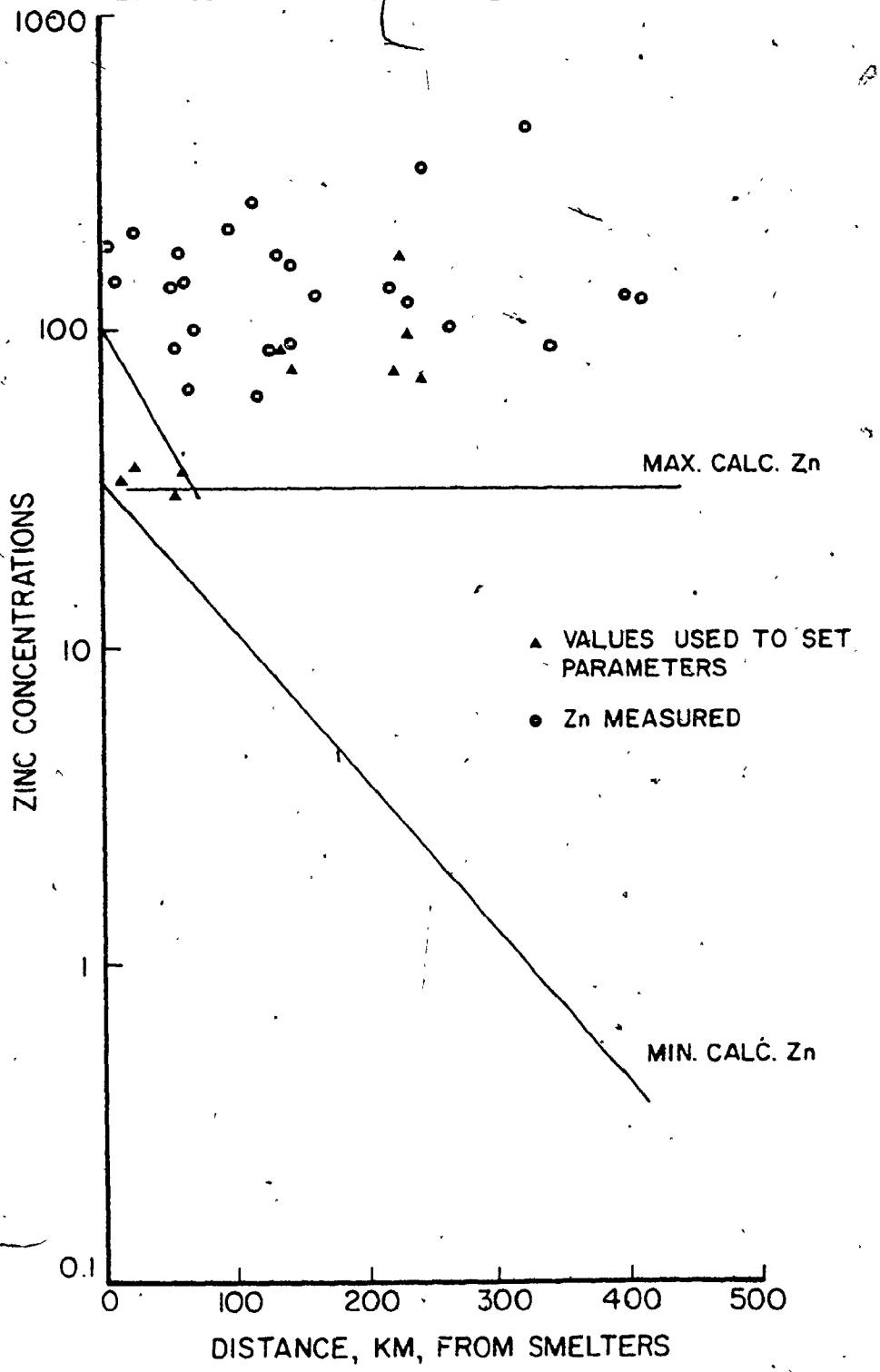

FIGURE 27
CALCULATED AND MEASURED Fe CONCENTRATIONS, PLOTTED AGAINST DISTANCE

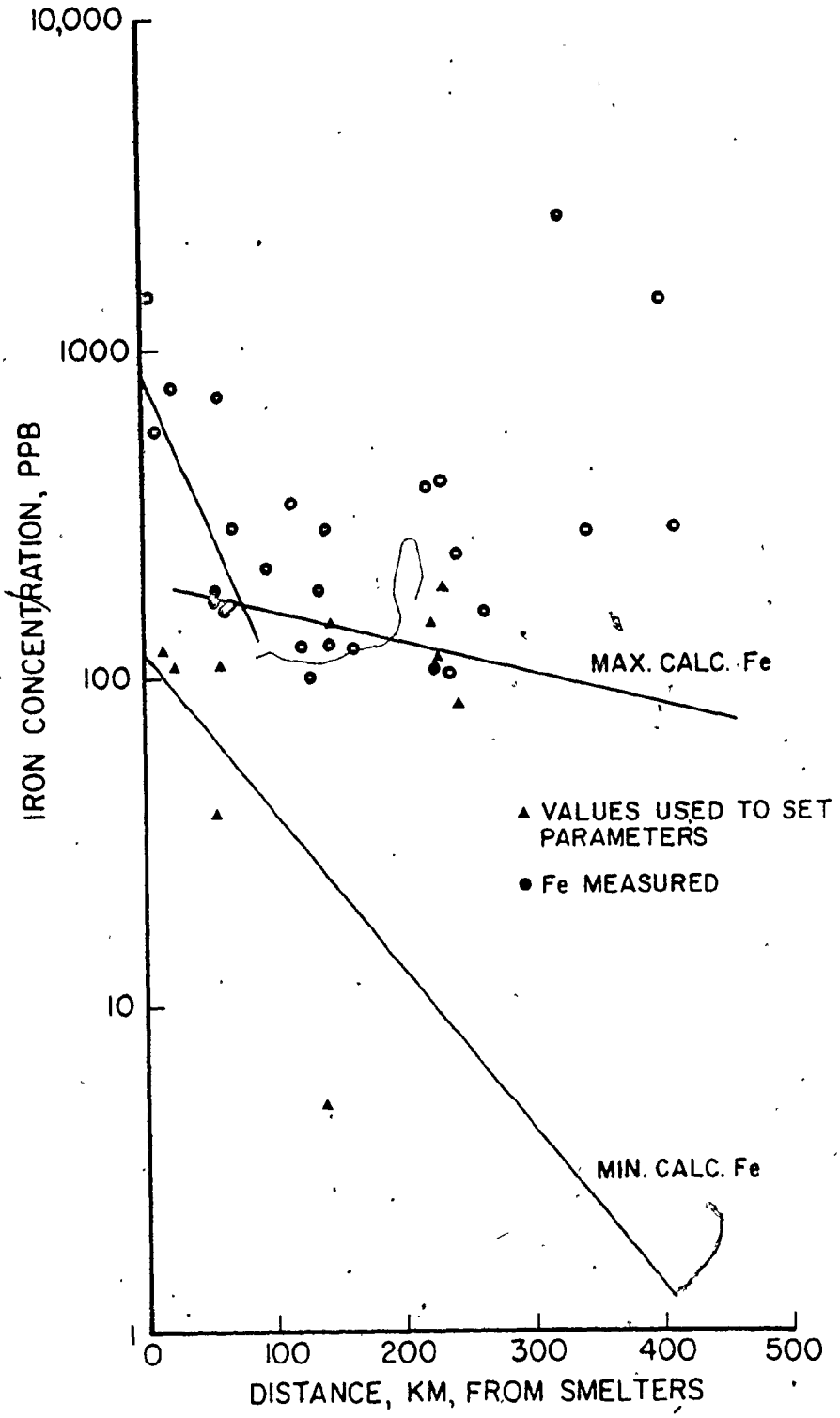

scatter in the measurements (Figure 23). Measured nickel concentrations are close to the maximum calculated limitation (Figure 24). Between distances from the source of 10 to 150 kilometres measured nickel concentrations are adequately modeled. Beyond 150 kilometres the concentration component from the smelters is obscured. Within a distance of 100 kilometres from the source measured sulphate concentrations fall between the predicted maximum and minimum limitations (Figure 21). Beyond 100 kilometres the influence of the smelters at Sudbury is obscured. Within approximately 250 kilometres measured iron concentrations in precipitation are approximated by the maximum calculated iron concentration (Figure 27). Beyond 250 kilometres the contribution to total precipitation concentrations of iron from the Sudbury area smelters is obscured. Figure 27 (iron) indicates, as do Figures 19 and 20, that major sources of atmospheric iron concentrations and loadings in the study area exist other than the Sudbury smelters (including sources at Wawa, Temagami, and Kirkland Lake). Beyond 150 kilometres from Sudbury these sources obscure the contributions of the Sudbury smelters (the Falconbridge smelter, where the ore contains a high percentage of iron, and the INCO iron ore recovery operation at Copper Cliff).

Figure 26 (zinc) indicates, as does Figures 17 and 18, that the major sources of atmospheric zinc concentrations and loadings in the study area are not from the Sudbury smelters (sources include Timmins and Manitouwadge).

Figures 15, 16 and 25 (lead) indicate the importance of sources of atmospheric lead concentrations and loadings other than the Sudbury smelters (including Sturgeon Lake, Manitouwadge, and Timmins). As previously noted, the lead emission rate was originally underestimated (Figures 15, 16 and 25). Calculations for average meteorological conditions (years 1972, 1973, and 1974) with corrected lead emission rates (Copper Cliff, 3.47×10^5 gm/day; Falconbridge, 8.16×10^4 gm/day) indicate increased calculated lead concentrations in precipitation and lead loading rates by between one and two orders of magnitude.

Results in tabular form consist of Tables 35 and 36, and Appendix B, presenting calculated atmospheric concentrations, minimum and maximum calculated concentrations and loading rates for seven constituents at 27 receptor sites. Measured concentrations are arithmetic means and standard deviations for from 12 to 36 sampling periods (Kramer, 1974). Maximum and minimum calculated values are for the same receptor sites and sampling periods. Table 31 is a cross-

correlation matrix for measured atmospheric concentrations of the seven constituents: pH and hydrogen ion, sulphate, copper, nickel, lead, zinc, and iron. Table 35, analogous to Table 31, is a cross-correlation matrix for measured precipitation concentrations. Values in Table 35 are correlation coefficients for pairs of constituents measured at 15 receptor sites less than 150 kilometres from Sudbury. Table 36 compares measured concentrations to the controlling parameters, including distance from the source, precipitation event duration, and wind heading, and compares measured to calculated concentrations for the seven constituents.

The results of the cross-correlation matrix for measured precipitation concentrations (Table 35) are similar to the results exhibited by the cross-correlation matrix for measured atmospheric concentrations (Table 31). Significant pairs of constituents expected were: pH or hydrogen ion and sulphate, hydrogen ion and copper, hydrogen ion and nickel, hydrogen ion and iron, sulphate and copper, sulphate and nickel, sulphate and iron, lead and zinc, and zinc and iron. Significant correlations between constituents in these pairs indicate sources in common. Strong significant correlations in other pairs with hydrogen ion may be indicative of a controlling effect exerted on raindrop chemistry by pH.

TABLE 35

Cross Correlations Between Pollutant Species, for Measured Precipitation Chemistry (15 sites)

Pollutant Species	pH	H^+ ion	Sulphate	Copper	Nickel	Lead	Iron
Sulphate	0.3722	-0.4613[b]					
Copper	-0.3870	0.3500	0.1133				
Nickel	-0.4250	0.3895	0.0681	0.9850[a]			
Lead	0.1473	-0.0285	0.8091[a]	0.5240[a]	0.4967[b]		
Zinc	0.0471	-0.1624	0.3369	0.2893	0.2745	0.5472[a]	
Iron	0.0663	0.1402	0.7061[a]	0.7488[a]	0.7054[a]	0.8999[a]	0.3380

[a]Significant at the 95 percent confidence level

[b]Correlations considered marginally significant if equal to or larger than the average cross correlation

TABLE 36

Correlation Coefficients of Measured Precipitation Chemistry Concentrations to Distance from Source and to Calculated Concentrations (15 sites)

Pollutant Species	Correlation Coefficients				
	meas/min calc	meas/max calc	meas/distance[c] conc log conc	meas/event time	meas/angle to the wind
Sulphate	0.1292	-0.0113	-0.2878	0.343	0.204
pH	0.3521	0.4992[b]	0.6417	0.588[a]	0.639[a]
Copper	0.9117[a]	0.9008[a]	-0.8504[a]	-0.264	-0.279
Nickel	0.5937[a]	0.8731[a]	-0.8181[a]	-0.249	-0.326
Lead	-0.0316	-0.1568	-0.4083	0.164	-0.066
Zinc	-0.1136	-0.1898[b]	-0.1810	0.014	0.098
Iron	0.7035[a]	0.6191[a]	-0.6827[a]	-0.070	-0.214

[a] Significant at the 95 percent confidence level

[b] Considered significant if larger than the correlation with distance or the average correlation with distance

[c] For receptors up to 150-kilometre distance. Beyond 150 kilometres observed improvements in correlations are deemed spurious

Eight significant and two marginally significant pairs of constituents are indicated by the cross-correlation matrix for measured precipitation chemistry (Table 35), six were expected. The six expected constituent pairs are: pH or hydrogen ion and sulphate, sulphate and iron, copper and nickel, copper and iron, nickel and iron, and zinc and lead.

The oxidation of sulphur dioxide to sulphate in the atmosphere is indicated to be a major source of hydrogen ion in precipitation near Sudbury. Common sources are indicated for sulphur, iron, copper and nickel, all products of the Sudbury smelters. These elements are the major constituents of the ore minerals smelted in the Sudbury Basin. Zinc and lead are assumed to be products of the urbanization of the Sudbury Basin (lead is also a significant smelter effluent).

The presence of iron in the copper/nickel sulphide ores (a mixture including pentlandite, chalcopyrite and pyrrhotite) mined at Copper Cliff and Falconbridge is sufficient to produce a significant correlation of iron and sulphur in precipitation, even when the effects of the major iron and sulphur source at Wawa are ignored in calculations.

As illustrated in Table 31, nickel and sulphur dioxide concentrations in the atmosphere exhibit a strong positive correlation, while in precipitation (Table 35), nickel and sulphate exhibit no significant correlation. This negative evidence indicates that the oxidation of sulphur dioxide to sulphate is not linearly related to the concentration of nickel. Nickel, and the other trace metals present, may play a role as catalysts (Cheng et al, 1971).

Three meteorological and geographical parameters controlling precipitation chemistry were chosen to illustrate the degree of correlation between driving parameters and precipitation chemistry. The three parameters chosen exhibited the highest ratio of standard deviation to total range (Table 29). This aided in the calculation of reliable correlation coefficients. The three parameters are: distance from the source to the receptor, precipitation event time or duration, and the angle made by the mean wind direction with the vector from the source to the receptor (Table 36). Distance was chosen as a plotting parameter instead of plume travel time since the average wind velocity and direction, averaged over the approximately 3-year study period, varied little over the 27 receptor sites in the study area (Table 29). Therefore

plume travel time and distance from source to receptor are equivalent in the study areas. Averaged over the study period, total rain volume per sample period, average rainfall rate, windspeed and heading variability over 24 hours exhibited only small ranges of values over the 27 receptor sites in the study area (Table 29).

Copper, nickel, lead, zinc, and iron concentrations in precipitation correlate more strongly with distance than with precipitation event duration or with the wind heading angle (Table 36). The correlation of distance to measured precipitation zinc concentration is weak. Measured sulphate concentrations in precipitation correlate almost equally well with distance, precipitation event duration and with wind heading angle (Table 36). Plume travel time, and therefore sulphur dioxide oxidation time, deposition by rainfall scavenging, and crosswind dispersion by daily wind variability and eddy diffusion are all of nearly equal importance to the average measured pH and sulphate concentration in Sudbury area precipitation.

The very weak correlation of zinc with all three parameters indicates a zinc source that is not associated with the Sudbury smelters, such as other smelters outside the Sudbury area, and the possible reentrainment of soil and surface dust.

Significant correlations are indicated between pairs of measured and calculated concentrations of copper, nickel and iron in precipitation (Table 36). These correlations indicate the level of accuracy attained by the model in predicting concentrations of these metals. Weaker but still significant correlations are exhibited by pairs of measured and calculated values for pH and zinc concentrations in precipitation (Table 36).

4.2 - Lake Model

4.2.1 - Lake Characteristics and Driving Parameters

The basic driving parameters for lake water and sediment concentration calculations are the precipitation chemistry calculations performed by the atmospheric model program. The lakes and lake basins are treated in calculations as if they were very large rainfall receptors, so few additional parameters are required to make the relatively simple calculations. These additional parameters fall into two classifications

- basic calculation parameters
- lake and lake basin parameters.

Basic calculation parameters are parameters that are

assumed to be constant for all the lakes examined, and lake and lake basin parameters are those parameters that vary from lake to lake. Basic parameters are the evaporation rate, the bulk sedimentation rate, the sedimentation rates for the five metal particulates: copper, nickel, lead, zinc, and iron (Table 22), their background levels in sediments (Table 23), and the background level of the five metals and sulphate in lake water (Table 21). The lake basin parameters are latitude and longitude of the approximate centre of the lake basin, the area of the lake basin, the area of the lake, the depth of the lake, and the estimated area of water surfaces upstream of the lake. These parameters are estimated by tracing basin and lake outlines on topographic maps (EMR, 1975a, 1975b, 1975c) with a planimeter. Lake depths utilized in the model are depths at the position sampled, or an assumed figure of 10 meters for those lakes that were not accessible by road or float plane.

A series of small, relatively unbuffered lakes, were chosen for study in order to verify results of model predictions for lakes. These lakes have small drainage basins relative to the lake's surface areas, are all sited in the orthoquartzite of the Lorraine formation, and had only atmospheric input. A second series of lakes of various sizes, drainages, and lake basin geologies in the same area

were also investigated, primarily to indicate the relative importance of buffering capacity mediated by geology on trace metal chemistry (Kramer, 1971). Lake locations are indicated in Figures 6, 28 and 29. Figure 6, as previously noted, is a general map of the study area, including an indication of the area of the study lakes. Figure 28 is a larger scale map of the detail area of Figure 6, indicating the locations of most of the smaller study lakes in relation to the Lorraine quartzite ridges of the LaCloche mountains, the north channel of Lake Huron, and the important towns of the area. Most of the small unbuffered lakes are located in a small, approximately 30 km^2 area of the LaCloche mountains south and east of Lake LaCloche. This area is shown in more detail in Figure 29. Lake locations and some basic characteristics are listed in Table 37. The larger lakes are listed by names given on topographic maps (EMR, 1975a, 1975b and 1975c). The majority of the small unbuffered lakes are not officially named, and are designated by numbers (Figure 29, Table 37). Exceptions are White's Lake A, a small lake immediately to the northeast of White's Lake, and Microwave Lake, where Highway 68 crosses the LaCloche mountain ridge 2 kilometres north of the village of Whitefish Falls, Ontario. Both names are unofficial, and are used as convenient designations for the purpose of this study.

FIGURE 28
LAKES SAMPLED, IN AND NEAR THE LACLOCHE MOUNTAINS

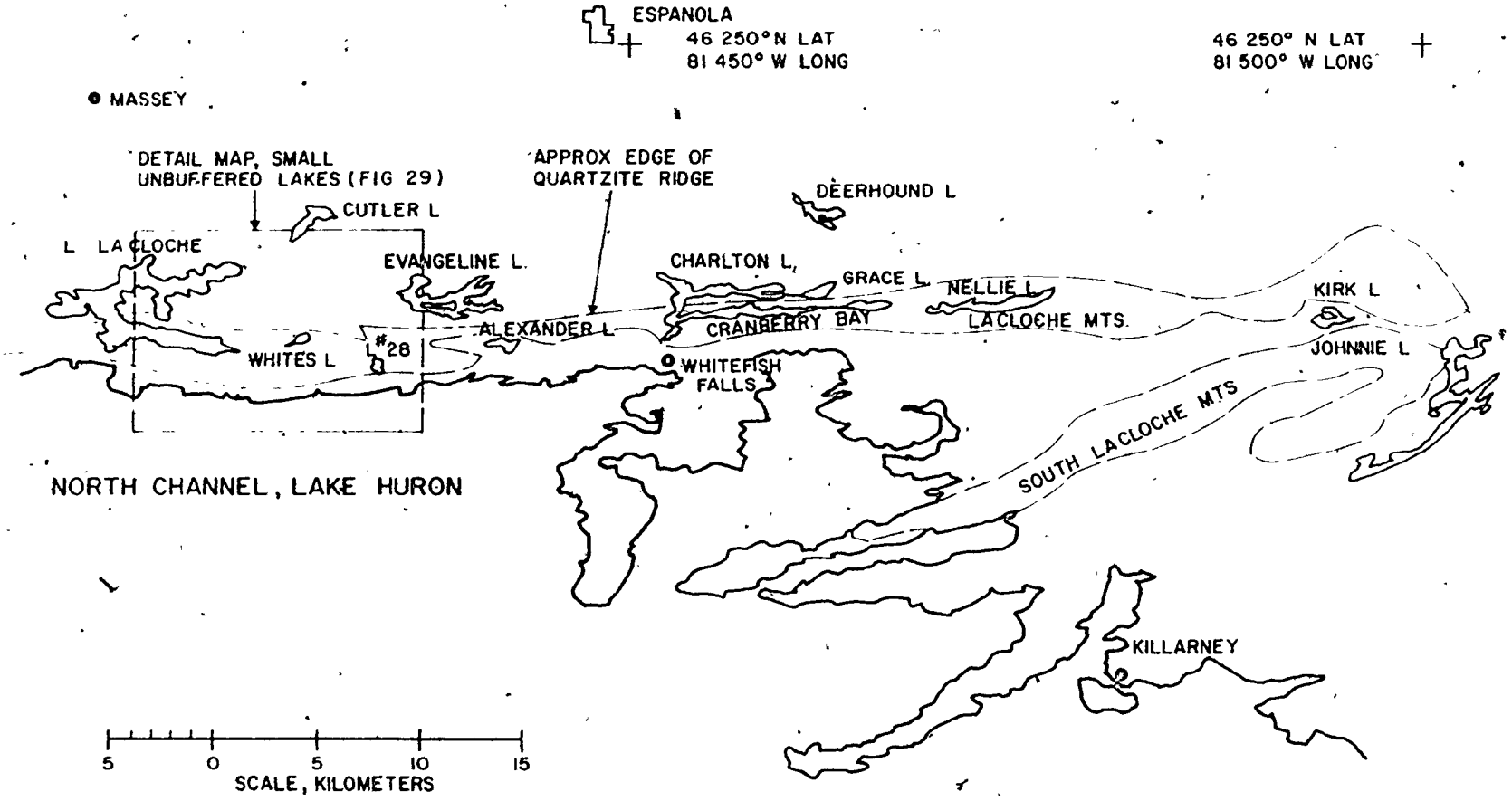

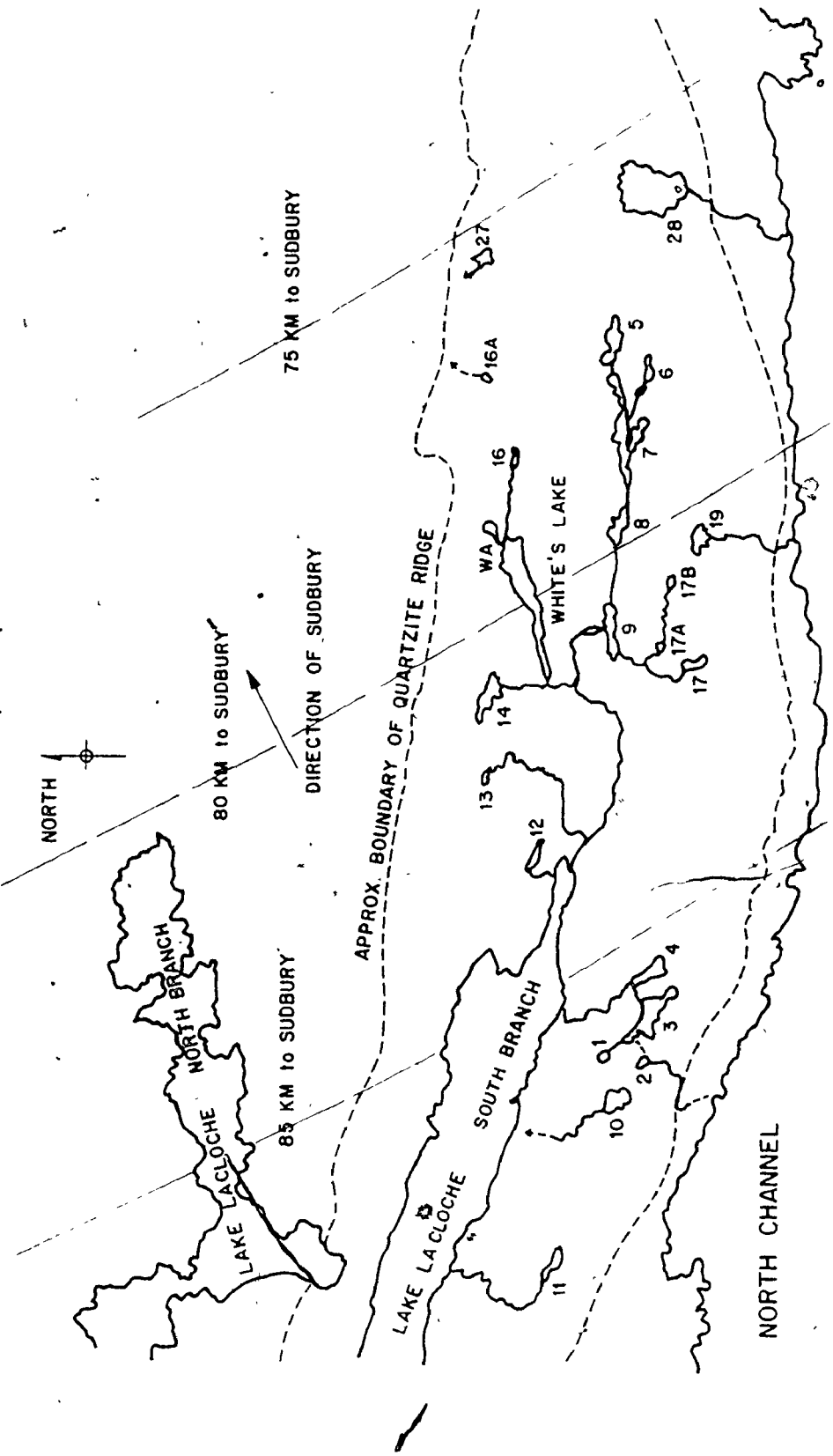

FIGURE 29
LOCATION OF QUARTZITE RIDGE STUDY LAKES, 1976; F.J. HUHN

Included in Table 37 are lake names, (with an indicator for lakes considered to be unbuffered for the purpose of this study), the latitude and longitude of the approximate center of the lake basin, the approximate relative proportion of the lake basin on the Lorraine quartzite formation of the LaCloche mountain ridge, measured alkalinity, pH, sulphate ion concentration, conductivity, lake and lake basin areas, and lake depths. In addition measured concentrations of total phosphate, total nitrate and nitrite, total suspended particulates, and chlorophyll a concentrations are listed to indicate the relative level of biological activity in the lakes. Quartzite ridge area, alkalinity, conductivity and pH are indicators of the relative buffering capacity of the lakes. Sulphate ion concentrations indicate atmospheric inputs. Only the basic geographical parameters of the lakes are utilized in the calculation of pollutant mass balances (location, distance from estimated lake basin centre to source, basin area, lake surface area, and lake depth). In addition to the major driving parameters of the lake model, basin geology affects water chemistry. This is illustrated by Table 38. Also illustrated by Table 38 are the spurious correlations between percentage quartzite ridge and distance and between lake basin size and distance. These real and apparent parameter interrelations must be noted when assessing measured lake water and sediment chemistry.

TABLE 37

Locations and Major Characteristics of Study Area Lakes

Lake Designation	Location Lat (deg)	Location Long (deg)	Distance (km)	Basin Area (km^2)	Lake Area (km^2)	Lake Depth (m)	Quartzite Ridge Area (percent)	Alkalinity (mg/L $CaCO_3$)	Conductivity (umho)	pH	Sulphate (10^{-6} gm/cm^3)	Total PO_4 (ug/L)	Total NO_3 and NO_2 (ug/L)	Total Particulates (mg/L)	Chlorophyll a (ug/L)
LaCloche N	46 147	82 008	78 5	1 435	62 50	5.5	21 0	6.24	50 0	7 05	11 4	11 5	-	2 180.0	1.10
LaCloche S	46 117	82 000	85 0	1 777	56.50	15.2	85.5	4.06	48.4	6.85	10.0	8.2	4 0	296.0	1.12
Johnnie 1*	46 067	81 250	38 6	1 024	11.20	23 0	48 5	0 37	44.0	4 85	13 1	5.5	-	15 2	0.47
Johnnie 2*	46 133	81 183	40 5	1 362	49 50	11.5	27.0	0.84	44.0	4 70	12 1	4.9	-	14 7	-
Evangeline E	46 138	81 850	71 3	447	42.7	5 5	25 0	8 72	45 0	6 40	11 5	31.0	-	13 3	0.08
Evangeline W	46.138	81 850	71.3	447	42 7	13.3	25.0	2.18	52.0	6 92	13.8	10.3	-	10.4	1 17
Cranberry Bay	46 132	81.633	59.0	65	6.50	5.8	99	1 62	46 0	6.10	11 8	15.8	-	14.2	1.11
Charleton	46.158	81.517	50.3	1 131	11 50	11 0	33 5	1.94	65 0	6.82	14 5	8.5	-	9.3	0 71
Cutler	46 167	81 950	77 0	72	11 70	5 7	0	2 70	58.0	7.15	11 5	13 0	-	2 060 0	0.74
Deerhound	46 175	81 625	55.3	92	12 30	5 5	0	6 87	55.0	7.50	11 2	11 7	-	2 565 0	2 63
Kirk*	46.093	81.300	44.0	149	8 00	5.5	83 5	1 04	35.0	4 81	10.4	6 0	-	9 1	0 26
Microwave*	46 125	81 744	-	1 9	0 25	-	100	-	36 3	4 28	8.4	15 8	-	840 0	-
Alexander	46 113	81 837	73 5	59	5 00	10.0	78	2 58	42 0	6 81	10 7	6 3	-	1 440 0	0.38
White's	46.117	81.950	79.4	23.3	1 87	10 0	100	2.24	44.3	6 43	9 1	7.1	5.5	564.0	0.71
Grace*	46 133	81 598	56 5	29	5 20	12 5	100	1 24	41 0	4 72	12 3	4 0	-	815 0	0.53
Nellie*	46.133	81 500	50.8	152	26.80	45.0	100	0.63	55 0	4 38	11 8	2.9	-	695 0	0 15
White's A	46 118	81 950	79 0	1 0	0 50	-	99	1 80	25 0	5.79	9.4	8 0	1.5	7 5	1 23
Lake 1*	46 105	82 020	86 5	0 8	0.33	-	100	1 17	35 2	4 20	9 2	5 4	145 0	7 5	3 15
Lake 2*	46 105	82 020	86.7	0 8	0 25	-	100	1 07	43 5	4 12	8.3	4.1	93.5	0.5	0.03
Lake 3*	46 105	82 015	86 0	3 8	1.00	-	100	0 55	43 5	4 30	11 0	2 4	100 0	1 0	0 58
Lake 4*	46 103	82.004	85 5	13 0	0 83	-	100	0 98	33.8	4.62	10 1	4.5	3.0	8 0	0 39
Lake 5*	46.110	81.926	77 5	4 4	-	-	99	0 74	26.0	4.65	10.4	28 0	4 5	3.6	2.45
Lake 6*	46 107	81 927	78.1	2.2	0.33	-	99	0 90	29 3	4 33	9.5	10.0	4 0	4.5	1.58
Lake 7*	46.108	81 940	78.5	16 8	1 50	-	99	0 84	29 8	4 55	8 9	6 8	25.5	2 5	1 03
Lake 8*	46 108	81 948	79 8	25.5	0 67	-	99	0.94	27 8	4 82	9 0	3.2	10 0	2 0	0 56
Lake 9*	46 108	81 958	81 0	41 7	0 50	-	99	1 09	19 0	4 70	9 4	6 0	1 0	3 6	0 25
Lake 10	46 107	82.026	87 0	2 0	0 70	-	100	6.79	37 0	4 30	11 0	1 5	71 5	2 2	0.72
Lake 11	46 113	82 044	89 0	1 8	0 65	-	100	2 86	25 5	6 10	7 8	6 8	4 5	4 0	0 67
Lake 12*	46 117	81 988	83.5	1.0	0.63	-	100	0 93	36 5	4 22	12 0	4.7	10 0	3 5	0 58
Lake 13*	46 118	81 980	8. 0	0 5	0 30	-	100	0 27	48 5	4 19	9 4	10 0	1 0	13 5	2 69
Lake 14*	46 118	81.969	81 0	4 1	0 90	-	100	0 10	26.0	4.50	10 4	4 0	25 5	7 0	0 55
Lake 16	46 118	81 938	78 0	1 2	0.28	-	98	1 45	24 0	5.70	8 4	5 0	24 5	5 6	2.11
Lake 16A*	46 120	81 920	77 0	0 3	0 15	-	85	0 70	22 5	4 39	7.2	9 5	10 0	5 9	0 72
Lake 17*	46 102	81 799	82 0	0 8	0 33	-	100	0 94	37 5	4 71	12 6	6.0	88 5	4 0	3.79
Lake 17A*	46 103	81.798	81 5	0 1	0 20	-	99	1 17	30.5	4 34	7 2	22 0	5 5	9 5	1.25
Lake 17B*	46 105	81 790	81 0	0 8	0.20	-	99	1 84	21 5	4 90	6 2	47 0	4 0	12 0	5.71
Lake 19	46 100	81 785	80 5	4 0	0.65	-	100	0.69	29.5	4 55	10.4	2 0	8 0	9 0	0 48
Lake 27*	46.122	81 913	75 5	0 5	-	-	100	0.69	33 5	4.31	12 4	18.0	45 5	5 0	0.72
Lake 28	46 113	81 006	78 0	18 0	1.75	-	85	2.19	33.0	6.15	10 4	2.5	12.5	4.0	0.96

*Designates lakes considered to be relatively unbuffered

A cross correlation matrix was constructed to compare the major driving parameters of the atmospheric model: distance from the source, percent quartzite ridge in the lake basin, and lake basin area, with total alkalinity, conductivity, and pH. Percentage of quartzite ridge in the lake basin is assumed to have an important effect on the buffering capacity of the lake (Semkin, 1975; Conroy, 1971). The pH, known to be a controlling factor in lake water chemistry (Stumm and Morgan, 1970), is assumed to be in part an air pollution controlled factor (Table 38).

It was expected that distance and pH would exhibit a significant correlation, that total alkalinity and pH would exhibit a significant correlation, but that distance and basin area, distance and percent of quartzite ridge in the lake basin, would not exhibit any significant degree of correlation. As expected pH (expressed as hydrogen ion concentration) exhibited significant correlation with distance from the smelters. Total alkalinity and pH did not exhibit a significant correlation, due to the very low buffering capacity of these small lakes.

Eleven pairs of parameters, out of a possible 15, exhibited correlation coefficients significant at the 95 percent confidence level (Table 38). Plausible connections

exist between the elements in eight of the pairs exhibiting significant correlations. The eight parameter pairs are: conductivity and distance from the source, percent quartzite ridge and total alkalinity, percent quartzite ridge and pH, percent quartzite ridge and conductivity, total alkalinity and conductivity, pH and conductivity, basin area and conductivity, pH and basin area. Two pairs of parameters exhibit spurious correlations. These two parameter pairs are: distance and percent quartzite ridge in the lake basin, and lake basin area and distance. These spurious correlations are due to the character of the 39 lake sample chosen for study. All of the very small lakes are in the Lorraine formation quartzite ridge near Massey, Ontario, at distances from Sudbury between 75 and 90 kilometres (Figure 29). All the larger lakes, in softer bedrock or unconsolidated sediments are closer to Sudbury (Figure 28). This size and distance distribution is the cause of the observed spurious correlations. The two spuriously correlating pairs are linked by a correlation between percent of quartzite ridge in the lake basin and the size of the lake basin (Table 38).

The existence of these spurious correlations must be considered in examining correlation coefficients of measured and calculated pollutant concentrations in lake water.

TABLE 38

Significant and Spurious Cross Correlations of Controlling Parameters for Lake Water Measured Pollutant Species Concentrations (39 lakes)

Pollutant Species	Distance Linear	Exponential	Percent Quartzite Ridge	Total Alkalinity	Conductivity	pH
Percent quartzite ridge	0.515[a]	0.163				
Total alkalinity	0.038	0.057	-0.537[b]			
Conductivity	-0.459[b]	-0.421[b]	-0.639[b]	0.335[b]		
pH	-0.161	-0.793[b]	-0.678[b]	0.081	0.505[b]	
Basin area	-0.391[a]	-0.636[a]	-0.542[a]	0.289	0.488[b]	0.421[b]

[a]Relatively large spurious correlations

[b]Significant at the 95 percent confidence level

4.2.2 - Lake Water Concentrations

Cross correlation matrices were constructed for measured pollutant species concentrations in lake water (Table 39). The purpose of this study was to indicate to what degree the common sources for sulphate, hydrogen ion, copper, nickel, and iron would be exhibited in lake water. This provides an indication of the validity of the measured lake water concentrations as a check on concentrations calculated by the model. Two cross correlation matrices were constructed, one for the 15 large, relatively well buffered lakes not in the Lorraine quartzite ridge, and one for all 39 lakes examined. Pairs expected to exhibit relatively significant correlations were: pH and sulphate, pH and copper, pH and nickel, pH and iron, sulphate and copper, sulphate and nickel, sulphate and iron, copper and nickel, nickel and iron. On lake water zinc concentrations, pH was also expected to have a controlling influence, but not as an indicator of a common source. For the total 39 lake sample, 7 significant and 4 marginally significant correlations out of a possible 21 were observed. Six of these pairs were expected: pH and copper, pH and nickel, pH and zinc, sulphate and iron, and copper and nickel. Of the other 5 significant and marginally significant correlations observed, all are plausible if it is considered that pH exerts a controlling influence on both members of the pair (Table 39).

TABLE 39

Cross Correlations Between Pollutant Species, for Measured Lake Water Concentrations

15 relatively well buffered lakes (upper values)
39 lakes total (lower values)

Pollutant Species	pH	Sulphate	Copper	Nickel	Lead	Zinc
Sulphate	0.086					
	0.311[b]					
Copper	-0.219	-0.517[a]				
	-0.353[a]	-0.569[a]				
Nickel	-0.842[a]	0.110	0.298[b]			
	-0.293[b]	0.024	0.408[a]			
Lead	0.043	0.173	-0.038	-0.250[b]		
	0.020	0.308[b]	-0.350[a]	-0.031		
Zinc	-0.249[b]	0.175	0.222	0.249[b]	0.303[b]	
	-0.459[a]	-0.174	0.291[b]	0.062	0.168	
Iron	0.146	0.248[b]	-0.125	-0.282[b]	0.559[a]	0.212
	-0.166	-0.372[a]	0.134	-0.091	0.184	0.425[a]

[a]Significant at the 95 percent confidence level

[b]Correlations considered significant if equal to or larger than the average cross correlations measured for the total 39 lake sample

For the smaller sample of 15 lakes with basins not confined to the Lorraine quartzite, 3 significantly and 7 marginally correlated pairs were observed (Table 39). Five of these pairs are the same as for the total lake sample. These pairs are: pH and nickel, pH and zinc, sulphate and copper, sulphate and iron, and copper and nickel. Copper and sulphate correlate equally well in the total lake and the small lake sample, indicating the same reason , probably their common source, for the correlation in each sample. The degree of correlation changes by large factors, in the case of iron and sulphate changing from a significant negative correlation in the total lake sample to a positive correlation in the 15 lake sample. This is indicative of different factors controlling the concentrations of iron, zinc, and nickel in the large and in the small lakes.

In the relatively unbuffered small lakes significant correlations may be largely controlled by common source relationships through atmospheric deposition, while in the relatively well buffered large lakes, pH may be controlled by the varied characteristics of the different lake basins.

In the total 39 lake sample, pair correlations are significant enough to allow the conclusion that pH, sulphate, copper, nickel, and iron have sources in common, and that

iron and zinc have sources in common. When the small and distant lakes in the Lorraine quartzite ridge are excluded, this pattern is more clearly observed.

Concentrations measured in the 39 lakes and model calculations of concentrations of sulphate, copper, nickel, lead, zinc, iron, and hydrogen ion, expressed as pH, are compared in Tables 40 and 41. Table 40 is a comparison of measured and calculated sulphate ion concentration and pH in lake water. Measured values are averages of from 2 to 6 measurements for the named lakes. With the exception of White's and White's A, measurements are averages of near surface and near bottom samples. The numbered lakes were all sampled near the surface only. White's Lake, Lakes 1 through 4, and Lakes 6 through 9 were sampled twice in succeeding years. Calculated concentrations and pH are expressed as maximum and minimum calculated values, and sulphate concentrations are in units of micro grams, or 10^{-6} grams, per cubic centimetre.

Table 41 is a comparison of measured and calculated copper, nickel, lead, zinc, and iron concentrations, with concentrations expressed in units of nanograms, or 10^{-9} grams, per cubic centimetre. The same samples were used to determine the measured values in both Tables 40 and 41.

TABLE 40

Comparison of Calculated and Measured pH and Sulphate ion in Lake Water

Lake Designation	Sulphate, 10^{-6} gm/cm^3 Meas.	calc (min-max)	pH Meas.	calc (min-max)
LaCloche N	11.4	3.89-6.63	7.05	5.08-6.23
LaCloche S	10.0	3.75-5.48	6.85	5.30-6.64
Johnnie 1	13.1	4.02-11.72	4.85	4.66-6.03
Johnnie 2	12.1	3.94-7.74	4.70	4.95-6.15
Evangeline E	11.5	3.76-4.67	6.40	5.55-6.60
Evangeline W	13.8	3.73-4.10	6.92	5.92-6.82
Cranberry Bay	11.8	3.77-5.13	6.10	5.39-6.57
Charleton	14.5	4.25-11.80	6.82	4.65-5.82
Cutler	11.5	3.74-4.33	7.15	5.74-6.73
Deerhound	11.2	3.76-4.77	7.50	5.52-6.64
Kirk	10.4	3.80-5.02	4.81	5.54-6.48
Microwave	8.4	3.73-4.20	4.27	5.83-6.82
Alexander	10.7	3.74-4.42	6.81	5.68-6.71
White's	9.1	3.74-4.34	5.71	5.73-6.70
Grace	12.3	3.72-4.06	4.72	5.96-6.88
Nellie	11.8	3.71-3.80	4.38	6.43-6.99
White's A	9.4	3.71-3.87	5.79	6.25-6.95
Lake 1	9.2	3.71-3.91	4.20	6.18-6.44
Lake 2	8.3	3.71-3.91	4.12	6.17-6.93
Lake 3	11.0	3.72-3.99	4.30	6.05-6.88
Lake 4	10.1	3.76-4.52	4.62	5.62-6.63
Lake 5	10.4	3.72-4.03	4.65	6.00-6.86
Lake 6	9.5	3.72-4.06	4.33	5.97-6.85
Lake 7	8.9	3.74-4.29	4.55	5.76-6.73
Lake 8	9.0	3.83-5.57	4.82	5.27-6.83
Lake 9	9.4	3.97-7.57	4.70	4.96-6.10
Lake 10	11.0	3.71-3.90	4.30	6.19-6.93
Lake 11	7.8	3.71-3.90	6.10	6.19-6.94
Lake 12	12.0	3.71-3.86	4.22	6.28-6.96
Lake 13	9.4	3.71-3.86	4.19	6.28-6.96
Lake 14	10.4	3.72-3.96	4.50	6.09-6.89
Lake 16	8.4	3.72-3.96	5.70	6.10-6.90
Lake 16A	7.2	3.71-3.88	4.39	6.23-6.95
Lake 17	12.6	3.71-3.94	4.71	6.13-6.93
Lake 17A	7.2	3.73-4.23	4.39	5.81-6.80
Lake 17B	6.2	3.72-4.02	4.90	6.01-6.90
Lake 19	10.4	3.72-4.13	4.55	5.90-6.85
Lake 27	12.0	3.72-4.13	4.55	5.90-6.85
Lake 28	10.4	3.73-4.20	6.15	5.83-6.78

TABLE 41

Comparison of Calculated and Measured Metal Concentrations in Lake Water

Lake Designations	Concentrations									
	Copper, 10^{-9} gm/cm^3		Nickel, 10^{-9} gm/cm^3		Lead, 10^{-9} gm/cm^3		Zinc, 10^{-9} gm/cm^3		Iron, 10^{-9} gm/cm^3	
	Meas	calc (min-max)	Meas	calc (min-max)	Meas	calc (min-max)	Meas	calc (min-max)	Meas	calc (min-max)
LaCloche N	2.5	0.84-7.35	1.3	0.46-16.77	1.1	0.76-4.05	17.5	6.07-32.29	80.0	25.94-139.42
LaCloche S	2.3	0.63-10.85	1.0	0.32-8.89	2.2	0.47-3.88	16.7	3.71-29.91	65.3	14.91-107.74
Johnnie 1	2.0	1.82-93.97	4.3	0.84-40.71	2.7	0.47-2.14	12.0	3.99-20.00	71.3	24.65-190.04
Johnnie 2	1.9	4.02-81.63	4.2	1.20-26.08	1.9	0.53-2.39	13.8	4.33-20.37	55.8	21.41-115.64
Evangeline E	2.7	0.66-9.78	1.5	0.33-6.10	3.0	0.57-2.60	27.0	4.36-19.59	310.5	16.15-64.43
Evangeline W	1.0	0.57-4.33	1.0	0.29-2.67	1.9	0.38-1.22	8.5	2.97-9.26	258.3	11.95-31.87
Cranberry Bay	1.9	0.79-40.86	1.9	0.40-7.57	1.6	0.57-2.64	9.1	4.42-20.25	85.3	16.53-80.85
Charleton	1.5	5.93-153.82	3.1	3.20-26.26	1.9	1.26-7.78	22.7	10.30-63.66	71.3	46.81-346.72
Cutler	1.5	0.60-6.03	2.0	0.30-4.44	1.1	0.45-1.77	4.8	3.52-13.35	59.0	13.56-44.20
Deerhound	0.8	0.64-26.07	1.3	0.33-7.74	1.1	0.51-2.16	3.1	3.93-16.52	45.5	14.85-61.33
Kirk	1.0	0.76-30.35	3.4	0.38-5.82	1.6	0.69-3.21	15.0	5.28-24.48	65.0	18.70-90.96
Microwave	4.3	0.57-10.74	4.3	0.29-3.81	1.8	0.38-1.25	13.0	3.00-9.51	114.5	12.00-34.70
Alexander	1.8	0.61-10.07	2.3	0.31-5.28	1.5	0.46-1.80	6.3	3.56-13.65	29.5	13.77-47.23
White's	6.8	0.62-4.71	1.3	0.31-3.22	1.1	0.48-1.96	8.8	3.72-14.77	23.3	14.17-48.39
Grace	2.5	0.63-11.26	5.4	0.31-1.86	0.5	0.34-0.90	16.3	2.65-6.90	30.5	11.00-28.07
Nellie	7.0	0.65-3.14	5.5	0.33-0.56	0.5	0.28-0.44	19.0	2.20-3.46	88.8	9.68-14.60
White's A	7.3	0.53-1.64	2.8	0.27-1.05	1.2	0.31-0.72	16.0	2.47-5.51	64.2	10.41-19.76
Lake 1	9.6	0.53-2.24	3.0	0.27-1.59	1.5	0.32-0.76	39.0	2.51-5.82	138.0	10.53-20.82
Lake 2	18.1	0.54-1.86	4.1	0.27-1.29	1.5	0.33-0.84	32.0	2.59-6.36	113.0	10.75-22.33
Lake 3	7.4	0.55-2.34	9.8	0.28-1.64	2.1	0.36-1.04	42.8	2.79-7.89	94.5	11.40-27.24
Lake 4	7.4	0.65-5.44	5.4	0.33-3.93	2.1	0.54-2.44	27.5	4.22-18.50	55.0	15.88-60.68
Lake 5	3.0	0.56-3.25	0.8	0.28-2.10	2.1	0.36-1.10	12.0	2.85-8.33	140.0	11.54-28.58
Lake 6	4.8	0.56-3.55	1.7	0.28-2.30	2.6	0.37-1.16	160.0	2.91-8.80	276.0	11.73-30.06
Lake 7	5.3	0.60-5.06	2.4	0.30-3.40	1.1	0.45-1.75	24.0	3.51-13.24	82.0	13.57-44.08
Lake 8	3.0	0.82-14.15	1.4	0.42-9.89	1.5	0.88-4.93	25.3	8.74-37.27	40.0	23.60-120.78
Lake 9	4.8	1.18-26.94	1.1	0.62-19.23	0.5	1.55-9.98	18.5	11.86-75.31	150.0	39.55-242.26
Lake 10	12.3	0.54-1.84	2.4	0.27-1.28	1.1	0.32-0.80	39.0	2.55-6.12	70.0	10.66-21.61
Lake 11	20.2	0.54-1.95	11.4	0.27-1.40	0.5	0.32-0.79	9.0	2.55-6.06	95.0	10.63-21.46
Lake 12	7.8	0.53-1.56	9.5	0.27-1.04	2.1	0.31-0.68	87.8	2.43-5.22	128.0	10.30-18.87
Lake 13	6.0	0.53-1.57	5.6	0.27-1.03	1.1	0.31-0.69	77.5	2.49-5.28	353.0	10.32-19.04
Lake 14	8.8	0.55-2.18	1.4	0.28-1.49	1.1	0.35-0.96	115.0	2.71-7.31	76.0	11.14-25.24
Lake 16	8.8	0.55-2.32	3.6	0.27-1.51	0.0	0.34-0.94	34.0	2.69-7.12	75.5	11.06-24.72
Lake 16A	9.0	0.53-1.93	1.9	0.27-1.22	0.5	0.31-0.72	33.5	2.47-5.52	90.0	10.41-19.85
Lake 17	9.2	0.53-4.26	4.5	0.27-1.97	1.5	0.32-0.76	90.0	2.51-5.83	55.0	10.53-21.54
Lake 17A	10.6	0.57-10.34	3.1	0.29-3.95	1.5	0.39-1.32	87.5	3.07-10.02	498.0	12.24-36.32
Lake 17B	11.4	0.54-6.80	2.1	0.27-2.51	1.1	0.34-0.91	53.5	2.86-6.95	490.0	10.98-25.83
Lake 19	14.7	0.56-8.83	2.6	0.28-3.22	1.1	0.37-1.11	45.5	2.86-8.48	40.0	11.59-31.04
Lake 27	4.9	0.53-2.15	2.6	0.26-1.29	1.1	0.30-0.66	22.0	2.41-5.03	40.0	10.22-18.47
Lake 28	9.1	0.58-5.02	1.2	0.29-3.20	1.5	0.42-1.50	39.0	3.25-11.34	33.0	12.75-38.04

Calculated values of sulphate ion are consistently 25 to 50 percent of measured concentrations, which reflects the ratio of calculated to measured atmospheric loading rates for sulphate (approximately 26 to 90 percent).

Calculated pH values are lower than measured for the larger and better buffered lakes, but higher than measured pH values for the smaller and very poorly buffered lakes on the Lorraine quartzite ridge. This is due to differences in actual buffering capacities and errors in retention time and initial pH estimates. The lakes on the Lorraine quartzite ridge have virtually no buffering capacity: those of the other lakes vary.

Retention time is based on lake depth , which was estimated for the ridge lakes, assuming no retention in the drainage basin. The model runs for one retention time period, assuming an initial pH of 7.0. Other factors include an incorrect assumption for NH_4^+ concentrations in precipitation (Section 3.1.5).

Sulphur dioxide oxidation and other aspects of aquatic sulphur chemistry were not considered in calculating lake water pH. The interactive chemistry of pH and trace metals was ignored in lake water and sediment chemistry calculations.

Correlations between calculated and measured concentrations in lakes are expected to be weaker than the correlations observed between measured and calculated precipitation concentrations. There are three reasons for this expectation

- the smaller sample size and temporal extent of the measured lake sample
- the entrance into the system of a large number of uncontrolled and poorly documented or understood variables
- lake water chemistry predictions are calculated utilizing atmospheric model predictions.

The choice of very small lakes on the Lorraine quartzite ridge formation was an effort to minimize some of these variables, chiefly pH control by lake basin factors and the entrance into the lake of pollutant species by non-atmospheric fallout routes. It was expected therefore, that correlations of measured and calculated concentrations would be stronger for the total 39 lake sample, including the relatively unbuffered lakes. This was not observed to be the case (Table 42). A comparison of measured and calculated lake water concentrations, for the 15 large lake basin (greater than 50 km^2), and for the total 39 lake sample, indicates only three pollutant species for which the calculations correlate significantly with the measurements, which are sulphate, pH and copper. Correlation

TABLE 42

Correlation Coefficients of Measured Lake Water Concentrations to Calculated Lake Water Concentrations, and to Distance from Source, Total Alkalinity, and Lake Basin Surface Area

Pollutant Species	Correlation Coefficients Meas/Calc min 15 large lks[c]	Meas/Calc min All 39 lks	Meas/Calc max 15 large lks[c]	Meas/Calc max All 39 lks	Meas/Distance Conc	Meas/Distance Log conc	Meas/Total Alkalinity	Meas/Basin Area
Sulphate	0.6029[a]	0.4348[a]	0.5758[a]	0.4516[a]		-0.5238[a]	0.131	0.409[a]
pH	-0.4220	-0.4621[a]	-0.2685	-0.2808	-0.161		0.081	0.425[a]
Copper	-0.2295	-0.2997	-0.3424	-0.3855[a]		0.6581[a]	-0.148	-0.404[a]
Nickel	0.1964	-0.0155	0.2683	-0.0832		-0.3062	-0.192	-0.136
Lead	0.2560	0.0276	0.3571[b]	0.0636		-0.0608	0.115	0.351[a]
Zinc	0.3595	-0.2429	0.3821[b]	-0.2576		0.3695[a]	-0.275[a]	-0.254
Iron	-0.0751	-0.0886	-0.1028	-0.1444		0.2111	0.022	-0.115

[a] Significant at the 95 percent confidence level

[b] Considered to be significant if larger than the correlation coefficient of measured concentrations to distance from source, to total alkalinity, or to lake basin area

[c] Lakes with drainage basins larger than 50 km^2

coefficients for measured and calculated lead and zinc are marginally significant in lake water. Correlations of measured and calculated lead and zinc concentrations are negligible for air and precipitation. For all three cases the 15 lake sample exhibits a better correlation. This and the fact that lead and zinc are not important atmospheric emissions from the smelters at Sudbury, indicate that distance from the source may not be the controlling factor in determining measured lake water concentrations. For example, measured zinc values exhibit significant correlation with total alkalinity, and lead is significantly correlated with basin area (Table 42). Also compared in Table 42 are the correlation coefficients of measured concentrations in lake water to distance, to total alkalinity, and to basin area. Correlations with distance are strong with sulphate, copper, and lead. Correlations with basin area are strong for sulphate, pH, copper, and zinc. Correlations between measured concentrations and total alkalinity are uniformly weak. The correlations between basin size and measured concentrations of sulphate and lead are positive; larger lake basins collect more atmospheric depositions, and this relationship is reflected in lake water concentrations. However, the correlations between basin size and concentrations of hydrogen ion, copper, and nickel are negative; larger basins allow less of these

pollutant species to find their way into the lakes. This effect can be explained if it is postulated that the organic upper soil layers in the drainage basin of the lake contain ion absorption sites capable of taking up these ions. If the rate of uptake per unit surface area exceeds the deposition per unit surface, a larger basin area would result in a smaller lake water concentration. These results indicate that the adsorption parameter, F_s, should be larger than 1.00. While this effect may play a part in producing the observed correlation coefficients, the effect may also be in part explained by the spurious correlation between basin size and distance (Table 38). If absorption by the soil is more important, it must be concluded that a simple mass balance is not entirely adequate for modeling lake water concentrations, even for the relatively simple case of the very small unbuffered lakes on the Lorraine quartzite ridge. The water balance must be more precisely characterized, and the ion exchange capacity of the soil in the lake basin must be estimated.

4.2.3 - Sediment Concentrations

One of the important pathways by which some pollutants leave lake water is by sedimentation. This especially applies to the trace metals copper, lead, and nickel. The amount of these trace metals, iron, and zinc found in the

lake sediments is related to the lake water pH, and to concentrations in the lake water. These are related to the atmospheric input rates of these metals to the lake basin, assuming that atmospheric deposition of trace metal particulates will pass through the basin essentially unmodified by the lake water. Atmospheric inputs were assumed to be especially important for the small unbuffered lakes in relatively small drainage basins on the Lorraine quartzite formation ridge. For the case of the larger drainage basin lakes other factors can be assumed to have major effects, especially on sediment concentrations of zinc and iron. All sediment samples analyzed came from the bottoms of large drainage basin lakes (Table 43).

It is assumed that coefficients of correlation between pairs of metals with common sources in lake sediments would be strong (Table 44). It was assumed that sediments accumulate in the lake bottom and hence tend to accumulate trace metals from the lake water. Migration of ions is relatively slow in the sediment, therefore most of these trace metals are assumed to be effectively isolated from the lake water. Based on the ratio of lake basin areas (catchment) to lake surface areas (equivalent to deposition area), higher trace metal concentrations and stronger correlations between source related pairs are expected in sediments than in lake water.

TABLE 43

Comparison of Calculated and Measured Surface (approx 0 to 1/2 cm) Sediment Metal Concentrations

Lake Designations	Concentrations									
	Copper, 10^{-6} gm/gm		Nickel, 10^{-6} gm/gm		Lead, 10^{-6} gm/gm		Zinc, 10^{-6} gm/gm		Iron, percent	
	Meas	calc (min-max)	Meas	calc (min-max)	Meas	calc (min-max)	Meas	calc (min-max)	Meas	calc (min-max)
Johnnie 1	356.3	124.6-5418.0	231.6	55.3-799.4	235.7	82.9-343.3	303.6	414.8-2164.0	2.77	3.89-4.53
Johnnie 2	281.7	251.2-4710.0	210.6	61.9-513.7	171.1	92.6-382.2	243.0	169.1-1553.0	2.08	3.88-4.24
Grace	196.6	56.4-666.8	98.0	45.7-73.8	205.4	62.5-150.1	196.0	64.9-483.5	2.30	3.84-3.91
Nellie	119.7	57.4-200.4	78.7	45.9-50.2	150.8	53.0-78.9	260.7	62.5-267.6	2.70	3.84-3.86
LaCloche S	50.2	64.5-643.3	60.3	47.5-201.5	83.6	124.8-613.8	195.5	231.9-2317.0	3.05	3.88-4.21
LaCloche N	24.9	68.2-1017.0	27.1	48.7-344.5	26.1	128.3-640.1	78.1	189.3-2358.0	1.56	3.90-4.34
Charleton	107.6	360.6-8857.0	177.0	98.0-516.9	90.5	206.4-1222.0	314.0	1063.0-7000.0	2.69	3.98-5.13
Cranberry Bay	73.3	65.6-2368.0	108.0	47.2-177.5	63.3	99.0-421.5	213.0	94.3-1367.0	2.17	3.86-4.11
Alexander	66.3	54.8-598.5	82.5	45.6-135.8	150.6	81.3-289.6	353.1	92.0-949.5	3.88	3.85-3.98
Evangeline E	53.3	57.8-582.1	73.4	46.1-150.8	60.1	98.1-415.0	218.0	95.6-1328.0	3.15	3.86-4.05
Evangeline W	60.7	52.5-268.8	76.6	45.2-88.4	80.7	69.2-200.0	261.0	81.1-653.8	4.00	3.85-3.92
Deerhound	50.0	57.0-1518.0	53.8	45.9-180.6	48.8	88.9-346.8	124.0	79.4-1103.0	1.50	3.86-4.04
Cutler	66.7	54.6-366.6	92.6	45.5-120.7	113.0	80.8-285.8	250.0	71.7-891.8	3.24	3.85-3.97

A cross correlation matrix of measured trace metal; zinc, and iron concentrations in sediments was constructed (Table 44) to test these assumptions. This also provided an indication of the validity of the measured sediment concentrations as a check on concentrations calculated by the model. Copper, nickel and iron have common sources in smelter emissions from Sudbury and Falconbridge. Iron and zinc are major constituents of the soil in the lake basin. Hence the pairs copper and nickel, copper and iron, nickel and iron, and zinc and iron were expected to exhibit strong correlations. Of the six strongly correlated pairs observed, only two, copper and nickel, and iron and zinc were expected. The other two pairs expected to exhibit strong correlations due to a common origin, copper and iron, and nickel and iron exhibited weak negative correlations. This is due to the large contribution to total sediment iron concentration made by the natural mineral iron in the bulk sediment, which is largely unrelated to atmospheric deposition. The other measured sediment metal concentration pairs exhibiting strong correlations are copper and lead, nickel and lead, nickel and zinc, and lead and zinc. Originally, the assumption was made that the Sudbury area would be a source of atmospheric emissions of lead and zinc. Although correlations between pairs of the metals copper and nickel, and lead and zinc in the atmosphere, precipitation, and lake

TABLE 44

Cross Correlations Between Pollutant Species, for Measured Lake Sediment Concentrations (13 sites)

Pollutant Species	Copper	Nickel	Lead	Zinc
Nickel	0.867*			
Lead	0.855*	0.658*		
Zinc	0.356	0.563*	0.557*	
Iron	-0.128	-0.010	0.178	0.713*

*Significant at the 95 percent confidence level

water are relatively weak, they are relatively strong in sediments. This is due to the accumulation effect of sedimentation. While each measured atmosphere, precipitation, and lake water sample represents only a short accumulation time, a sediment sample represents approximately three years of accumulation.

In order to sort out the effect of pH on lake sediment metal concentrations, a table of correlation coefficients for pairs of measured metal concentrations with pH and hydrogen ion concentrations was constructed (Table 45). Also

compared in Table 45 are the observed distribution coefficient ratios (the measured concentration in the sediment divided by the measured concentration in the lake water) for the five metals: copper, nickel, lead, zinc, and iron, given for minimum, maximum and arithmetic mean (and standard deviation). Only nickel and iron concentrations exhibit strong correlations between measured values in lake water and lake bottom sediments. While this indicates important controlling factors in common for concentrations in water and sediments, it does not indicate what the common factor may be. The controlling factor may be a common origin for nickel and iron in lake water and sediment, pH control of sedimentation distribution coefficient, or the return of sediment components to the lake water. For the case of nickel, the distribution coefficient is negatively correlated with hydrogen ion. This indicates that a common source for both nickel and hydrogen ion has a relatively smaller effect in controlling the distribution coefficient than does the effect of pH on the solubility of nickel in the lake water. The distribution coefficient for iron exhibits no significant correlation with pH. This is because the major portions of the measured iron in the sediment are insoluble natural constituents of the minerals of the bulk sediment, relatively unaffected by lake water chemistry. Copper and lead distribution coefficients

TABLE 45

Dependence of the Distribution Coefficient on the pH of the Lake Water

Pollutant Species	Distribution Coefficient x 10^{-3}				Correlation Coefficients	
	min	max	mean	std	sed/water	Distribution Coefficient/$[H^+]$
Copper	9.96	178.2	60.7	50.7	0.060	0.412*
Nickel	14.31	76.6	44.4	18.4	0.532*	-0.195
Lead	20.03	410.8	103.7	117.7	-0.047	0.531*
Zinc	4.46	56.1	23.8	16.6	0.135	0.350
Iron	101.45	1 315.3	424.5	318.0	0.413*	0.003

*Significant at the 95 percent confidence level

correlate significantly with hydrogen ion, indicating that the effect of lower pH in increasing the solubility of these metals in the lake water (decreasing the rate of removal from the water to the sediments) has a relatively smaller effect than does the effect of a common source for hydrogen ion and copper, and for hydrogen ion and lead.

These arguments are dependent on the assumption that the five trace metals, copper, nickel, lead, zinc and iron tend to be in more soluble forms at lower pH values (in the measured pH range, approximately 4.00 to 7.00), and that metal sedimentation is independent of suspended organic and inorganic particulates. In order to find some indication of the correctness or error of these assumptions the ratio of suspended to dissolved metal species was measured for the five metals for three classes of lakes. The three classes are a subjective division into relatively strongly buffered lakes, relatively unbuffered lakes, and relatively weakly buffered lakes. The basis of this division is total suspended particulate concentration and total alkalinity. Only 2 of the lakes sampled, Deerhound and Cutler, both with pH values greater than 7.00 (Table 37), and with total suspended particulates approximately an order of magnitude higher than the average for all the lakes sampled (Table 46), were classified as relatively strongly buffered. These two lakes

were included to provide an indication of the effects of strong buffering, high pH and high suspended particulate concentrations, on the relationship of sediment chemistry to water chemistry. The relatively unbuffered class of lakes consists of the numbered lakes, White's Lake, White's Lake A, Grace Lake and Microwave Lake. These lakes are small, on the Lorraine formation, have an average pH value less than 5.00, and have total suspended particulates between one and two orders of magnitude lower than the average for all the lakes sampled (Table 46). The 11 remaining lakes have pH values between 4.5 and 7.00 and average total particulate concentrations of approximately 0.38 gm/L (Table 46).

Metal concentrations for filtered and unfiltered samples of lake water for the three classes of lakes outlined above are compared in Table 47. For each lake classification total measured concentrations of metals in unfiltered water samples, the ratio of total to filtered water concentrations, and filtered water sample concentrations are given. The higher the ratio, the larger the proportion of the metal in particulate form, either as insoluble chemical species or adsorbed on particles suspended in the water (Table 47). The largest ratios are usually for iron, indicating that most of the iron in the lake water is in

TABLE 46

Means and Standard Deviations for some Measured Lake Parameters, Including some Biological Indicator Parameters

	Chlorophyll a	Total Phosphate (10^{-9} gm/cm^3)	Nitrite-nitrate (10^{-9} gm/cm^3)	Specific Conductivity (μmho)	Total Alkalinity (10^{-3} gm/L) $CaCO_3$	Total Particulates (10^{-3} gm/L)
	Mean±std	Mean±std	Mean±std	Mean±std	Mean±std	Mean±std
A	1.6±1.6	9.4±10.0	28.6±39.3	30.8±6.8	1.11±0.61	5.6±3.4
B	1.7	6.1	-	56.5	4.8	2 312.5
C	0.7±0.4	7.5±7.5	-	47.9±7.8	2.8±2.6	379.3±753.2
All	1.2±1.2	8.7±9.3	28.3±5.3	37.9±11.1	2.0±2.0	235.2±232.5

A Lakes numbered 1 through 28, White's, Whites A, Grace and Microwave lakes (comparatively unbuffered)

B Cutler Lake and Deerhound Lake (comparatively strongly buffered and eutrophic)

C Remaining 11 larger lakes (comparatively weakly buffered)

TABLE 47

The Relative Proportion of Soluble and Particulate Metals Measured in Lake Water; a Comparison of Unbuffered, Weakly Buffered, and Comparatively Strongly Buffered Lakes

Metals Measured (10^{-9} gm/cm^3)	Lake Classifications: Comparatively Strongly Buffered (2 lakes) Total	Filter	Filt/Tot Ratio	Unbuffered (26 lakes) Total	Filter	Filt/Tot Ratio	Weakly Buffered (11 lakes) Total	Filter	Filt/Tot Ratio
Copper	1.4	0.9	0.6	12.0	5.3	0.4	3.0	1.4	0.5
Nickel	2.4	0.9	0.4	4.3	2.8	0.7	3.1	1.4	0.4
Lead	1.8	0.5	0.3	-	1.4	-	2.8	1.2	0.5
Zinc	4.8	3.1	0.6	60.2	24.4	0.4	15.5	14.6	0.9
Iron	54.8	49.8	0.9	158.0	123.5	0.8	126.3	80.3	0.6

suspended form, and is susceptible to sedimentation. The major portion of this iron is probably in the iron minerals of bulk sediment particles suspended in the lake water. In the comparatively eutrophic lakes, with high pH values and large concentrations of suspended particulates, most of the iron in the lake water is probably in the form of suspended particulates, which can sediment out, leading to high distribution coefficients for iron (Tables 45 and 47). The ratio of total measured iron to filtered lake water sample measured iron is approximately 33 percent lower for the comparatively weakly buffered lakes, with suspended total particulate concentrations approximately one order of magnitude lower, and hydrogen ion concentrations one to two orders of magnitude higher (Tables 46 and 47). Copper, nickel, lead and zinc exhibit lower ratios of total measured metal to filtered lake water sample measured metal concentrations, indicating that a greater proportion of these metals is in the form of dissolved species, which are not susceptible to sedimentation (Table 47). This is also indicated by the lower distribution coefficients for these metals (Table 45).

For all five metals: copper, nickel, lead, zinc, and iron, there is a trend from more metal in suspended particulate form in comparatively eutrophic lakes, to more

metal in dissolved forms in unbuffered lakes. This trend is parallel to trends toward lower pH values and lower total suspended particulate concentrations in the series of increasingly unbuffered lakes (Tables 46 and 47). It can be concluded from these observations that both pH and the availability of suspended particulates play an important role in determining the rate of sedimentation of trace metals: copper, nickel, lead, zinc and iron, from lake water.

Measured and calculated sediment concentrations of these five metals are compared in Tables 43 and 48. Values for each lake are listed as measured minimum and maximum calculated values (Table 43), and as correlation coefficients for the five metals (Table 48). Also given are correlation coefficients between the measured sediment metal concentrations and distance to the source, total alkalinity, and lake basin area (Table 48). Correlations of measured sediment metal concentrations with lake characteristics indicate the validity of measured sediment metal concentrations as a check on concentrations calculated by the model. Measured copper, nickel, zinc and iron concentration are correlated to the 95 percent confidence level with distance. Measured trace metal correlations do not correlate significantly with basin size. However, measured sediment

TABLE 48

Correlation Coefficients of Measured Lake Sediment Concentrations to Calculated Concentrations, Distance from Source, Total Alkalinity, and Lake Basin Area

Pollutant Species	Correlation Coefficients				
	meas/calc min conc conc	meas/calc max conc conc	log meas/distance[b] conc	meas/total conc alkalinity	meas/basin conc area
Copper	0.385	0.509[a]	-0.829[a]	-0.616[a]	0.098
Nickel	0.583[a]	0.798[a]	-0.739[a]	-0.615[a]	0.241
Lead	-0.405	-0.343	-0.524	-0.747[a]	-0.128
Zinc	0.344	-0.122	-0.558[a]	-0.588[a]	-0.162
Iron	-0.206	-0.195	-0.565[a]	-0.183	-0.141

[a]Significant to the 95 percent confidence level

[b]Distance from source to approximate centre of lake drainage basin, as estimated from topographic maps

concentrations of copper, nickel, lead and zinc are significantly correlated with total alkalinity. These results indicate that total alkalinity should be accounted for in the lake model.

It must be noted that some of the trace metal in the sediments is due to the erosion of the soil in the lake basin, which is independent of atmospheric trace element loading rates. The diluting effect of erosion is approximated by the bulk sedimentation rate (Huhn, 1974). Direct sedimentation rate measurements were not made in the very small lakes in the Lorraine quartzite ridge. This bulk sedimentation rate may not apply to these lakes. Correlations between calculated and measured metals in lake sediments are better for sediment copper and nickel than for lake water concentrations of these metals (Tables 42 and 48). This is due to the distribution coefficient of these metals in the sediments compared to their concentrations in lake water. This is also indicated by the stronger correlations of measured copper and nickel concentrations in the sediment with distance from the source, when compared to their correlation with distance in lake water (Tables 42 and 48). Lead, zinc, and iron did not exhibit strong correlations between measured and calculated sediment concentrations (Table 48). For the case of iron this is again due to the

large proportion of mineral iron in the measured iron concentration values, which is not a direct function of atmospheric iron concentrations, basin size, or distance from the smelters, three of the important driving parameters for calculating sediment metal concentrations. Lead and zinc exhibit stronger correlations with total alkalinity than with distance from the source. Distance from the source is one of the driving parameters for modeling sediment metal concentrations, while total alkalinity is not; therefore it is apparent that correlations between measured and calculated concentrations of lead and zinc in sediments are weaker than the corresponding correlations for copper and nickel (Table 48).

5 - SUMMARY AND CONCLUSIONS

The utility of the model can be briefly summarized as

- loading rates and precipitation concentrations can be effectively modeled by the modified box model

- atmospheric concentrations can be modeled adequately but conclusive results require more comprehensive measured atmospheric concentration data

- lake water concentration can be only poorly modeled. Due to a large number of complicating factors governing lake water chemistry a simple mass balance is inadequate. However, the effectiveness of the lake model cannot be tested unambiguously with the limited test data available. Sediment metal concentrations can be adequately modeled. Many of the governing factors complicating the calculation of concentrations in lake water are minimized by the accumulation and direct sedimentation of metals.

Atmospheric concentrations of sulphur dioxide are predicted effectively (approximately 69±26 percent of measured values) within 80 kilometres of the smelters at Sudbury, as are copper (approximately 81±11 percent of measured values)

and nickel (approximately 105±37 percent of measured values).

These sulphur dioxide predictions compare well with atmospheric modeling studies that indicate that Sudbury contributes approximately 45 percent of the total sulphur dioxide concentration in the 80 kilometre diameter around Sudbury (Acres 1975, 1980). These good results are due in part to the relatively isolated point source nature of the sulphur dioxide copper, and nickel emissions from the Sudbury smelters. Beyond 80 kilometres other sources of these pollutants (including Wawa, Manitouwadge and Timmins) becomes important.

Atmospheric concentrations of iron are less effectively predicted (approximately 77±16 percent of measured values). This is due in part to strong geological control of atmospheric iron concentration (reentrainment of surface dust and soil, which contains high concentrations of iron), and to the presence of other major sources of atmospheric iron concentrations (including the smelter at Wawa). Neither factor was incorporated in the model.

Atmospheric concentrations of zinc are effectively predicted (approximately 76±23 percent of measured values).

Lead can be effectively modeled if sources of atmospheric lead are adequately characterized. Recent literature (Conroy et al, 1978) indicated that lead emissions from the Sudbury smelters may be as much as 25 percent of the emission rates of copper or nickel. Utilizing these lead emission rates, lead is predicted effectively (approximately 76±14 percent of measured values).

Predicted atmospheric concentrations can only be verified to the accuracy of the available measured concentration data. Scatter in the measured concentration data is large. Only measured sulphur dioxide and nickel concentrations exhibit significant correlation with distance from the source. For copper, nickel and sulphur dioxide, correlation coefficients for calculated to measured values are larger than correlation coefficients for measured values to distance from the source.

Precipitation chemistry and loading rates are also effectively predicted. Predictions of sulphate loading rates and precipitation concentrations are excellent and the pH of precipitation is adequately predicted within 100 kilometres of Sudbury. Calculated pH values are

approximately 0.66±0.44 orders of magnitude high. (Calculated hydrogen ion concentrations are approximately 22±36 percent of measured values.) Calculated sulphate concentrations and loadings are approximately 112±198 percent of measured values. The difference in precipitation sulphate concentration predictions and pH (hydrogen ion concentration) predictions are due in part to sulphate from other sources (approximately 55 percent). This does not account for all of the extra hydrogen ion measured. Some hydrogen ion may come from background loadings of nitrates. However, other loading studies indicate that nitrate loadings contribute between approximately 18 and 27 percent of the total hydrogen ion loading rates in the Sudbury area (Acres 1975, 1980). The remaining discrepancy is probably due to error in the specification of the oxidation rate on the adsorption parameter utilized in calculating postdepositional chemistry. Modeling of pH and sulphate would be substantially improved by the incorporation of important sulphur dioxide sources beyond 200 kilometres from the Sudbury smelters (including Wawa, Noranda, and Timmins).

Precipitation concentrations and loading rates of copper and nickel are effectively predicted within 100 kilometres of Sudbury. Predicted copper values are

approximately 242±179 percent of measured values. Predicted nickel values are approximately 77±54 percent of measured values. Modeling of copper and nickel could be improved, especially beyond 100 to 200 kilometres from Sudbury, by the incorporation of other sources of atmospheric copper and nickel. Potential sources of copper and nickel include Timmins/Porcupine, Cobalt, Noranda, and Manitouwadge.

Concentrations of iron in precipitation and loading rates are predicted adequately within 100 kilometres of the smelters. Calculated iron values are approximately 48±18 percent of measured values. Reentrained dust containing iron may account for these consistently low predictions. Beyond 200 kilometres of Sudbury iron cannot be adequately modeled unless other sources of atmospheric iron are included in the model. Potential sources include Kirkland Lake, Temagami, and Wawa. Wawa produces measured precipitation iron concentrations near the smelter approximately four times as large as those near Sudbury.

Zinc precipitation chemistry and loading rates are predicted adequately close (50 kilometres) to the smelters. Calculated zinc values are approximately 32±21 percent of measured values. Reentrained dust containing zinc may

account for the consistently low predictions. In order to adequately model zinc in the study area at distances greater than 50 kilometres from the smelters, other sources of atmospheric zinc must be incorporated into the model. Zinc emission sources larger than the Sudbury smelters include Manitouwadge and Timmins.

Lead precipitation concentrations and loading rates can be adequately modeled (within 100 kilometres) if more recent estimates of the lead emission rate at Sudbury are included. Then calculated lead values are approximately 100±53 percent of measured values. Modeling of lead would be further improved by the incorpororation of other sources of atmospheric lead emissions (including mining and smelting areas such as Manitouwadge and Timmins).

Atmospheric concentrations, modeled precipitation concentrations and loading rates can only be verified to the accuracy of the available measured precipitation chemistry data. Scatter in the measured data is not as large as for measured atmospheric concentration data. Only measured pH, copper, nickel, and iron concentrations exhibit significant correlations with distance from the source. For pH and copper correlations between predicted and measured values are larger than the correlations between measured values and distance from the source.

Lake water pH and concentrations of sulphate and trace metal predictions are not as good as atmospheric concentrations and loading rate predictions. The lake model is driven by atmospheric loading rates calculated by the atmospheric model, which therefore defines an upper limit to predictions of lake chemistry. Lake chemistry predictions are further reduced by the accuracy with which the other controlling parameters of the lake model are measured. These factors include the accuracy with which lake basin areas can be determined and the absorption of pollutants in the watershed. The lake model parameter exhibits a large range. This is reflected in predicted lake chemistry by the large range between minimum and maximum predicted values.

Predicted lake water concentrations of sulphate are 44±12 percent of measured values. This compares well with atmospheric loading studies that indicate that Sudbury contributes approximately 45 percent of the total sulphate loadings in the 80 kilometre diameter area around Sudbury (Acres 1975, 1980).

However, pH predictions are approximately 1.0±1.2 orders of magnitude too high. (Calculated hydrogen ion concentrations are approximately 10±6 percent of measured

values.) Part of the hydrogen ion may also be due to nitrate loadings (Acres 1975, 1980). Predicted concentrations of iron and nickel are closer to measured values than are copper or lead predictions. Calculated iron values are approximately 107 ± 104 percent of measured values and calculated nickel values are approximately 140 ± 120 percent of measured values. Calculated zinc values are approximately 270 ± 265 percent of measured values. Calculated copper values are approximately 215 ± 185 percent of measured values. Calculated lead values are approximately 195 ± 175 percent of measured values.

It must be noted that predicted lake water chemistry can only be verified to the accuracy of the available measured lake water concentrations. Only measured sulphate, copper and zinc concentrations exhibit significant correlations with distance from the source. These measured values were obtained from the analysis of from one to four water samples per lake. In the case of LaCloche Lake, twelve water samples were taken. It is clear from the literature that lake chemistry is not uniform. It varies with depth from place to place in the lake and with time. The numbers of samples obtained from each lake are not large enough to adequately characterize lake chemistry. Therefore, no useful calculation of a normal range of measured pH, sulphate and trace metal concentrations could be made. Moreover, the lake model makes predictions in the

form of values averaged over three years, assuming uniform concentrations throughout the lake. Comparison of measured and predicted lake water concentrations can therefore provide rough indications of modeling accuracy only.

Comparisons of modeled and measured lake water concentrations do indicate the importance of geological factors in controlling lake chemistry. Modeling of lake water chemistry would be substantially improved if the role of total alkalinity and pH in controlling trace metal chemistry were incorporated in the model.

Concentrations of trace metals in lake sediment are calculated from lake water trace metal concentrations. Therefore the accuracy of sediment chemistry predictions are further reduced by the accuracy with which sedimentation rates can be estimated. This is reflected in the modeled sediment trace metal concentrations by the wide range between minimum and maximum calculated concentrations.

Sediment copper concentrations are effectively predicted. Copper predictions are approximately 155±120 percent of measured values. Nickel concentrations are approximately 102±78 percent of measured values.

Predicted iron concentrations are approximately 178±84 percent of measured values and predicted zinc concentrations are approximately 133±103 percent of measured values. The prediction of lead in lake sediments was less effective than for the other trace metals (approximately 263±228 percent of measured values).

Sediment modeling accuracy can only be verified to the accuracy of the available measured sediment concentration data. Of the five trace metals measured in the sediments, all but lead exhibited significant correlations with distance from the smelters. However, all but iron also exhibited significant correlations with total alkalinity. These measured values were obtained from analysis of the upper 1/2 centimetre of sediments from eleven of the lakes studied (13 cores analyzed). Therefore a calculation of a normal range of trace metal concentrations was not made. Comparison of measured and predicted sediment concentrations can therefore provide only a rough indication of modeling accuracy. Measured and modeled sediment concentrations correspond better than measured and modeled lake water concentrations. This apparent contradiction is explained by the nature of the measured data in each case. Measured sediment concentrations represent an average rate of accumulation over a longer time scale than measured lake

water concentrations. Calculated sediment concentrations are average values for a three year modeling period, as are calculated lake water concentrations. This is comparable to the time scale for accumulation of sediments. Water chemistry, however, changes substantially from place to place in the lake and from season to season. As each water sample obtained during the field program represents only a single location and time, while modeled lake water concentrations are calculated for average lake basin conditions for a three year modeling period, a poor correspondence of measured and calculated concentrations is to be expected.

In addition to the recommendations previously suggested, the incorporation of inputs in addition to atmospheric inputs (including soil erosion rates) of trace metals and bulk sediment to the lake bottom would substantially improve the modeling of sediment trace metal concentrations.

Modeling effectiveness for atmospheric, precipitation, lake water, and sediment chemistry predictions can be summarized as follows.

Modeled pollutant	Ratios, predicted to measured values as percent			
	Atmospheric	Precipitation	Lake water	Sediment
SO_2	69±26[a]	-	-	-
SO_4	-	112±198	44±12[a]	-
pH[b]	-	22±36[a]	10±6[a]	-
Cu	81±11	242±179[a]	215±185[a]	155±120[a]
Ni	105±39[a]	77±54[a]	140±120	102±78[a]
Pb[c]	76±14	100±53	195±175	263±228
Zn	76±23	32±21	270±265	133±103
Fe	77±16	48±18	107±104	178±83

[a]significant at the 95 percent confidence level.
[b]ratios for hydrogen ion concentrations.
[c]calculated utilizing average meteorological parameters for the three year period of study.

6 - FUTURE WORK

This section outlines some areas in which improvements and future studies related to the modified box model could be made. It is not meant to be complete, and will only cover some aspects of the atmospheric model. Lake water chemistry, sedimentation, and the modeling of lake basins are a few of the areas in which the need for more work is clear.

6.1 - Receptor Locations

The receptor locations are not evenly distributed over the study area (Figure 6), which leads to problems in interpreting the isopleth maps. The receptor sites are confined to a "bow tie" shaped area defined by Lake Huron, Georgian Bay, Lake Superior, and the border of the province of Quebec. In the narrowest portion of this area, around North Bay, Ontario, isopleths are poorly defined due to boundary effects. In order to completely define a point on a plotted isopleth there must be data points on each side of the isopleth. Therefore the portions of each isopleth that lie between a data point and the edge of the study area are not completely defined. This is compensated for

to an extent by the greater density of receptors in the North Bay area. On the extreme north, northwest and southern edges of the study area the spacing of the receptors is inadequate. The distance between receptors in these areas often exceeds the scale of the well defined portion of the Sudbury area deposition pattern. In the north this is due to practical considerations, such as a scarcity of roads. The practical result of this very uneven distribution of data points is to introduce a subjective northwest-southeast bias to the plotted isopleth patterns.

The calculated and measured patterns of concentrations and loading rates could be more clearly compared if a number of approximately equally spaced precipitation measurements in Quebec, Michigan, and southern Ontario could be added to the study area.

6.2 - Temporal Scale

For the mixing height, a critical parameter in driving the modified box model, average mixing height values for the Great Lakes area are utilized on a seasonal basis. A more accurate calculation could be made by incorporating daily average mixing heights into the model. This information is not always available for a study area, in which

case an extensive program of windspeed and temperature gradient measurements would be required.

Mixing heights can change very significantly over the course of a day. A night time inversion can be broken up at midmorning by sun induced turbulence, causing erratic episodes of short-lived high pollutant concentrations at the ground level in the near field. In the evening as the ground cools an inversion can again be set up. The inversion height may be lower than the expected average mixing height deduced from meteorological considerations, and hence ground level pollutant concentrations may be higher than predicted.

This fractional daytime scale may not appear as a significantly time correlated concentration variation at far field distances (beyond 25 to 50 kilometres), however, the overall effect on far field concentration values may not reflect a simple daily average mixing height. More studies in this area are required.

6.3 - Spatial Scale

At very short distances (less than 10 to 20 kilometres) from the source the modified box model is not

appropriate, as at these distances the vertical pollutant concentration profile has not had sufficient time to attain uniformity. At these distances a two dimensional Gaussian model is more appropriate. At greater distances, by which time it is assumed that a uniform vertical profile has been formed, the box model, though more effective than the two dimensional Gaussian model, still suffers from some basic design problems. The most important of these is the assumption of uniform vertical mixing up to the mixing height, which is assumed to be perfectly reflecting. Improved calculated results may be obtainable by the incorporation of an imperfectly reflecting mixing height. A term, or terms, in the basic function would account for the proportion of pollutants escaping from the top of the box. Alternatively, a "multibox" model may be used to account for the nonuniform vertical distribution of pollutants and vertical migrations. Two or more box models are stacked one above the other with the interfaces determined by vertical discontinuities (in wind regime, in atmospheric stability or temperature), such as an inversion. Each box would be specified with its own dispersion angle appropriate to the atmospheric conditions at its own range of altitude. A two-box model may be especially appropriate for very high sources, such as the 381-metre INCO stack at Copper Cliff, where a portion of the plume is often injected into the atmosphere above the mixing height determined by a nighttime inversion.

To judge the practical value of a multibox model, beyond some special cases, requires an extensive program of wind, temperature, and pollutant concentration profiles for the study area in which the model will be used.

The mixing height, wind velocity, wind direction, and dispersion angle, as well as deposition velocities, may vary from place to place over a large study area. These parameters are to some extent dependent upon topography of the study area, the character of the surface (water, open fields, bush, etc), and upon meteorological factors (Denison et al, 1979). These differences can have significant effects on the calculation of concentrations and loading rates (Acres, 1975, 1977, 1980). The model, as utilized in this study, accounts for varying meteorological parameters over the study area by combining weather data from five meteorological stations distributed over the study area. The combining schemes utilized the locations of the meteorological stations and of the receptors only. Weather parameters estimated for the locations of the receptors determine all aspects of the model.

The opposite approach, to have all aspects determined by the location of the source, is not usually an improvement. A possible improvement would be to have a

combination of both approaches, where some aspects, such as dispersion angle and losses, are determined by source area weather parameters; and other aspects, such as deposition, are determined by receptor area weather parameters (Acres, 1975, 1977, 1980). More effective, but with increased computing cost, would be to compute a pollutant plume trajectory through a series of steps, with different mixing heights, dispersion angles, and losses for each step determined by the position of the step in relation to the meteorological stations, by the conditions prevailing during the previous step, and by the topography of the area that the plume is traversing.

6.4 - Chemistry

A more complex treatment of atmospheric chemistry is required. In this study separate loss and scavenging coefficients are utilized for each pollutant species being considered, without allowance for any pollutant species overlap. For example, because there is a loss factor for iron and a separate one for sulphate, the iron and the sulphate in ferrous and ferric sulphates, and any sulphate adsorbed on the surfaces of iron-containing particulates, is double counted. In the Sudbury area this may not be a problem, however, in applying the box model to problems

of the transport of photochemical smog, for one example, the interaction of different chemical species must be accounted for. This can be accomplished by the simultaneous solution of the differential equations that describe losses and scavenging.

In this study a simple first order rate constant for the oxidation of sulphur dioxide to sulphate is modified to account for a decreasing rate constant with plume age (Lusis, 1975). This is a purely analytical relationship that does not attempt to relate the oxidation rate to the underlying chemistry. This appears to be adequate for the far field in the Sudbury area, but may be inadequate in the near field (less than 25 kilometres), due to the complex interaction of water vapor, particulates, and sulphur dioxide. If attempts are made to apply the model to other situations, such as sources in a highly industrialized area, the chemical interaction of plumes composed of different pollutants (i.e. sulpur dioxide, nitrogen oxides, fluorides, ammonia, hydrocarbons) must be accounted for.

6.5 - Deposition

Dry deposition velocities vary with the nature of the scavenged species, the stability of the atmosphere,

wind velocity, and the nature of the deposition surface. In this study no accounting for different surface character has been made, and only the simplest relationships, in part theoretical and in part based on measurements in the literature, have been incorporated to account for the effects of wind velocity and effective particle diameters.

Similarly, for wet deposition a simple washout coefficient relationship has been utilized.

Deposition processes are probably the most complex and least understood area in the study of pollutant transport and scavenging. Field and laboratory studies agree broadly, but many discrepancies are apparent in specific situations (Denison et al, 1979). Attempts to tie together theory and measurement have met with limited success.

In part this is due to the difficulties involved in attempting to identify and control the relevant variables in an experiment, and the difficulty in making useful measurements in the field. In the field, wet and dry deposition components in the total deposition must be measured separately, the relative capture efficiency of samplers under different conditions must be known, and the

concentration gradient with altitude must be measured and compared to the vertical wind speed and direction profiles. Measurements of very small differences must be made, hence, experiment design and analytical controls are critically important.

In future work, better and more extensive programs of measurement should be undertaken to determine wet and dry scavenging mechanisms, which would lead to more effective descriptions of these mechanisms in theoretical terms. It is probable that the degree of sophistication now available for the construction of transport and dispersion models cannot be properly evaluated until the results of such programs are available.

Examination of the literature indicates that this is the first atmospheric modeling program designed to calculate minimum and maximum concentrations and loading rates from ranges of input parameters. Outputs in the form of ranges of minimum to maximum calculated values, when compared to measured values, allow more realistic interpretations and projections to be made.

Only minimum and maximum calculated values are selected (from a field of 16) by the program. An

improvement in assessing the modeled chemistries can be gained by modifications to the program to output all standard statistical parameters (means, standard deviations, correlation coefficients, etc).

As far as I have been able to determine this is the first attempt to tie an atmospheric model directly to a lake chemistry model. This is a concept that must be further developed if useful predictions of lake basin chemistry are to be modeled.

REFERENCES CITED (APPENDIX A)

Acres Consulting Services Limited. Atmospheric Loading of the Upper Great Lakes, Canada Center for Inland Waters. 1975.

Acres Consulting Services Limited. Atmospheric Loading of the Lower Great Lakes and the Great Lakes Drainage Basin, Canada Center for Inland Waters. 1977.

Acres Consulting Services Limited. Acid Deposition in Ontario and Neighboring Regions, Ontario Hydro. 1980.

Altshuller, A. P. Model Predictions of the Rates of Homogeneous Oxidation of Sulfur Dioxide to Sulfate in the Troposphere. ATM ENVR 13(12): pp 1653 - 1661. 1979.

Altshuller, A. P., W. A. Lonneman, F. D. Sutterfield and S. L. Kopczyniski. Hydrocarbon Composition of the Atmosphere of the Los Angeles Basin - 1967, Environ. Sci. and Tech. 5:10, p 1009. 1971.

Atkins, P. R. Lead in a Suburban Environment, J. Air Pollution Control Assoc. 19: pp 591 - 596. 1969.

Batchelor, G. K. The Theory of Homogenous Turbulence, Cambridge University Press. 1953.

Beamish, R. J. Loss of Fish Population from Unexploited Remote Lakes in Ontario, Canada as a Consequence of of Atmospheric Fallout of Acid, Water Res. 8, pp 85 - 95. 1974.

Beamish, R. J., J. C. Van Loon, G. A. McFarlane and J. Lichwa. The Effects of Sudbury Nickel Smelter Emissions on Lakes within the Whitefish Lake Indian Reserve. 1974

Beilke, S. and G. Gravenhorst. Heterogeneous SO_2 - Oxidation in the Droplet Phase, ATM ENVR 12(1 - 3): pp 231 - 239. 1978.

Beilke, S. Laboratory Investigations on Washout of Trace Gases, Proc. Symp. on Precip. Scavenging, USAEC Symp. Series 22: pp 261 - 269. 1970.

Bird, R. B., W. E. Stewart and E. N. Lightfoot. Transport Phenomena, Wiley, N.Y.C. 1960.

Bosanquet, C. H. and J. L. Pearson. The Spread of Smoke and Gases from Chimneys, Trans. Faraday Soc. 32: p 1249. 1936.

Boray, E. Les Depots de Plumb sur la Vegetation le Long des Auto Routes, Mitl. Geb. Lebensmittel Centers Hyg., 61: pp 303 - 321. 1970.

Bowen, H.J.M. Trace Elements in Biochemistry, Academic Press N.Y.C. 1966.

Briggs, G. A. Plume Rise, AEC Crit. Rev. Ser. TID-25075, U.S. At. Energy Comm., Div. Tech. Inform. Ext., Oak Ridge, Tenn. 1969.

Briggs, G. A. Some Recent Analyses of Plume Rise Observations, Proc. 2nd Int. Clean Air Congr., Wash., D.C. 1970.

Briggs, G. A. Chimney Plumes in Neutral and Stable Surroundings, ATM ENVR 6: p 507. 1972.

Bringfelt, B. Plume Rise Measurements at Industrial Chimneys, ATM ENVR 2: p 575. 1968.

Bringfelt, B. A Study of Bouyant Chimney Plumes in Neutral and Stable Atmospheres, ATM ENVR 3: p 609. 1969.

Bufalini, M. Oxidation of Sulfur Dioxide in Polluted Atmospheres - A Review, Environ. Sci. and Tech. 5:8, pp 685 - 700. 1971.

Calvert, J. G., F. Su, J. W. Bottenheim and O. P. Strausz. Mechanism of the Homogeneous Oxidation of Sulfur Dioxide in the Troposphere, ATM ENVR 12(1 - 3): pp 197 - 226. 1978.

Carpenter, S. B., W. C. Colbaugh, J. M. Leavitt, W. B. Morris and T. L. Montgomery. A Study of Limited Layer Mixing Dispersion-Bull Run Steam Plant, TVA, Div. Envron. Planning E-AQ-76-2. 1976.

Carpenter, S. B., T. L. Montgomery, J. M. Leavitt, W. C. Colbaugh and F. W. Thomas. Principal Plume Dispersion Models: TVA Power Plants, J. Air Pollut. Contr. Assoc. 21: p 491. 1971.

Cawse, P. A. A Survey of Atmospheric Trace Elements in the U.K., (1972-3), AERE-R 7669 HMSO, London. 1974.

Chamberlain, A. C. Aspects of Travel and Deposition of Aerosol and Vapour Clouds, A.E.R.E. HP/R 1261, Harwell, G.B. 1955.

Chamberlain, A. C. Travel and Deposition of Lead Aerosols, AERE-R7679 Harwell, Oxfordshire, G.B. 1974.

Chamberlain, A. C. Transport of Lycopodium Spores and Other small Particles to Rough Surfaces, Proc. Roy. Soc.A. 296: pp 45 - 70. 1967.

Chamberlain, A. C. Approach to Evaluating Dry Deposition of Atmospheric Aerosol Pollutant onto Lake Surfaces, Great Lakes Res, Proc. 1st Spec. Symp. 2, Sup. 1, pp 38 - 41. 1976.

Chan, W. H., R. J. Vet, M. A. Lusis, J. E. Hunt and R.D.S. Stevens. Airborne Sulfur Dioxide to Sulfate Oxidation Studies of the INCO 381 M Chimney Plume, ATM ENVR 14(10): pp 1159 - 1170. 1980.

Cheng, R. T., M. Corn and J. O. Frohliger. Contribution to the Reaction Kinetics of Water-Soluble Aerosols and Sulfur Dioxide in Air at ppm Concentrations, ATM ENVR 5: pp 987 - 1000. 1971.

Chun, K. C. and J. E. Quon. Capacity of Ferric Oxide Particles to Oxidize Sulfur Dioxide in Air, Air Environ. Sci. and Tech. 7: p 532 - 538. 1973.

Clough, W. S. Transport of Particles to a Surface, J. Aerosol Science, 4: pp 227 - 234. 1973.

Conroy, N., K. Hawley and W. Keller. Extensive Monitoring of Lakes in the Greater Sudbury Area 1974 - 1976, Ontario Ministry of the Environment, Sudbury Environmental Study Report, Water Resources Assessment, Northeastern Region. 1978.

Conroy, N. Classification of Precambrian Shield Lakes Based on Factors Controlling Biological Activity, M.Sc. Thesis, McMaster University. 1971.

Costescu, L. M. and T. C. Hutchinson. The Ecological Consequences of Soil Pollution by Metallic Dust from the Sudbury Smelters, Inst. Environ. Sci., 18th Annual Tech. Sess. Proc., N.Y.C., pp 540 - 545. 1972.

Coutant, R. W., E. L. Merryman, R. E. Barrett, R. D. Giammer and A. Levy. A Study of the Fate of SO_2 in Flue Gas. Battelle Columbus Laboratories Final Report, EPA/API/BCR, Inc./EEI (March 1972), 12 p.

Cox, R. A. and S. A. Penkett. The Photo-oxidation of Sulphur Dioxide in Sunlight, ATM ENVR 4: pp 425 - 433. 1970.

Crowther, C. and H. G. Rustan. The Nature, Distribution, and Effect Upon Vegetation of Atmospheric Impurities in and Near an Industrial Town, J. Agric. Sci. 4: pp 25 - 55. 1911.

Dana, M. T., J. M. Hales, W.G.V. Slinn and M. A. Wolf. Natural Precipitation Washout of Sulphur Compounds from Plumes, USEPA, EPA-R3-73-047:202. 1973.

Davenport, A. G. In "Wind Effects on Buildings and Structures", Symp. No. 16, Dept. Sci. Ind. Res., Nat. Phys. Lab., HM Stationary Office, London, U.K. 1965.

DeMarris, G. A. Wind-speed Profiles at Brookhaven National Laboratory, J. Meteorol, 16: p 181. 1959.

Denison, P. J., T. A. McMahon and J. R. Kramer. Literature Review on Pollution Deposition Processes, Alberta Oil Sands Environmental Research Program and Syncrude Canada Limited, Project ME 3, 6, AOSERP Rpt. 50. 1979.

Dennis, R., C. E. Billings, F. A. Recond, P. Warneck and M. L. Arin. Measurements of Sulfur Dioxide Losses from Stack Plumes, APCA 69th Annual Meeting, June, N.Y.C., 1969.

Dingle, A. N. Scavenging and Dispersal of Tracer by a Self-Propagating Convective Shower System, ERDA Symp. Series 41, Tech. Info. Center, Energy Res. & Dev. Admin. Argonne, Ill. 1977.

DiToro, D. M., D. J. O'Conner and R. V. Thomman. A Dynamic Model of the Phytoplankton Population in the Sacramento-San Joaquin Delta, in "Non-equilibrium Systems in Natural Water Chemistry", Amer. Chem. Soc., Advances in Chemistry Series 106: pp 131 - 180. 1972.

Dreisinger, B. R. SO_2 Levels and Vegetation Injury in the Sudbury Area during the 1969 Season, Dept. Energy and Res. Mgmnt., Ontario Min. Nat. Res. 1970.

Eggleton, A.E.J. and R. A. Cox. Homogeneous Oxidation of Sulphur Compounds in the Atmosphere, ATM ENVR 12 (1 - 3): pp 227 - 230. 1978.

Englemann, R. J. The Calculation of Precipitation Scavenging, Battelle Northwest Laboratory, USAEC Rpt. BNWL-77. 1965.

Energy, Mines and Resources. Army Survey Establishment, 1:250,000 Topographic Map, 41-I, Edition 1, Sudbury, Ontario. 1960.

Energy, Mines and Resources. Surveys and Mapping Branch, 1:50,000 Topographic Map, 41-I/4, Edition 3, Whitefish Falls, Ontario. 1975a.

Energy, Mines and Resources. Surveys and Mapping Branch, 1:50,000 Topographic Map, 41-I/1, Edition 3, Spanish, Ontario. 1975b.

Energy, Mines and Resources. Surveys and Mapping Branch, 1:50,000 Topographic Map, 41-I/3, Edition 4, Lake Panache, Ontario. 1975c.

Environment Canada. Meteorological Data, Atmospheric Environment Service. 1972-73-74.

Environment Canada. A Nationwide Inventory of Air Pollutant Emissions (1972), Econo and Tech. Rev. Rpt. EPS 3-AP-77-2. 1977.

Environment Canada. A Nationwide Inventory of Air Pollutant Emissions (1974), Econ. and Tech. Rev. Rpt. EPS 3-AP-78-2. 1978.

Esmen, N. A. Particle Retention Efficiency of Scavenging Rainfall, Presented to Water, Air and Waste Chem. Div., Amer. Chem. Soc., Boston, 1972.

Esmen, N. A. and M. Corn. Residence Time of Particles in Urban Air, ATM ENVR, Vol 8, pp 571 - 578. 1971.

Falk, M. and P. A. Giguere. "On the Nature of Sulphurous Acid", Can. J. Chem. 36:1121. 1958.

Falkowski, P. The INCO Stack-Engineering Triumph or Biological Disaster?, Steel Labor 38:10, p 2. 1973.

Fay, J. A., M. Escudier and D. P. Hoult. A Correlation of Field Observations of Plume Rise, J. Air. Pollut. Contr. Assc., 20:391. 1970.

Foster, P. M. Oxidation of Sulfur Dioxide in Power Station Plumes. ATM ENVR, 3:157. 1969.

Fuller, E. C. and R. H. Crist. The Rate of Oxidation of Sulfite Ions by Oxygen, J. Am. Chem. Soc., 63:644. 1941.

Garland, J. A., W. S. Clough and D. Fowler. Deposition of SO_2 on Grass, Nature, Vol 242, pp 256 - 257. 1973.

Gartrell, F. E., F. W. Thomas and S. B. Carpenter. Atmospheric Oxidation of SO_2 in Coal-burning Power Plant Plumes, Am. Ind. Hyg. Assc. J. 24: p 113 - 120. 1963.

Gatz, D. F. Scavenging Ratios in METROMEX, Precipitation Scavenging (1974), ERDA Symp. Series 41, pp 71 - 87. 1977.

Gatz, D. F. Wet Deposition Estimation using Scavenging Ratios, Great Lakes Res., Proc. 1st Special Symp., 2:Sup. 1, pp 21 - 29. 1976.

Gerhard, E. R. and H. F. Johnstone. Photochemical Oxidation of Sulfur Dioxide in Air, Ind. and Eng. Chem., 47: pp 972 - 976. 1955.

Gifford, F. A. Jr. Uses of Routine Meteorological Observations for Estimates of Atmospheric Dispersion, Nucl. Safety 2:4, pp 47 - 51. 1961.

Gorham, E. and A. G. Gordon. Some Effects of Smelter Pollution Northeast of Falconbridge, Ontario, Can. J. Bot., 38: p 307 - 312. 1960.

Gorham, E. and A. G. Gordon. Some Effects of Smelter Pollution Northeast of Falconbridge, Ontario, Can. J. Bot., 41: pp 378 - 380. 1963.

Greenfield, S. M. Rain Scavenging of Radioactive Particulate Matter from the Atmosphere, J. Met., 14: pp 115 - 125. 1957.

Gunn, R. and G. D. Kinzer. Terminal Velocity of Fall for Water Droplets in Stagnant Air, J. Meteorol. 6:246. 1949.

Hales, J. M., J. M. Thorp and M. A. Wolf. Washout of SO_2 from the Plume of a Coal Fired Power Plant by Natural Precipitation, In Proc. Symp. Precip, Scavenging, (1970) USAEC, Sypm, Series 22. 1970.

Hallsworth, E. G. and W. A. Adams. The Heavy Metal Content of the East Midlands, Environ. Pollut. 4:3, pp 231. 1973.

Harrison, P. R., K. A. Rahn, R. Dans, J. A. Robbins, J. W. Winchester, S. S. Brar and D. M. Nelson. Areawide Trace Metal Concentrations Measured by Multielement Neutron Activation Analysis - A One Day Study in Northwest Indiana, APCA Journal 21:9, pp 563 - 570. 1971.

Hegg, D. A. and P. V. Hobbs. Oxidation of Sulfur Dioxide In Aqueous Systems with Particular Reference to the Atmosphere, ATM ENVR 12(1 - 3): pp 241 - 254. 1978.

Hinds, W. T. Diffusion Over Coastal Mountains of Southern California, ATM ENVR 4: pp 107 - 124. 1970

Holland, J. Z. Meteorology Survey of the Oak Ridge Area, ORO-99. USAEC, Oak Ridge, Tenn. 1953.

Howard-White, F. B. "Nickel, an Historical Review, Methuen, London, U.K. 1963.

Huhn, F. J. Lake Sediment Records of Industrialization in the Sudbury Area of Ontario, MSc Thesis, University of Toronto. 1974.

INCO. The Land Above the Ore Below, Publicity Brochure, International Nickel Company. 1971.

Johnston, H. F. and D. R. Coughanowr. Absorption of Sulfur Dioxide from the Air, Ind. Eng. Chem. 50: pp 1169 - 1172. 1958.

Johnstone, H. F. and A. J. Woll. Formation of Sulfuric Acid in Fogs, Ind. Eng. Chem. 52: pp 861 - 863. 1960.

Jones, P. M., M.A.B. de Larrinaga and C. B. Wilson. The Urban Wind Velocity Profile, Atmos. Environ. 5:89. 1971.

Junge, C. E. "Air Chemistry and Radioactivity" Academic Press, N.Y.C. 1963.

Junge, C. E. and T. G. Ryan. Study of the SO_2 Oxidation in Solution and its Role in Atmospheric Chemistry, Royal Meteorol. Soc. Quart. Jour. 84: pp 46 - 55. 1958.

Katz, M. Photoelectric Determination of Atmospheric Sulfur Dioxide, Anal. Chem. 22:1040-7. 1950.

Kramer, J. R. Geology of Manitoulin Island and the North Shore to Espanola, Ontario Dept. of Geology, McMaster University. 1971.

Kramer, J. R. Fate of Atmospheric Sulphur Dioxide and Related Substances as Indicated by Chemistry of Precipitation (Part I), Rpt. submitted to Air Res. Branch, Min. Environ., Ontario. 1973.

Kramer, J. R. Fate of Atmospheric Sulphur Dioxide and Related Substances as Indicated by Chemistry of Precipitation (Part II), Rpt. submitted to Air Res. Branch, Min. Environ., Ontario. 1974.

Kramer, J. R. Fate of Atmospheric Sulphur Dioxide and Related Substances as Indicated by Chemistry of Precipitation (Part III), Rpt. submitted to Air Res. Branch, Min. Environ., Ontario. 1975.

Kramer, J. R. Fate of Atmospheric Sulphur Dioxide and Related Substances as Indicated by Chemistry of Precipitation (Part IV), Rpt. submitted to Air Res. Branch, Min. Environ., Ontario. 1976.

Kopp, J. F. and R. C. Kroner. Trace Metals in Water of the United States (Oct. 1, 1962 - Sept. 30, 1967), US Dept. Intr. Fed. Water. Pollu. Contr. Admin., Div. of Pollut. Surveillance, Cinn., Ohio. 1969.

Lazrus, A. L., E. Lorange and J. P. Lodge Jr. Lead and Other Metal Ions in United States Precipitation, Environ. Sci. and Tech. 4:1, pp 55. 1970.

Ledbetter, J. O. "Air Pollution", Marcel Dekker Inc., N.Y.C. 1972.

Lee, R. E. Jr., and R. K. Patterson Size Determination of Atmospheric Phosphate, Nitrate, Chloride, and Ammonium Particulate in Several Urban Areas, Atmos. Envrn., 3:249. 1969.

Lettau, H. Note on Aerodynamic Roughness - Parameter Estimation on the Basis of Roughness - Element Description, J. Appl. Meteorol., 8:828. 1969.

Levy, A., Drewes, D. R., and Hales, J. M. SO_2 Oxidation In Plumes: A Review and Assessment of Relevant Mechanistic and Rate Studies, BNWL, Richland, Wash., EPA-450/3-76-022. 1976.

Liberti, A. The Nature of Particulate Matter Int. Symp. on the Chemical Aspects of Air Pollution., Cortina d'Anpezzo, Italy, p631-642. 1969.

Lin, C. C. "Statistical Theories of Turbulence", Princeton University Press, Princeton NJ 1961.

Linzon, S. N., P. J. Temple and R. G. Pearson Sulphur Concentration in Plant Foliage and Related Effects APCA 29(5): 520-525. 1979.

Liss, P. S. Gas Transfer Across Natural Air-Water Interfaces with Special References to Lake Surfaces, Proc. Second Fed Conf. on the Great Lakes. Interagency Comm. on Marine Sci. and Eng. pp248-254. 1976.

Little, P. and Wiffen, R. D. Emission and Deposition of Petrol Engine Exhaust Pb-1 Deposition of Exhaust Pb to Plant and Soil Surfaces, Atm Envr. 11(5): 437-447. 1977.

Lumley, J. L. and H. A. Panofsky "The Structure of Atmospheric Turbulence". Wiley, NYC. 1964.

Lundgren, D. A. Atmospheric Aerosol Composition and Concentration as a Function of Particle Size and of Time, J. Air Pollut. Contr. Assc. 20:603. 1970.

Lusis, M., H. A. Wiebe, K. G. Anlauf and H. P. Sanderson The Rate of Oxidation of Sulphur Dioxide to Sulfuric Acid and Sulfate in the Plume of the INCO Superstack at Sudbury, Ontario, Atm. Envr. Services, Rpt. AEQA:26-75. 1975.

Makhon'ko, K. P. Simplified Theoretical Notion of Contaminant Removal by Precipitation from the Atmosphere, Tellus 19:3, p467 / 1967.

Manowitz, B. L., Newman, et al, The Atmospheric Diagnostic Program at Brookhaven National Laboratory, Status Rpt BNL 50361. 1972

Marcello, J. M. "Control of Air Pollution Sources", Marcel Dekker Inc. NYC. 1976.

Martens, C. S. and R. G. Harriss. Chemistry of Aerosols, Cloud Droplets and Rain in the Puerto Rican Marine Atmosphere. J. of Geophys. Res. 78:6, p949. 1973.

Mason, B., and L. G. Berry. "Elements of Mineralogy". W. H. Freeman Co., San Fransisco, Calif. 1968.

Massachusetts Institute of Technology. Man's Impact on the Global Environment, Rpt. of the Study of Critical Environmental Problems, M.I.T. Press, Cambridge, Mass. 1970.

McElroy, J. L. A Comparative Study of Urban and Rural Dispersion, J. Appl. Meteorol. 8:19. 1969.

McGovern, P. C. and D. Balsillie, Sulphur Dioxide (1972) Metal (1971), Levels and Vegetation Effects in the Sudbury Area, Air Management Branch, Ont. Min Envr, Sudbury, Ontario. 1973.

McMahon T. A., P. J. Denison and R. Fleming. A Long Distance Air Pollution Transportation Model Incorporating Washout and Dry Deposition Components, Atm. Envr. 10:751-761. 1976.

Miller, M. E., and G. C. Holzworth. An Atmospheric Diffusion Model for Metropolitan Areas, J. APCA 17:4, p232-4. 1967.

Möller, D. Kinetic Model of Atmospheric SO_2 Oxidation Based on Published Data, Atm. Envr. 14(9): 1067-1076. 1980.

Montgomery, T. L., S. B. Carpenter, W. C. Colbaugh and F. W. Thomas. Results of Recent TVA Investigation of Plume Rise, J. Air Pollut. Contr. Assc. 22:779. 1972.

Montgomery, T. L., W. B. Norris, F. W. Thomas and S. B. Carpenter. A Simplified Technique Used to Evaluate Atmospheric Dispersion of Emissions from Large Power Plants. J. Air. Pollut. Contr. Assc. 23:388. 1973.

Moses, H. "Mathematical Air Pollution Models", Argonne Nat. Lab. 1969.

Moses, H. and J. E. Carson. Stack Design Parameters Influencing Plume Rise, J. Air Pollut. Contr. Assc. 18:454. 1968.

Munn, R. E. "Descriptive Micrometeorology", Academic Press NYC. 1966.

Muller, E. F. and J. R. Kramer. Precipitation Scavenging in Central and Northern Ontario, ERDA Symp. Series 41, pp 560 - 601. 1977.

Newman, L., J. Forest and B. Monowitz. The Application of an Isotopic Ratio Technique to a Study of the Atmospheric Oxidation of Sulphur Dioxide in the Plume from a Coal-Fired Power Plant, Atm. Envr. 9: pp 969 - 977. 1975.

Obukhoff, A. M. "On the Energy Distribution in the Spectrum of a Turbulent Flow", Compt. Rend. Acad. Sci. U.R.S.S. 31:19. 1941.

O'Connor, D. J. An Analysis of the Dissolved Oxygen Distribution in the East River, J. Water Pollut. Contr. Fed. 38:11, pp 1813 - 1830. 1966.

O'Connor, D. J. and J. A. Mueller. A Water Quality Model of Chloride in Great Lakes, Proc. ASCE, Jour. Sed. 96:SA4, pp 955 - 975. 1970.

Ontario Department of Lands and Forests. Algoma, Sudbury, Timiskaming and Nipissing, 1:506,880 Surficial Geology Map, S465. 1962.

Ontario Ministry of Environment. High Volume Air Sampler Data, Air Resources Branch. 1973, 1974, 1975 and 1976.

Ontario Ministry of Environment. Air Quality Monitoring Reports, Volume I and III, Air Resources Branch. 1973, 1974, 1975 and 1976.

Ontario Ministry of Natural Resources. Blind River, 1:125,000 Geological Map, 41-JSE. 1972.

Ontario Ministry of Natural Resources. Espanola, 1:125,000 Geological Map, 41-ISW. 1976.

Orlenko, L. R. Wind and its Technical Aspects, Tech. Note No. 109, World Meteorol. Org. Geneva, Switz. 1970.

Pasquill, F. The Estimation of the Dispersion of Windborne Material, Meteorol. Mag. 90:33. 1961.

Pasquill, F. "Atmospheric Diffusion", Van Nostrand, London U. K., 1962.

Peirson, D. H., P. A. Cawse, L. Solman and R. S. Cambary. Trace Elements in the Atmospheric Environment, Nature, Vol. 241, pp 252 - 256. 1973.

Penzhorn, R. D., W. G. Filby and H. Guestin. Photochemically Induced Homogeneous Removal Rate of Sulphur Dioxide from the Lower Atmosphere of Central Europe, Z. Naturforsch. 29(A): pp 1449 - 1453. 1974.

Phillips, P. W. and J.A.W. McCulloch. Climatological Studies, 20: Envr. Canada. 1972.

Plate, E. J. "Aerodynamic Characteristics of Atmospheric Boundary Layers", AEC Crit. Rev. Ser., TID-25465, USAEC, Wash., D.C. 1971.

Priestly, C.H.B. "Turbulent Transfer in the Lower Atmosphere", Univ. of Chicago Press, Chicago, Ill. 1959.

Roberts, J. J., E. S. Croke and A. S. Kennedy. An Urban Atmospheric Dispersion Model, Proc. Symp. Mult. Source Urban Diff. Models, Chapel Hill, N.C., Air Poll. Contr. Office Pub. AP-86 USEPA. 1970.

Roberts, J. J., J. E. Norco, A. S. Kennedy and E. J. Croke. A Model for Simulation of Air Pollution Transients, Proc. 2nd Int. Clean Air Congress: pp 1161 - 1167. 1971.

Roberts, J. J., E. J. Croke and A. S. Kennedy. An Urban Atmospheric Dispersion Model, Proc. Symp. Multiple Source Urban Diffusion Models, USEPA: pp 61 - 62. 1970.

Roberts, P. T. and S. K. Friedlander. Conversion of SO_2 to Sulfur Particulate in the Los Angeles Atmosphere, Envr. Health Perspectives, 10: pp 103 - 108. 1975.

Robinson, E. and F. L. Ludwig. Particle Size Distribution of Urban Lead Aerosols, J. Air Pollut. Contr. Assc. 17:664. 1967.

Rohsenow, W. M. and H. Y. Choi. "Heat, Mass and Momentum Transfer", Prentice Hall, Englewood Cliffs, N.J. 1961.

Roth, M. R., M. A. Yocke, J. P. Meyer, M. K. Liu, J. P. Killus and C. S. Burton. An Examination of the Accuracy and Adequacy of Air Quality Models and Monitoring Data for use in Assessing the Impact of EPA Significant Deterioration Regulations on Energy Developments, Amer. Petr. Inst. TR(F)-10700-2. 1975.

Scott, W. D. and Hobbs, P. V. Formation of Sulphate in Water Droplets, J. Atmos. Sci. 24:54. 1967.

Sehmel, G. A. Particle and Gas Deposition; a Review, Atm. Envr. 14(9): pp. 983 - 1012. 1980.

Sehmel, G. A. and S. L. Sutter. Particle Deposition Rates on a Water Surface as a Function of Particle Diameter and Air Velocity. BNWL-1850, Prt. 3: pp 171 - 174. 1974.

Semkin, R. G. A Limnogeochemical Study of Sudbury Area Lakes, M. Sc. Thesis, McMaster University. 1974.

Shieh, L. J., B. Davidson and J. P. Friend. A Model of Diffusion in Urban Atmospheres: SO_2 in Greater New York, Proc. Symp. Multiple Source Urban Diffusion Model. Chapel Hill, N.C., Air Poll. Contr. Office Pub. AP-86, USEPA: pp 10.1 - 10.39. 1970.

Shirai, T., S. Hamada, H. Takahashi, T. Ozawa, T. Ohmuro and T. Kawakami. Photooxidation of SO_2 in Air, Kogyo-Kagaku Zasshi. 65:1906. 1962.

Sidle, A. B. Amino Acid Content of Atmospheric Precipitation, Tellus, 19:1. pp 128. 1967.

Sillen, L. G. Stability Constant of Metal Ion Complexes, Section I. Chem. Soc. Special Publ. No 17. 1964.

Slade, D. H. Modeling Air Pollution in the Washington D.C., to Boston, Megalopolis, Science 157: pp 1304 - 1307. 1967.

Slade, D. H. ed. "Meteorology and Atomic Energy - 1968" TID-24190 USAEC. Oak Ridge, Tenn. 1968.

Slinn, W.G.M. and J. M. Hales. Phoretic Processes in Scavenging, in Proc. Symp. Precipitation Scavenging-1970 USAEC Symp. Series 22. 1970.

Smith, F. B. and T. S. Hay. The Expansion of Clusters of Particles in the Atmosphere, Roy. Meteorol. Soc. Quart. J. 87: pp 82 - 101. 1961.

Smith, M. E. and I. A. Singer. An Improved Method of Estimating Concentrations and Related Phenomena from a Point Source Emission, J. Appl. Meteorol. 5(5) pp 631 - 639. 1966.

Snodgrass, W. J. and C. R. Omelia. A Predictive Model for Phosphorous in Lakes, Dept. Envrn. Sci. and Eng., Univ. North Carolina, Chapel Hill, N.C. 1974.

Soo, S. L. Modeling and Similarity Relations of Physical and Chemical Processes, Int. Symp. on the Chemical Aspects of Air Pollut., Cortina d'Anpezzo, Italy. pp 721 - 9. 1969.

Stephens, N. T. and R. O. McCaldin. Attenuation of Power Station Plumes as Determined by Instrumented Aircraft, Envr. Sci. Tech. 5: pp 615 - 21. 1971.

Stern, A. C. "Air Pollution", 3rd ed, Academic Press, N.Y.C. 1976.

Stern, A. C., H. C. Wohlers, R. W. Boubel and W. P. Lowry. "Fundamentals of Air Pollution", Academic Press, N.Y.C. 1973.

Stokes, P. M., T. C. Hutchinson and K. Krauter. Heavy Metal Tolerance in Algae Isolated from Polluted Lakes Near the Sudbury, Ontario Smelters, Water Pollut. Res. in Canada Vol 8, Inst. Envr. Sci. and Eng., University of Toronto. 1973.

Strickland, J.D.H. and T. R. Parsons. "A Practical Handbook of Seawater Analysis", Fish. Res. Board of Canada, Bull.167, 1968.

Stumm, W. and J. J. Morgan. "Aquatic Chemistry", Wiley Interscience. 1970.

Sutton, O. G. The Theoretical Distribution of Airborne Pollution from Factory Chimneys, Quart. J. Roy. Meteorol. Soc. 73: p 426. 1947.

Sutton, O. G. "Micrometeorology", McGraw-Hill, N.Y.C. 1953.

Thomann, R. V., D. J. O'Connor and D. M. DiToro. Mathematical Modeling of Phytoplankton in Lake Ontario, USEPA, Corvallis, Oregon, 660-3-75-005. 1975.

Thomas, M. D. and R. H. Hendricks. Effects of Air Pollution on Plants, in "Air Pollution Handbook", McGraw-Hill, N.Y.C. 1956.

Turner, D. B. A Diffusion Model for an Urban Area, J. Appl. Meteorol. 3: pp 83 - 91. 1964.

Turner, D. B. "Workbook of Atmospheric Dispersion Estimates", US Dept. of HEW. 1969.

Turner, D. B. "Workbook of Atmospheric Diffusion Estimates", Pub. 999-AP-26 Public Health Services, Nat. Air. Poll. Contr. Admin., Cinn., Ohio. 1970.

Turner, D. B. "Workbook of Dispersion Estimates", USEPA, Publ. No. AP-26. 1971.

Tverskoi, P. N. "Physics of the Atmosphere", Israel Prog. for Scientific Trans., Jerusalem. 1962 (Trans, 1965).

United States Bureau of Mines. Minerals Yearbook, U.S. Dept. Interior, US Gov. Publ., Wash., D.C. 1953 through 1972.

United States Environmental Protection Agency. 1973 National Emissions Report National Emissions Data System (NEDS) of the Aerometric and Emission Reporting System (AEROS) US EPA-450/2-76-007. 1976.

University of Utah Research Institute. Rate of Conversion of Sulfur Dioxide in a Power Plant Plume to Particulate Sulfate, Final Report, Phase I, APS Contract No. 75-00634. 1975.

Van den Heuvel, A. P. and B. J. Mason. The Formation of Ammonium Sulphate in Water Droplets Exposed to Gaseous Sulphur Dioxide and Ammonia, Roy. Meteorol. Soc. Quart. J. 89: pp 271 - 275. 1963.

Van der Westhuizen, M. Radioactive Nuclear Bomb Fallout - A Relationship Between Deposition, Air Concentration and Rainfall, Atm. Envr. 3: pp 241 - 248. 1969.

Weber, E. Determination of the Lifetime of SO_2 by Simultaneous CO_2 and SO_2 Monitoring, 2nd Int. Clean Air Cong., Wash. D.C., December 6 - 11. 1970.

Whelpdale, D. M. and R. W. Shaw. Sulphur Dioxide Removal by Turbulent Transfer Over Grass, Snow and Water Surfaces, 1974, Accpt. for Publ. by Tellus, Feb. 5. 1974.

Whitby, K. T., B. C. Cantrel, R. B. Husar, N. V. Gillani, J. A. Anderson, D. C. Blumenthal and W. E. Wilson Jr. Aerosol Formation in a Coal-Fired Power Plant Plume, Presented Div. Envr. Chem., Am. Chem. Soc., April 1976.

Winchester, J. W. and G. D. Nifong. Water Pollution in Lake Michigan by Trace Elements from Pollution Aerosol Fallout, Water, Air and Soil Pollut., 1: pp 50 - 64. 1971.

Yue, G. K., C. S. Kiang, V. A. Mohnen and E. Danielsen. The Interaction of Atmospheric Sulfur Compounds with Cloud and Precipitation Elements, Intrm. Rpt. Nat. Sci. Foundt., State University of New York, (Albany), p 143. 1975.

APPENDIX B
Measured and calculated
precipitation concentrations

1 2*SHEAD

CONSTITUENT		AVERAGE CONC	STD DEV	AVERAGE LOADING	STD DEV
SO4 CONC IN 10(-6) GM/CM3, LOADINGS IN 10(-6) GM/CM2/DAY					
20	MIN CALC	1.945	.969	.500	.249
21	MAX CALC	26.413	19.464	6.793	5.006
34	AVE MEAS	5.127	3.443	.935	.631
ATM CONC IN 10(-12) GM/M3					
60	ATM CALC	.136E-08	.596E-08		
57	DISSOLVED SO2	.182E-06	.810E-06		
58	DISSOLVED SO4	.876E-07	.290E-06		
59	PRTCULATE SO4	.149E-08	.731E-08		
PH LOADINGS IN (EXP) MEQ/CM2/DAY					
22	MIN CALC	5.312	.245	1366.230	62.884
23	MAX CALC	4.245	.353	1091.606	90.713
35	AVE MEAS	4.077	.332	746.720	60.833
ATM CONC IN 10(-12) GM/M3					
61	ATM CALC	.122E-07	.516E-08		
CU CONC IN 10(-9) GM/CM3, LOADINGS IN 10(-9) GM/CM2/DAY					
24	MIN CALC	17.669	14.750	4.544	3.793
25	MAX CALC	425.832	374.520	109.512	96.316
36	AVE MEAS	194.407	145.872	35.602	26.714
ATM CONC IN 10(-12) GM/M3					
62	ATM CALC	.210E-11	.859E-11		
NI CONC IN 10(-9) GM/CM3, LOADINGS IN 10(-9) GM/CM2/DAY					
26	MIN CALC	2.597	1.931	.771	.497
27	MAX CALC	69.340	51.399	17.832	13.218
37	AVE MEAS	152.814	113.096	27.985	20.711
ATM CONC IN 10(-12) GM/M3					
63	ATM CALC	.111E-11	.460E-11		
PB CONC IN 10(-9) GM/CM3, LOADINGS IN 10(-9) GM/CM2/DAY					
28	MIN CALC	3.064	1.773	.788	.456
29	MAX CALC	4.082	2.151	1.050	.553
38	AVE MEAS	41.593	27.363	7.616	5.011
ATM CONC IN 10(-12) GM/M3					
64	ATM CALC	.682E-13	.188E-13		
ZN CONC IN 10(-9) GM/CM3, LOADINGS IN 10(-9) GM/CM2/DAY					
30	MIN CALC	25.039	15.460	6.439	3.976
31	MAX CALC	42.301	20.654	10.879	5.312
39	AVE MEAS	204.161	275.522	37.388	50.457
ATM CONC IN 10(-12) GM/M3					
65	ATM CALC	.536E-12	.367E-12		
FE CONC IN 10(-9) GM/CM3, LOADINGS IN 10(-9) GM/CM2/DAY					
32	MIN CALC	103.813	68.796	26.698	17.693
33	MAX CALC	498.762	336.362	126.268	86.503
40	AVE MEAS	777.568	657.301	142.397	120.373
ATM CONC IN 10(-12) GM/M3					
66	ATM CALC	.585E-11	.213E-10		

2 3 KILLARNEY

CONSTITUENT		AVERAGE CONC	STD DEV	AVERAGE LOADING	STD DEV
SO4 CONC IN 10(-6) GM/CM3, LOADINGS IN 10(-6) GM/CM2/DAY					
29	MIN CALC	1.166	.758	.265	.188
21	MAX CALC	3.755	2.010	.933	.499
34	AVE MEAS	3.590	1.830	.712	.372
ATM CONC IN 10(-12) GM/M3					
60	ATM CALC	.147E-09	.438E-10		
57	DISSOLVED SO2	.992E-08	.523E-08		
58	DISSOLVED SO4	.649E-08	.512E-08		
59	PRTCULATE SO4	.311E-10	.645E-10		
PH LOADINGS IN (EXP) MEQ/CM2/DAY					
22	MIN CALC	5.610	.342	1393.873	84.949
23	MAX CALC	5.030	.288	1249.676	71.573
35	AVE MEAS	4.290	.795	872.242	161.591
ATM CONC IN 10(-12) GM/M3					
61	ATM CALC	.780E-08	.702E-08		
CU CONC IN 10(-9) GM/CM3, LOADINGS IN 10(-9) GM/CM2/DAY					
24	MIN CALC	3.976	5.957	.988	1.480
25	MAX CALC	59.063	73.724	14.675	18.318
36	AVE MEAS	15.479	18.565	3.147	3.775
ATM CONC IN 10(-12) GM/M3					
62	ATM CALC	.219E-13	.655E-14		
NI CONC IN 10(-9) GM/CM3, LOADINGS IN 10(-9) GM/CM2/DAY					
26	MIN CALC	.929	.691	.231	.172
27	MAX CALC	9.127	10.342	2.268	2.570
37	AVE MEAS	35.768	144.300	7.272	29.339
ATM CONC IN 10(-12) GM/M3					
63	ATM CALC	.222E-13	.663E-14		
PB CONC IN 10(-9) GM/CM3, LOADINGS IN 10(-9) GM/CM2/DAY					
28	MIN CALC	2.337	1.286	.581	.320
29	MAX CALC	4.051	2.131	1.007	.529
39	AVE MEAS	20.768	19.995	5.849	4.065
ATM CONC IN 10(-12) GM/M3					
64	ATM CALC	.666E-13	.199E-13		
ZN CONC IN 10(-9) GM/CM3, LOADINGS IN 10(-9) GM/CM2/DAY					
30	MIN CALC	16.634	11.451	4.680	2.845
31	MAX CALC	32.470	17.981	8.068	4.468
39	AVE MEAS	143.446	227.411	29.166	46.237
ATM CONC IN 10(-12) GM/M3					
65	ATM CALC	.444E-12	.133E-12		
FE CONC IN 10(-9) GM/CM3, LOADINGS IN 10(-9) GM/CM2/DAY					
32	MIN CALC	68.382	51.625	16.916	12.877
33	MAX CALC	137.649	74.331	34.201	18.444
40	AVE MEAS	163.554	147.751	33.254	30.041
ATM CONC IN 10(-12) GM/M3					
66	ATM CALC	.106E-11	.300E-12		

3 4 GORE BAY

CONSTITUENT		AVERAGE CONC	STD DEV	AVERAGE LOADING	STD DEV
SO4 CONC IN 10(-6) GM/CM3, LOADINGS IN 10(-6) GM/CM2/DAY					
20	MIN CALC	.586	.333	.147	.083
21	MAX CALC	2.393	1.202	.599	.301
34	AVE MEAS	3.493	2.199	.504	.326
ATM CONC IN 10(-12) GM/M3					
60	ATM CALC	.159E-09	.362E-10		
57	DISSOLVED SO2	.837E-08	.254E-08		
58	DISSOLVED SO4	.281E-08	.462E-08		
59	PRTCULATE SO4	.546E-11	.214E-11		
PH LOADINGS IN (EXP) MEQ/CM2/DAY					
22	MIN CALC	5.900	.340	1476.490	85.125
23	MAX CALC	5.256	.255	1316.399	63.786
35	AVE MEAS	4.985	1.318	738.099	195.122
ATM CONC IN 10(-12) GM/M3					
61	ATM CALC	.261E-08	.479E-08		
CU CONC IN 10(-9) GM/CM3, LOADINGS IN 10(-9) GM/CM2/DAY					
24	MIN CALC	1.471	1.383	.368	.346
25	MAX CALC	16.131	17.273	4.037	4.322
36	AVE MEAS	9.734	11.952	1.441	1.770
ATM CONC IN 10(-12) GM/M3					
62	ATM CALC	.313E-13	.423E-13		
NI CONC IN 10(-9) GM/CM3, LOADINGS IN 10(-9) GM/CM2/DAY					
26	MIN CALC	.546	.471	.137	.118
27	MAX CALC	4.427	4.491	1.108	1.124
37	AVE MEAS	6.131	6.103	.908	.904
ATM CONC IN 10(-12) GM/M3					
63	ATM CALC	.287E-13	.268E-13		
PB CONC IN 10(-9) GM/CM3, LOADINGS IN 10(-9) GM/CM2/DAY					
28	MIN CALC	1.522	.731	.381	.183
29	MAX CALC	3.909	1.861	.978	.466
38	AVE MEAS	19.771	16.591	2.928	2.457
ATM CONC IN 10(-12) GM/M3					
64	ATM CALC	.722E-13	.165E-13		
ZN CONC IN 10(-9) GM/CM3, LOADINGS IN 10(-9) GM/CM2/DAY					
30	MIN CALC	12.117	5.319	3.032	1.456
31	MAX CALC	30.644	15.117	7.669	3.783
39	AVE MEAS	171.551	237.339	25.403	35.144
ATM CONC IN 10(-12) GM/M3					
65	ATM CALC	.481E-12	.110E-12		
FE CONC IN 10(-9) GM/CM3, LOADINGS IN 10(-9) GM/CM2/DAY					
32	MIN CALC	42.160	22.230	10.551	5.563
33	MAX CALC	109.552	54.460	27.416	13.629
40	AVE MEAS	184.300	232.039	27.291	34.360
ATM CONC IN 10(-12) GM/M3					
66	ATM CALC	.109E-11	.255E-12		

4 5 JAMOT

CONSTITUENT	AVERAGE CONC	STD DEV	AVERAGE LOADING	STD DEV
SO4 CONC IN 10(-6) GM/CM3, LOADINGS IN 10(-6) GM/CM2/DAY				
20 MIN CALC	.969	.604	.249	.176
21 MAX CALC	7.706	5.844	1.983	1.502
34 AVE MEAS	3.445	2.334	.834	.430
ATM CONC IN 10(-12) GM/M3				
60 ATM CALC	.155E-09	.429E-10		
57 DISSOLVED SO2	.118E-07	.101E-07		
58 DISSOLVED SO4	.141E-07	.444E-07		
59 PRTCULATE SO4	.359E-10	.661E-10		
PH LOADINGS IN (EXP) MEQ/CM2/DAY				
22 MIN CALC	5.651	.366	1452.148	78.537
23 MAX CALC	4.744	.258	1219.117	66.190
35 AVE MEAS	4.517	.726	831.336	133.609
ATM CONC IN 10(-12) GM/M3				
61 ATM CALC	.776E-08	.785E-08		
CU CONC IN 10(-9) GM/CM3, LOADINGS IN 10(-9) GM/CM2/DAY				
24 MIN CALC	6.107	5.715	1.590	1.468
25 MAX CALC	205.658	177.527	52.845	45.616
36 AVE MEAS	17.098	19.009	3.146	3.499
ATM CONC IN 10(-12) GM/M3				
62 ATM CALC	.320E-12	.160E-11		
NI CONC IN 10(-9) GM/CM3, LOADINGS IN 10(-9) GM/CM2/DAY				
26 MIN CALC	1.078	.628	.277	.161
27 MAX CALC	29.493	21.235	7.578	5.456
37 AVE MEAS	9.414	9.427	1.733	1.735
ATM CONC IN 10(-12) GM/M3				
63 ATM CALC	.163E-12	.752E-12		
PB CONC IN 10(-9) GM/CM3, LOADINGS IN 10(-9) GM/CM2/DAY				
28 MIN CALC	1.956	1.132	.502	.291
29 MAX CALC	3.966	2.109	1.019	.542
38 AVE MEAS	25.493	15.204	4.692	2.798
ATM CONC IN 10(-12) GM/M3				
64 ATM CALC	.662E-13	.185E-13		
ZN CONC IN 10(-9) GM/CM3, LOADINGS IN 10(-9) GM/CM2/DAY				
30 MIN CALC	15.678	9.814	4.029	2.522
31 MAX CALC	33.659	18.682	8.649	4.800
39 AVE MEAS	103.793	74.929	19.105	13.792
ATM CONC IN 10(-12) GM/M3				
65 ATM CALC	.466E-12	.131E-12		
FE CONC IN 10(-9) GM/CM3, LOADINGS IN 10(-9) GM/CM2/DAY				
32 MIN CALC	56.111	44.243	14.932	11.368
33 MAX CALC	221.244	149.282	56.850	38.359
40 AVE MEAS	174.276	120.335	32.078	22.149
ATM CONC IN 10(-12) GM/M3				
66 ATM CALC	.132E-11	.159E-11		

5 6 WINDY LAKE

CONSTITUENT	AVERAGE CONC	STD DEV	AVERAGE LOADING	STD DEV
SO4 CONC IN 10(-6) GM/CM3, LOADINGS IN 10(-6) GM/CM2/DAY				
20 MIN CALC	2.074	1.254	.346	.201
21 MAX CALC	10.811	7.146	1.802	1.191
34 AVE MEAS	3.360	2.644	.920	.724
ATM CONC IN 10(-12) GM/M3				
60 ATM CALC	.232E-09	.206E-16		
57 DISSOLVED SO2	.586E-07	.171E-13		
58 DISSOLVED SO4	.243E-06	.446E-13		
59 PETCULATE SO4	.503E-10	.515E-17		
PH LOADINGS IN (EXP) MEQ/CM2/DAY				
22 MIN CALC	5.326	.313	887.611	52.149
23 MAX CALC	4.618	.309	769.611	51.429
35 AVE MEAS	4.259	.392	1166.246	107.279
ATM CONC IN 10(-12) GM/M3				
61 ATM CALC	.102E-07	.280E-14		
CU CONC IN 10(-9) GM/CM3, LOADINGS IN 10(-9) GM/CM2/DAY				
24 MIN CALC	8.655	3.721	1.447	.620
25 MAX CALC	21.575	7.863	3.596	1.311
36 AVE MEAS	16.460	19.779	4.507	5.416
ATM CONC IN 10(-12) GM/M3				
62 ATM CALC	.864E-11	.204E-17		
NI CONC IN 10(-9) GM/CM3, LOADINGS IN 10(-9) GM/CM2/DAY				
26 MIN CALC	4.611	2.179	.769	.363
27 MAX CALC	19.456	11.087	3.243	1.848
37 AVE MEAS	12.020	13.968	3.291	3.825
ATM CONC IN 10(-12) GM/M3				
63 ATM CALC	.407E-11	.966E-18		
PB CONC IN 10(-9) GM/CM3, LOADINGS IN 10(-9) GM/CM2/DAY				
28 MIN CALC	16.613	8.335	2.769	1.389
29 MAX CALC	27.107	12.750	4.518	2.125
39 AVE MEAS	22.157	14.495	6.067	3.969
ATM CONC IN 10(-12) GM/M3				
64 ATM CALC	.579E-13	.128E-19		
ZN CONC IN 10(-9) GM/CM3, LOADINGS IN 10(-9) GM/CM2/DAY				
30 MIN CALC	54.315	27.076	9.052	4.513
31 MAX CALC	89.093	42.054	14.849	7.009
38 AVE MEAS	39.723	115.857	24.567	31.723
ATM CONC IN 10(-12) GM/M3				
65 ATM CALC	.716E-12	.127E-18		
FE CONC IN 10(-9) GM/CM3, LOADINGS IN 10(-9) GM/CM2/DAY				
32 MIN CALC	64.659	28.546	10.776	4.808
33 MAX CALC	138.633	55.610	23.105	9.268
40 AVE MEAS	183.350	135.750	50.203	37.170
ATM CONC IN 10(-12) GM/M3				
66 ATM CALC	.945E-11	.232E-17		

6 8 MOUNT LAKE

CONSTITUENT		AVERAGE CONC	STD DEV	AVERAGE LOADING	STD DEV
SO4 CONC IN 10(-6) GM/CM3, LOADINGS IN 10(-6) GM/CM2/DAY					
20	MIN CALC	.527	.263	.132	.066
21	MAX CALC	2.169	1.010	.542	.252
34	AVE MEAS	3.753	3.201	.685	.585
ATM CONC IN 10(-12) GM/M3					
60	ATM CALC	.156E-09	.705E-10		
57	DISSOLVED SO2	.913E-08	.447E-08		
58	DISSOLVED SO4	.325E-08	.466E-09		
59	PRTCULATE SO4	.134E-10	.311E-10		
PH LOADINGS IN (EXP) MEQ/CM2/DAY					
22	MIN CALC	5.891	.361	1471.359	95.041
23	MAX CALC	5.263	.325	1314.108	81.252
35	AVE MEAS	4.278	.462	781.881	84.373
ATM CONC IN 10(-12) GM/M3					
61	ATM CALC	.377E-08	.590E-08		
CU CONC IN 10(-9) GM/CM3, LOADINGS IN 10(-9) GM/CM2/DAY					
24	MIN CALC	1.099	.714	.272	.178
25	MAX CALC	4.425	5.058	1.105	1.263
36	AVE MEAS	6.214	9.206	1.136	1.683
ATM CONC IN 10(-12) GM/M3					
62	ATM CALC	.233E-13	.105E-13		
NI CONC IN 10(-9) GM/CM3, LOADINGS IN 10(-9) GM/CM2/DAY					
26	MIN CALC	.459	.313	.115	.078
27	MAX CALC	1.598	1.781	.399	.445
37	AVE MEAS	5.189	9.924	.948	1.814
ATM CONC IN 10(-12) GM/M3					
63	ATM CALC	.236E-13	.107E-13		
PB CONC IN 10(-9) GM/CM3, LOADINGS IN 10(-9) GM/CM2/DAY					
28	MIN CALC	1.403	.624	.350	.156
29	MAX CALC	3.923	1.731	.980	.432
38	AVE MEAS	21.321	21.075	3.897	3.852
ATM CONC IN 10(-12) GM/M3					
64	ATM CALC	.708E-13	.320E-13		
ZN CONC IN 10(-9) GM/CM3, LOADINGS IN 10(-9) GM/CM2/DAY					
30	MIN CALC	11.056	4.650	2.761	1.211
31	MAX CALC	30.403	13.492	7.591	3.369
39	AVE MEAS	66.268	97.156	15.768	17.758
ATM CONC IN 10(-12) GM/M3					
65	ATM CALC	.472E-12	.213E-12		
FE CONC IN 10(-9) GM/CM3, LOADINGS IN 10(-9) GM/CM2/DAY					
32	MIN CALC	37.441	16.345	9.349	4.081
33	MAX CALC	100.691	45.240	25.142	11.296
40	AVE MEAS	101.529	97.599	18.630	17.838
ATM CONC IN 10(-12) GM/M3					
66	ATM CALC	.107E-11	.482E-12		

7 9 GOGAMA

CONSTITUENT	AVERAGE CONC	STD DEV	AVERAGE LOADING	STD DEV
SO4 CONC IN 10(-6) GM/CM3, LOADINGS IN 10(-6) GM/CM2/DAY				
20 MIN CALC	.357	.244	.090	.062
21 MAX CALC	2.715	1.106	.687	.280
34 AVE MEAS	3.261	2.281	.571	.399
ATM CONC IN 10(-12) GM/M3				
60 ATM CALC	.142E-09	.391E-10		
57 DISSOLVED SO2	.771E-08	.227E-08		
58 DISSOLVED SO4	.286E-08	.618E-08		
59 PRTCULATE SO4	.101E-11	.221E-11		
PH LOADINGS IN (EXP) MEQ/CM2/DAY				
22 MIN CALC	6.175	.385	1537.015	97.299
23 MAX CALC	5.135	.260	1299.265	65.784
35 AVE MEAS	4.413	.477	772.526	83.482
ATM CONC IN 10(-12) GM/M3				
61 ATM CALC	.264E-08	.555E-08		
CU CONC IN 10(-9) GM/CM3, LOADINGS IN 10(-9) GM/CM2/DAY				
24 MIN CALC	1.939	3.323	.491	.841
25 MAX CALC	46.359	44.393	11.730	11.232
36 AVE MEAS	8.296	7.238	1.452	1.267
ATM CONC IN 10(-12) GM/M3				
62 ATM CALC	.416E-13	.107E-12		
NI CONC IN 10(-9) GM/CM3, LOADINGS IN 10(-9) GM/CM2/DAY				
26 MIN CALC	.487	.574	.123	.145
27 MAX CALC	8.894	8.434	2.250	2.134
37 AVE MEAS	3.861	3.897	.676	.682
ATM CONC IN 10(-12) GM/M3				
63 ATM CALC	.305E-13	.470E-13		
PB CONC IN 10(-9) GM/CM3, LOADINGS IN 10(-9) GM/CM2/DAY				
29 MIN CALC	.866	.570	.219	.144
29 MAX CALC	3.974	1.869	1.005	.473
38 AVE MEAS	27.800	19.607	4.867	3.432
ATM CONC IN 10(-12) GM/M3				
64 ATM CALC	.648E-13	.178E-13		
ZN CONC IN 10(-9) GM/CM3, LOADINGS IN 10(-9) GM/CM2/DAY				
30 MIN CALC	6.633	4.334	1.691	1.097
31 MAX CALC	31.133	14.652	7.877	3.707
39 AVE MEAS	162.964	129.222	20.529	22.622
ATM CONC IN 10(-12) GM/M3				
65 ATM CALC	.432E-12	.118E-12		
FE CONC IN 10(-9) GM/CM3, LOADINGS IN 10(-9) GM/CM2/DAY				
32 MIN CALC	22.556	13.905	5.707	3.518
33 MAX CALC	123.431	50.352	31.231	12.740
40 AVE MEAS	286.321	214.922	50.124	37.625
ATM CONC IN 10(-12) GM/M3				
66 ATM CALC	.991E-12	.275E-12		

8 10 TEMAGAMI

CONSTITUENT		AVERAGE CONC	STD DEV	AVERAGE LOADING	STD DEV
SO4 CONC IN 10(-6) GM/CM3, LOADINGS IN 10(-6) GM/CM2/DAY					
20	MIN CALC	.497	.283	.126	.072
21	MAX CALC	3.279	1.668	.833	.424
34	AVE MEAS	4.856	3.093	.826	.526
ATM CONC IN 10(-12) GM/M3					
60	ATM CALC	.147E-09	.284E-10		
57	DISSOLVED SO2	.766E-08	.124E-08		
58	DISSOLVED SO4	.267E-08	.903E-08		
59	PRTCULATE SO4	.240E-11	.973E-11		
PH LOADINGS IN (EXP) MEQ/CM2/DAY					
22	MIN CALC	5.936	.349	1507.208	88.528
23	MAX CALC	5.085	.258	1291.224	65.419
35	AVE MEAS	4.270	1.006	726.180	171.091
ATM CONC IN 10(-12) GM/M3					
61	ATM CALC	.138E-08	.428E-08		
CU CONC IN 10(-9) GM/CM3, LOADINGS IN 10(-9) GM/CM2/DAY					
24	MIN CALC	1.767	2.165	.449	.555
25	MAX CALC	85.907	72.923	21.613	18.516
36	AVE MEAS	17.066	16.156	2.902	2.748
ATM CONC IN 10(-12) GM/M3					
62	ATM CALC	.567E-13	.196E-12		
NI CONC IN 10(-9) GM/CM3, LOADINGS IN 10(-9) GM/CM2/DAY					
26	MIN CALC	.549	.474	.139	.120
27	MAX CALC	15.136	12.346	3.843	3.135
37	AVE MEAS	6.728	6.683	1.144	1.137
ATM CONC IN 10(-12) GM/M3					
63	ATM CALC	.402E-13	.101E-12		
PB CONC IN 10(-9) GM/CM3, LOADINGS IN 10(-9) GM/CM2/DAY					
28	MIN CALC	1.266	.636	.327	.174
29	MAX CALC	3.872	1.761	.983	.447
38	AVE MEAS	23.875	19.952	4.911	3.393
ATM CONC IN 10(-12) GM/M3					
64	ATM CALC	.666E-13	.132E-13		
ZN CONC IN 10(-9) GM/CM3, LOADINGS IN 10(-9) GM/CM2/DAY					
30	MIN CALC	10.096	5.370	2.563	1.363
31	MAX CALC	30.726	13.990	7.802	3.552
39	AVE MEAS	251.922	686.695	42.846	117.132
ATM CONC IN 10(-12) GM/M3					
65	ATM CALC	.445E-12	.872E-13		
FE CONC IN 10(-9) GM/CM3, LOADINGS IN 10(-9) GM/CM2/DAY					
32	MIN CALC	34.407	18.131	8.736	4.604
33	MAX CALC	148.108	69.759	37.606	17.713
40	AVE MEAS	340.656	408.604	57.938	69.495
ATM CONC IN 10(-12) GM/M3					
66	ATM CALC	.101E-11	.194E-12		

9 11 ESPANOLA

CONSTITUENT		AVERAGE CONC	STD DEV	AVERAGE LOADING	STD DEV
SO4 CONC IN 10(-6) GM/CM3, LOADINGS IN 10(-6) GM/CM2/DAY					
20	MIN CALC	1.035	.531	.258	.132
21	MAX CALC	2.129	.820	.531	.205
34	AVE MEAS	11.115	8.452	2.250	1.711
ATM CONC IN 10(-12) GM/M3					
60	ATM CALC	.159E-09	.407E-10		
57	DISSOLVED SO2	.160E-07	.484E-08		
58	DISSOLVED SO4	.644E-08	.426E-08		
59	PRTCULATE SO4	.746E-10	.404E-10		
PH	LOADINGS IN (EXP) MEQ/CM2/DAY				
22	MIN CALC	5.623	.310	1403.138	77.210
23	MAX CALC	5.279	.222	1316.178	55.373
35	AVE MEAS	5.029	.874	1018.301	176.990
ATM CONC IN 10(-12) GM/M3					
61	ATM CALC	.125E-07	.629E-08		
CU CONC IN 10(-9) GM/CM3, LOADINGS IN 10(-9) GM/CM2/DAY					
24	MIN CALC	2.325	1.698	.580	.423
25	MAX CALC	14.827	20.440	3.697	5.096
36	AVE MEAS	17.876	16.436	3.619	3.328
ATM CONC IN 10(-12) GM/M3					
62	ATM CALC	.236E-13	.604E-14		
NI CONC IN 10(-9) GM/CM3, LOADINGS IN 10(-9) GM/CM2/DAY					
26	MIN CALC	.804	.387	.201	.097
27	MAX CALC	3.994	5.403	.996	1.347
37	AVE MEAS	10.942	10.426	2.216	2.111
ATM CONC IN 10(-12) GM/M3					
63	ATM CALC	.239E-13	.610E-14		
PB CONC IN 10(-9) GM/CM3, LOADINGS IN 10(-9) GM/CM2/DAY					
28	MIN CALC	2.459	1.141	.613	.285
29	MAX CALC	3.165	1.225	.789	.305
38	AVE MEAS	51.686	37.386	10.465	7.570
ATM CONC IN 10(-12) GM/M3					
64	ATM CALC	.718E-13	.183E-13		
ZN CONC IN 10(-9) GM/CM3, LOADINGS IN 10(-9) GM/CM2/DAY					
30	MIN CALC	19.708	9.455	4.914	2.357
31	MAX CALC	24.832	9.849	6.191	2.465
39	AVE MEAS	173.636	218.179	34.549	44.175
ATM CONC IN 10(-12) GM/M3					
65	ATM CALC	.479E-12	.122E-12		
FE CONC IN 10(-9) GM/CM3, LOADINGS IN 10(-9) GM/CM2/DAY					
32	MIN CALC	69.565	36.085	17.344	8.997
33	MAX CALC	88.737	36.717	22.124	9.154
40	AVE MEAS	716.939	881.391	145.159	178.455
ATM CONC IN 10(-12) GM/M3					
66	ATM CALC	.108E-11	.276E-12		

10 12 SUISUPY S.

CONSTITUENT		AVERAGE CONC	STD DEV	AVERAGE LOADING	STD DEV
SO4 CONC IN 10(-6) GM/CM3, LOADINGS IN 10(-6) GM/CM2/DAY					
21	MIN CALC	2.632	1.267	.676	.326
21	MAX CALC	47.650	31.915	12.319	8.200
34	AVE MEAS	4.203	3.207	.798	.609
ATM CONC IN 10(-12) GM/M3					
60	ATM CALC	.390E-09	.174E-07		
57	DISSOLVED SO2	.235E-06	.876E-06		
58	DISSOLVED SO4	.153E-06	.513E-06		
59	PRTCULATE SO4	.692E-09	.271E-08		
PH LOADINGS IN (EXP) MEQ/CM2/DAY					
22	MIN CALC	5.156	.273	1332.907	70.195
23	MAX CALC	3.975	.346	1021.320	88.894
35	AVE MEAS	4.257	.332	808.092	63.115
ATM CONC IN 10(-12) GM/M3					
61	ATM CALC	.144E-07	.489E-08		
CU CONC IN 10(-9) GM/CM3, LOADINGS IN 10(-9) GM/CM2/DAY					
24	MIN CALC	21.595	16.146	5.548	4.148
25	MAX CALC	535.943	380.591	137.698	97.783
36	AVE MEAS	146.110	141.647	28.116	26.889
ATM CONC IN 10(-12) GM/M3					
62	ATM CALC	.320E-11	.118E-10		
NI CONC IN 10(-9) GM/CM3, LOADINGS IN 10(-9) GM/CM2/DAY					
26	MIN CALC	3.618	2.286	.930	.587
27	MAX CALC	93.118	71.581	23.924	18.417
37	AVE MEAS	109.524	164.625	20.791	31.251
ATM CONC IN 10(-12) GM/M3					
63	ATM CALC	.131E-11	.493E-11		
PB CONC IN 10(-9) GM/CM3, LOADINGS IN 10(-9) GM/CM2/DAY					
28	MIN CALC	2.923	1.702	.751	.437
29	MAX CALC	3.972	2.086	1.021	.536
38	AVE MEAS	36.697	47.943	7.004	9.102
ATM CONC IN 10(-12) GM/M3					
64	ATM CALC	.694E-13	.202E-13		
ZN CONC IN 10(-9) GM/CM3, LOADINGS IN 10(-9) GM/CM2/DAY					
30	MIN CALC	24.611	14.753	6.323	3.790
31	MAX CALC	62.099	28.235	15.955	7.254
39	AVE MEAS	144.000	208.276	27.336	39.537
ATM CONC IN 10(-12) GM/M3					
65	ATM CALC	.612E-12	.137E-11		
FE CONC IN 10(-9) GM/CM3, LOADINGS IN 10(-9) GM/CM2/DAY					
32	MIN CALC	100.889	65.397	25.921	16.802
33	MAX CALC	525.500	324.739	135.014	83.434
41	AVE MEAS	568.241	651.016	107.870	123.583
ATM CONC IN 10(-12) GM/M3					
66	ATM CALC	.442E-11	.169E-10		

11 13 S.S.MARIE

CONSTITUENT		AVERAGE CONC	STD DEV	AVERAGE LOADING	STD DEV
SO4 CONC IN 10(-6) GM/CM3, LOADINGS IN 10(-6) GM/CM2/DAY					
	20 MIN CALC	.165	.136	.042	.035
	21 MAX CALC	2.024	.965	.521	.249
	34 AVE MEAS	3.260	2.360	.749	.465
ATM CONC IN 10(-12) GM/M3					
	60 ATM CALC	.146E-09	.423E-10		
	57 DISSOLVED SO2	.760E-08	.217E-08		
	58 DISSOLVED SO4	.219E-08	.508E-08		
	59 PRTCULATE SO4	.121E-11	.260E-11		
PH LOADINGS IN (EXP) MEQ/CM2/DAY					
	22 MIN CALC	6.627	.792	1705.997	203.906
	23 MAX CALC	5.310	.286	1364.580	73.612
	35 AVE MEAS	4.713	.619	929.241	122.108
ATM CONC IN 10(-12) GM/M3					
	61 ATM CALC	.218E-09	.518E-08		
CU CONC IN 10(-9) GM/CM3, LOADINGS IN 10(-9) GM/CM2/DAY					
	24 MIN CALC	.301	.219	.077	.056
	25 MAX CALC	3.767	3.849	.975	.989
	36 AVE MEAS	4.677	3.551	.922	.700
ATM CONC IN 10(-12) GM/M3					
	62 ATM CALC	.223E-13	.634E-14		
NI CONC IN 10(-9) GM/CM3, LOADINGS IN 10(-9) GM/CM2/DAY					
	26 MIN CALC	.151	.124	.039	.032
	27 MAX CALC	1.643	1.581	.422	.407
	37 AVE MEAS	2.562	2.256	.505	.445
ATM CONC IN 10(-12) GM/M3					
	63 ATM CALC	.225E-13	.641E-14		
PB CONC IN 10(-9) GM/CM3, LOADINGS IN 10(-9) GM/CM2/DAY					
	28 MIN CALC	.554	.457	.143	.118
	29 MAX CALC	3.981	1.633	1.025	.421
	38 AVE MEAS	27.323	16.581	5.387	3.269
ATM CONC IN 10(-12) GM/M3					
	64 ATM CALC	.676E-13	.193E-13		
ZN CONC IN 10(-9) GM/CM3, LOADINGS IN 10(-9) GM/CM2/DAY					
	30 MIN CALC	4.162	3.327	1.072	.851
	31 MAX CALC	30.693	12.821	7.953	3.301
	39 AVE MEAS	322.538	753.858	63.592	148.632
ATM CONC IN 10(-12) GM/M3					
	65 ATM CALC	.450E-12	.128E-12		
FE CONC IN 10(-9) GM/CM3, LOADINGS IN 10(-9) GM/CM2/DAY					
	32 MIN CALC	12.686	9.437	3.266	2.430
	33 MAX CALC	102.310	44.295	26.340	11.404
	41 AVE MEAS	236.404	114.236	46.610	22.523
ATM CONC IN 10(-12) GM/M3					
	66 ATM CALC	.102E-11	.290E-12		

12 14 CHAPLEAU

CONSTITUENT		AVERAGE CONC	STD DEV	AVERAGE LOADING	STD DEV
SO4 CONC IN 10(-6) GM/CM3, LOADINGS IN 10(-6) GM/CM2/DAY					
20	MIN CALC	.141	.135	.036	.034
21	MAX CALC	2.245	1.152	.566	.290
34	AVE MEAS	3.296	1.594	.595	.272
ATM CONC IN 10(-12) GM/M3					
63	ATM CALC	.146E-09	.368E-10		
57	DISSOLVED SO2	.745E-08	.179E-08		
58	DISSOLVED SO4	.111E-08	.345E-08		
59	PRTCULATE SO4	.505E-12	.159E-11		
PH	LOADINGS IN (EXP) MEQ/CM2/DAY				
22	MIN CALC	6.639	.958	1723.539	241.481
23	MAX CALC	5.247	.245	1322.469	61.795
35	AVE MEAS	4.986	.767	399.202	138.420
ATM CONC IN 10(-12) GM/M3					
61	ATM CALC	.106E-08	.328E-08		
CU CONC IN 10(-9) GM/CM3, LOADINGS IN 10(-9) GM/CM2/DAY					
24	MIN CALC	.357	.527	.090	.133
25	MAX CALC	11.286	9.295	2.592	2.342
36	AVE MEAS	11.011	10.430	1.988	1.883
ATM CONC IN 10(-12) GM/M3					
62	ATM CALC	.219E-13	.553E-14		
NI CONC IN 10(-9) GM/CM3, LOADINGS IN 10(-9) GM/CM2/DAY					
26	MIN CALC	.156	.190	.039	.048
27	MAX CALC	3.462	2.872	.872	.724
37	AVE MEAS	3.350	3.119	.605	.563
ATM CONC IN 10(-12) GM/M3					
63	ATM CALC	.222E-13	.559E-14		
PB CONC IN 10(-9) GM/CM3, LOADINGS IN 10(-9) GM/CM2/DAY					
28	MIN CALC	.444	.439	.112	.111
29	MAX CALC	4.211	1.869	1.061	.471
38	AVE MEAS	39.625	31.508	7.155	5.690
ATM CONC IN 10(-12) GM/M3					
64	ATM CALC	.666E-13	.168E-13		
ZN CONC IN 10(-9) GM/CM3, LOADINGS IN 10(-9) GM/CM2/DAY					
30	MIN CALC	3.319	3.168	.837	.799
31	MAX CALC	32.690	15.053	8.289	3.794
39	AVE MEAS	122.232	101.420	22.072	18.314
ATM CONC IN 10(-12) GM/M3					
65	ATM CALC	.444E-12	.112E-12		
FE CONC IN 10(-9) GM/CM3, LOADINGS IN 10(-9) GM/CM2/DAY					
32	MIN CALC	10.113	8.949	2.549	2.255
33	MAX CALC	113.070	53.235	28.496	13.416
41	AVE MEAS	396.500	522.358	71.598	94.325
ATM CONC IN 10(-12) GM/M3					
66	ATM CALC	.100E-11	.253E-12		

13 15 HAHA

CONSTITUENT	AVERAGE CONC	STD DEV	AVERAGE LOADING	STD DEV
SO4 CONC IN 10(-6) GM/CM3, LOADINGS IN 10(-6) GM/CM2/DAY				
20 MIN CALC	.650	.117	.015	.330
21 MAX CALC	1.593	1.191	.612	.305
34 AVE MEAS	8.258	6.546	1.522	1.207
ATM CONC IN 10(-12) GM/M3				
60 ATM CALC	.151E-09	.442E-10		
57 DISSOLVED SO2	.757E-08	.222E-08		
58 DISSOLVED SO4	0.	0.		
59 PRTCULATE SO4	0.	0.		
PH LOADINGS IN (EXP) MEQ/CM2/DAY				
22 MIN CALC	7.471	.953	1914.764	244.316
23 MAX CALC	5.326	.266	1365.034	68.138
35 AVE MEAS	4.301	.787	792.969	145.041
ATM CONC IN 10(-12) GM/M3				
61 ATM CALC	0.	0.		
CU CONC IN 10(-9) GM/CM3, LOADINGS IN 10(-9) GM/CM2/DAY				
24 MIN CALC	.100	.144	.026	.037
25 MAX CALC	6.659	6.057	1.707	1.552
36 AVE MEAS	6.158	5.784	1.135	1.066
ATM CONC IN 10(-12) GM/M3				
62 ATM CALC	.226E-13	.664E-14		
NI CONC IN 10(-9) GM/CM3, LOADINGS IN 10(-9) GM/CM2/DAY				
26 MIN CALC	.047	.074	.012	.019
27 MAX CALC	2.723	2.357	.698	.604
37 AVE MEAS	3.229	3.041	.595	.561
ATM CONC IN 10(-12) GM/M3				
63 ATM CALC	.223E-13	.671E-14		
PB CONC IN 10(-9) GM/CM3, LOADINGS IN 10(-9) GM/CM2/DAY				
28 MIN CALC	.193	.320	.050	.082
29 MAX CALC	4.260	2.089	1.092	.535
38 AVE MEAS	30.004	57.968	5.532	10.687
ATM CONC IN 10(-12) GM/M3				
64 ATM CALC	.687E-13	.202E-13		
ZN CONC IN 10(-9) GM/CM3, LOADINGS IN 10(-9) GM/CM2/DAY				
30 MIN CALC	1.463	2.392	.375	.613
31 MAX CALC	33.603	16.714	8.458	4.284
39 AVE MEAS	439.896	1036.949	81.098	191.170
ATM CONC IN 10(-12) GM/M3				
65 ATM CALC	.453E-12	.134E-12		
FE CONC IN 10(-9) GM/CM3, LOADINGS IN 10(-9) GM/CM2/DAY				
32 MIN CALC	4.427	6.843	1.134	1.754
33 MAX CALC	109.863	59.175	28.156	15.166
40 AVE MEAS	2536.958	2525.490	467.708	465.594
ATM CONC IN 10(-12) GM/M3				
66 ATM CALC	.103E-11	.304E-12		

14 16 TINKINS

CONSTITUENT	AVERAGE CONC	STD DEV	AVERAGE LOADING	STD DEV
SO4 CONC IN 10(-6) GM/CM3, LOADINGS IN 10(+6) GM/CM2/DAY				
20 MIN CALC	.159	.144	.040	.036
21 MAX CALC	2.313	.841	.582	.212
34 AVE MEAS	5.124	14.517	1.013	2.869
ATM CONC IN 10(-12) GM/M3				
60 ATM CALC	.147E-09	.402E-10		
57 DISSOLVED SO2	.754E-08	.219E-08		
58 DISSOLVED SO4	.219E-08	.635E-08		
59 PRTCULATE SO4	.847E-12	.240E-11		
PH LOADINGS IN (EXP) MEQ/CM2/DAY				
22 MIN CALC	6.697	.861	1684.333	216.619
23 MAX CALC	5.205	.251	1308.996	62.945
35 AVE MEAS	5.991	.804	1184.106	158.823
ATM CONC IN 10(-12) GM/M3				
61 ATM CALC	.222E-08	.654E-08		
CU CONC IN 10(-9) GM/CM3, LOADINGS IN 10(-9) GM/CM2/DAY				
24 MIN CALC	.263	1.415	.217	.356
25 MAX CALC	40.704	31.138	10.237	7.831
36 AVE MEAS	14.641	14.918	2.933	2.948
ATM CONC IN 10(-12) GM/M3				
62 ATM CALC	.220E-13	.601E-14		
NI CONC IN 10(-9) GM/CM3, LOADINGS IN 10(-9) GM/CM2/DAY				
26 MIN CALC	.239	.239	.060	.073
27 MAX CALC	6.630	5.770	2.012	1.451
37 AVE MEAS	7.566	25.987	1.495	5.136
ATM CONC IN 10(-12) GM/M3				
63 ATM CALC	.222E-13	.608E-14		
PB CONC IN 10(-9) GM/CM3, LOADINGS IN 10(-9) GM/CM2/DAY				
28 MIN CALC	.492	.432	.124	.109
29 MAX CALC	3.855	1.627	.969	.409
38 AVE MEAS	26.617	20.305	5.261	4.013
ATM CONC IN 10(-12) GM/M3				
64 ATM CALC	.667E-13	.183E-13		
ZN CONC IN 10(-9) GM/CM3, LOADINGS IN 10(-9) GM/CM2/DAY				
30 MIN CALC	3.666	3.135	.922	.789
31 MAX CALC	30.024	12.508	7.551	3.146
39 AVE MEAS	139.672	114.785	27.606	22.667
ATM CONC IN 10(-12) GM/M3				
65 ATM CALC	.445E-12	.122E-12		
FE CONC IN 10(-9) GM/CM3, LOADINGS IN 10(-9) GM/CM2/DAY				
32 MIN CALC	11.438	9.215	2.869	2.317
33 MAX CALC	119.739	39.413	30.114	9.912
41 AVE MEAS	362.707	297.684	75.641	58.836
ATM CONC IN 10(-12) GM/M3				
66 ATM CALC	.190E-11	.275E-12		

15 17 KAPUSKASIN

CONSTITUENT		AVERAGE CONC	STO DEV	AVERAGE LOADING	STO DEV
SO4 CONC IN 10(-6) GM/CM3, LOADINGS IN 10(-6) GM/CM2/DAY					
20	MIN CALC	.039	.062	.010	.016
21	MAX CALC	1.740	.826	.447	.212
* 34	AVE MEAS	3.496	2.066	.610	.350
ATM CONC IN 10(-12) GM/M3					
60	ATM CALC	.145E-09	.462E-10		
57	DISSOLVED SO2	.727E-08	.232E-08		
58	DISSOLVED SO4	0.	0.		
59	PRTCULATE SO4	0.	0.		
PH LOADINGS IN (EXP) MEQ/CM2/DAY					
22	MIN CALC	7.529	.918	1933.797	235.657
23	MAX CALC	5.338	.304	1370.925	78.131
35	AVE MEAS	6.179	.615	1078.926	107.327
ATM CONC IN 10(-12) GM/M3					
61	ATM CALC	0.	0.		
CU CONC IN 10(-9) GM/CM3, LOADINGS IN 10(-9) GM/CM2/DAY					
24	MIN CALC	.135	.155	.027	.040
25	MAX CALC	18.841	16.377	4.839	4.206
36	AVE MEAS	7.519	8.829	1.313	1.542
ATM CONC IN 10(-12) GM/M3					
62	ATM CALC	.217E-13	.694E-14		
NI CONC IN 10(-9) GM/CM3, LOADINGS IN 10(-9) GM/CM2/DAY					
26	MIN CALC	.044	.061	.011	.016
27	MAX CALC	4.423	3.047	1.137	.783
37	AVE MEAS	7.019	29.817	1.365	5.207
ATM CONC IN 10(-12) GM/M3					
63	ATM CALC	.219E-13	.701E-14		
PB CONC IN 10(-9) GM/CM3, LOADINGS IN 10(-9) GM/CM2/DAY					
28	MIN CALC	.139	.222	.036	.052
29	MAX CALC	3.666	1.641	.942	.421
38	AVE MEAS	15.804	12.715	2.760	2.220
ATM CONC IN 10(-12) GM/M3					
64	ATM CALC	.660E-13	.211E-13		
ZN CONC IN 10(-9) GM/CM3, LOADINGS IN 10(-9) GM/CM2/DAY					
30	MIN CALC	1.037	1.451	.266	.373
31	MAX CALC	26.110	12.524	7.220	3.217
39	AVE MEAS	89.558	81.611	15.638	14.251
ATM CONC IN 10(-12) GM/M3					
65	ATM CALC	.439E-12	.140E-12		
FE CONC IN 10(-9) GM/CM3, LOADINGS IN 10(-9) GM/CM2/DAY					
32	MIN CALC	3.123	3.911	.802	1.004
33	MAX CALC	99.613	40.903	25.584	10.507
40	AVE MEAS	274.212	330.708	47.882	57.747
ATM CONC IN 10(-12) GM/M3					
66	ATM CALC	.992E-12	.317E-12		

16 18 SPARROW L.

CONSTITUENT		AVERAGE CONC	STD DEV	AVERAGE LOADING	STD DEV
SO4 CONC IN 10(-6) GM/CM3, LOADINGS IN 10(-6) GM/CM2/DAY					
	20 MIN CALC	.123	.118	.031	.030
	21 MAX CALC	2.355	1.071	.599	.272
	34 AVE MEAS	3.637	1.804	.893	.420
ATM CONC IN 10(-12) GM/M3					
	69 ATM CALC	.141E-09	.296E-10		
	57 DISSOLVED SO2	.717E-08	.134E-08		
	58 DISSOLVED SO4	.115E-08	.346E-08		
	59 PRTCULATE SO4	.484E-12	.148E-11		
PH LOADINGS IN (EXP) MEQ/CM2/DAY					
	22 MIN CALC	6.657	.895	1744.502	227.753
	23 MAX CALC	5.206	.254	1324.936	64.655
	35 AVE MEAS	4.389	.451	1321.109	104.993
ATM CONC IN 10(-12) GM/M3					
	61 ATM CALC	.111E-08	.328E-08		
CU CONC IN 10(-9) GM/CM3, LOADINGS IN 10(-9) GM/CM2/DAY					
	24 MIN CALC	.294	.179	.052	.045
	25 MAX CALC	43.761	29.753	11.138	7.570
	36 AVE MEAS	3.722	3.755	.866	.874
ATM CONC IN 10(-12) GM/M3					
	62 ATM CALC	.211E-13	.445E-14		
NI CONC IN 10(-9) GM/CM3, LOADINGS IN 10(-9) GM/CM2/DAY					
	26 MIN CALC	.104	.100	.026	.025
	27 MAX CALC	9.089	5.459	2.312	1.389
	37 AVE MEAS	2.722	3.556	.633	.816
ATM CONC IN 10(-12) GM/M3					
	63 ATM CALC	.213E-13	.450E-14		
PB CONC IN 10(-9) GM/CM3, LOADINGS IN 10(-9) GM/CM2/DAY					
	28 MIN CALC	.384	.371	.098	.094
	29 MAX CALC	3.943	1.736	1.003	.442
	38 AVE MEAS	23.033	13.958	5.358	3.247
ATM CONC IN 10(-12) GM/M3					
	64 ATM CALC	.641E-13	.135E-13		
ZN CONC IN 10(-9) GM/CM3, LOADINGS IN 10(-9) GM/CM2/DAY					
	30 MIN CALC	2.878	2.691	.732	.685
	31 MAX CALC	30.639	13.466	7.794	3.426
	39 AVE MEAS	90.352	53.996	18.693	12.562
ATM CONC IN 10(-12) GM/M3					
	65 ATM CALC	.427E-12	.901E-13		
FE CONC IN 10(-9) GM/CM3, LOADINGS IN 10(-9) GM/CM2/DAY					
	32 MIN CALC	8.703	7.714	2.214	1.962
	33 MAX CALC	122.144	50.564	31.073	12.863
	40 AVE MEAS	105.889	67.257	25.332	15.647
ATM CONC IN 10(-12) GM/M3					
	66 ATM CALC	.964E-12	.204E-12		

17 23 L ST PETER

CONSTITUENT		AVERAGE CONC	STD DEV	AVERAGE LOADING	STD DEV
SO4 CONC IN 10(-6) GM/CM3, LOADINGS IN 10(-6) GM/CM2/DAY					
	20 MIN CALC	.090	.094	.022	.023
	21 MAX CALC	2.461	2.032	.603	.493
	34 AVE MEAS	2.976	1.826	.767	.470
ATM CONC IN 10(-12) GM/M3					
	60 ATM CALC	.153E-09	.346E-10		
	57 DISSOLVED SO2	.796E-08	.172E-08		
	58 DISSOLVED SO4	.156E-09	.390E-08		
	59 PRTCULATE SO4	.664E-12	.175E-11		
PH LOADINGS IN (EXP) MEQ/CM2/DAY					
	22 MIN CALC	7.049	.889	1711.976	215.576
	23 MAX CALC	5.264	.293	1278.493	71.218
	35 AVE MEAS	4.166	.397	1073.398	102.187
ATM CONC IN 10(-12) GM/M3					
	61 ATM CALC	.152E-08	.372E-09		
CU CONC IN 10(-9) GM/CM3, LOADINGS IN 10(-9) GM/CM2/DAY					
	24 MIN CALC	.155	.141	.038	.034
	25 MAX CALC	47.508	45.887	11.539	11.145
	36 AVE MEAS	4.160	3.317	1.077	.855
ATM CONC IN 10(-12) GM/M3					
	62 ATM CALC	.230E-13	.519E-14		
NI CONC IN 10(-9) GM/CM3, LOADINGS IN 10(-9) GM/CM2/DAY					
	26 MIN CALC	.068	.074	.017	.018
	27 MAX CALC	10.163	7.062	2.470	1.715
	37 AVE MEAS	4.352	4.921	1.121	1.268
ATM CONC IN 10(-12) GM/M3					
	63 ATM CALC	.232E-13	.525E-14		
PB CONC IN 10(-9) GM/CM3, LOADINGS IN 10(-9) GM/CM2/DAY					
	28 MIN CALC	.251	.264	.061	.069
	29 MAX CALC	4.044	2.201	.982	.534
	38 AVE MEAS	24.388	14.159	6.284	3.648
ATM CONC IN 10(-12) GM/M3					
	64 ATM CALC	.698E-13	.156E-13		
ZN CONC IN 10(-9) GM/CM3, LOADINGS IN 10(-9) GM/CM2/DAY					
	31 MIN CALC	1.947	2.068	.473	.502
	31 MAX CALC	32.046	19.088	7.783	4.636
	39 AVE MEAS	102.100	95.323	26.327	24.561
ATM CONC IN 10(-12) GM/M3					
	65 ATM CALC	.465E-12	.105E-12		
FE CONC IN 10(-9) GM/CM3, LOADINGS IN 10(-9) GM/CM2/DAY					
	32 MIN CALC	6.361	6.026	1.545	1.464
	33 MAX CALC	133.432	94.513	32.407	22.955
	42 AVE MEAS	159.640	173.422	41.184	44.683
ATM CONC IN 10(-12) GM/M3					
	66 ATM CALC	.105E-11	.237E-12		

18 24 TRAVERSE

CONSTITUENT	AVERAGE CONC	STD DEV	AVERAGE LOADING	STD DEV
SO4 CONC IN 10(-6) GM/CM3, LOADINGS IN 10(-6) GM/CM2/DAY				
20 MIN CALC	.124	.120	.030	.029
21 MAX CALC	2.610	2.071	.633	.502
34 AVE MEAS	2.932	2.703	.589	.543
ATM CONC IN 10(-12) GM/M3				
60 ATM CALC	.193E-09	.349E-10		
57 DISSOLVED SO2	.765E-08	.159E-08		
58 DISSOLVED SO4	.133E-08	.370E-08		
59 PRTCULATE SO4	.506E-12	.155E-11		
PH LOADINGS IN (EXP) MEQ/CM2/DAY				
22 MIN CALC	6.844	.868	1658.724	210.353
23 MAX CALC	5.229	.261	1267.091	63.292
35 AVE MEAS	4.121	.322	828.215	64.690
ATM CONC IN 10(-12) GM/M3				
61 ATM CALC	.132E-08	.375E-08		
CU CONC IN 10(-9) GM/CM3, LOADINGS IN 10(-9) GM/CM2/DAY				
24 MIN CALC	.219	.187	.053	.045
25 MAX CALC	57.511	50.787	13.939	12.308
36 AVE MEAS	4.568	6.709	.922	1.348
ATM CONC IN 10(-12) GM/M3				
62 ATM CALC	.229E-13	.524E-14		
NI CONC IN 10(-9) GM/CM3, LOADINGS IN 10(-9) GM/CM2/DAY				
26 MIN CALC	.107	.096	.026	.023
27 MAX CALC	10.954	7.465	2.662	1.809
37 AVE MEAS	2.628	2.985	.527	.600
ATM CONC IN 10(-12) GM/M3				
63 ATM CALC	.232E-13	.530E-14		
PB CONC IN 10(-9) GM/CM3, LOADINGS IN 10(-9) GM/CM2/DAY				
28 MIN CALC	.390	.358	.095	.087
29 MAX CALC	4.019	2.227	.974	.540
38 AVE MEAS	17.676	11.619	3.593	2.335
ATM CONC IN 10(-12) GM/M3				
64 ATM CALC	.696E-13	.159E-13		
ZN CONC IN 10(-9) GM/CM3, LOADINGS IN 10(-9) GM/CM2/DAY				
30 MIN CALC	2.966	2.660	.719	.645
31 MAX CALC	31.855	19.324	7.721	4.683
39 AVE MEAS	79.160	52.487	15.910	10.549
ATM CONC IN 10(-12) GM/M3				
65 ATM CALC	.464E-12	.106E-12		
FE CONC IN 10(-9) GM/CM3, LOADINGS IN 10(-9) GM/CM2/DAY				
32 MIN CALC	9.160	7.983	2.220	1.934
33 MAX CALC	140.120	101.262	33.958	24.545
40 AVE MEAS	103.600	71.989	20.822	14.469
ATM CONC IN 10(-12) GM/M3				
66 ATM CALC	.105E-11	.239E-12		

19 25 SHAWANAGA

CONSTITUENT		AVERAGE CONC	STD DEV	AVERAGE LOADING	STD DEV
SO4 CONC IN 10(-6) GM/CM3, LOADINGS IN 10(-6) GM/CM2/DAY					
20	MIN CALC	.363	.216	.088	.052
21	MAX CALC	3.473	2.276	.839	.550
34	AVE MEAS	3.058	2.139	.755	.528
ATM CONC IN 10(-12) GM/M3					
60	ATM CALC	.172E-09	.856E-10		
57	DISSOLVED SO2	.103E-07	.471E-08		
58	DISSOLVED SO4	.724E-08	.130E-07		
59	PRTCULATE SO4	.238E-11	.329E-11		
PH	LOADINGS IN (EXP) MEQ/CM2/DAY				
22	MIN CALC	6.083	.378	1469.611	91.368
23	MAX CALC	5.112	.352	1234.876	85.018
35	AVE MEAS	4.228	.196	1044.299	48.534
ATM CONC IN 10(-12) GM/M3					
61	ATM CALC	.712E-08	.962E-08		
CU CONC IN 10(-9) GM/CM3, LOADINGS IN 10(-9) GM/CM2/DAY					
24	MIN CALC	1.502	1.118	.242	.270
25	MAX CALC	83.637	56.699	20.205	13.695
36	AVE MEAS	10.142	26.793	2.505	6.618
ATM CONC IN 10(-12) GM/M3					
62	ATM CALC	.684E-13	.148E-12		
NI CONC IN 10(-9) GM/CM3, LOADINGS IN 10(-9) GM/CM2/DAY					
26	MIN CALC	.273	.160	.066	.039
27	MAX CALC	12.712	7.560	3.071	1.826
37	AVE MEAS	9.092	26.415	2.443	7.019
ATM CONC IN 10(-12) GM/M3					
63	ATM CALC	.406E-13	.515E-13		
PB CONC IN 10(-9) GM/CM3, LOADINGS IN 10(-9) GM/CM2/DAY					
28	MIN CALC	.842	.417	.204	.101
29	MAX CALC	4.040	2.425	.976	.586
38	AVE MEAS	19.875	11.443	4.910	2.827
ATM CONC IN 10(-12) GM/M3					
64	ATM CALC	.760E-13	.387E-13		
ZN CONC IN 10(-9) GM/CM3, LOADINGS IN 10(-9) GM/CM2/DAY					
30	MIN CALC	6.718	3.368	1.623	.790
31	MAX CALC	32.336	21.120	7.812	5.102
39	AVE MEAS	63.792	33.976	15.758	8.393
ATM CONC IN 10(-12) GM/M3					
65	ATM CALC	.520E-12	.258E-12		
FE CONC IN 10(-9) GM/CM3, LOADINGS IN 10(-9) GM/CM2/DAY					
32	MIN CALC	23.599	12.093	5.699	2.921
33	MAX CALC	149.450	103.688	36.104	25.049
40	AVE MEAS	125.917	82.104	31.105	20.282
ATM CONC IN 10(-12) GM/M3					
66	ATM CALC	.120E-11	.584E-12		

20 26 HATTAWA

CONSTITUENT		AVERAGE CONC	STD DEV	AVERAGE LOADING	STD DEV
SO4 CONC IN 10(-6) GM/CM3, LOADINGS IN 10(-6) GM/CM2/DAY					
	20 MIN CALC	.275	.161	.070	.041
	21 MAX CALC	2.626	.998	.674	.256
	34 AVE MEAS	3.336	2.672	.716	.565
ATM CONC IN 10(-12) GM/M3					
	60 ATM CALC	.140E-09	.276E-10		
	57 DISSOLVED SO2	.756E-08	.177E-08		
	58 DISSOLVED SO4	.143E-08	.338E-08		
	59 PRTCULATE SO4	.467E-12	.108E-11		
PH	LOADINGS IN (EXP) MEQ/CM2/DAY				
	22 MIN CALC	6.174	.357	1563.968	91.595
	23 MAX CALC	5.139	.218	1318.526	55.979
	35 AVE MEAS	4.188	.273	884.958	57.707
ATM CONC IN 10(-12) GM/M3					
	61 ATM CALC	.170E-08	.411E-08		
CU CONC IN 10(-9) GM/CM3, LOADINGS IN 10(-9) GM/CM2/DAY					
	24 MIN CALC	.729	.767	.187	.197
	25 MAX CALC	58.538	32.177	15.018	8.255
	36 AVE MEAS	6.658	7.053	1.449	1.490
ATM CONC IN 10(-12) GM/M3					
	62 ATM CALC	.210E-13	.415E-14		
NI CONC IN 10(-9) GM/CM3, LOADINGS IN 10(-9) GM/CM2/DAY					
	26 MIN CALC	.260	.166	.067	.048
	27 MAX CALC	11.035	7.791	2.844	1.996
	37 AVE MEAS	3.973	3.743	.839	.791
ATM CONC IN 10(-12) GM/M3					
	63 ATM CALC	.212E-13	.419E-14		
PB CONC IN 10(-9) GM/CM3, LOADINGS IN 10(-9) GM/CM2/DAY					
	28 MIN CALC	.767	.444	.194	.114
	29 MAX CALC	3.871	1.641	.993	.421
	38 AVE MEAS	23.646	17.272	4.996	3.649
ATM CONC IN 10(-12) GM/M3					
	64 ATM CALC	.637E-13	.126E-13		
ZN CONC IN 10(-9) GM/CM3, LOADINGS IN 10(-9) GM/CM2/DAY					
	30 MIN CALC	5.671	3.318	1.506	.851
	31 MAX CALC	33.247	12.759	7.760	3.274
	39 AVE MEAS	129.646	170.162	27.223	35.953
ATM CONC IN 10(-12) GM/M3					
	65 ATM CALC	.425E-12	.839E-13		
FE CONC IN 10(-9) GM/CM3, LOADINGS IN 10(-9) GM/CM2/DAY					
	32 MIN CALC	19.291	10.285	4.949	2.639
	33 MAX CALC	130.775	45.537	33.552	11.683
	40 AVE MEAS	125.019	139.244	26.415	29.420
ATM CONC IN 10(-12) GM/M3					
	66 ATM CALC	.959E-12	.189E-12		

21 27 HEARST

CONSTITUENT		AVERAGE CONC	STD DEV	AVERAGE LOADING	STD DEV
SO4 CONC IN 10(-6) GM/CM3, LOADINGS IN 10(-6) GM/CM2/DAY					
	20 MIN CALC	.012	.022	.003	.006
	21 MAX CALC	1.372	.702	.352	.180
	34 AVE MEAS	3.564	2.449	.667	.458
ATM CONC IN 10(-12) GM/M3					
	60 ATM CALC	.148E-09	.554E-10		
	57 DISSOLVED SO2	.745E-08	.279E-08		
	58 DISSOLVED SO4	0.	0.		
	59 PRTCULATE SO4	0.	0.		
PH	LOADINGS IN (EXP) MEQ/CM2/DAY				
	22 MIN CALC	7.934	.746	2035.596	191.393
	23 MAX CALC	5.469	.339	1403.799	86.918
	35 AVE MEAS	7.412	.494	1386.340	75.634
ATM CONC IN 10(-12) GM/M3					
	61 ATM CALC	0.	0.		
CU CONC IN 10(-9) GM/CM3, LOADINGS IN 10(-9) GM/CM2/DAY					
	24 MIN CALC	.027	.033	.007	.009
	25 MAX CALC	9.195	8.392	2.357	2.153
	36 AVE MEAS	21.045	24.332	3.936	4.551
ATM CONC IN 10(-12) GM/M3					
	62 ATM CALC	.222E-13	.832E-14		
NI CONC IN 10(-9) GM/CM3, LOADINGS IN 10(-9) GM/CM2/DAY					
	26 MIN CALC	.011	.021	.003	.005
	27 MAX CALC	2.789	2.578	.716	.662
	37 AVE MEAS	7.695	17.203	1.422	3.217
ATM CONC IN 10(-12) GM/M3					
	63 ATM CALC	.225E-13	.841E-14		
PB CONC IN 10(-9) GM/CM3, LOADINGS IN 10(-9) GM/CM2/DAY					
	28 MIN CALC	.053	.082	.014	.021
	29 MAX CALC	3.235	1.495	.830	.384
	38 AVE MEAS	61.255	51.712	11.270	9.672
ATM CONC IN 10(-12) GM/M3					
	64 ATM CALC	.676E-13	.253E-13		
ZN CONC IN 10(-9) GM/CM3, LOADINGS IN 10(-9) GM/CM2/DAY					
	30 MIN CALC	.395	.581	.101	.149
	31 MAX CALC	24.690	11.396	6.335	2.924
	39 AVE MEAS	132.295	157.572	24.728	29.473
ATM CONC IN 10(-12) GM/M3					
	65 ATM CALC	.450E-12	.168E-12		
FE CONC IN 10(-9) GM/CM3, LOADINGS IN 10(-9) GM/CM2/DAY					
	32 MIN CALC	1.183	1.535	.303	.394
	33 MAX CALC	82.490	35.927	21.165	9.218
	40 AVE MEAS	1402.692	1487.601	262.364	278.285
ATM CONC IN 10(-12) GM/M3					
	66 ATM CALC	.102E-11	.380E-12		

22 28 HORNEPAYNE

CONSTITUENT		AVERAGE CONC	STD DEV	AVERAGE LOADING	STD DEV
SO4 CONC IN 10(-6) GM/CM3, LOADINGS IN 10(-6) GM/CM2/DAY					
	20 MIN CALC	.014	.025	.003	.006
	21 MAX CALC	1.372	.691	.337	.170
	34 AVE MEAS	2.600	3.103	.525	.582
ATM CONC IN 10(-12) GM/M3					
	60 ATM CALC	.142E-09	.436E-10		
	57 DISSOLVED SO2	.712E-08	.204E-08		
	58 DISSOLVED SO4	0.	0.		
	59 PRTCULATE SO4	0.	0.		
PH	LOADINGS IN (EXP) MEQ/CM2/DAY				
	22 MIN CALC	7.915	.707	1945.581	173.803
	23 MAX CALC	5.454	.321	1340.614	78.951
	35 AVE MEAS	6.056	.919	1135.991	172.378
ATM CONC IN 10(-12) GM/M3					
	61 ATM CALC	0.	0.		
CU CONC IN 10(-9) GM/CM3, LOADINGS IN 10(-9) GM/CM2/DAY					
	24 MIN CALC	.048	.098	.012	.024
	25 MAX CALC	5.599	4.582	1.376	1.126
	36 AVE MEAS	8.558	14.212	1.605	2.666
ATM CONC IN 10(-12) GM/M3					
	62 ATM CALC	.213E-13	.609E-14		
NI CONC IN 10(-9) GM/CM3, LOADINGS IN 10(-9) GM/CM2/DAY					
	26 MIN CALC	.020	.054	.005	.013
	27 MAX CALC	2.302	1.969	.566	.484
	37 AVE MEAS	7.125	17.829	1.337	3.344
ATM CONC IN 10(-12) GM/M3					
	63 ATM CALC	.215E-13	.615E-14		
PB CONC IN 10(-9) GM/CM3, LOADINGS IN 10(-9) GM/CM2/DAY					
	28 MIN CALC	.055	.097	.013	.022
	29 MAX CALC	3.363	1.521	.828	.374
	38 AVE MEAS	14.525	13.799	2.725	2.588
ATM CONC IN 10(-12) GM/M3					
	64 ATM CALC	.646E-13	.185E-13		
ZN CONC IN 10(-9) GM/CM3, LOADINGS IN 10(-9) GM/CM2/DAY					
	30 MIN CALC	.417	.628	.102	.154
	31 MAX CALC	25.731	11.647	6.325	2.863
	39 AVE MEAS	125.625	119.316	23.566	22.382
ATM CONC IN 10(-12) GM/M3					
	65 ATM CALC	.431E-12	.123E-12		
FE CONC IN 10(-9) GM/CM3, LOADINGS IN 10(-9) GM/CM2/DAY					
	32 MIN CALC	1.318	1.801	.324	.443
	33 MAX CALC	83.639	35.824	20.607	8.805
	40 AVE MEAS	285.708	482.983	53.595	90.601
ATM CONC IN 10(-12) GM/M3					
	66 ATM CALC	.973E-12	.278E-12		

23 29 POHASSAN

CONSTITUENT	AVERAGE CONC	STD DEV	AVERAGE LOADING	STD DEV
SO4 CONC IN 10(-6) GM/CM3, LOADINGS IN 10(-6) GM/CM2/DAY				
20 MIN CALC	.364	.233	.093	.059
21 MAX CALC	2.993	1.262	.764	.327
34 AVE MEAS	3.290	1.848	.706	.396
ATM CONC IN 10(-12) GM/M3				
61 ATM CALC	.146E-09	.714E-10		
57 DISSOLVED SO2	.776E-08	.351E-08		
58 DISSOLVED SO4	.131E-08	.287E-08		
59 PRTCULATE SO4	.551E-11	.175E-10		
PH LOADINGS IN (EXP) MEQ/CM2/DAY				
22 MIN CALC	6.674	.420	1546.707	137.161
23 MAX CALC	5.888	.225	1297.983	57.315
35 AVE MEAS	4.620	.666	991.299	142.646
ATM CONC IN 10(-12) GM/M3				
61 ATM CALC	.158E-08	.363E-08		
CU CONC IN 10(-9) GM/CM3, LOADINGS IN 10(-9) GM/CM2/DAY				
24 MIN CALC	1.109	1.054	.283	.269
25 MAX CALC	71.776	35.114	18.312	8.959
36 AVE MEAS	6.333	10.510	1.359	2.255
ATM CONC IN 10(-12) GM/M3				
62 ATM CALC	.223E-13	.107E-13		
NI CONC IN 10(-9) GM/CM3, LOADINGS IN 10(-9) GM/CM2/DAY				
26 MIN CALC	.357	.244	.091	.062
27 MAX CALC	13.246	6.282	3.379	1.603
37 AVE MEAS	11.445	28.924	2.456	6.206
ATM CONC IN 10(-12) GM/M3				
63 ATM CALC	.223E-13	.107E-13		
PB CONC IN 10(-9) GM/CM3, LOADINGS IN 10(-9) GM/CM2/DAY				
28 MIN CALC	.930	.557	.237	.142
29 MAX CALC	4.060	1.822	1.036	.465
38 AVE MEAS	12.766	10.722	2.743	2.300
ATM CONC IN 10(-12) GM/M3				
64 ATM CALC	.665E-13	.321E-13		
ZN CONC IN 10(-9) GM/CM3, LOADINGS IN 10(-9) GM/CM2/DAY				
30 MIN CALC	7.321	4.356	1.868	1.111
31 MAX CALC	31.911	14.397	8.141	3.673
39 AVE MEAS	90.119	53.365	19.335	11.453
ATM CONC IN 10(-12) GM/M3				
65 ATM CALC	.443E-12	.214E-12		
FE CONC IN 10(-9) GM/CM3, LOADINGS IN 10(-9) GM/CM2/DAY				
32 MIN CALC	25.159	14.826	6.419	3.782
33 MAX CALC	140.901	57.375	35.948	14.638
40 AVE MEAS	126.262	84.909	27.089	18.217
ATM CONC IN 10(-12) GM/M3				
66 ATM CALC	.100E-11	.484E-12		

24 31 HARTEN RIV

CONSTITUENT	AVERAGE CONC	STD DEV	AVERAGE LOADING	STD DEV
SO4 CONC IN 10(-6) GM/CM3, LOADINGS IN 10(-6) GM/CM2/DAY				
20 MIN CALC	.654	.298	.169	.077
21 MAX CALC	4.164	1.833	1.474	.472
34 AVE MEAS	3.960	1.716	.653	.283
ATM CONC IN 10(-12) GM/M3				
60 ATM CALC	.135E-09	.672E-10		
57 DISSOLVED SO2	.917E-08	.653E-08		
58 DISSOLVED SO4	.247E-07	.818E-07		
59 PRTCULATE SO4	.296E-10	.415E-10		
PH LOADINGS IN (EXP) MEQ/CM2/DAY				
22 MIN CALC	5.695	.398	1468.935	102.546
23 MAX CALC	4.874	.295	1257.245	76.127
35 AVE MEAS	4.291	.413	707.147	68.039
ATM CONC IN 10(-12) GM/M3				
61 ATM CALC	.532E-08	.631E-08		
CU CONC IN 10(-9) GM/CM3, LOADINGS IN 10(-9) GM/CM2/DAY				
24 MIN CALC	5.355	4.713	1.381	1.216
25 MAX CALC	121.804	92.373	31.419	23.828
36 AVE MEAS	14.147	16.024	2.331	2.640
ATM CONC IN 10(-12) GM/M3				
62 ATM CALC	.757E-12	.286E-11		
NI CONC IN 10(-9) GM/CM3, LOADINGS IN 10(-9) GM/CM2/DAY				
26 MIN CALC	.951	.481	.246	.124
27 MAX CALC	22.335	15.750	5.761	4.063
37 AVE MEAS	7.733	4.775	1.274	.787
ATM CONC IN 10(-12) GM/M3				
63 ATM CALC	.376E-12	.139E-11		
PB CONC IN 10(-9) GM/CM3, LOADINGS IN 10(-9) GM/CM2/DAY				
28 MIN CALC	1.466	.733	.378	.189
29 MAX CALC	3.767	1.853	.972	.478
38 AVE MEAS	27.093	9.747	4.465	1.606
ATM CONC IN 10(-12) GM/M3				
64 ATM CALC	.579E-13	.242E-13		
ZN CONC IN 10(-9) GM/CM3, LOADINGS IN 10(-9) GM/CM2/DAY				
30 MIN CALC	11.623	5.884	3.014	1.518
31 MAX CALC	31.275	14.350	7.609	3.701
39 AVE MEAS	209.700	423.145	34.555	69.728
ATM CONC IN 10(-12) GM/M3				
65 ATM CALC	.396E-12	.179E-12		
FE CONC IN 10(-9) GM/CM3, LOADINGS IN 10(-9) GM/CM2/DAY				
32 MIN CALC	43.175	19.959	11.137	5.156
33 MAX CALC	166.830	81.561	43.562	21.039
40 AVE MEAS	216.633	144.886	35.731	23.875
ATM CONC IN 10(-12) GM/M3				
66 ATM CALC	.132E-11	.169E-11		

25 32 VERNIER

CONSTITUENT	AVERAGE CONC	STD DEV	AVERAGE LOADING	STD DEV
SO4 CONC IN 10(-6) GM/CM3, LOADINGS IN 10(-6) GM/CM2/DAY				
20 MIN CALC	.974	.680	.252	.176
21 MAX CALC	5.859	5.366	1.518	1.390
34 AVE MEAS	5.421	4.568	1.017	.857
ATM CONC IN 10(-12) GM/M3				
60 ATM CALC	.138E-09	.504E-10		
57 DISSOLVED SO2	.785E-08	.425E-08		
58 DISSOLVED SO4	.267E-08	.409E-08		
59 PRTCULATE SO4	.116E-10	.277E-10		
PH LOADINGS IN (EXP) MEQ/CM2/DAY				
22 MIN CALC	5.602	.337	1451.262	87.180
23 MAX CALC	4.619	.270	1249.379	69.833
35 AVE MEAS	4.550	.327	853.362	155.184
ATM CONC IN 10(-12) GM/M3				
61 ATM CALC	.315E-08	.513E-08		
CU CONC IN 10(-9) GM/CM3, LOADINGS IN 10(-9) GM/CM2/DAY				
24 MIN CALC	4.727	5.236	1.225	1.356
25 MAX CALC	152.838	166.933	39.594	43.245
36 AVE MEAS	22.563	27.475	4.232	5.153
ATM CONC IN 10(-12) GM/M3				
62 ATM CALC	.205E-13	.749E-14		
NI CONC IN 10(-9) GM/CM3, LOADINGS IN 10(-9) GM/CM2/DAY				
26 MIN CALC	1.043	.775	.270	.201
27 MAX CALC	21.568	14.975	5.328	3.879
37 AVE MEAS	7.795	6.632	1.462	1.244
ATM CONC IN 10(-12) GM/M3				
63 ATM CALC	.207E-13	.757E-14		
PB CONC IN 10(-9) GM/CM3, LOADINGS IN 10(-9) GM/CM2/DAY				
28 MIN CALC	2.128	1.169	.551	.303
29 MAX CALC	4.503	2.244	1.166	.581
38 AVE MEAS	24.363	14.896	5.310	2.794
ATM CONC IN 10(-12) GM/M3				
64 ATM CALC	.622E-13	.228E-13		
ZN CONC IN 10(-9) GM/CM3, LOADINGS IN 10(-9) GM/CM2/DAY				
30 MIN CALC	17.166	10.453	4.447	2.708
31 MAX CALC	36.601	20.292	9.534	5.257
39 AVE MEAS	101.395	68.400	19.017	12.829
ATM CONC IN 10(-12) GM/M3				
65 ATM CALC	.415E-12	.152E-12		
FE CONC IN 10(-9) GM/CM3, LOADINGS IN 10(-9) GM/CM2/DAY				
32 MIN CALC	63.572	49.937	16.469	12.937
33 MAX CALC	207.445	179.139	53.740	46.407
40 AVE MEAS	286.866	230.545	54.178	43.239
ATM CONC IN 10(-12) GM/M3				
66 ATM CALC	.937E-12	.342E-12		

26 33 RIVER.V.

CONSTITUENT	AVERAGE CONC	STD DEV	AVERAGE LOADING	STD DEV
SO4 CONC IN 10(-6) GM/CM3, LOADINGS IN 10(-6) GM/CM2/DAY				
20 MIN CALC	.843	.388	.217	.100
21 MAX CALC	4.842	2.094	1.244	.538
34 AVE MEAS	3.142	2.529	.736	.593
ATM CONC IN 10(-12) GM/M3				
60 ATM CALC	.165E-09	.901E-10		
57 DISSOLVED SO2	.971E-08	.536E-08		
58 DISSOLVED SO4	.467E-08	.401E-08		
59 PRTCULATE SO4	.133E-10	.296E-10		
PH LOADINGS IN (EXP) MEQ/CM2/DAY				
22 MIN CALC	5.672	.382	1457.010	77.532
23 MAX CALC	4.899	.266	1258.561	68.245
35 AVE MEAS	4.268	.695	999.903	160.355
ATM CONC IN 10(-12) GM/M3				
61 ATM CALC	.536E-08	.499E-08		
CU CONC IN 10(-9) GM/CM3, LOADINGS IN 10(-9) GM/CM2/DAY				
24 MIN CALC	3.716	3.521	.955	.904
25 MAX CALC	126.830	91.181	32.582	20.855
36 AVE MEAS	16.175	15.514	3.789	3.634
ATM CONC IN 10(-12) GM/M3				
62 ATM CALC	.245E-13	.136E-13		
NI CONC IN 10(-9) GM/CM3, LOADINGS IN 10(-9) GM/CM2/DAY				
26 MIN CALC	1.802	.811	.257	.208
27 MAX CALC	16.381	8.459	4.208	2.173
37 AVE MEAS	11.775	18.291	2.758	4.285
ATM CONC IN 10(-12) GM/M3				
63 ATM CALC	.248E-13	.137E-13		
PB CONC IN 10(-9) GM/CM3, LOADINGS IN 10(-9) GM/CM2/DAY				
28 MIN CALC	2.537	.980	.523	.252
29 MAX CALC	3.694	1.611	1.000	.414
38 AVE MEAS	14.856	9.369	3.481	2.195
ATM CONC IN 10(-12) GM/M3				
64 ATM CALC	.745E-13	.412E-13		
ZN CONC IN 10(-9) GM/CM3, LOADINGS IN 10(-9) GM/CM2/DAY				
30 MIN CALC	16.121	7.303	4.141	1.876
31 MAX CALC	31.058	12.140	7.979	3.119
39 AVE MEAS	67.167	38.671	15.735	9.059
ATM CONC IN 10(-12) GM/M3				
65 ATM CALC	.496E-12	.275E-12		
FE CONC IN 10(-9) GM/CM3, LOADINGS IN 10(-9) GM/CM2/DAY				
32 MIN CALC	56.266	22.696	14.454	5.830
33 MAX CALC	162.262	50.646	41.684	13.011
40 AVE MEAS	168.433	79.174	39.457	18.547
ATM CONC IN 10(-12) GM/M3				
66 ATM CALC	.112E-11	.620E-12		

27 34 SUDBURY N.

CONSTITUENT		AVERAGE CONC.	STD DEV	AVERAGE LOADING	STD DEV
SO4 CONC IN 10(-6) GM/CM3, LOADINGS IN 10(-6) GM/CM2/DAY					
20	MIN CALC	5.674	2.896	1.421	.734
21	MAX CALC	124.568	60.719	31.683	15.395
34	AVE MEAS	7.175	4.069	1.344	.762
ATM CONC IN 10(-12) GM/M3					
60	ATM CALC	.949E-08	.215E-07		
57	DISSOLVED SO2	.709E-06	.155E-05		
58	DISSOLVED SO4	.191E-06	.420E-06		
59	PRTCULATE SO4	.393E-08	.862E-08		
PH	LOADINGS IN (EXP) MEQ/CM2/DAY				
22	MIN CALC	4.664	.265	1233.221	67.133
23	MAX CALC	3.522	.292	892.843	74.158
35	AVE MEAS	4.646	.727	870.286	136.194
ATM CONC IN 10(-12) GM/M3					
61	ATM CALC	.139E-07	.638E-09		
CU CONC IN 10(-9) GM/CM3, LOADINGS IN 10(-9) GM/CM2/DAY					
24	MIN CALC	40.573	29.297	10.287	7.174
25	MAX CALC	934.954	505.363	237.049	128.130
36	AVE MEAS	541.600	396.335	101.441	74.327
ATM CONC IN 10(-12) GM/M3					
62	ATM CALC	.524E-11	.117E-10		
NI CONC IN 10(-9) GM/CM3, LOADINGS IN 10(-9) GM/CM2/DAY					
26	MIN CALC	7.114	3.998	1.804	1.014
27	MAX CALC	186.246	91.927	47.221	23.307
37	AVE MEAS	231.260	145.792	43.315	27.307
ATM CONC IN 10(-12) GM/M3					
63	ATM CALC	.221E-11	.487E-11		
PB CONC IN 10(-9) GM/CM3, LOADINGS IN 10(-9) GM/CM2/DAY					
28	MIN CALC	3.451	1.681	.879	.477
29	MAX CALC	4.520	2.277	1.146	.577
38	AVE MEAS	70.500	47.259	13.205	8.852
ATM CONC IN 10(-12) GM/M3					
64	ATM CALC	.666E-13	.229E-13		
ZN CONC IN 10(-9) GM/CM3, LOADINGS IN 10(-9) GM/CM2/DAY					
30	MIN CALC	31.398	17.168	7.961	4.338
31	MAX CALC	120.253	52.969	30.489	13.430
39	AVE MEAS	136.700	154.904	34.969	29.013
ATM CONC IN 10(-12) GM/M3					
65	ATM CALC	.128E-11	.184E-11		
FE CONC IN 10(-9) GM/CM3, LOADINGS IN 10(-9) GM/CM2/DAY					
32	MIN CALC	142.752	88.860	36.201	22.530
33	MAX CALC	1034.132	563.343	262.194	147.901
40	AVE MEAS	1445.700	1559.104	270.779	292.019
ATM CONC IN 10(-12) GM/M3					
66	ATM CALC	.783E-11	.152E-10		

APPENDIX C
atmospheric box model program

```
FTN,OPT=1.
1         6400 END OF RECORD
      PROGRAM SC480X (INPUT=100 ,OUTPUT,FILE2,FILE3,FILE4,FILE5,FILE6,
     1 FILE7,FILE8,TAPE5=INPUT,TAPE6=OUTPUT                ,TAPE9=FILE2,
     2 TAPE10=FILE3,TAPE10=FILE4,TAPE11=FILE5,TAPE12=FILE6,TAPE13=FILE7,
     3 TAPE14=FILE8,                    SUOSTS,MYCATA,TAPE16=SUOSTS,
     4 TAPE17=MYDATA,CTUT12,TAPE19=OTUT12)
      DIMENSION                                      SMI(50,4),NMM(50),
     1 S4M(50),CWE(5) ,SS2W(50)
      DIMENSION RMI(50),RMF(50)
      DIMENSION XLS(5),XLS(5),XLM(50),YLM(50),ZSM(50)
      DIMENSION CFF(50),DRC(50), CL4(50),PDM(50),ZNM(50)
      DIMENSION VLM(50),CKM(50),TPM(50),TIM(50),SCK(50),TMS(50)
      DIMENSION CST(5),WF(5),OHT(5),OFE(5),FEM(50)
      DIMENSION MSS(5),SIPS(5,4),ZBS(5)       ,CH(5),OS2(5),OS4(5),
     1  Y(5),F(5),QSA(5),ICU(5),QNI(5),QP3(5),QZN(5)
      DIMENSION SAPX(50),S20X(50),S40X(50),SCCX(50),TEN(50)
      DIMENSION SAC(50),S20(50),S40(50),S80(50),SPT(50),SGS2(50),
     1 SHS4(50),SOF4(50),SWS2(50),SG2X(50),SW2X(50),SW4X(50),SD4X(50),
     2 TWSX(50),TCSY(50),TF2X(50),TS4X(50),TRSX(50),CSCX(50)
      DIMENSION THF(50),III(50),TWS(50),TDS(50),TRS2(50),TFS4(50)
      DIMENSIONIW1(5),IW2(5),IW3(5),IW4(5),IW5(5),IW6(5),W7(5),W3(5),
     1 W9(5),W10(5),W11(5),IW12(5),IW13(5),IW14(5),W15(5),W16(5),W17(5),
     2 W18(5),W19(5),W20(5)
      DIMENSION ATSS(50),ATRSX(50),AOPC(50),AOPCX(50)
      DIMENSION SWCU(50),SWNI(50),SWP3(50),SWFE(50),SWZN(50),SWCUX(50),
     1 SWNIX(50),SWP3X(50),SWFEX(50),SWZNX(50),SWC(50),SWN(50),SWP(50),
     2 SW2(50),SWF(50),SWCX(50),SWNX(50),SWPX(50),SWZX(50),SWFX(50)
      DIMENSION                        SPH(50),SPHX(50),PH(50),PHX(50)
      DIMENSION DAYC(50),DXS(50)
      DIMENSION WFM(50),WPHX(50)
      DIMENSION SOWF(50),SSDV(50),SAV(50),SSOH(50),SAH(50)
      INTEGER STF,STFS,YR3,CYR,THR,SNR,FGR,YMI(50),DMI(50),YMF(50),
     1 CWF(50)
      REAL HP,HPX,HMIN(50),HIM(50),NIMM,NIMX
      WRITE(6,108)
      WRITE(6,600)
      WRITE(6,602)
      WRITE(6,602)
C  READ PHYSICAL DATA
      READ(5,109) IWT,NCX,NIX,NSI
      WRITE(6,100) IWT,NCX,NIX,NST
      READ(5,327) XMAX,YMIN
      WRITE(6,616)
      WRITE(6,327)XMAX,YMIN
      READ  (5,510) CXST,DS,FO2,CF,ESJ,EHK
      WRITE(6,511)  CXST,DS,FO2,CF,ESJ,EHK
      READ(5,530)  CS2AM,CS4PM,CHICN,CNH3,CPRT
      WRITE(6,618)
      WRITE(6,531) CS2AM,CS4PM,CHICN,CNH3,CPRT
      READ (5,520) SCUM,SNIM,SP3M,SZNM,SFEM
      WRITE(6,619)
      WRITE(6,531) SCUM,SNIM,SP3M,SZNM,SFEM
      READ (5,610) CFC,CFN,CFP,CFZ,CFF
      WRITE(6,620)
      WRITE(6,531) CFC,CFN,CFP,CFZ,CFF
      READ (5,612) FOP,FOL,ROS4,ROCU,RONI,ROPB,ROZN,ROFE
      WRITE(6,621)
      WRITE(6,513) FOP,FOL,ROS4,ROCU,RONI,ROPB,ROZN,ROFE
      WRITE(6,602)
```

```
C  READ INDEXED DATA
      READ(5,540)  NPT,NDI,NP,NSS,NH
      WRITE(6,541) NPT,NDI,NP,NSS,NH
      WRITE( 6,650)    HIX,IST,NSS,XMAX,YMIN,CS2AM,CS4PM,CHION,CNH3,CPRT,
     1  SCUM,SAIM,SPRM,SZNM,SFEM,FO2,DF,CFC,CFN,CFF,CFZ,CFF,ROP,ROC,ROS4,
     2  RCCU,CONI,FOZN,FOFE
C  READ SOURCES DATA
C  XLS,LAT  XMS,LONG  ZBS,HEIGHT OF STACK BASE ABOVE DATUM,M  QS,RATE OF
C  XLS,LAT  XMS,LONG  ZBS,HEIGHT OF STACK BASE ABOVE DATUM,M  QH,RATE OF
C  HEAT EMMISSION,CAL/SEC  QS2,RATE OF SO2 EMMISSION,GM/DAY  QS4,RATE OF
C  SO4 PARTICULATE EMMISSION,GM/DAY  H,HEIGHT OF STACK,KM  Y,EFFECTIVE
C  SOURCE DIAM,KM  QWP,RATE OF WATER VAPOR EMMISSION,GM/DAY
      READ(5,536)  (NNSS(K),(SMPS(K,K2),K2=1,4),XMS(K),XLS(K),ZBS(K),
     1  QH(K),QS2(K),QS4(K),H(K),Y(K),QWP(K),QSA(K),QCU(K),QNI(K),QPB(K)
     2 ,QZN(K), QFE(K),QHI(K),K=1,NSS)
      WRITE(6,536) (NNSS(K),(SMPS(K,K2),K2=1,4),XMS(K),XLS(K),ZBS(K),
     1  QH(K),QS2(K),QS4(K),H(K),Y(K),QWP(K),QSA(K),QCU(K),QNI(K),QPB(K)
     2 ,QZN(K), QFE(K),QHI(K),K=1,NSS)
      WRITE(6,602)
C  READ MEASURED DATA
      JJ=1
      JJC=0
 6000 CONTINUE
      READ (17,26) NNN(JJ),(SMI(JJ,JJA),JJA=1,4),XNM(JJ),YLM(JJ),ZBM(JJ)
     1 ,VLM(JJ),CXM(JJ),TPM(JJ)
     2 ,YMI(JJ),MMI(JJ),DMI(JJ),YMF(JJ),MMF(JJ),DMF(JJ),S4M(JJ),CUM(JJ),
     3 NIM(JJ),PBM(JJ),ZNM(JJ),FEM(JJ),HIM(JJ)
      IF(NNM(JJ).GT.32.AND.NMI(JJ).GT.6)  GO TO 6597
      IF(NNM(JJ).NE.12.AND.NNM(JJ).NE.24.AND.NNM(JJ).NE.26.AND.NNM(JJ).
     1 NE.33) GO TO 6000
      IF(NMI(JJ).NE.6) GO TO 6000
      GO TO 6500
 6597 NNM(JJ)=0
 6500 WRITE (14   )NNM(JJ),(SMI(JJ,JJA),JJA=1,4),XNM(JJ),YLM(JJ),ZBM(JJ)
     1 ,VLM(JJ),CXM(JJ),TPM(JJ)
     2 ,YMI(JJ),MMI(JJ),DMI(JJ),YMF(JJ),MMF(JJ),DMF(JJ),S4M(JJ),CUM(JJ),
     3 NIM(JJ),PBM(JJ),ZNM(JJ),FEM(JJ),HIM(JJ)
      IF(NNM(JJ).EQ.0) GO TO 6599
      JJC=JJC+1
      GO TO 6000
 6999 CONTINUE
      WRITE(6,*) JJC
      IIC=0
 5000 CONTINUE
      READ(16,135) INC,IN3,STR,YRR,MNR,DYR,RT,DMP,DMFX,HP,HPX,THR,SNR,
     1 FGR,AVP,AHP,SDVW,SDHH
      WRITE(13   )INC,IN3,STR,YRR,MNR,DYR,RT,DMP,DMFX,HP,HPX,THR,SNR,
     1 FGR,AVP,AHP,SDVW,SDHH
      IF(STR.EQ.0) GO TO 5999
      IIC=IIC+1
      GO TO 5000
 5999 CONTINUE
      WRITE(6,*) IIC
      REWIND13
      WRITE(6,602)
      WRITE(6,168)
      WRITE(6,601)
      WRITE(6,602)
      WRITE(6,602)
      II=0
```

```
      IIT=0
      J=1
      AA=1.0
      AAA=1.0
      SSDX=0.
      SM2)=0.
      XL4=0.
      YL4=0.
      SC52=0.
      SCD2(X=0.
      SS44=0.
      STP3=0.
      STP3X=0.
      SC2=0.
      SL2X=0.
      SI=0.0
      CO 8000 J=1, JJC
      III(J)=0
      IIF(J)=0
      CAYC(J)=0.
      SS2H(J)=0.
      TS3X(J)=0.
      IPS(J)=0.
      CR2X(J)=0.
      DS2(J)=0.
      CS4(J)=0.
      AC32C(J)=0.
      AC32X(J)=0.
      SC4)(J)=0.
      SH4X(J)=0.
      SH2X(J)=0.
      SG2X(J)=0.
      SHCX(J)=0.
      SH4X(J)=0.
      SHCX(J)=0.
      SH7X(J)=0.
      SHFX(J)=0.
      SPT1J)=0.
      SDS((J)=0.
      SHS4(J)=0.
      SHS2(J)=0.
      SGS2(J)=0.
      SHC(J)=0.
      SH2(J)=0.
      SH8(J)=0.
      SH7(J)=0.
      SHF(J)=0.
      III3(J)=0
      AT32S(J)=0.
      AT32X(J)=0.
      SPH(J)=0.
      SPHX(J)=0.
      SSDF(J)=0.
      SSDV(J)=0.
      SS44(J)=0.
      SAV(J)=0.
      SDM2(J)=0.
 8000 CONTINUE
      ACL=550.
      TKY=0.0351
```

A

```
      TKYOP=0.006
      ELN=        (64.3-FO2)       *RCL**2 /(RCP+RCL) * 2.47E+3
      ES4N=       (64.3-OF)*        RCS4**2 /(RCP+RCS4)* 2.73E+3
      ECUN=       (64.3-FFC)        *RCCU**2 /(RCP+RCCU)* 9.96E+3
      ENIN=     (64.3-9FN)*       RCNI**2 /(RCP+RCNI)* 11.67E+3
      EZNN=     ( 64.3-3FZ)       *RCZN**2 /(RCP+RCZN)* 10.11E+3
      EPBN=       (64.3-9FB)       *RCPB**2 /(RCP+RCPB)* 15.36E+3
      EFEN=       (64.3-3FE)       *RCFE**2 /(RCP+RCFE)*11.11E+3
      EL=ELNN**2 /(ELN+0.06)**2
      ES4=ES4N**2 /(ES4N+0.06)**2
      ECU=ECUN**2 /(ECUN+0.06)**2
      ENI=ENIN**2 /(ENIN+0.06)**2
      EPB=EPBN**2 /(EPBN+0.06)**2
      EZN=EZNN**2 /(EZNN+0.06)**2
      EFE=EFEN**2 /(EFEN+0.06)**2
      ECL=EL
      TKL=RCL**3*EL**3*NCL*(RCP+RCL*EL)**2*0.4112
      TKG=TKYOP*1064.4*FOO**2
      CXSI=TKL/(TKL+TKG)
      ESR=TKY*RCL**2 *RCL*2.513E+3
      FOFE=(RCFE/RCL)**2 *(EFE/EL)
      FOZN=(RCZN/RCL)**2 *(EZN/EL)
      FOPB=(RCPB/RCL)**2 *(EPB/EL)
      RCNI=(RCNI/RCL)**2 *(ENI/EL)
      RCCL=(RCCL/RCL)**2 *(ECU/EL)
      RCS4=(RCS4/RCL)**2 *(ES4/EL)
  900 CONTINUE
      IT=IT+1
  READ EARLY WEATHER STATISTICS
      READ( 13     )IND,INR,STR,YRR,MNR,DYR,RT,DMP,DMPX,HP,HPX,THR,SNR,
     1 FOS,AVE,AHR,SOVW,S3HW
  SELECTION OF WEATHER STATIONS
      IF(STR.EQ.6057552)  IND=1
      IF(STR.EQ.6066150) IND=2
      IF(STR.EQ.6076265) IND=3
      IF(STR.EQ.6055700) IND=4
      IF(STR.EQ.6092925) IND=5
      IF(STR.EQ.0) IND=6
      IF(NIX.LT.1.OR.NIX.GT.5) GO TO 1100
      IF (IND.LE.NIX) GO TO 1000
  100 CONTINUE
      IF(NIX.EQ.11) GO TO 1101
      IF(NIX.LT.6.OR.NIX.GT.9) GO TO 9151
  101 CONTINUE
      IF(IND.NE.1) GO TO 9100
      XLW=84.3333
      YLW=46.5333
      WRITE(9     ) IND,INR,STR,YRR,MNR,DYR,RT,DMP,DMPX,HP,HPX,THR,SNR,
     1 FOS,AVE,AHR,SOVW,S3HW,XLW,YLW
      GO TO 1000
  100 IF(IND.NE.2) GO TO 9110
      XLW=80.5000
      YLW=46.6162
      WRITE(9     ) IND,INR,STR,YRR,MNR,DYR,RT,DMP,DMPX,HP,HPX,THR,SNR,
     1 FOS,AVE,AHR,SOVW,S3HW,XLW,YLW
      GO TO 1000
  110 IF(IND.NE.3) GO TO 9120
      XLW=81.3333
      YLW=45.5000
      WRITE(10    )IND,INR,STR,YRR,MNR,DYR,RT,DMP,DMPX,HP,HPX,THR,SNR,
```

```
     1 FSR,AVE,AHP,SDVH,SDHH,XBH,YLH
      GO TO 1000
 8120 IF(IND.NE.4) GO TO 8130
      XBH=79.4333
      YLH=46.3333
      WRITE(11    )IND,IWR,STR,YRR,MNR,DYR,RT,DHP,DHPX,HP,HPX,THR,SNR,
     1 FSR,AVE,AHP,SDVH,SDHH,XBH,YLH
      GO TO 1000
 8130 IF(IND.NE.5) GO TO 1000
      XBH=82.4667
      YLH=45.5000
      WRITE(12    )IND,IWR,STR,YRR,MNR,DYR,RT,DHP,DHPX,HP,HPX,THR,SNR,
     1 FSR,AVE,AHP,SDVH,SDHH,XBH,YLH
      IF(STR.EQ.0) GO TO 901
      GO TO 1000
  901 CONTINUE
      REWIND8
      REWIND9
      REWIND10
      REWIND11
      REWIND12
      II=0
  900 CONTINUE
      II=II+1
      READ(12    )IW1( 5),IW2( 5),IW3( 5),IW4( 5),IW5( 5),IW6( 5),W7( 5)
     1 ,W8( 5),W9( 5),W10( 5),W11( 5),IW12( 5),IW13( 5),IW14( 5),W15( 5)
     2,W16( 5),W17( 5),W18( 5),W19( 5),W20( 5)
      IF(IW3( 5).EQ.0) GO TO 1001
      READ(8     ) IW1( 1),IW2( 1),IW3( 1),IW4( 1),IW5( 1),IW6( 1),W7( 1)
     1 ,W8( 1),W9( 1),W10( 1),W11( 1),IW12( 1),IW13( 1),IW14( 1),W15( 1)
     2,W16( 1),W17( 1),W18( 1),W19( 1),W20( 1)
      READ(9     ) IW1( 2),IW2( 2),IW3( 2),IW4( 2),IW5( 2),IW6( 2),W7( 2)
     1 ,W8( 2),W9( 2),W10( 2),W11( 2),IW12( 2),IW13( 2),IW14( 2),W15( 2)
     2,W16( 2),W17( 2),W18( 2),W19( 2),W20( 2)
      READ(10    )IW1( 3),IW2( 3),IW3( 3),IW4( 3),IW5( 3),IW6( 3),W7( 3)
     1 ,W8( 3),W9( 3),W10( 3),W11( 3),IW12( 3),IW13( 3),IW14( 3),W15( 3)
     2,W16( 3),W17( 3),W18( 3),W19( 3),W20( 3)
      READ(11    )IW1( 4),IW2( 4),IW3( 4),IW4( 4),IW5( 4),IW6( 4),W7( 4)
     1 ,W8( 4),W9( 4),W10( 4),W11( 4),IW12( 4),IW13( 4),IW14( 4),W15( 4)
     2,W16( 4),W17( 4),W18( 4),W19( 4),W20( 4)
      YRR=IW4(1)
      MNR=IW5(1)
      DYR=IW6(1)
      GO TO 8152
 8151 CONTINUE
      IF(STR.EQ.0) GO TO 1001
 8152 CONTINUE
      SDT=360.
      IWM=1
      DO 2002 IW=1,5
      EST(IW)=0.
 2002 CONTINUE
      REWIND14
      NNC=0
      J2C=2+JJC/50
      DO 2995 J2=1,J2C
      J=1
      DO 2000 J=1,50
      JJ=J
      READ (14    )XNM(JJ),(SMI(JJ,JJA),JJA=1,4),XNH(JJ),YLH(JJ),ZBH(JJ)
```

```
     1 ,VLM(JJ),CXM(JJ),TPM(JJ)
     2 ,YMI(JJ),MMI(JJ),DMI(JJ),YMF(JJ),MMF(JJ),DMF(JJ),S4M(JJ),CUM(JJ),
     3 RTM(JJ),EBM(JJ),ZMM(JJ),FEM(JJ),HIM(JJ)
      IF(NRN(J).EQ.0) GO TO 2999
      M75=0
      IF(YMF(JJ).LT.75)  GO TO 2122
      M75=1
      IYF=YMF(JJ)
      IMF=MMF(JJ)
      IDF=DMF(JJ)
      YMF(JJ)=74
      MMF(JJ)=12
      DMF(JJ)=31
 2122 CONTINUE
      NRC=NRC+1
      IF(II.NE.1) GO TO 2003
      WRITE(6,  27) NM(JJ),(SMI(JJ,JJA),JJA=1,4),XNM(JJ),YLM(JJ),ZBM(JJ)
     1 ,VLM(JJ),CXM(JJ),TPM(JJ)
     2 ,YMI(JJ),MMI(JJ),DMI(JJ),YMF(JJ),MMF(JJ),DMF(JJ),S4M(JJ),CUM(JJ),
     3 RTM(JJ),EBM(JJ),ZMM(JJ),FEM(JJ),HIM(JJ)
 2003 CONTINUE
      GS2=0.0
      WS2=0.0
      WS4=0.0
      GS4=0.0
C ELIMINATION OF DAYS NOT IN MEASURED TIME PERIODS
      IF(YRR.EQ.YMI(J).AND.MRR.EQ.MMI(J).AND.DYR.EQ.DMI(J)) III(J  )=II
      IF(YRR.EQ.YMF(J).AND.MRR.EQ.MMF(J).AND.DYR.EQ.DMF(J)) IIF(J  )=II
      IF(III(J).EQ.0) GO TO 2100
      IF(IIF(J).EQ.II) GO TO 2001
      IF(IIF(J).NE.0) GO TO 2000
 2001 CONTINUE
      IF(NIX.EQ.11) GO TO 2121
      IF(NIX.LT.5.OR.NIX.GT.9) GO TO 2114
 2121 CONTINUE
C   CALC DISTANCES, STATIONS TO RECEPTORS, AND MIN DISTANCE STATIONS
      DO 2111 IW=1,5
      XLAD=3185.6*ABS(XRM(JJ)-W19))*(COS(YLM(JJ)/57.3)+COS(W20(IW)
     1 /57.3))/57.3
      YLAD=6371.2*ABS(YLM(JJ)-W20(IW))/57.3
      DST(IW)=SQRT(XLAD**2+YLAD**2)
      IF((DST(IW).EQ.0.) DST (IW)=0.0001
      IF(DST(IW).GT.SDT) GO TO 2111
      SDT=DST(IW)
      IWW=IW
 2111 CONTINUE
C   WEATHER FOR NEAREST STATION
      IF(NIX.NE.8) GO TO 2112
      IWD=IW1(IWW)
      IFR=IW2(IWW)
      STR=IW3(IWW)
      RT=W7(IWW)
      CMR=W8(IWW)
      OMR=W9(IWW)
      MR=W10(IWW)
      MRX=W11(IWW)
      THR=IW12(IWW)
      SNR=IW13(IWW)
      FGR=IW14(IWW)
      AVR=W15(IWW)
```

```
      AHP=W16(IHP)
      SCVH=W17(IHP)
      SCHH=W18(IHP)
      XNH=W19(IHP)
      YLH=W20(IHP)
 2117 CONTINUE
      IF(NIX.EQ.6. OR.NIX.EQ.7. OR.NIX.EQ.11) GO TO 2116
      GO TO 2115
 2116 CONTINUE
      SRT=0.
      SCHF=0.
      SCHPX=0.
      SHP=0.
      SHPX=0.
      ISTH=0
      ISSH=0
      STHP=0.
      SSHP=0.
      SFGP=0.
      SAVP=0.
      SAHF=0.
      SSDVH=0.
      SSCHH=0.
      SXNH=0.
      SYLH=0.
      WFS=0.
      DO 2113 IH=1,5
      WF(IH)=1.
C  AVERAGE WEATHER FOR ALL STATIONS
      IF(NIX.EQ.6) WF(IH)=1.0
C  WEIGHTED AVERAGE, INVERSE DISTANCE,STATION TO RECEPTORS
      IF(NIX.EQ.7) WF(IH)=SDT/DST(IH)
C  WEIGHTED AVERAGE, INVERSE SQUARE DISTANCE,STATION TO RECEPTORS
      IF(NIX.EQ.11) WF(IH)=(SDT/DST(IH)) **2
      IHP=NIX
      IHP=0
      STP=0
      SRT=SRT+W7(IH)*WF(IH)
      SCHFX=SCHFX+W8(IH)*WF(IH)
      SCHP=SCHP+WF(IH)*WF(IH)
      SHP=SHP+W17(IH)*WF(IH)
      SHPX=SHPX+W11(IH)*WF(IH)
      WW12=IW12(IH)
      STHP=STHP+WW12*WF(IH)
      WW13=IW13(IH)
      SSHP=SSHP+WW13*WF(IH)
      WW14=IW14(IH)
      SFGP=SFGP+WW14*WF(IH)
      SAVP=SAVP+W15(IH)*WF(IH)
      SAHP=SAHP+W16(IH)*WF(IH)
      SSDVH=SSDVH+W17(IH)*WF(IH)
      SSCHH=SSCHH+W18(IH)*WF(IH)
      SXNH=SXNH+W19(IH)*WF(IH)
      SYLH=SYLH+W20(IH)*WF(IH)
      WFS=WFS+WF(IH)
 2113 CONTINUE
      RT=SRT/WFS
      CHP=SCHF/WFS
      CHPX=SCHFX/WFS
      HP=SHP/WFS
```

```
      HPX=SHPX/WFS
      THS=STHS/WFS
      SHS=SSHP/WFS
      FGS=SFGP/WFS
      AVS=SAVP/WFS
      AHP=  SAHP/WFS
      SCVH=SSCVH/WFS
      SDHH=SSDHH/WFS
      XMH=SXMH/WFS
      YLH=SYLH/WFS
 2115 CONTINUE
C  TREND SURFACE WEATHER CALCULATION
      IF(NYX.NE.9) GO TO 2114
 2114 CONTINUE
      SAVX(J)=0.
      SPVX(J)=0.
      SAVX(J)=0.
      SDVX(J)=0.
      SWCUX(J)=0.
      SWNIX(J)=0.
      SWPEX(J)=0.
      SWZNX(J)=0.
      SWFEX(J)=0.
      WFHX(J)=0.
      SAV(J)=1.0E5
      SPV(J)=1.0E5
      SAV(J)=1.0E5
      SDV(J)=1.0E5
      SWCU(J)=1.0E5
      SWNI(J)=1.0E5
      SWPE(J)=1.0E5
      SWZN(J)=1.0E5
      SWFE(J)=1.0E5
      WFH(J)=1.0E5
      AGS2S=0.
      AHS2S=0.
      AHS4S=0.
      AGS4S=0.
      AWSHS=0.
      AWCUS=0.
      AWNIS=0.
      AWPES=0.
      AWFES=0.
      AWZNS=0.
C  CALC OF MAX,MIN WIND,MAX,MIN RAINFALL DURATION AND RATES
      DO 2600 IP=1,4
      HP=HPX
      DHS=DHPX
      AHQ=AHP
      AVQ=AVP+SCVH
      IF(IP.EQ.3.OR.IP.EQ.4) AVQ=AVP-SCVH
      IF(IP.EQ.2.OR.IP.EQ.4) HP=HPX
      IF(IP.EQ.2.OR.IP.EQ.4) DHS=DHPX
C  MEASUREMENT ACCURACY OF INPUT DATA
      DO 2600 IV=1,4
      AHW=AHQ+0.0871
      AVW=AVQ+0.20
      IF(IV.EQ.2.OR.IV.EQ.4) AHW=AHQ-0.0871
      IF(IV.EQ.3.OR.IV   .EQ.4) AVW=AVQ-.20
      IF(AVW.LT.0.) AHW=AHW+3.1416
```

```
      IF(AHH.GT.3.14159) AHH=AHH-6.28319
      AVH=ABS(AVH)
      XR=(XMAX-XMM(J))*76.
      YR=(YLM(J)-YMIN)*105.
C  MAX MIXING HEIGHTS FROM TURNER (IN AGRES BOX MODEL)
      HMAC=0.616+0.497*SIN((HNF-4.)*0.524)
      HMAX=HMAC+.025
      IF(IV.EQ.3.OR.IV   .EQ.4) HMAX=HMAC-.025
C  CALCULATION OF THE CONCENTRATIONS AND LOADINGS
      CLH=AVH*24.
      ADXL=SQHW*2.
C  TD IS DURATION OF RAINFALL ETC EVENT
C  CALC OF LOSS FACTORS FOR DIFFERENT SPECIES FOR DRY AND RAINFALL CONDITIONS
C  STANDARDIZED LOSS FACTORS, IN HR-1, EST FROM JR KRAMER 1976 (GREEN BFT)
C  GI IS EFFECT GAS IMPINGEMENT COEF EST.  WO1 IS WASHOUT COEF OF GASEOUS SO2
C  WO2 IS WASHOUT COEF OF CLOUD DROPLETS.  SUM EQUALS WASHOUT FROM ENGELMANN,
C  REKATED BY EFFECTIVE CROSS SECTION OCCUPIED BY CLOUD DROPLETS  CXST IS CROSS
C  SECTION
C  SCAVENGING COEFFICIENTS ARE ESTIMATES FROM SLINN AND HALES,1970,JR KRAMER,
C  ETC, IN PARTS PER HOUR  OR HR-1,
C  WASHOUT COEFFICIENT FROM ANGELMANN,1965
      WOA=0.
      IF(TR    .EQ.0.) GO TO 3010
      WOA=EXP(2.3026* (-0.24+0.5*ALOG10(0.5)))
 3010 CONTINUE
      WO1=WOA*(1.-CXST)
      WO2=WOA*CXST
      WO3=WOA*FOS4
      CY=1.002
      TC=HR
      CS2AI=0.
      CS4FI=0.
      CH2I=0.
      SCU=0.
      SNI=0.
      SPB=0.
      SZN=0.
      SFE=0.
      SCA=0.
      S2H=0.
      S4H=0.
      SCP=0.
      SCH=0.
      SGSAV=1.006
      GS2S=0.
      HS2S=0.
      HS4S=0.
      GS4S=0.
      HCUS=0.
      HPBS=0.
      HFES=0.
      HZNS=0.
      HSHS=0.
      K=1
      DO 4000 K=1,NSS
      GI=1.0
      CCA=0.
      C2H=0.
      C4H=0.
```

```
      CCP=0.
      CCU=0.
      CPI=0.
      CPS=0.
      CZH=0.
      CPE=0.
      XLS(K)=YMAX-XLS(K)
      XLS(K)=XLS(K)-YMIN
C     CONVERSION OF LAT AND LONG TO KM
      XS=XLSK*76.
      YS=XLSK*105.
C     WIND ANGLE CALCULATIONS, ETC.
C     XPS IS DISTANCE SOURCE TO RECEPTOR
      XSR=SQRT((YR-YS)**2 +(XR-XS)**2 )
      ASR=ATAN((YR-YS)/(XR-XS))
      XLA=59.5851*    (XLS(K)-XLW(JJ))*(COS(YLM(JJ)/57.3)+COS(XLS(K)/57.3
     1 ))
      YLA=111.1902*    (YLM(JJ)-YLS(K))
      XSR=SQRT(XLA**2+YLA**2)
      ASR=ATAN(YLA/XLA)
      IF(XLA.LT.0.) ASR=ASR-3.14159
      IF( K.EQ.1) XSR1=XSR
      IF( K.EQ.2) XSR2=XSR
      IF( K.EQ.3) XSR3=XSR
      IF(K.EQ.1) ASR1=ASR
      IF(K.EQ.2) ASR2=ASR
      IF(K.EQ.3) ASR3=ASR
C     AUX IS THE ANGLE, RECEPTOR TO SOURCE, TO THE WIND DIRECTION
      AUX=ABS(ASR-AHW)
      IF(AUX.GT.3.14159) AUX=ABS(6.28318 -AUX)
C     STOP CALC FOR CASES WHEN WIND  VELOCITY IS TOO LOW TO REACH RECEPTOR IN 24 HRS
      IF(CCH.LT.XSR) GO TO 4000
C     STOP CALC FOR CASES OF WIND HEADING MORE THEN 2 STD DEV FROM RECEPTOR HEADING
      IF(AUX.GT.3.14159) GO TO 4000
C     UX AND UY ARE COMPONENTS OF WIND FROM SOURCE TO RECEPTOR AND AT RIGHT
C     ANGLES TO THAT LINE, RESPECTIVELY
      UX=AVH              *COS(AUX)
      UY=AVH              *SIN(AUX)
      UY=ABS(UY)
      XCH=ABS(XSR*SIN(AUX))
C     LOFT, BRIGGS REVISED FORMULAE
C     DISTANCE IN M SECH KM
      HMM=H(K)*1.0E3
      X=XSR*1.0E3
C     VELOCITY IN M/SEC FROM KM/HR
      UXX=AVH    *0.2778E
      F=3.7E-5*CH(K)
      CB=14.
      IF(F.GT.55.) CB=34.
      F13=F**0.33333
      CH=1.6*F13          *X**(.66667)/UXX
      EVPP=1.6*F13          /X**(.33333)
      XC=3.5*CB*F**(.625)
      IF(X.GT.XC) CH=1.6*F13          *(10*HMM )**(.6667)/UXX
      IF(X.GT.XC) EVPP=1.6*F13          *(10*HMM)**(.6667)/X
      EVP=EVPP
C     LOFT IN KM ABOVE STACK BASE
      HK=H(K)+CH*1.0E-3
      IF(HK.GT.HMAX) HK=HMAX
C     EST WIND PROFILE WITH ALTITUDE
```

```
C  GROUND WIND IN M/SEC
       UXH=AVH*0.27768
       AVH=AVH*SQRT(SQRT(HK/0.013))
       UXF=UXH*SQRT(SQRT(HK/0.013))
       WFAC=10**(0.063*UXF)
C  TIME TO REACH RECEPTOR DISTANCE ALONG WIND HEADING, CALCULATED IN HOURS
       T=XSR/AVH
C  TT IS THE PROBABLE EVENT TIME PORTION OF TOTAL TRAVEL TIME T
       TT=T*TO/24.
C  DISPERSION
C  VERTICAL DISPERSION ANGLE, SMITH-SINGER RELATIONSHIP
       ADY=.33/XSR**(.14)
C  STD DEV OF WIND HEADINGS OVER 24 HRS USED AS DISPERSION ANGLE
C  DISPERSION AFTER SUTTON, TURNER,ETC
       DX=.30*SQRT*XSR**0.86
C  VERTICAL DISPERSION AT THE RECEPTOR
       CYX=HK+ABS(XSR*ADY)
       CYH=HK-ABS(XSR*ADY)
       IF(CYX.GT.HMAX) CYX=HMAX
       IF(CYH.LT.0.) CYH=0.
       CY=CYX-CYH
       CYD=(CYX+CYH)/2.
C  OXIDATION RATES FROM H. LUSIS IN PARTS/HR
       RO1=0.01
       RO2=0.0
       RO3=0.0025
       PO1=10.**(-1.45-0.45*T)
       IF(T.GT.2.) PO1=0.0
       RO2=0.5E-4
       PO3=(PO1+RO2)*0.75
C  INITIAL CONCENTRATIONS AT RECEPTOR VICINITY
       YC=Y(K)
C  BOX DISTRIBUTION
C  INPUTS IN GM/DAY
C  CONVERT GM/KM3 TO UG/C13, OR PPM OF SULFUR SPECIES IN VOL VH OF WATER
C  OR IN A 1 CM3 VOL OF AIR
       CILF=          1.0E-9/((DX+YC)*AVH*DY*24.)
       CS2AC=QS2(K)*CILF
       CS4PC=QS4(K)*CILF
       CHAO =QH=(K)*CILF
       CSAO =QSA(K)*CILF
       CCUC =QCU(K)*CILF
       CNIC =QNI(K)*CILF
       CPBC =QPB(K)*CILF
       CZNO =QZN(K)*CILF
       CFEC=QFE(K) *CILF
C  HORIZONTAL GAUSSIAN DISTRIBUTION.  CONCENTRATIONS UNIFORM IN VERTICAL DIM
       GCF=.398   *EXP(-0.5*AUX**2 *XSR**2 /((DX+YC)   )**2)
       IF(AST.EQ.0) GO TO 4002
       GCF=0.
       CXY(=2.*(CX+YC)
       IF(AUX.GE.CXYC) GO TO 4002
       GCF=1.
 4002  CONTINUE
       IF(GCF.LE.1.00) GO TO 4001
       WRITE(6,*) J,II,IP ,K,AUX,DX,XSR,GCF
 4001  CONTINUE
       CS2AI=CS2AC*GCF
       CS4PI=CS4PC*GCF
       CSAI=CSAC*GCF
```

```
      CHAI=CHAO*GCF
      CCUI=CCUO*GCF
      CNII=CNIO*GCF
      CP3I=CP3O*GCF
      CZNI=CZNO*GCF
      CFEI=CFEO*GCF
      CS2AI=CS2AI*(.9000+.1000*(1.-EXP(-.02091*XSR)))
      CCUI =CCUI *(.0065+.2483*(1.-EXP(-.00620*XSR)))
      CNII =CNII *(.0050+.1968*(1.-EXP(-.00362*XSR)))
      CZNI=CZNI*(.010+0.9551*(1.-EXP(-.00310*XSR)))
      CP3I=CP3I*(.0040+.1245*(1.-EXP(-.00200*XSR)))
      CFEI =CFEI *(.0040+.0167*(1.-EXP(-.00400*XSR)))
C     ESTABLISH THE EFFECTIVE SOLUTION RATE OF SO2 AND EFFCTV HENRY S LAW CONSTNT
C     INPUT OF SO2 GAS
      CCAA=CS2AI
C     OXIDATION OF SO2
      CCA3=CCAA*EXP(-T*(RO1+RO2+RO3))*1.99
C     DISSOLVED PRODUCT SO4 ION
      C4HA=CCAA*(1.-EXP(-T*(RO1+RO2+RO3)))
C     ADD H2SO4
      C4HB=C4HA+CSAI
C     H+ ION CALCULATED FROM H2SO4 AND O IDATION OF SO2 IN TGE ATMOSPHERE
      CCH=C4HB*1E-3/49.+CHIO-CNH3*1E-3/17.
C     REMAINING GASEOUS SO2
      CCA=CCAB*EXP(      -T*ESR)
C     DISSOLVED SO2
      C2H =CCAB*(1.-EXP(      -T*ESR))
C     PARTICULATE SO4 BY EVAPORATION PLUS INPUT PARTICULATES
      CCP=CS4PI+C4HB*(1.-EXP(-T*EVR))
C     DISSOLVED SO4 ION
      C4H=C4HB*EXP(-T*EVR)
      OFA=EXP(-TT*HO1)
C     APPROX GAS LOSS DUE TO DIFF THROUGH AIR DRIVEN BY GAUSSIAN CONC GRADIENT
      GI=CS*(2.*CCA-CS2AM)/CY**2*0.9E-9
      SGSAV=SGSAV+CY
      TTHA=TT*HCA
      OF2=EXP(-TT*HO2)
      OFP=EXP(-TT*HO3)
      OFCU=EXP(-TTHA  *RCCU)
      OFNI=EXP(-TTHA  *RCNI)
      OFPB=EXP(-TTHA  *RCPB)
      OFZN=EXP(-TTHA  *RCZN)
      OFFE=EXP(-TTHA  *RCFE)
      ALTF=0.03E/DY
      WHFC=10.**(0.065*UXH)
      ALTFC=ALTF*WHFC
      OCA=EXP((TT-T)*GI*ALTFC)
      OC2=EXP((TT-T)*FO2   *ALTFC  )
      OCP=EXP((TT-T)*OF    *ALTFC  )
      OCCU=EXP((TT-T)*OFC  *ALTFC  )
      OCNI=EXP((TT-T)*OFN  *ALTFC  )
      OCPB=EXP((TT-T)*OFP  *ALTFC  )
      OCZN=EXP((TT-T)*OFZ  *ALTFC  )
      OCFE=EXP((TT-T)*OFF  *ALTFC  )
      CCA=CCA-OCA*CCA
      C2H=C2H*OC2*OC2
      C4H=C4H*OC2*OC2
      CCP=CCP*OCP*OCP
      CCU=CCUI*OCCU*OCCU
      CNI=CNII*OCNI*OCNI
```

```
      CPB=CPBI*CFPB*DCPB
      CZH=CZHI*CFZN*DCZN
      CFE=CFEI*CFFE*DCFE
      CCH=CCH*CS2*DD2
      SCA=SCA+CCA
      S2H=S2H+C2H
      S4H=S4H+C4H
      SCP=SCP+CCP
      SCU=SCU+CCU
      SNI=SNI+CNI
      SPB=SPB+CPB
      SZN=SZN+CZN
      SFE=SFE+CFE
      SCH=SCH+CCH
 4000 CONTINUE
      K=J
C  DAILY RAINFALL CALCULATED, IN CM
      TP(K    )=PT*CXP(K)*2.54
      SCA=SCA+CS2AM
      SCP=SCP+CS4PM
      SCU=SCU+SCUM
      SNI=SNI+SNIM
      SPB=SPB+SPBM
      SZN=SZN+SZNM
      SFE=SFE+SFEM
C  CALCULATION OF SULFATE AND SO2 SCAVENGED EACH DAY, IN UG
      TO2=TO*HO2*DYA*1E+6
      FO24=(24.-TO)*FO2*3600.
      TCHA=TO*HOA
      AKSS=HSS
      DYA=SGSAV/AKSS
      GI=GS*(2.*SCA-CS2AM)/DYA**2*0.9E-9
      GS2=SCA*(24-TO)*GI*3600.
      HS2=SCA*(TO*HO1)+S2H*(TO2+FO24)
      HS4=S4H*(TO2+FO24)
      HSH=SCH*(TO2+FO24)
      CS4=SCP*(24-TO)*DF*3600.
      HCL=SCU*(TCHA*RCCU+(24-TO)*DFC*3600.)
      HNI=SNI*(TCHA*RCNI+(24-TO)*DFN*3600.)
      HPB=SPB*(TCHA*RCPB+(24-TO)*DFP*3600.)
      HZN=SZN*(TCHA*RCZN+(24-TO)*DFZ*3600.)
      HFE=SFE*(TCHA*RCFE+(24-TO)*DFF*3600.)
      SBT=S2H+SCA
      SCT=S4H+SCP
      IF(SCA.EQ.0.)  RW2=0.
      IF(SBT.EQ.0.)  RW2=0.
      IF(SCT.EQ.0.)  RW4=0.
      IF(SCP.EQ.0.)  RWP=0.
      IF(SCA.EQ.0.)  GO TO 8001
      RWG=GS2/SCA
 8001 CONTINUE
      IF(SBT.EQ.0.) GO TO 8002
      RW2=HS2/(S2H+SCA)
 8002 CONTINUE
      IF(SCT.EQ.0.) GO TO 8003
      RW4=HS4/(S4H+SCP)
 8003 CONTINUE
      IF(SCP.EQ.0.) GO TO 8004
      RWP=CS4/SCP
 8004 CONTINUE
```

```
      IF(SHG.GT.1.) GS2=SCA
      IF(SH2.GT.1.) WS2=S2W+SCA
      IF(SHP.GT.1.) DS4=SCP
      IF(SH4.GT.1.) WS4=WS4W+SCP
C     DAILY SCAVENGED TOTALS IN UG FROM DAILY CONCS IN UG/CM3=FPM  DY IS BOX HEIGHT
C     IN KM AND CX(K) IS SAMPLED CROSS SECTION AREA IN CM2
      CY5=CXM(K)
      CY11=CY5*1.0E6
      GS2=GS2*CY5
      WS2=WS2*CY5
      WS4=WS4*CY5
      DS4=DS4*CY5
C     IN  UUG/CM3=FPM
      WCU=WCU*CY11
      WNI=WNI*CY11
      WPB=WPB*CY11
      WZN=WZN*CY11
      WFE=WFE*CY11
      WSH=WSH*    CXM(K)*1.0E2
      WW4=GS2+WS2+WS4+DS4
C     FIND MAX,MIN CONCNS FOR DIFFERENT CONDITIONS
      IF(SAD(K).GT.GS2) SAD(K)=GS2
      IF(S2D(K).GT.WS2) S2D(K)=WS2
      IF(S4D(K).GT.WS4) S4D(K)=WS4
      IF(SDD(K).GT.DS4) SDD(K)=DS4
      IF( SWCU(K).GT.WCU) SWCU(K)=WCU
      IF(SWNI(K).GT.WNI) SWNI(K)=WNI
      IF(SWPB(K).GT.WPB) SWPB(K)=WPB
      IF(SWFE(K).GT.WFE) SWFE(K)=WFE
      IF(SWZN(K).GT.WZN) SWZN(K)=WZN
      IF(WPH(K).GT.WSH) WPH(K)=WSH
      IF(SADX(K).LT.GS2) SADX(K)=GS2
      IF(S2DX(K).LT.WS2) S2DX(K)=WS2
      IF(S4DX(K).LT.WS4) S4DX(K)=WS4
      IF(SDDX(K).LT.DS4) SDDX(K)=DS4
      IF(SWCUX(K).LT.WCU) SWCUX(K)=WCU
      IF(SWNIX(K).LT.WNI) SWNIX(K)=WNI
      IF(SWPBX(K).LT.WPB) SWPBX(K)=WPB
      IF(SWZNX(K).LT.WZN) SWZNX(K)=WZN
      IF(SWFEX(K).LT.WFE) SWFEX(K)=WFE
      IF(WPHX(K).LT.WSH) WPHX(K)=WSH
      GS2S=GS2S+SCA
      WS2S=WS2S+S2W
      WS4S=WS4S+S4W
      WSHS=WSHS+SCH
      DS4S=DS4S+SCF
      WCUS=WCUS+SCU
      WNIS=WNIS+SNI
      WPBS=WPBS+SPB
      WZNS=WZNS+SZN
      WFES=WFES+SFE
 2500 CONTINUE
 2500 CONTINUE
      K=J
      SMOX=(SG2X(K)+SW2X(K)+SW4X(K)+SD4X(K))
      IF(SMOX.EQ.0.) SMOX=1.0E-10
      SPT(K)=SPT(K)+TFN(K    )
      SGS2(K)=SGS2(K)+SAD(K)
      SWS2(K)=SWS2(K)+S2D(K)
      SWS4(K)=SWS4(K)+S4D(K)
```

```
      SDS4(K)=SDS4(K)+SDD(K)
      SWC(K)=SWC(K)+ SWCU(K)
      SWN(K)=SWN(K)+SWNI(K)
      SWP(K)=SWP(K)+SWPP(K)
      SWZ(K)=SWZ(K)+SWZI(K)
      SWF(K)=SWF(K)+SWFF(K)
      SPT(K)=SPT(K)+WPH(K)
      SG2X(K)=SG2X(K)+SADX(K)
      SW2X(K)=SW2X(K)+S2DX(K)
      SW4X(K)=SW4X(K)+S4DX(K)
      SD4X(K)=SD4X(K)+SDDX(K)
      SWCX(K)=SWCX(K)+SWCUX(K)
      SWNX(K)=SWNX(K)+SWNIX(K)
      SWZX(K)=SWZX(K)+SWZIX(K)
      SWPX(K)=SWPX(K)+SWPPX(K)
      SWFX(K)=SWFX(K)+SWFFX(K)
      AGS2S=AGS2S+GS2S/16.
      AWS2S=AWS2S+WS2S/16.
      AWS4S=AWS4S+WS4S/16.
      ADS4S=ADS4S+DS4S/16.
      AWSHS=AWSHS+WSHS/16.
      AWCUS=AWCUS+WCUS/16.
      AWNIS=AWNIS+WNIS/16.
      AWPPS=AWPPS+WPPS/16.
      AWZIS=AWZIS+WZIS/16.
      AWFFS=AWFFS+WFFS/16.
      SDHP(K)=SDHP(K)+( DIP+DMPX)/2.
      SAV(K)=SAV(K)+AVP
      SSDV(K)=SSDV(K)+SDVH
      SSDH(K)=SSDH(K)+SDHW
      SAH(K)=SAH(K)+AHP
      SSDX=SADX(K)+S2DX(K)+S4DX(K)+SDDX(K)
      SPPX(K)=SPHX(K)+WPHX(K)
      SSSX=SSDX/SWDX
      IF(SSSX.LT..50) GO TO 2101
 2101 CONTINUE
      AAA=AAA+1.
C  CALC AND WRITE CONC AS EACH SAMPLE PERIOD IS TERMINATED
      IF(III.NE.IIP(K)) GO TO 2000
      DAY(K)=IIP(K)-III(K)+1
      AA=AA+1.0
      FDHP=SDHP(K)/DAYC(K)
      FAVH    =SAV(K)/DAYC(K)
      FSDVH    =SSDV(K)/DAYC(K)
      FSDHW    =SSDH(K)/DAYC(K)
      FAHW=SAH(K)/DAYC(K)
      AGS2=AGS2S/DAYC(K)
      AWS2=AWS2S/DAYC(K)
      AWS4=AWS4S/DAYC(K)
      ADS4=ADS4S/DAYC(K)
      AWSH=AWSHS/DAYC(K)
      AWCL=AWCUS/DAYC(K)
      AWNI=AWNIS/DAYC(K)
      AWPP=AWPPS/DAYC(K)
      AWZI=AWZIS/DAYC(K)
      AWFF=AWFFS/DAYC(K)
      CSTI= SWS2(K)+SWS4(K)+SDS2(K)+SDS4(K)
      IF((SPT(K).EQ.0.) GO TO 2100
      CSTI=CSTI/SPT(K)
 2100 CONTINUE
```

```
C  TOTAL WET DEPOSITION
      TWS(K)=SWS2(K)+SWS4(K)
      TWSX(K)=SW2X(K)+SW4X(K)
C  TOTAL DRY DEPOSITION
      TDS(K)=SGS2(K)+SDS4(K)
      TDSX(K)=SG2X(K)+SD4X(K)
C  TOTAL SO2 DEPOSITION
      TRS2(K)=SWS2(K)+SGS2(K)
      TR2X(K)=SW2X(K)+SG2X(K)
C  TOTAL SO4 DEPOSITION
      TRS4(K)=SWS4(K)+SDS4(K)
      TR4X(K)=SW4X(K)+SD4X(K)
C  TOTAL SULFUR DEPOSITION
      TRS(K)=TRS2(K)+TRS4(K)
      TRSX(K)=TR2X(K)+TR4X(K)
C  CALC OF RECEPTOR CONC IN UG/CM3 OF PPM,UUG/CM3 OR PPB, AND IN GM/CM3FOR H+
      IF(SPT(K).EQ.0.) GO TO 5001
      TRS(K)=TRS(K)/SPT(K)
      TRSX(K)=TRSX(K)/SPT(K)
      SWC(K)=SWC(K)/SPT(K)
      SWN(K)=SWN(K)/SPT(K)
      SWP(K)=SWP(K)/SPT(K)
      SWZ(K)=SWZ(K)/SPT(K)
      SWF(K)=SWF(K)/SPT(K)
      SWCX(K)=SWCX(K)/SPT(K)
      SWNX(K)=SWNX(K)/SPT(K)
      SWPX(K)=SWPX(K)/SPT(K)
      SWZX(K)=SWZX(K)/SPT(K)
      SWFX(K)=SWFX(K)/SPT(K)
      IF(TRS(K).EQ.0.) TRS(K)=1.0E-10
      IF(TRSX(K).EQ.0.) TRSX(K)=1.0E-10
C  EST TOTAL PARTICULATES ,UG, MULT BY ION ABSRPTION , IN EQUIV/UG = EFCTV EQUIV
      CCPRT=CPRT*.162E-14+(SWC(K)+SWN(K)+SWP(K)+SWZ(K)+SWF(K))*.05E-14
      CCPRTX=CPRT*.162E-14+(SWCX(K)+SWNX(K)+SWPX(K)+SWZX(K)+SWFX(K))*
     1 0.05E-14
C  ASSUMED THAT REMAINING SCAVENGED SO2 IS OXIDIZED IN THE SAMPLER
      CXS(K)=1.-EXP(-CAYC(K)*0.4066E-5)
      SPH(K)=SPH(K)+TRS2(K)*1E-3/48.*CXS(K)*1.5
      SPHX(K)=SPHX(K)+TR2X(K)*1E-3/48.*CXS(K)*1.5
C  CALC H+ ION CONC, IN GM/LITER
      SPH(K)=SPF(K)/SPT(K)*1E3*CCPRT
      SPHX(K)=SPHX(K)/SPT(K)*1E3*CCPRTX
C  CRP(K) IS MEASURED OVER CALCULATED RAINFALL AND ORC(K) IS MEASURED OVER
C  CALCULATED CONCENTRATIONS
      CRP(K)=VLM(K)*1000./SPT(K)
 5001 CONTINUE
C  CALC OF MAX AND MIN PH
      PH(K)=0.
      IF(SPH(K).LE.0.) GO TO 5006
      PH(K)=-ALOG10(SPH(K))
 5006 CONTINUE
      PHX(K)=0.
      IF(SPHX(K).LE.0.) GO TO 5007
      PHX(K)=-ALOG10(SPHX(K))
 5007 CONTINUE
      PHA=(PH(K)+PHX(K))/2.
      S4MM=S4M(K)*.40
      S4MX=S4M(K)*1.60
      CUMM=CUM(K)*.4
      CUMX=CUM(K)*1.6
```

```
      NIMM=NIM(K)*.4
      NIMX=NIM(K)*1.6
      PBMM=PBM(K)*.4
      PBMX=PBM(K)*1.6
      ZNMM=ZNM(K)*.4
      ZNMX=ZNM(K)*1.6
      FEMM=FEM(K)*.4
      FEMX=FEM(K)*1.6
      HIMM=HIM(K)*.4
      HIMX=HIM(K)*1.6
      CRCA=0.
      TRSA=(TRS(K)+TRSX(K))/2.
      IF(SUM(K).EQ.0.) GO TO 5005
      CRCA=TRSU/SUM(K)
 5005 CONTINUE
      SWCA=(SWC(K)+SWCX(K))/2.
      SWNA=(SWN(K)+SWNX(K))/2.
      SWFA=(SWF(K)+SWFX(K))/2.
      SWPA=(SWP(K)+SWPX(K))/2.
      SWZA=(SWZ(K)+SWZX(K))/2.
      PCR=0.
      IF(CUM(K).EQ.0.) GO TO 5009
      PCR=SWCA/CUM(K)
 5009 CONTINUE
      ANR=0.
      IF(ANM(K).EQ.0.) GO TO 5010
      ANR=SWNA/NIM(K)
 5010 CONTINUE
      AFR=0.
      IF(FEM(K).EQ.0.) GO TO 5011
      AFR=SWFA/FEM(K)
 5011 CONTINUE
      APR=0.
      IF(HIM(K).EQ.0.) GO TO 5012
      APR=PHA/HIM(K)
 5012 CONTINUE
      AER=0.
      IF(PBM(K).EQ.0.) GO TO 5013
      AER=SWPA/PBM(K)
 5013 CONTINUE
      AZR=0.
      IF(ZNM(K).EQ.0.) GO TO 5014
      AZR=SWZA/ZNM(K)
 5014 CONTINUE
      WRITE(6,168)
      WRITE(6,602)
      WRITE(6,602)
      SPT(K)=SPT(K)/1E3
      XSRA=(XSR1+XSR2+XSR3)/3.
      ASRA=(ASR1+ASR2+ASR3)/3.
      AUXA=ABS(ASRA-FLHW)
      IF(N75.NE.1) GO TO 2123
      WRITE(6,658) IMF,IOF,IYF
 2123 CONTINUE
      WRITE(6,603) ANM(K),(SMI(K,JJA),JJA=1,4)
      WRITE(6,602)
      WRITE(6,604)YMI(K),XMI(K),OMI(K),YMF(K),XMF(K),OMF(K),XNM(K),
     1 YLM(K),ZEM(K)
      WRITE(6,602)
      WRITE(6,659) FOAR,FAVH,FSOVH,FSOHW,FAHW
```

```
      WRITE(6,663) XSP1,ASR1,XSP2,ASR2,XSP3,ASP3,XSPA,ASPA,AUXA
      WRITE(6,654) VLM(K),SPT(K),CXM(K)
      WRITE(6,602)
      WRITE(6,167)
      WRITE(6,602)
      WRITE(6,166) AGS2,AWS2,AWS4,AOS4,AWSH,AWCU,AWNI,AWP8,AWZN,AWFE
      WRITE(6,612)
      WRITE(6,605)
      WRITE(6,606)
      WRITE(6,607) TPS(K),TRSA,TPSX(K),PH(K),PHA,PHX(K),SWC(K),SWCA,
     1 SWCX(K),SWN(K),SWNA,SWNX(K)
      WRITE(6,608) S4M4,S4M(K),S4MX,HIMM,HIM(K),HIMX,CUMM,CUM(K),CUMX,
     1 AIMM,AIM(K),AIMX
      WRITE(6,609) DPCA,RPHR,PCR,PNO
      WRITE(6,602)
      WRITE(6,610)
      WRITE(6,614)
      WRITE(6,611)SHP(K),SHPA,SHPX(K),SHZ(K),SHZA,SHZX(K),SHF(K),SHFA,
     1 SHFX(K)
      WRITE(6,612) PBHM,PBM(K),PBMX,ZNMM,ZNM(K),ZNMX,FEMM,FEM(K),FEMX
      WRITE(6,613)PPP,RZR,RPC
      WRITE(6,602)
      WRITE(6,602)
      IDAY=DAYC(K)
      WRITE(19,661) MNH(K),(SWS(K,JJA),JJA=1,4),YMI(K),PMI(K),QMI(K),
     1 YMF(K),PPF(K),QMF(K),XAM(K),YLM(K),ZBM(K),FDPR,FAVM,FSCVM,FSCHM,
     2 PBHM,TPS(K),TPSX(K),PH(K),PHX(K),SWC(K),SWCX(K),SWN(K),SWNX(K),
     3  SHP(K),SHPX(K),SHZ(K),SHZX(K),SHF(K),SHFX(K), S4M(K),HIM(K),
     4  CUM(K),AIM(K),PEP(K),ZNM(K),FEM(K),VLM(K),CXM(K),SPT(K),IDAY
      WRITE(19,659)XSP1,ASR1,XSR2,ASR2,XSR3,ASP3,XSPA,ASRA,AUXA
     5            ,VLM(K),SPT(K),CXM(K)
     7            ,AGS2,AWS2,AWS4,AOS4,AWSH,AWCU,AWNI,AWP8,AWZN,AWFE
      STRS=STRS+TPS(K)
      STRSX=STRSX+TPSX(K)
      IF(MIX.NE.10) GO TO 2200
      ATRS(K)=ATRS(K)+TRS(K)
      ATRSX(K)=ATRSX(K)+TRSX(K)
      IF(STR.NE. 6092925.) GO TO 2200
      ATRS(K)=ATRS(K)/5.
      ATRSX(K)=ATRSX(K)/5.
      WRITE(6,152)
      WRITE(6,306) ATRS(K)
      WRITE(6,309) ATRSX(K)
      ATRS(K)=0.
      ATRSX(K)=0.
 2200 CONTINUE
      III(K)=0
      IIF(K)=0
      SPT(J)=0.
      SGS2(J)=0.
      SWS2(J)=0.
      SWS4(J)=0.
      SOS4(J)=0.
      SG2X(J)=0.
      SW2X(J)=0.
      SW4X(J)=0.
      SO4X(J)=0.
      SHC(K)=0.
      SHN(K)=0.
      SHP(K)=0.
```

```
      SH2(K)=0.
      SHF(K)=0.
      SHCX(K)=0.
      SHNX(K)=0.
      SHPX(K)=0.
      SH2X(K)=0.
      SHFX(K)=0.
      DPR(J)=0.
      DPC(J)=0.
      DPCX(J)=0.
      TPS(J)=0.
      TPSX(J)=0.
      SPH(K)=0.
      SPHX(K)=0.
      SS2X(J)=0.
      AAA=1.
      SSO)=0.
      SMOX=0.
      DAYC(J)=0.
      SCMS(J)=0.
      SSDV(J)=0.
      SAM(J)=0.
      SSOH(J)=0.
      SAH(J)=0.
      N75=0
 2000 CONTINUE
 2995 CONTINUE
 2999 CONTINUE
      IF(NIX.EC.11) GC TO 900
      IF(NIX.GE.6.AND.NIX.LE.9) GO TO 900
      GO TO 1000
 3001 CONTINUE
  600 FORMAT(1X,* MODIFIED ECX MODEL FOR SULFUR AND METAL LOADINGS
     1 F J HUHR, 1977 *)
  601 FORMAT(1X,* CALCULATED AND MEASURED LOADINGS *)
  602 FORMAT(/)
  603 FORMAT(1X,I5,5X,4A4)
  604 FORMAT(1X,3I3,* TO *,3I3,*  AT*,F8.4,* DEG. W. LONG. AND *,F8.4,
     1 * DEG. N. LAT.  ELEV. IS *,F8.4,1 M*)
  605 FORMAT(15X,*SO4,PPM                PH                    CU,PPB
     1          NI,PPB                *)
  606 FORMAT(12X,4(* MIN   ( MEAN )  MAX    *))
  607 FORMAT(1X,*CALCULATED *,4(F6.2,*(*,F6.2,*)*,F6.2,1X))
  608 FORMAT(1X,*MEASURED   *,4(F6.2,*(*,F6.2,*)*,F6.1,1X))
  609 FORMAT(1X,*RATIOS     *,7X,4(F6.2,15X))
  610 FORMAT(15X,*PB,PPB                ZN,PPB                FE,PPB    *)
  611 FORMAT(1X,*CALCULATED *,3(F6.2,*(*,F6.2,*)*,F6.2,1X))
  612 FORMAT(1X,*MEASURED   *,3(F6.2,*(*,F6.1,*)*,F6.1,1X))
  613 FORMAT(1X,*RATIOS     *,7X,3(F6.2,15X))
  614 FORMAT(12X,3(* MIN   ( MEAN )  MAX    *))
  616  FORMAT (1X,* LONG AND LAT OF PLOT ORIGIN*)
  618 FORMAT(1X,*AMBIENT SO2,SO4,H+,NH3,AND PARTUCULATES*)
  619 FORMAT(1X,*AMBIENT CU,NI,PB,ZN,FE *)
  620 FORMAT(1X,*DRYFALL   CL,NI,PB,ZN,FE*)
  621 FORMAT(1X,*CIAMS,RAINDROPS, CLOUD DROPLETS, SO4,CL,NI,PB,ZN,FE,AN,
     1D PARTICULATES*)
  650 FORMAT(1X,3I4,2F8.4,/,1X,12E10.4,/,1X,12E10.4)
  651 FORMAT  (1X,I5,4A4,6I2,3F8.4,/,1X,5F3.4,/,1X,12F8.2,/,1X,12F8.2,I5)
  659 FORMAT  (1X,12F8.2,/,1X,10E10.4)
  662 FORMAT  (1X,* AVE RAIN RATE, MM/HR *,F8.4,/,1X,* AVE WIND, KM/HR *,
```

```
     1  ,F9.4,/,1X,* STD DEV OF VELOCITY *,F9.4,/,1X,* STD DEV OF HEADING
     2 *,F9.4,/,1X,* AVE WIND HEADING *,F9.4)
653  FORMAT (1X,* DISTANCE IN KM AND HEADING FROM SOURCES *,6(1X,F6.2),
     1 /,1X,* AVERAGE DISTANCE AND HEADING *,2F7.2,/,1X,* AVE ANGLE HEAD
     2ING TO WIND *,F6.2)
654  FORMAT(1X,* MEASURED AND CALCULATED VOLUME, L *,2F6.2,/,1X,*  SAM
     1PLER CROSS SECTIONAL AREA *,F6.2)
658  FORMAT (1X,* SAMPLE PERIOD END TRUNCATED FROM *,3I3,* TO 12 31 74*)
668  FORMAT   (3X,*    MEASURED SO4 = *,E13.6,* PPM *)
669  FORMAT   (3X,* CALCULATED SO4 = *,E13.6,* PPM *)
530  FORMAT     (5E10.4)
531  FORMAT(1X, 5E10.4)
510  FORMAT     (6E10.4)
511  FORMAT(1X, 6E10.4)
512  FORMAT (   6E10.4)
513  FORMAT (1X, 6E10.4)
540  FORMAT     (5I4)
541  FORMAT(1X,5I4)
535  FORMAT    (1X,I5,4A4,3F6.4,3E10.3,4X/,1X,7E10.3,E9.2,/,1X,2E10.3)
536  FORMAT   (1X,I5,4A4,3F5.4,6E10.3,/,4E10.3)
135  FORMAT  (1X,I1,I6,I7,3I2,F6.3,2F3.5,2F3.0,3I1,2F7.4,2F3.4)
136  FORMAT  (2X,I1,I6,I7,3I2,F6.3,2F8.6,2F3.0,3I1,4F7.4,/,2X,2F9.4)
300  FORMAT(11,6,17,3I2,F6.3,2F8.5,2F3.0,3I1,2F7.4,2F3.5)
100  FORMAT (2I6,I2,I1)
131  FORMAT(1X,I4,4A4,3F3.4)
 26  FORMAT(1X,I4,4A4,3F3.4,F6.4,F6.2,I1,6I2,F6.2,4X,/,16X,3F6.2,2F6.1,
     1   F6.2)
 27  FORMAT(1X,I4,4A4    ,3F8.4,F6.2,F6.2,I1,6I2,F6.2,4X,/,16X,5F6.1,
     1 F6.2)
327   FORMAT   (2F8.4)
 60  FORMAT  (4X,19A4)
 61  FORMAT   (2I5)
 70  FORMAT   (2I8)
150  FORMAT  (1X,I6,I7,I2,5E12.5)
151  FORMAT  (1X,I3,E12.6)
152  FORMAT(1X,* AVERAGE OF 5 OUTPUTS*)
153  FORMAT(1X,* TOTAL AVERAGE RATIO,MEAS OVER MIN AND MAX CALC CONC*)
154  FORMAT(1X,* TOTAL RMS DIFF, MEAS TO MIN AND MAX CALC CONC *)
161  FORMAT  (1X,* SAULT ST. MARIE *)
162  FORMAT  (1X,*  SUDBURY AIRPORT*)
163  FORMAT  (1X,*  TIMMINS *)
164  FORMAT  (1X,* NORTH BAY AIRPORT *)
165  FORMAT  (1X,*  GORE BAY *)
166  FORMAT  (1X,5(5X,E10.4),/,1X,5(5X,E10.4))
167  FORMAT  (1X,*   GASEOUS SO2     DISSOLVED SO2  DISSOLVED SO4  PARTCLE
    1SO4     HYDROGEN ION   *,/,1X,*     COPPER          NICKEL          LE
    2AD          ZINC            IRON        *)
168  FORMAT  (1H1)
     STOP
     END
```

APPENDIX D

LAKE subroutine

```
      SUBROUTINE LAKE(PRC,CPP,ALB,ALS,AUL,EVP,RSED,FS,D,VDB,CWØ,CSØ,
     1 CW,CSED)
C  WATER BALANCE
C  QWIN IS AVERAGE WATER INFLUX FROM PRECIPITATION
      QWIN = 2.9E10*PRC*ALB
C  QWOUT IS AVERAGE STREAM FLOW OUTPUT FLUX
      QWOUT = QWIN*(1-EVP)
C  QSED IS FLUX LEAVING LAKE BY SEDIMENTATION
      QSED = 1.369E9*RSED*ALS*D
C  FSED IS ESTIMATED SEDIMENTATION FACTOR
C  CPP IS THE AVERAGE POLLUTANT CONCENTRATION IN PRECIPITATION
      FSED = 1-QSED/(QWIN*CPP)
C  BFACT IS LAKE BASIN FACTOR
      BFACT = (ALS+FSED*AUL+FS*(ALB-AUL-ALS))/ALB
C  QPIN IS POLLUTANT INPUT FLUX TO LAKE
      QPIN = QWIN*BFACT*CPP
C  TAW IS AVERAGE WATER DETENTION TIME
      V = D*ALS
      TAW = V/QWOUT
C  CW IS LAKEWATER POLLUTANT CONCENTRATION
      CW = (1-EXP(-TAW*(QWOUT+QSED)/V)*QPIN)/(QWOUT+QSED)+CWØ
C  CSED IS POLLUTANT CONCENTRATION IN SURFACE SEDIMENT LAYER
      CSED = 50.0*C*RSED*D/VDB+CSØ
      CALL SUBROUTINEWRITLK(CW,CSED)
      RETURN
      END
```